Gauge-gravity duality, phase transition of nuclear matter, beyond the Einstein gravity limit

Dissertation
zur Erlangung des Doktorgrades
der Naturwissenschaften

vorgelegt beim Fachbereich Physik
der Johann Wolfgang Goethe -Universität
in Frankfurt am Main

von

Antonia Micol Frassino
aus Rom, Italien

Frankfurt 2016
(D 30)

vom Fachbereich Physik der
Johann Wolfgang Goethe - Universität
als Dissertation angenommen.

Dekan:	Prof. Dr. Rene Reifarth
Gutachter :	Prof. Dr. Marcus Bleicher
	PD Dr. Piero Nicolini

Datum der Disputation :

Preface

This dissertation is submitted to the Faculty of Physics of the Johann Wolfgang Goethe University for attaining the Ph.D. degree of Natural Sciences.
The research described herein was conducted under the supervision of Prof. Dr. Marcus Bleicher and PD Dr. Piero Nicolini at the Frankfurt Institute for Advanced Studies, between January 2012 and April 2016. The results of this work have been presented in the following publications:

- A. M. Frassino, S. Köppel and P. Nicolini,
  "Geometric model of black hole quantum N-portrait, extradimensions and thermodynamics," [arXiv:1604.03263 [gr-qc]].
  (Invited paper to the special issue "Entropy in Quantum Gravity and Quantum Cosmology" edited by R. Garattini). Entropy **18** (2016), 181.

- M. Cadoni, A. M. Frassino and M. Tuveri,
  "On the universality of thermodynamics and η/s ratio for the charged Lovelock black branes," [arXiv:1602.05593 [hep-th]]
  (accepted for publication in JHEP, in press).

- A. M. Frassino, R. B. Mann and J. R. Mureika, "Lower-Dimensional Black Hole Chemistry," Phys. Rev. D **92**, no. 12, 124069 (2015)
  [arXiv:1509.05481 [gr-qc]].

- A. M. Frassino, "Phase transitions of regular Schwarzschild-Anti-deSitter black holes," Springer Proc. Phys. **170** (2016) 241
  [arXiv:1502.01305 [hep-th]].

- A. M. Frassino, D. Kubiznak, R. B. Mann and F. Simovic, "Multiple Reentrant Phase Transitions and Triple Points in Lovelock Thermodynamics," JHEP **1409** (2014) 080 [arXiv:1406.7015 [hep-th]].

- A. M. Frassino and O. Panella, "The Casimir Effect in Minimal Length Theories Based on a Generalized Uncertainity Principle," Phys. Rev. D **85** (2012) 045030 [arXiv:1112.2924 [hep-th]].

Zusammenfassung

In den vergangen Jahren wurde erkannt, dass eine Quantenfeldtheorie (QFT) namens Quantenchromodynamik (QCD) die richtige Theorie der starken Wechselwirkungen ist. QCD beschreibt erfolgreich die starken Wechselwirkungen, die Quarks zu Nukleonen und Nukleonen zu Atomkernen zusammenbinden. Jedoch ist die theoretische Beschreibung vieler Phänomene der starken Wechselwirkung aufgrund des starken Kopplungsverhaltens bei niedrigen Energien schwierig. Stoßexperimente mit Schwerionen sind ein möglicher Weg, um die charakteristischen Phänomene und Eigenschaften der QCD-Materie zu untersuchen. In Stoßexperimenten mit Schwerionen werden schwere (d.h. große) Atomkerne aufeinander geschossen, beispielsweise Gold (am RHIC) oder Blei (am CERN, LHC), mit einer ultrarelativistischen Energie $\sqrt{s}$ im Schwerpunktsystem. Auf diese Art ist es möglich, eine große Menge von Materie mit hoher Energiedichte hervorzubringen. Das Ziel von Schwerionenkollisionen ist die Erzeugung und Charakterisierung einer makroskopischen Phase von freien Quarks und Gluonen im lokalen thermischen Gleichgewicht. Ein solcher Aggregatzustand kann neue Informationen über das QCD-Phasendiagramm und den QCD-Phasenübergang liefern. Man nimmt an, dass ein solcher Übergang stattfand, als sich die Materie des frühen Universums von einem Plasma aus Quarks und Gluonen (QGP) in ein Gas von Hadronen umwandelte.

Die Phänomenologie der Schwerionenphysik erfordert Techniken zur Behandlung starker Kopplung sowohl für thermodynamische Größen wie die QCD – Zustandsgleichung als auch für dynamische Größen bei Temperaturen $T \neq 0$, wie beispielsweise Transportkoeffizienten. Momentan betrifft eine der Hauptschwierigkeiten der verschiedenen Modelle zur Beschreibung von Schwerionenkollisionen den Abschnitt direkt nach der Kollision und vor der Bildung des QGP. Diese Anfangsphase ist außergewöhnlich komplex, weil sie die Entwicklung vieler Quarks und Gluonen in reeller Zeit betrifft. Prinzipiell sollte sie durch eine vollständig nichtperturbative

Rechnung beschreiben werden. Aktuell können diese nichtperturbativen Rechnungen nicht mittels QCD durchgeführt werden. In dieser Arbeit wird ein besonderer Ansatz zu diesem Problem verwendet, der *Holographie* genannt wird.

Das Konzept der Holographie geht auf eine Idee 't Hoofts aus dem Jahre 1974 zurück und besagt, dass eine vollständige Äquivalenz zwischen zwei verschiedenen Theorien möglich ist, die sich in ihren Dimensionen unterscheiden. Der Rand ("boundary") besitzt eine Dimension weniger als das Innere ("bulk") und wird mit dem Raum identifiziert, auf dem die duale Quantenfeldtheorie lebt. Darüber hinaus stellte 't Hooft in einer anderen Arbeit allgemeingültig fest, dass sich stark gekoppelte $SU(N_c)$-Eichtheorien mit Kopplungskonstante g vereinfachen können, falls N_c groß ist. Gemäß des holographischen Prinzips kann die Entwicklung einer nicht-abelschen Eichtheorie für große N_c auf eine Beschreibung mittels klassischer Gravitation führen. Daher ermöglicht Holographie vollständige Rechnungen bei starker Kopplung, auch wenn nicht in der QCD selbst (da $N_c > 3$). Trotzdem blieben die Berechnungen vor der Formulierung der sogenannten *AdS/CFT-Dualität* schwierig durchzuführen.

Die AdS/CFT-Korrespondenz, allgemeiner die Gauge/Gravity-Dualität, sind konkrete Realisierungen des holographischen Prinzips. Die Dualität besagt, dass bestimmte nicht-abelsche Eichtheorien als Theorien der Quantengravitation beschrieben werden können, die in einer höherdimensionalen Raumzeit mit dem asymptotischen Verhalten eines Anti-de-Sitter-Raums (AdS) leben. Die Stärke der Dualität liegt darin, dass sie die schwach koppelnden Bereiche im Inneren mit stark koppelnden auf dem Rand verbindet und damit ein Werkzeug zu nichtperturbativen Berechnungen dynamischer Grßen bereitstellt. Das Ziel der vorliegenden Arbeit ist es, mithilfe kürzlich vorgeschlagener Modelle fÃijr Gravitation dynamische Größen bei Temperaturen $T \neq 0$ wie beispielsweise das Verhältnis η/s zu bestimmen.

Einer der größten Erfolge der Dualität ist die Abschätzung des Quotienten der Scherviskosität η und der Entropiedichte s für das QGP. Im Besonderen wurde eine universelle Grenze dieser Größe vermutet, die sogenannte Kovtun-Son-Starinets (KSS) Grenze $\eta/s \geq 1/4\pi$.

Ein fundamentaler Baustein der Gauge/Gravity-Dualität ist das Schwarze Loch (BH). Schwarze Löcher sind Lösungen der klassischen Allgemeinen Relativitätstheorie (GR), die entscheidende Aspekte der Physik des Endstadiums eines Gravitationskollapses beinhalten.

Die erste Lösung der Einstein'schen Feldgleichungen im Vakuum ($T_{\mu\nu} = 0$) ist die Schwarzschild-Lösung eines Schwarzen Lochs, das auch als BH bezeichnet wird. Ein Durchbruch in der Untersuchung Schwarzer Löcher geschah mit der Entdeckung, dass sie eine thermodynamische Natur besitzen. Die Entdeckung der thermodynamischen Eigenschaften Schwarzer Löcher eröffnete faszinierende Möglichkeiten, warf aber auch verschiedene Fragen auf. Diese Fragen betreffen beispielsweise das Informationsparadoxon oder das Schicksal der Unitarität in der Theorie. Die Beantwortung dieser Fragen benötigt eine vollständige quantendynamische Beschreibung in Bereichen fernab der semiklassischen Fälle. Insbesondere erfordert sie das Verständnis der Dynamik im gesamten Bereich der Krümmungssingularität, auch wenn diese hinter dem Ereignishorizont verborgen ist. Dies ist das Ziel der Theorie der Quantengravitation.

In den letzten Jahren wurde eine alternative Quantisierung der Raumzeit vorgeschlagen, die auf Heisenbergs Korollar basiert: **"physical quantities are governed by non-commutative algebra".** Ein möglicher Ansatz für diese Raumzeitquantisierung basiert auf der Benutzung kohärenter Zustände des quantenmechanischen Ortsoperators $\mathbf{x}^\mu$, für den $[\mathbf{x}^\mu, \mathbf{x}^\nu] \neq 0$ gilt. Jedoch verhindert der nichtverschwindende Kommutator die Existenz einer gemeinsamen Basis in der Koordinatendarstellung und fordert eine Unschärferelation zwischen ihnen, wobei er eine fundamentale Längenskala einführt. Das beste Vorgehen in einem solchen Fall ist die Einführung eines Mittelwerts zwischen geeignet gewählten, d.h. kohärenten, Zuständen. Die kohärenten Zustände sind Zustände kleinster Unschärfe, deren Mittelwerte den klassischen kommutierenden Koordinaten am nächsten kommen, wobei ihre Breite von einer fundamentalen Länge abhängt. In der Beschreibung mit kohärenten Zuständen gibt es keine UV-Divergenzen, aus denen Anomalien resultieren. Die Möglichkeit, eine fundamentale Länge zu nutzen, wird in dieser Arbeit aus der Sicht der Allgemeinen Relativitätstheorie untersucht: Reguläre Schwarze Löcher (RBH) sind eine Familie von Schwarzen Löchern als Lösungen der Einstein'schen Feldgleichungen, die den Effekt der Planck-Länge im Bereich kleiner Längen/hoher Energien des Gravitationsfelds beinhalten. Die Herleitung des Wegelements dieser Lösungen basiert auf der Möglichkeit, eine effektive minimale Länge in die Allgemeine Relativitätstheorie einzuführen. Mit diesen Lösungen können verschiedene Bereiche in AdS/CFT-Berechnungen untersucht werden.

Im Zusammenhang mit Quantenkorrekturen der Feldgleichungen ist auch ein weiterer Ansatz möglich. Krümmungskorrekturen höherer Ordnung (*Higher curvature corrections*) können in die Allgemeine Relativitätstheorie eingeführt werden, weil man erwartet, dass die Quantengravitation eine bedeutende Rolle bei starken

Krümmungen spielt. Die nützlichste Klasse von Theorien ist die der sogenannten Lovelock-Gravitationstheorien. Diese Theorien erweitern die Allgemeine Relativitätstheorie in Raumzeiten mit mehr als vier Dimensionen und sind die einzigen Theorien mit höheren Ableitungen, die Differentialgleichungen zweiter Ordnung für die metrischen Funktionen zulassen. Die Lovelock-Korrektur zweiter Ordnung wird Gauß-Bonnet genannt und liefert Korrekturen zu den Einstein'schen Feldgleichungen in Raumzeitdimensionen $d \geq 5$. Im Kontext der Gauge/Gravity-Dualität leben die Felder auf dem Rand in einer Dimension weniger als die Gravitation im Inneren. Um eine realistische Feldtheorie in vier Dimensionen zu modellieren, muss die relevante Raumzeit im Inneren fünf Dimensionen besitzen. Um alle mÃűglichen Szenarien, die die Allgemeine Relativitätstheorie bietet, zu untersuchen, können die Gauß-Bonnet-Terme nicht willkürlich vernchlässigt werden. Aufgrund der Gauge/Gravity-Dualität können weiterhin einige Krümmungsterme höherer Ableitung in der Entwicklung der dualen Feldtheorie als Korrekturen bei hohem N_c angesehen werden.

In dieser Arbeit werden ausgehend von der Gauge/Gravity-Dualität und der Teilchenphysik mehrere Modelle untersucht, die interessante Gravitationsphänomene beschreiben

- Im ersten Kapitel wird ein Überblick über die für diese Arbeit relevanten Konzepte vorgestellt: Lösungen der Einstein'schen Feldgleichungen für Schwarze Löcher werden diskutiert, um die Notation einzufüren. Die Paradoxa, die aus der klassischen Allgemeinen Relativitätstheorie hervorgehen, werden beschrieben. Ein besonderes Augenmerk gilt der AdS/CFT-Dualität und dem Wörterbuch, das die Größen des Rands mit denen des Inneren verbindet.

- Im zweiten Kapitel werden Phasenübergänge von regulären Schwarzen Löchern und Gauß-Bonnet Schwarzen Branen analysiert. Es hat sich herausgestellt, dass Gauß-Bonnet Schwarze Branen ein universelles thermodynamisches Verhalten aufweisen, d.h. ausgedrückt mittels effektiver Masse und Temperatur können sie von geladenen Schwarzen Branen nicht unterschieden werden.

- Im dritten Kapitel wird eine detaillierte Untersuchung der Thermodynamik Schwarzer Löcher aus einer anderen Perspektive vorgeschlagen. Die Idee besteht darin, dass die kosmologische Konstante Λ als charakteristische Größe der AdS-Raumzeit selbst als thermodynamische Variable betrachtet werden muss, analog zum Druck im Ersten Hauptsatz der Thermodynamik. Diese Interpretation erweitert den Phasenraum der thermodynamischen Parameter.

In diesem Zusammenhang wurden Phasenübergänge von RBH und Lovelock-BHs studiert. Es wurde herausgefunden, dass ungeladene Lovelock-Schwarze Löcher dritter Ordnung ein spezielles thermodynamisches Verhalten aufweisen: Die Zustandsgleichung hat eine ungewöhnliche Entwicklung in der Umgebung eines besonderen kritischen Punkts, die auf eine Verletzung bestimmter Skalenbeziehungen und ungewöhnliche kritische Exponenten hindeutet. Dies ist das erste Beispiel eines ungewöhnlichen kritischen Exponenten in einer Gravitationstheorie. Kürzlich wurde die Rolle einer dynamischen Kosmologischen Konstante in der AdS/CFT-Korrespondenz untersucht, die mit der Anzahl der Farben der Eichtheorie auf dem Rand in Verbindung gesetzt wurde.

- Im vierten Kapitel wird das Verhältnis von Scherviskosität und Entropiedichte in den dualen Feldtheorien auf dem Rand berechnet. Die untersuchten Modelle sind eine reguläre und eine Gauß-Bonnet Schwarze Brane in einer asymptotischen AdS Raumzeit. Es wurden interessante Konsequenzen hinsichtlich der Universalität der Wertes von η/s gefunden.

Zusammenfassend wurden in dieser Arbeit die geometrischen, thermodynamischen und holographischen Eigenschaften von geladenen GB Schwarzen Branen in fünf Dimensionen, geladenen Lovelock-Schwarzen Löchern und regulären Schwarzen Löchern und Branen detailliert untersucht. Im Fall von Gauß-Bonnet wurde herausgefunden, dass in Übereinstimmung mit der geometrischen und thermodynamischen Vorstellung die Universalität von η/s im UV verloren geht, aber im IR wiederhergestellt wird. Das Verhältnis η/s hat ein nichtuniverselles temperaturabhängiges Verhalten für nichtextreme Gauß-Bonnet Schwarze Branen, erreicht aber den universellen Wert $1/4\pi$ im Extremalfall. Dieses Ergebnis legt nahe, dass η/s ausschließlich durch das IR-Verhalten bestimmt wird und unempfindlich gegen den UV-Bereich der dualen QFT ist. Bei niedrigen Temperaturen nähert sich das Verhältnis η/s dem universellen Wert $1/4\pi$, aber dieser Wert stellt ein *Minimum* für die Gauß-Bonnet Kopplungskonstante $\lambda < 0$ und ein *Maximum* für $\lambda > 0$ dar. Deshalb ist die zur GB-Maxwell duale QFT für $\lambda < 0$ ein schönes Beispiel für ein temperaturabhängiges η/s mit einer unteren Schranke von $1/4\pi$. Aber die Temperaturabhängigkeit, die für $0 < \lambda < 1/4$ erhalten wird und die KSS-Grenze verletzt, ist ein interessantes Thema für weitere Untersuchungen.

Contents

List of Figures

Dedicated to Franca and Arcangelo

Chapter 1

Introduction

In the past years, a quantum field theory (QFT) called Quantum Chromodynamics (QCD) has been recognized to be the correct theory of the strong interactions. QCD successfully describes the strong interactions that bind quarks together to form nucleons and nucleons to nuclei. However, many strong interaction phenomena are difficult to describe theoretically because of the strongly coupling at low energies. At low energy, quarks are confined within nucleons and the degrees of freedom that are observable are not the solutions of the corresponding free theory. At this regime, a perturbative approach (i.e., an expansion of the theory in the coupling constant) is not possible. The coupling constant becomes of the order one at an energy scale Λ_{QCD} of several hundred MeV. Therefore, the perturbative approach, which is possible at higher energies, is not sufficient to gain a complete picture of QCD.[1]

A possible way to study phenomena and properties that characterize the strongly interacting matter is to do heavy-ion collision experiments. Heavy-ion collision experiments consist in the collisions of heavy (i.e., large) nuclei, such as gold (at RHIC) or lead (at the CERN, LHC), at an ultra-relativistic center of mass energy $\sqrt{s}$. In this way, it is possible to create a large volume of matter at high energy density. The aim of heavy-ion collisions is to create and characterize a macroscopic state (in QCD scale where $\Lambda_{QCD} > 1\text{GeV}$) of deconfined quarks and gluons in local thermal equilibrium. Such state of matter can give new information regarding the QCD phase diagram (see Fig.1.1) and the QCD phase transition between confined and deconfined matter. This transition is supposed to have occurred when the matter in the early Universe turned from a plasma of quarks and gluons (QGP) into a gas of hadrons.

[1] The Λ_{QCD} corresponds to the scale where the perturbatively-defined coupling would diverge.

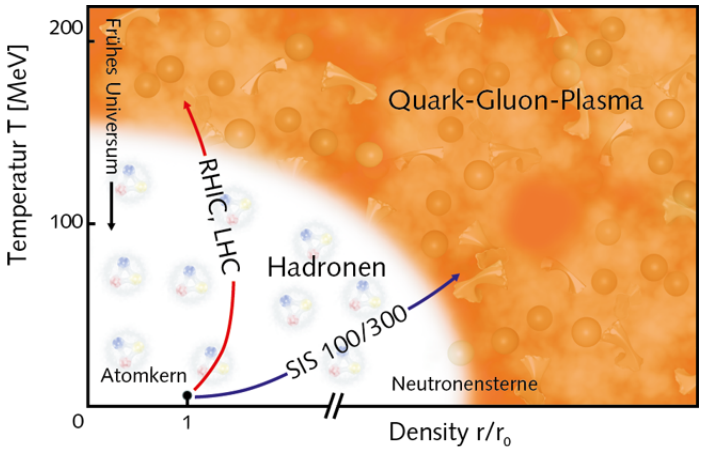

FIGURE 1.1: **Nuclear matter phase diagram.** The plot shows the temperature in units of one million electron-volt against the density in units of normal nuclear density ρ_0. At very high temperatures and densities, it is expected that the quarks and the gluons (usually locked up inside the nucleons) become freed from their confinement and move as free particles in a so-called quark-gluon plasma

At the moment, one of the main difficulties in the different models describing heavy-ion collisions regards the stage directly after the collision and before the quark-gluon plasma creation. This initial phase is remarkably complex since it concerns the real-time evolution of many quarks and gluons and, it should be expressed by a fully non-perturbative calculation. Currently, these non-perturbative calculations cannot be achieved in QCD. In this thesis, a particular approach called *gauge/gravity duality* it is used to explore the properties of this phase. Indeed, it has been proved that the duality is a useful tool for probing thermal and hydrodynamic properties of field theories at strong coupling.

The seed of the gauge/gravity duality can be found in the concept of *holography* that goes back to a 't Hooft's idea [1]; the holographic principle postulates a full equivalence between certain theories formulated in different number of dimensions. However, at the core of the gauge/gravity duality, there is a relation between string theory (in the bulk) and certain conformal QFTs in one lower dimension (on the boundary) making, therefore, the correspondence holographic.
In [2], 't Hooft noticed, with a very general argument, that strongly coupled $SU(N_c)$ gauge theories with coupling constant g may simplify when N_c is large. In virtue of the gauge/gravity duality, the large-N_c expansion of a non-Abelian gauge theory may have a classical gravitational description in one higher dimension. Thus, holography and more generally, the gauge/gravity duality, allows for doing a full strongly coupled calculation, although not in QCD itself. Indeed, QCD is not conformal (although the duality has been extended to some non-conformal

field theories) and it has $N_c = 3$. Quantum corrections in the bulk are only suppressed, in the duality, if $N_c >> 1$.
Since the goal of heavy-ion collisions is to study the properties of QCD at extreme temperature and energy density, any successful phenomenology should be based on QCD. However, heavy ion phenomenology requires strong coupling techniques both for thermodynamic quantities like the QCD equation of state, and also for dynamical quantities at $T \neq 0$ such as transport coefficients or quantities accessed by probes propagating through a plasma. For now, lattice-regularized QCD calculations provide well-controlled results for some of these bulk quantities. But, holography provides a tool for performing non-perturbative calculations of dynamical quantities. This method can lead to a better understanding of the initial stage of the heavy-ion collisions.

A particular example of gauge/gravity duality is the AdS/CFT (Anti-de-Sitter/ Conformal Field Theory) correspondence. In [3], J. Maldacena proposed the AdS/CFT correspondence while he was studying D-branes in string theory[2]. The AdS/CFT duality allows one to describe the strong coupling limit of a large class of non-Abelian quantum field theories in terms of *black holes* (BH) in AdS space. More precisely, this correspondence indicates that an evaporating BH in AdS background is dual to a unitary conformal field theory on the boundary of AdS [4]. Although the AdS/CFT correspondence was originally discovered by studying D-branes and BHs in string theory, the duality seems to have deep roots in certain more general aspects of gauge theories.

A short introduction to the AdS/CFT duality would start stating that there was a close link between string theory and QCD since the beginning. In fact, string theory was originally introduced to describe strong interactions already by the 60s (for a historical review see for example [5]). In that framework, gluons at low energies can be thought, because of the confinement property, like flux tubes (strings) that can close on themselves or connect a quark-antiquark pair. Strings nicely explained several features of the hadron spectrum: Different vibration modes of a string provided a way to describe many hadronic resonances of high spin discovered in the 1960s. However, such a low-energy effective description does not extend to high energies where the theory becomes weakly coupled. Then, in the mid-70s, it was realized that string theory is also a theory of gravity and it

[2] In the perturbative approach (see Eq. (1.4)), string theory is just a theory of extended one-dimensional objects, namely strings. Non-perturbatively, the theory also contains a variety of higher-dimensional solitonic objects. D-branes are a particularly relevant extended objects of this non-perturbative regime. Introducing a D-brane adds an entirely new sector to the theory of closed strings, consisting of open strings whose endpoints must satisfy the boundary condition that they lie on the D-brane.

was proposed as a fundamental theory. The already mentioned 't Hooft's large N_c expansion is an indication that a fundamental (as opposite to effective) string theory description may exist for any non-Abelian gauge theory. The basic idea of 't Hooft was to treat the number of colors N_c for a non-Abelian gauge theory as a parameter, take it to be large, and expand physical quantities in $1/N_c$. For example, consider a generic Euclidean partition function for a $U(N_c)$ gauge theory with gauge coupling g [6]:

$$Z = \int DA_\mu \, \exp\left(-\frac{1}{4g^2}\int d^4x \, \mathrm{Tr} F^2\right), \tag{1.1}$$

introducing the 't Hooft coupling

$$\lambda_{tH} \equiv g^2 N_c \tag{1.2}$$

one finds that the sum over the connected vacuum-to-vacuum amplitude, $\log Z$, can be expanded in $1/N_c$ as

$$\log Z = \sum_{h=0}^{\infty} N_c^{2-2h} f_h(\lambda_{tH}) = N_c^2 \, f_0(\lambda_{tH}) + f_1(\lambda_{tH}) + \frac{1}{N_c^2} f_2(\lambda_{tH}) + \ldots, \tag{1.3}$$

where $f_h(\lambda_{tH})$, with $h = 0, 1, \ldots$, are only functions of the 't Hooft coupling λ_{tH}. The large-N_c expansion (1.3), at a fixed λ_{tH}, turns out to be an expansion in terms of the topology of compact two-dimensional surfaces. Given that the topology of a two-dimensional compact orientable surface is classified by its number of holes, in the large-N_c expansion, one can suppose that Feynman diagrams are organized by their topologies. For example, the "planar diagrams"[3] are all proportional to N_c^2 and are included in $f_0(\lambda_{tH})$. Similarly, the generic functions $f_h(\lambda_{tH})$ include the contributions of all diagrams that can be drawn on a two dimensional surface with h holes without crossing any lines. The diagrams with $h = 0$ in (1.3) are the dominant ones in the large-N_c expansion. This is the reason to call the large-N_c limit, the planar limit of the gauge theory.

The large-N_c expansion goes in parallel with the perturbative expansion of a closed string theory. The worldsheet[4] of a closed string is a two dimensional compact surface and the string perturbative expansion is given by a sum over the topologies of two dimensional surfaces. For example the vacuum-to-vacuum amplitude A in

[3] Diagrams that can be drawn on a plane without crossing any lines

[4] The worldsheet is the surface area swept by the string as it propagates through spacetime.

a string theory can be written as

$$A = \sum_{h=0}^{\infty} g_s^{2h-2} F_h(\alpha') = \frac{1}{g_s^2} F_0(\alpha') + F_1(\alpha') + g_s^2 F_2(\alpha') + \dots \tag{1.4}$$

where g_s is the string coupling, $2\pi\alpha'$ is the inverse of the string tension, and $F_h(\alpha')$ is the contribution of two-dimensional surfaces with h holes. Topological considerations suggest the conjecture of identifying $f_0(\lambda_{tH})$ with $F_0(\alpha')$ for some closed string theory, if one recognize the string coupling constant to be

$$g_s \sim \frac{1}{N_c}, \tag{1.5}$$

but leaves open what the specific string theory is. The AdS/CFT duality is a particular realization of this connection for planar theories in the strongly coupled regime (i.e., in the limit $N_c, \lambda_{tH} \to \infty$). One can also include quarks in this general picture, or more generally matter in the fundamental representation. Feynman diagrams with quark loops can also be classified by using topologies of two dimensional surfaces with boundaries. Each boundary can be identified with a quark loop. On the string side, two-dimensional surfaces with boundaries describe the worldsheet of a string theory containing both closed and open strings, with boundaries corresponding to the worldlines of endpoints of the open string. *Therefore, it is possible to reformulate a non-Abelian gauge theory as a string theory.*

Now the question is why does one need to consider AdS background? It is a symmetry reason. A generic CFT in d dimensions with Poincare and scaling symmetry is also invariant under d special conformal transformation, which altogether form the $d-$dimensional conformal group $SO(2, d)$ that is also the isometry group[5] of a $(d+1)$ $-$dimensional AdS spacetime. Thus one expects that a CFT should have a string theory description in AdS spacetime.

1.1 Black Holes

As stated in the previous paragraph, a fundamental ingredient of the gauge/gravity correspondence is the black hole. Black holes are solutions of the field equations of classical General Relativity (GR) that encode aspects of the physics of the final stage of the gravitational collapse of matter. GR is the theory that expands the concept of Minkowski spacetime of special relativity to a more general spacetime

[5] It is the set of the spacetime coordinate transformations that leave the metric invariant.

that under the effect of gravity can be curved. This new geometric object is called Lorentzian manifold, and the gravitational field is its metric $g_{\mu\nu}$. The curvature is related to the space-time distribution of the energy-momentum tensor $T_{\mu\nu}$ of the matter content. The Einstein's field equations give the connection between the matter distribution and the curvature of the space-time

$$G_{\mu\nu} = R_{\mu\nu} - \frac{1}{2} g_{\mu\nu} R = \frac{8\pi G_N}{4} T_{\mu\nu} \tag{1.6}$$

where $R_{\mu\nu}$ is the Ricci curvature tensor, R the Ricci scalar, $g_{\mu\nu}$ is the metric tensor and G_N is the Newton constant. GR can be intended as a purely geometrical theory: Space-time is curved by its energy content, and test particles move along geodesics. This point of view makes GR a theory radically different from the theories that describe all the other known interactions, i.e., special relativistic field theories that after quantization, explain the interaction between two bodies through the exchange of quanta of the field theory.

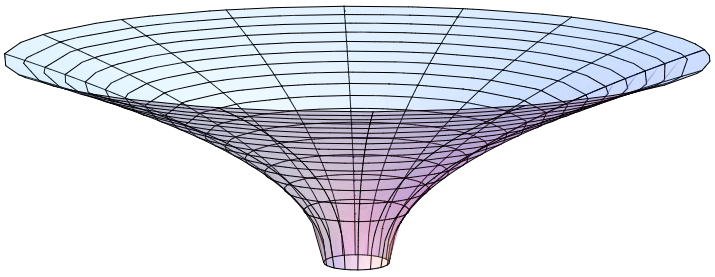

FIGURE 1.2: **Representation of black hole geometry.** The surface represents the outer region of the black hole at fixed time and shows its spatial curvature. In particular, this is the isometric embedding of the spatial Schwarzschild The foliation covers the entire space in the exterior region, and terminates with the final slice on the horizon.

1.1.1 Black Hole in Asymptotically Flat Spacetime

The Schwarzschild black hole (usually referred only as BH) was the first exact solution of the vacuum ($T_{\mu\nu} = 0$) Einstein's equations (1.6). In four space-time dimensions[6] the BH metric takes the form

$$ds^2 = -f(r)\, dt^2 + f(r)^{-1}\, dr^2 + r^2 d\Omega^2 \tag{1.7}$$

where

$$f(r) = 1 - \frac{2G_N M}{r} \tag{1.8}$$

[6]The metric signature convention will be $(-,+,+,+)$

and the line element $d\Omega^2$ is the unit sphere metric $d\Omega^2 = d\theta^2 + \sin^2\theta\, d\phi^2$. The mass M of the BH plays the fundamental role of the total energy of the system (so $M = E$) and it is defined as a surface integral over the asymptotic behavior of the gravitational field[7]. The BH metric (1.7) describes the gravitational field created by a spherically symmetric, massive object as seen from far away (in the vacuum region) by a static observer. The Schwarzschild spacetime satisfies the vacuum Einstein's equations everywhere except at the singular point $r = 0$. At this point of the Schwarzschild solution, there is a *curvature singularity*. At $r = 2MG_N$ instead, the Schwarzschild metric (1.7) has only a coordinate singularity, i.e., it can be removed performing a change of coordinates. The interpretation of vacuum solutions of the Einstein's equations is a difficult point since the possible source is located by definition in a region in which the Einstein's equations are not solved (e.g., $r = 0$). Another important feature of the Schwarzschild solution is the existence of an *event horizon*. The event horizon is a light-like hypersurface that separates the "exterior" and the "interior" regions of a BH. The presence of an event horizon has the consequence that a classical free falling observer can never come back from inside the BH and cannot send any information outside. Several observational data support the existence of BHs in our universe. However, real astrophysical BHs are not supposed to be in complete isolation neither vacuum solutions but surrounded by some matter. Theoreticians frequently call such BHs surrounded by an environment as "dirty BHs" [7].

It is better to emphasize here that in the gauge/gravity duality the relevant spacetime is a higher-dimensional one compared to the non-gravitational system it describes (remember the holographic principle). That means that if the gauge theory is four dimensional (as considered in this thesis), then the BH in the dual gravitational theory will be five-dimensional. For this reason in Chap.2 and Chap.3, higher dimensional BHs are studied. However, before going to the description of higher dimensional BHs, more details about four dimensional BHs will be presented in the next subsections.

1.1.2 Black Hole Thermodynamics

An initial hint of the thermodynamic nature of BHs was the fact that for null energy conditions (satisfied by classical matter fields), $T_{\mu\nu}k^\mu k^\nu \geq 0$ for arbitrary null vector k^μ, the area of a BH horizon can only increase in any physical process. This argument brought the irreversibility characteristic of thermodynamic systems

[7] See App. A.2.1 for further details.

into the context of BH physics and motivated Bekenstein to associate to BHs a notion of entropy proportional to their area [8]. The complete realization that BHs could be considered as thermodynamic objects in the semi-classical regime came with the discovery of the BH radiation (the so-called Hawking radiation). The thermodynamic nature of BHs is a prediction of the combination of GR and QFT as a first approximation to a full quantum gravity theory (semi-classical approach). An asymptotic observer measures a radiation coming from the horizon with a temperature

$$T_H = \frac{\hbar \kappa_h}{2\,\pi} = \frac{1}{8\pi M} \tag{1.9}$$

where $\kappa_h = f'(r_+)/2$ is the BH's surface gravity and r_+ is the event horizon radius $f(r_+) = 0$. BHs also have an associated entropy. However, the precise expression of this entropy is a question that should be answered within the framework of a complete quantum gravity theory. Up to now, the semi-classical entropy associated to a stationary BH is

$$S = \frac{A}{4G_N\hbar} \tag{1.10}$$

where A is the area of the event horizon. In the Schwarzschild solution, a small positive fluctuation in temperature makes the BH radiate some mass away increasing the temperature and lowering the mass further until the hot BH evaporates completely. On the other side, a small negative fluctuation in temperature makes the BH absorb more radiation than it radiates, increasing its mass. In this way, the BH cools down, absorbs mass at a faster rate and can grow indefinitely. Therefore, even if it appears somewhat counter-intuitive, small BHs radiate faster than bigger BHs. The zeroth law of BH mechanics says that the surface gravity κ_h is constant over the event horizon of a stationary BH. The first law states that

$$dM = \frac{\kappa_h}{8\pi} dA \tag{1.11}$$

i.e., it relates the change in the area to the change in mass for an adiabatic transition between nearby stationary BH solutions.

1.1.3 Black Hole in a Box: The Schwarzschild-Anti-deSitter Solution

Accordingly to the semi-classical description presented in the previous section, a Schwarzschild BH is thermodynamically unstable because its specific heat is negative:

$$C^{-1} = \frac{\partial T_H}{\partial M} = -\frac{1}{8\pi M^2}. \tag{1.12}$$

To restore stability, it was considered the case of putting the BH in a box of finite volume and finite heat capacity. In [9], the authors found that the BH is in a stable thermodynamic equilibrium against radiation when the radiation energy of the box satisfies $E_{rad} < M/4$. Therefore, putting a BH in a box does give a thermodynamically stable solution. To have a more physical situation one should consider, however, not a box but a spacetime that is no longer asymptotically flat. This is done using the Anti-de Sitter spacetime [9]. The AdS space is a valid box because can be thought to have a potential wall as one approaches the asymptotic infinity, namely, the gravitational potential relative to the origin increases as one moves away from the origin. The AdS space is a solution of the Einstein's equations (1.6) with a negative cosmological constant Λ (or alternatively AdS radius b) defined in the following way:

$$G_{\mu\nu} = \Lambda g_{\mu\nu}, \quad \Lambda = -\frac{3}{b^2} < 0\,. \tag{1.13}$$

The line element of AdS is

$$ds^2 = -\left(1 - \frac{\Lambda}{3}r^2\right) dt^2 + \left(1 - \frac{\Lambda}{3}r^2\right)^{-1} dr^2 + r^2 d\Omega^2. \tag{1.14}$$

A BH in an asymptotically AdS space has positive specific heat at high temperature and therefore is thermodynamically stable. The metric of a BH in AdS background is

$$ds^2 = -\left(1 + \frac{r^2}{b^2} - \frac{2G_N\,M}{r}\right) dt^2 + \frac{dr^2}{\left(1 + \frac{r^2}{b^2} - \frac{2G_N\,M}{r}\right)} + r^2 d\Omega^2 \tag{1.15}$$

and approaches (1.14) as r goes to infinity.

1.1.4 Charged Black Hole

Another exact mathematical BH solution, which illustrates some features that will be substantial in the next chapters, is the charged Reissner-Nordstrom (RN) black hole. In contrast to a Schwarzschild BH, a charged black hole is no longer in the vacuum since the charge generates a nonzero electromagnetic field, which acts as a source of the energy-momentum tensor

$$T_{\mu\nu} = F_{\mu\rho}F^{\rho}_{\nu} - \frac{1}{4}g_{\mu\nu}F_{\rho\sigma}F^{\rho\sigma} \tag{1.16}$$

where $F_{\mu\nu}$ is the electromagnetic field strength tensor. Using the spherical symmetry, the Einstein's and Maxwell's equations lead to the RN solution, described by

$$ds^2 = -\triangle(r)\,dt^2 + \triangle^{-1}(r)\,dr^2 + r^2 d\Omega^2\,, \tag{1.17}$$

$$\triangle(r) = 1 - \frac{2\,G_N M}{r} + \frac{G_N Q^2}{r^2} \tag{1.18}$$

where M is again interpreted as the mass of the BH and Q is the total electric charge. The RN solution, as the Schwarzschild one, has a curvature singularity in $r = 0$ (this can be checked by computing the curvature invariant scalar $R_{\mu\nu\rho\sigma}R^{\mu\nu\rho\sigma}$). The horizon structure, however, is more complicated than in the Schwarzschild BH. In the RN case, there can be one, two or zero solutions to the horizon equation $\triangle(r) = 0$. When the two horizons coincide at a single radius $r_+ = r_- = G_N M$, the BH is known as the *extremal* RN BH. The extremal solution is often analyzed in quantum gravity (e.g., string theory).

In general, the RN law of BH thermodynamics takes a form similar to that of a Schwarzschild BH. Although, in this case, the first law (1.11) requires the addition of another term that considers the possible changes in the BH mass due to changes in the charge. For large values of the RN mass, the temperature diminishes when the mass grows, just as in the Schwarzschild BH but, for values of the mass comparable to the charge Q and close to the extreme limit, the temperature grows with the mass as in an ordinary thermodynamic system. Between these two regions, there is a maximum temperature (for constant charge). At the point at which the temperature reaches its maximum value, one has $\partial T/\partial M = 0$ and the specific heat (1.12) diverges. The interesting feature of the RN solution is that there is an endpoint of the Hawking evaporation (corresponding to $T = 0$). However, assuming that nothing special happens when the mass is such that $\partial T/\partial M = 0$, one would expect that the RN BH approaches the extremal limit in a very long-lasting (maybe eternal) process in which the BH loses mass and temperature at lower and lower rates. It has been conjectured that there could be a BH *remnant* storing all the information contained in the original BH that is not radiated away. On the other hand, it has also been argued that the thermodynamical description of RN breaks down when we approach the extreme limit[8]. This is a very important issue

[8] Close enough to the extreme limit, the emission of a single quantum with energy equal to the Hawking temperature would take the mass of the RN beyond the extreme limit. Then, the change in the spacetime metric caused by Hawking radiation would be very big and HawkingâĂŹs calculation in which back-reaction of the metric to the radiation is ignored becomes inconsistent.

because essentially these are the only BHs for which a statistical computation of the entropy based on string theory has been performed [10].

1.2 The Problem of the Black Hole Singularity

The discovery of the thermodynamic properties of BHs opened new exciting possibilities but also several questions. These questions are related, for example, to the information paradox or the unitarity of the theory. It would be important to know how does the information of the quantum state of infalling particles re-emerge in the outgoing BH radiation. Moreover, the S-matrix between the ingoing and outgoing particles scattered off the horizon should be unitary. These questions necessitate a full control of the quantum dynamics in regimes away from the semi-classical one. In particular, answer these questions requires the understanding of the dynamics near and across the curvature singularity even though it is hidden within the event horizon.

It is believed that singularities should be generically avoided in virtue of the quantum gravity effects occurring at the Planck scale. This line of reasoning is inspired by the case of the classical electrodynamics, where sources can generate field singularities which are avoided in quantum electrodynamics. A possible way of identifying the object that could be the source of the full Schwarzschild gravitational field is to proceed by analogy with the Maxwell case [11]. However, in the BH case, the situation is more complicated especially because the spacetime is not even defined in $r = 0$. Proceeding in a way similar to the Maxwell case, one could introduce a massive point-like particle as the source of the Schwarzschild field, namely an energy-momentum tensor with the only non-vanishing component $T_{00} \sim \delta^3(r)$. This massive point-particle would give rise to a time-like singularity along its world-line (since massive particles are described by time-like geodesics). Thus, this result is not correct because the Schwarzschild singularity should be space-like. Interestingly, in [12], a distributional energy-momentum tensor has been found to satisfy the equation of motion for the Schwarzschild BH. This energy-momentum tensor is different from zero at the origin and in components, reads

$$G(x) = 8\pi T(x) = -8\pi M \delta^3(x) \left(dt \otimes \partial_t + dr \otimes \partial_r - \frac{1}{2} d\theta \otimes \partial_\theta - \frac{1}{2} d\phi \otimes \partial_\phi \right) \tag{1.19}$$

providing the Ricci scalar $R = 8\pi M \delta^3(x)$. In this way, it is possible to describe the singularity mathematically as a distributional energy-momentum tensor. However, this mathematical formulation (1.19) does not solve the singularity problem that

should be instead finally solved by a complete theory of quantum gravity. A possibility to do a step forward is, for example, to consider a source that can also describe the quantum nature of the matter effectively. This will be explained in sections 1.3.1, 1.3.2.

1.3 Non-Local Theories

Up to now, one of the key ingredients in the field of quantum gravity research has been non-locality. Assuming an uncertainty relation between position measurements implies a non-local theory. String theory is another example of a non-local theory. Indeed, the fundamental objects of string theory are essentially extended along some characteristic distance $l_s = \sqrt{\alpha'}$, and they become local in a particular regime called the point-like limit (i.e., $l_s \to 0$).

1.3.1 Non-Commutative Spacetime and Minimal Length Parameter

In the past years, a possible spacetime quantization has been proposed based on the Heisenberg's corollary: "physical quantities are governed by non-commutative algebra" [13]. This spacetime quantization is given by the *non-commutative geometry approach*, and the quantum features are encoded into a non-vanishing coordinate commutator. The technical difficulty of dealing with coordinates that are not c-numbers[9] but "operators" is usually avoided by using ordinary, commuting coordinates while shifting non-commutativity in a new multiplication rule, the so-called $*$-product between functions. The approach is the following: one should take standard commutative QFT results and substitute ordinary function multiplication by $*$-product multiplication. However, this prescription leaves quadratic terms in the action unaffected, as the explicit form of the $*$-product leads to surface terms only. Thus, the free dynamics encoded in kinetic terms and Green functions remains the same as in the commutative case. The presence of a non-commutative product becomes relevant only when more than two field variables couple together. The $*$-product is a non-local operation that gives rise to non-planar contributions to Feynman graphs at any perturbative order. These non-planar graphs introduce a problematic mixing of ultraviolet (UV) and infrared (IR) divergences. So far there has been no solution to this problem, and it has been accepted as an

[9] The term c-number is an abbreviation for classical number. This is an old nomenclature used by Paul Dirac, which refers to commuting real and complex numbers. Usually, this terminology is used in quantum mechanics to distinguish from operators that are defined as q-numbers or quantum numbers.

unavoidable consequence of non-commutativity. Anyway, this is only one of the technical problems which include also the possible breaking of Lorentz invariance and violation of unitarity.

An alternative approach to non-commutative geometry is based on the use of *coherent states* of the quantum position operator $\mathbf{x}^\mu$ satisfying $[\mathbf{x}^\mu, \mathbf{x}^\nu] \neq 0$ (see [14, 15, 16]). The idea is that the non-vanishing commutator prevents the existence of a common basis in coordinate representation. The best that one can do then is to define a mean value between appropriately chosen states, i.e. coherent states. The coherent states are minimum uncertainty states, and the mean values are the closest one can get to the classical commuting coordinates. In the coherent state approach, there are no UV divergences from which to extract anomalies and there is no $*$-product at all. The possibility of using a minimal length is explored in this thesis from the general relativity point of view (see Chap. 2 and Chap. 4).

1.3.2 Regular Black Holes

Regular black holes (RBH) are a family of BH solutions of the Einstein's equations which incorporate the effects of the Plank length in the short distance/high energy regime of the gravitational field. The derivation of the line element of these solutions is based on the possibility of implementing an effective minimal length directly in the classical GR. In this way, instead of the formulation of the full theory of quantum gravity, one can consider an effective theory that encodes quantum fluctuations. It has been shown in [17] that the effects of the quantum fluctuations of the manifold can be modeled by a non-standard form of the energy-momentum tensor while keeping unchanged the Einstein tensor $G_{\mu\nu}$ in gravity field equations (1.6). In this approach, for all RBHs, the curvature singularity at the origin is smeared out, and replaced by a regular de Sitter core (repulsive pressure). However, the hidden cost of this procedure is that the de Sitter core can only be attained in a non-classical gravity framework because of the energy condition violations at the origin.
An important feature of these RBHs concerns an "improved" thermodynamics. Indeed, even for neutral RBH, the Hawking temperature has a maximum and, after that, a cooling down phase, with positive heat capacity, toward a zero temperature remnant configuration (see Fig. 1.3). In the semi-classical description, there are limits to the validity of the approximation during the terminal phase of the evaporation (see footnote 8). In this scenario instead, the back-reaction should be suppressed giving the description of the final state of an RBH: a remnant.

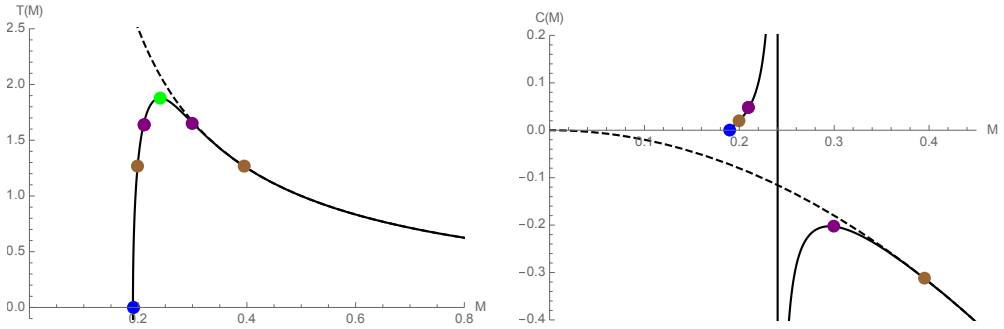

FIGURE 1.3: **Temperature and heat capacity for the 4d regular black hole.** On the left, we have the $4d$-regular black temperature T and on the right, its heat capacity C. In both plots, solid lines represents the behaviour for the regular black hole with $\theta = 0.1$ while dashed lines are the classical results. $C < 0$ is the unstable thermodynamic phase while $C > 0$, the positive heat capacity phase corresponding to the cool down phase. Blue dots represents the extremal BH; purple and brown dots are two values of the mass that have the same temperature; the green dot is the temperature maximum where the heat capacity diverges.

Before illustrating in the next chapter the line element of this RBH and other sophisticated geometrical objects, one needs to understand all the physical objects that are usually considered to be point-like and how to change them. We can note that a way to approach this issue is to estimate the mean position of an object by averaging coordinate operators on suitable coordinate *coherent states*. As a result, one finds that the mean position of a point-like object in this kind of manifold is no longer described by a Dirac delta function as in (1.19) but by a Gaussian distribution

$$f_\theta(\vec{x}) = \frac{1}{(4\pi\theta^2)^{n/2}} \exp\left(-\frac{|\vec{x}|^2}{4\theta^2}\right) \tag{1.20}$$

where n is the (space) manifold dimension and θ is the minimal length implemented through the non-commutative relation between coordinate operators. Field equations in the presence of this background can be obtained by substituting the conventional point-like source term with a Gaussian distribution while keeping formally unchanged differential operators [18]. For a static, spherically symmetric, diffused, gravitational source of mass M, one gets a Gaussian profile for the T_0^0 component of the energy momentum tensor

$$T_0^0 = -\rho_\theta(r) = -\frac{M}{(4\pi\theta^2)^{n/2}} \exp\left(-\frac{r^2}{4\theta^2}\right) \tag{1.21}$$

then, two components of the energy-momentum tensor are already determined $T_0^0 = T_r^r = -\rho_\theta(r)$ from the Schwarzschild-like condition $g_{00} = g_{11}^{-1}$, while the remaining $(n-1)$ components, which are identical because of the condition of

spherical symmetry, can be fixed using the covariant conservation law:

$$\nabla_\mu T^{\mu\nu} = 0. \tag{1.22}$$

In this way, the energy-momentum tensor is completely specified by

$$T^\mu_\nu = \text{Diag}\left(-\rho_\theta\left(r\right), p_r\left(r\right), p_\perp\left(r\right), \ldots, p_\perp\left(r\right)\right). \tag{1.23}$$

One should notice here that there are non-vanishing pressure terms with $p_r \neq p_\perp$ and that the geometry is effectively represented as a fluid diffused around the origin. From the conservation law Eq. (1.22), one then finds

$$T^i_i = -\rho_\theta - \frac{r}{d-1}\partial_r \rho_\theta \tag{1.24}$$

for all $i = 1, \ldots, n-1$ (without summation). Using all the properties, one can finally write the resulting Einstein's equations in the presence of a source term that encodes minimal length smearing effects

$$R^\mu_\nu = 8\pi G_N T^\mu_\nu - \frac{8\pi G_N}{n-1}\delta^\mu_\nu T\,, \tag{1.25}$$

where T is the trace of the energy-momentum tensor.
Summarizing, we have seen that there exists a solution of the Einstein's equations given by a particular ansatz that models a fluid with a Gaussian distribution from an energy density. Eventually, one chooses $p_r = -\rho_\theta$ and solves the conservation law for all the other components. Then, because it looks similar to the cosmological constant term in the Einstein's equations around the center, one gets a match to a de Sitter core. Thus, an important question would be: what is the global structure of this spacetime? The global structure is very similar to RN black hole but *without* the timelike singularity. This solution of the Einstein's equations will be one of the pillars of this thesis. Investigation about the phase structure of a RBH in AdS background are presented in Chap. 2 and Chap. 3 while the possible applications to AdS/CFT will be shown in Chap.4.

1.3.3 Lovelock Gravity

In the context of quantum gravity corrections to Einstein's equations, another approach is possible: Higher curvature corrections can be included in the GR theory. Higher-derivative theories have been a subject of long-standing interest. Indeed, these kind of corrections arise, for example, in the context of string theory as next

to leading order corrections in the low energy effective action. Or, they are motivated by the study of higher dimensional spacetimes.
Among all the higher derivative theories, Lovelock gravity theories [19] are extremely used, in large part because they admit second order differential equations for the metric functions and also because they represent a natural generalization of the standard GR to dimensions higher than four. These are the reasons why theories of gravity that include higher derivative curvature terms have received a lot of attention in the framework of BH thermodynamics (see for example [20]) and AdS/CFT. In particular, in the field of BH thermodynamics, higher derivative corrections are expected to give some insights into quantum gravity since the thermodynamic properties of BHs are essentially a quantum feature of gravity (see [21] for a review on BH in higher curvature theories of gravity). On the other hand, it is possible through the thermodynamics of BHs in AdS background to study the phase structure of a certain field theory via the AdS/CFT correspondence. Due to the AdS/CFT correspondence, some higher derivative curvature terms can be regarded as large N_c-corrections in the expansion of the dual field theory. More discussion about higher curvature gravity can be found in Chap. 3. The relevance of the Lovelock theory in the context of AdS/CFT will be discussed in Chap. 4

1.4 QCD and AdS/CFT

In the past twenty years, the gauge/gravity duality not only has provided new insights into the BH physics and quantum gravity but also has led to a new paradigm for probing strongly coupled gauge theories to which it is sometimes difficult to apply standard methods. An interesting question is if gauge/gravity duality may be applied to strongly coupled gauge theories such as QCD.

1.4.1 The Standard Model of Particle Physics

The Standard Model (SM) of particle physics describes elementary particles and their interactions via a quantum gauge field theory with symmetry group $U(1)_Y \times SU(2)_W \times SU(3)$. In the SM, fermion fields describe the matter particles and a complex scalar field spontaneously breaks the electroweak group $U(1)_Y \times SU(2)_W$ to its subgroup $U(1)_{EM}$, which is responsible for electromagnetism. The remaining unbroken $SU(3)$ group is the gauge group of the QCD and describes the strong interactions of colored quarks and gluons (the quanta of the non-Abelian

gauge field). Differently from photon in QED with Abelian gauge group $U(1)$, in non-Abelian theories, the gluons carry charge and self-interact. Neither quarks nor gluons are observed as free particles. This is because at low energies, non-Abelian theories display the property of confinement while in the UV the theory is asymptotically free.

Initially, the fermions are massless so they have well-defined chirality. Then introducing the Higgs vacuum expectation value, they acquire mass. This allows for the $SU(2)$ part of the electroweak of the gauge group to act only on the left-handed components. All the left-handed fermions are $SU(2)$ doublets and all the right handed are singlets. All the quarks are in the $SU(3)$ fundamental representation (anti-fundamental for the anti-quarks) that confine them in the hadrons. Hadrons are (color-neutral) color-singlet combinations of quarks, anti-quarks, and gluons. The gauge bosons of the $SU(3)$ are the eight gluons. In the SM, the electroweak symmetry breaking (EWSB) mechanism allows to keep untouched the structure of the gauge interactions at high energy and generate the observed masses of the W and Z gauge bosons. The mass generation of the W and Z bosons happen using charged and neutral Goldstone bosons that manifest themselves as the longitudinal components of the gauge bosons. Because of the EWSB mechanism, three massless Goldstone bosons are generated. The Goldstone bosons are absorbed to give masses to the W and Z gauge bosons. Then, the remaining component of the complex doublet becomes a new fundamental scalar particle: the Higgs boson. Also all the fermions masses are a consequence of EWSB because the Higgs doublet is postulated to couple to the fermions through Yukawa interactions. The resulting theory is in good agreement with experimental tests, and its consistency has been confirmed by the detection of the Higgs boson at the LHC [22, 23]. However, the structure behind the discovered boson, e.g., the exact dynamics that triggers the Higgs vacuum expectation value (VEV) and the corresponding UV completion, is still unsolved [24]. To this aim, research on nuclear and quark matter at high baryon (quark) density is expected to say a lot about our empirical understanding of the origin of matter in the Universe.

1.4.2 Phase Transitions in Quantum Chromodynamics

One of the fundamental phase transitions of the matter is that between the hadron gas and the quark-gluon plasma (QGP), i.e., a transition from a confined to a deconfined phase. The detailed structure of the QCD phase diagram is still an open question. However, experiments at RHIC and LHC, suggest that the QGP

observed at high temperatures is a strongly coupled state of matter and it shows a collective behaviour. This also suggests that the QGP can be well described by an hydrodynamical description. The deconfinement phase transition can be represented in the plane of temperature versus baryon chemical potential (T, μ_B) in the conjectured phase diagram for QCD (see Fig.1.1). As said before, the detailed character of this QCD phase diagram is still not known, and current theoretical knowledge is restricted primarily to the $\mu_B = 0$ axis. Indeed, a common approximation in studying the physics of the quark-gluon plasma is to neglect the chemical potential μ_B for baryons[10]. At present, it is believed that the cross-over at $\mu_B = 0$ between confined and deconfined phases in QCD sharpens into a phase transition as μ_B becomes non-zero, with a critical point at finite μ_B and T [25]. However, the order of the phase transition is not clear.

The search for the dynamic properties (such as the shear viscosity) of the quark-gluon plasma via the gauge/gravity duality is one of the driving motivation for this thesis. This is also related to the search for a critical point in the phase diagram of QCD matter where the cross-over from hadron resonance gas to the quark-gluon plasma can turn into an actual phase transition.

1.4.3 Gauge/gravity Duality

Since the formulation of QCD, there has been the idea that the theory might simplify in the limit of a large number of colors N_c [2]. This idea has directed the research to relevant conceptual progress. Non-planar diagrams emerge from perturbative calculations in the large-N_c when the 't Hooft coupling $\lambda_{tH} = g^2 N_c$ is kept finite. However, calculations remained difficult to address even in the large-N_c limit until the formulation of the AdS/CFT duality (or in general, the gauge/gravity duality). The AdS/CFT correspondence provided a concrete realization of the holographic principle, the idea that quantum gravitating theories contain more information than needed, and can be described by a non-gravitational theory in fewer dimensions. The holographic principle has been principally motivates by the fact that the BH entropy scales as the surface area rather than the volume. If one considers a QFT in a d-dimensional spacetime, then the number of d.o.f. of a system is given by the entropy. In QFT the entropy of a spatial region R_{d-1}

[10] At least at mid-rapidity, this can be quantitatively justified based on the relative abundance of particle species.

should be proportional to its volume in $(d-1)$ dimensions:

$$S_{QFT} \propto \mathrm{Vol}\left(R_{d-1}\right). \tag{1.26}$$

On the gravity side, on the other hand, the theory lives in a $(d+1)$ dimensional spacetime. The fundamental point here is that in a gravitational theory, the entropy in a volume is bounded by the entropy of a BH that fits inside the volume. The entropy of this BH is proportional to the BH surface A, that is the Bekenstein-Hawking formula (1.10). Then according to (1.10), the gravitational entropy associated to a spatial region R_d in $(d+1)$ dimensional spacetime and bounded by a $(d-1)$ dimensional manifold scales as

$$S_{GR}\left(R_d\right) \propto \mathrm{Area}\left(R_{d-1}\right) \propto \mathrm{Vol}\left(R_{d-1}\right) \tag{1.27}$$

which is in agreement with the entropy in QFT given by (1.26). The AdS/CFT correspondence relies also significantly on the asymptotic properties of anti-de Sitter space. In AdS space, massive particles must stay at finite spatial values (the "bulk"), but massless trajectories can reach spatial infinity, called the "boundary". As a consequence, describing physics in an asymptotically AdS space requires more than initial conditions: it requires boundary conditions that fix the behavior of the various dynamical fields at infinity. The ideal case would be a formulation via string theory of a gravity dual for QCD. There are several proposal about how to model QCD using AdS/CFT. In this thesis, it is used the duality in a phenomenological bottom-up approach, i.e., the possibility to "engineer" gravity duals that do not originate directly from string theory. Generally, the duality map in these so-called "bottom-up" models[11], is not precisely known, but some features, such as symmetries and thermodynamics, can be built-in. The hope is of matching certain aspects of QCD as closely as possible and find how useful gauge/gravity calculations can be. Indeed, the macroscopic behaviour of strongly correlated systems at large distances and long timescales generically exhibits features that are independent of the details of the underlying, difficult to describe, microscopic description. This thesis examines a particular feature in the gauge-gravity duality dictionary. The entry is based on the following property: the quasi-normal spectra of asymptotically AdS_{n+1} (and more general backgrounds) correspond to poles of the retarded thermal correlators of dual n-dimensional strongly interacting quantum gauge theories. In particular, the lowest quasi-normal frequencies

[11] In contrast to "top-down" studies of AdS/CFT based on sting theory constructions.

of black branes[12] can be interpreted in the dual theory as dispersion relations of hydrodynamic excitations.

1.5 Outline

Motivated by gauge/gravity duality and particle physics, in this thesis some models describing relevant gravitational phenomena are investigated. These models have a repercussion in the nuclear matter description via AdS/CFT.
In Chapter 2, RBH phase transitions and Gauss-Bonnet BH thermodynamics are presented. The chapter is divided into two parts: the first part is a study of the thermodynamics of RBH in different ensembles while the second part is an extensive study of the charged Gauss-Bonnet black brane solution and it is based on Ref. [26]. In Chapter 3, a detailed study of 3rd-order Lovelock BH and RBH thermodynamics from an alternative point of view is proposed. This new approach occurred within a proposal regarding the interpretation of BH thermodynamic system: The idea is that the cosmological constant Λ that define the AdS spacetime has to be considered itself as a thermodynamical variable analog to the pressure in the first law of thermodynamics. This interpretation extends the phase space of thermodynamic parameters. Recently, the role of a dynamical cosmological constant has been analyzed in the AdS/CFT correspondence [27, 28, 29]. Since, in string theory, the cosmological constant is related to the number of branes in the bulk, then it can be connected to the number of colors N_c of the boundary gauge theory. The contents of Chapter 3 are from the following papers [30, 31, 32]. In Chapter 4, the shear viscosity over entropy density ratio is calculated for the field theory dual to Gauss-Bonnet and RBH theory. The models in exam are a regular black brane in asymptotically AdS background and a 2-nd order Lovelock black brane (i.e., Gauss-Bonnet theory). The content of this chapter is partially from the following paper [26].

[12] A black brane is a solution of the Einstein's equations that generalizes a BH solution in generic spatial dimensions, and it is also translationally symmetric.

References

[1] Gerard 't Hooft. "Dimensional reduction in quantum gravity". In: *Salamfest 1993: 0284-296*. 1993, pp. 0284–296. arXiv: gr-qc/9310026 [gr-qc].

[2] Gerard 't Hooft. "A Planar Diagram Theory for Strong Interactions". In: *Nucl. Phys.* B72 (1974), p. 461.

[3] Juan Martin Maldacena. "The Large N limit of superconformal field theories and supergravity". In: *Int.J.Theor.Phys.* 38 (1999), pp. 1113–1133. arXiv: hep-th/9711200 [hep-th].

[4] Edward Witten. "Anti-de Sitter space and holography". In: *Adv.Theor.Math.Phys.* 2 (1998), pp. 253–291. arXiv: hep-th/9802150 [hep-th].

[5] J. Polchinski. *String Theory: Volume 1, An Introduction to the Bosonic String*. Cambridge Monographs on Mathematical Physics. Cambridge University Press, 1998.

[6] Professor Jorge Casalderrey-Solana et al. *Gauge/String Duality, Hot QCD and Heavy Ion Collisions*. 1st ed. Cambridge University Press, Aug. 2014.

[7] Matt Visser. "Dirty black holes: Thermodynamics and horizon structure". In: *Phys.Rev.* D46 (1992), pp. 2445–2451. arXiv: hep-th/9203057 [hep-th].

[8] Jacob D. Bekenstein. "Black holes and entropy". In: *Phys. Rev.* D7 (1973), pp. 2333–2346.

[9] S.W. Hawking and Don N. Page. "Thermodynamics of Black Holes in anti-De Sitter Space". In: *Commun.Math.Phys.* 87 (1983), p. 577.

[10] Andrew Strominger and Cumrun Vafa. "Microscopic origin of the Bekenstein-Hawking entropy". In: *Phys. Lett.* B379 (1996), pp. 99–104. arXiv: hep-th/9601029 [hep-th].

[11] Tomás Ortín. *Gravity and Strings*. Cambridge University Press, 2004.

[12] Herbert Balasin and Herbert Nachbagauer. "The energy-momentum tensor of a black hole, or what curves the Schwarzschild geometry?" In: *Class.Quant.Grav.* 10 (1993), p. 2271. arXiv: gr-qc/9305009 [gr-qc].

[13] A. Connes. *Noncommutative Geometry*. Elsevier Science, 1995.

[14] Michele Maggiore. "A Generalized uncertainty principle in quantum gravity". In: *Phys. Lett.* B304 (1993), pp. 65–69. arXiv: hep-th/9301067 [hep-th].

[15] Achim Kempf, Gianpiero Mangano, and Robert B. Mann. "Hilbert space representation of the minimal length uncertainty relation". In: *Phys. Rev.* D52 (1995), pp. 1108–1118. arXiv: hep-th/9412167 [hep-th].

[16] A. M. Frassino and O. Panella. "The Casimir Effect in Minimal Length Theories Based on a Generalized Uncertainity Principle". In: *Phys. Rev.* D85 (2012), p. 045030. arXiv: 1112.2924 [hep-th].

[17] Piero Nicolini, Anais Smailagic, and Euro Spallucci. "Noncommutative geometry inspired Schwarzschild black hole". In: *Phys. Lett.* B632 (2006), pp. 547–551. arXiv: gr-qc/0510112 [gr-qc].

[18] Leonardo Modesto and Piero Nicolini. "Charged rotating noncommutative black holes". In: *Phys. Rev.* D82 (2010), p. 104035. arXiv: 1005.5605 [gr-qc].

[19] D. Lovelock. "The Einstein tensor and its generalizations". In: *J.Math.Phys.* 12 (1971), pp. 498–501.

[20] Rong-Gen Cai. "A Note on thermodynamics of black holes in Lovelock gravity". In: *Phys.Lett.* B582 (2004), pp. 237–242. arXiv: hep-th/0311240 [hep-th].

[21] Robert C. Myers. "Black holes in higher curvature gravity". In: (1998). arXiv: gr-qc/9811042 [gr-qc].

[22] Georges Aad et al. "Observation of a new particle in the search for the Standard Model Higgs boson with the ATLAS detector at the LHC". In: *Phys. Lett.* B716 (2012), pp. 1–29. arXiv: 1207.7214 [hep-ex].

[23] Serguei Chatrchyan et al. "Observation of a new boson at a mass of 125 GeV with the CMS experiment at the LHC". In: *Phys. Lett.* B716 (2012), pp. 30–61. arXiv: 1207.7235 [hep-ex].

[24] K. Olive et al. "Review of Particle Physics". In: *Chin. Phys.* C38 (2014), p. 090001.

[25] Roy A. Lacey. "Indications for a Critical End Point in the Phase Diagram for Hot and Dense Nuclear Matter". In: *Phys. Rev. Lett.* 114.14 (2015), p. 142301. arXiv: 1411.7931 [nucl-ex].

[26] Mariano Cadoni, Antonia M. Frassino, and Matteo Tuveri. "On the universality of thermodynamics and η/s ratio for the charged Lovelock black branes". In: (2016). arXiv: 1602.05593 [hep-th].

[27] Clifford V. Johnson. "Holographic Heat Engines". In: *Class.Quant.Grav.* 31 (2014), p. 205002. arXiv: 1404.5982 [hep-th].

[28] Brian P. Dolan. "Bose condensation and branes". In: *JHEP* 1410 (2014), p. 179. arXiv: 1406.7267 [hep-th].

[29] Andreas Karch and Brandon Robinson. "Holographic Black Hole Chemistry". In: *JHEP* 12 (2015), p. 073. arXiv: 1510.02472 [hep-th].

[30] Antonia M. Frassino, Robert B. Mann, and Jonas R. Mureika. "Lower-Dimensional Black Hole Chemistry". In: *Phys. Rev.* D92.12 (2015), p. 124069. arXiv: 1509.05481 [gr-qc].

[31] Antonia M. Frassino et al. "Multiple Reentrant Phase Transitions and Triple Points in Lovelock Thermodynamics". In: *JHEP* 09 (2014), p. 080. arXiv: 1406.7015 [hep-th].

[32] Antonia Micol Frassino. "Phase transitions of regular Schwarzschild-Anti-deSitter black holes". In: *Springer Proc. Phys.* 170 (2016), pp. 241–247. arXiv: 1502.01305 [hep-th].

Chapter 2

Black Hole and Black Brane Thermodynamics and Phase Transitions

In the previous chapter, the Schwarzschild solution of the vacuum Einstein's equations has been introduced and related to the general concept of BH. Then, in the context of effective theories for a spacetime with a minimal length, it has been presented the regular black hole solution (RBH), i.e., a solution of the Einstein equations where the static interior of the BH is full of exotic matter. This matter mimics a repulsive pressure that encodes a quantum gravity effect that opposes to the gravitational collapse. In the case of the RBH, the matter cannot collapse into the singularity because of the presence the minimal length imposes a maximal resolution.

In this chapter, a thermodynamic analysis of the RBH in AdS-background is presented. Also, the charged Gauss-Bonnet black brane solution is investigated as a preliminary study to Chap. 4. The RBHs share common features with the charged, spherically symmetric so-called RN black holes presented in sec. 1.1.4. The RN solution has very interesting features. In particular, it has an *extreme limit* with a regular horizon and Hawking temperature equal to zero. This limit is approached with positive specific heat, as in the standard thermodynamic systems. Interestingly, the RBH solution shares with the RN solution the same kind of features.

In the whole chapter, the discussion about RBH will be for arbitrary space dimensions $n \geq 3$. Then, all the numerical calculations will use $n = 3$ or $n = 4$

dimensional spaces. The former case describes the usual four-dimensional spacetime while the latter will represent an RBH in AdS_5 background and hence it will be dual, via the gauge/gravity duality, to a four-dimensional field theory on the boundary. For the same reason, the analysis of the Gauss-Bonnet solution will be mainly in five spacetime dimensions. The aim of this chapter is to determine the thermal phase structure of the RBH (see Sec. 2.4) and of the charged Gauss-Bonnet black brane (see Sec. 2.6). We will show how to connect the thermodynamics to the properties of the dual field theory in the Chap. 4.

2.1 The Euclidean Path Integral Approach

A possible way to relate thermal properties to the geometry of the spacetime is via the Feynman path-integral approach. Gibbons and Hawking proposed this approach in the '70s in order to evaluate the black hole partition function. However, the main difficulty is that, in the context of standard thermodynamics, black holes have negative heat capacity and are unstable. While, in statistical mechanics, the partition function describes only stable systems with positive heat capacity. The key point for the path integral approach to gravity is the use of the Euclidean action for a static BH.
The idea behind the path integral formulation is to calculate the thermal partition function of quantum gravity through the path integral of a Euclidean version of the Einstein-Hilbert action I_{EH} in this way

$$\mathcal{Z} = \int \mathcal{D}g\, e^{-\frac{I_{EH}}{\hbar}}, \tag{2.1}$$

where one has to sum over all metrics g with period $\beta = \hbar c/T$ (β has dimension of length and T has dimension of energy).
In general the total Einstein-Hilbert action in $n = 3$ is defined as

$$I_{EH} = \frac{c^3}{16\pi G_N} \int_{\mathcal{M}} d^4x\, \sqrt{g}\, R + \frac{c^3}{8\pi G_N} \int_{\partial\mathcal{M}} d^3x\, \sqrt{h}\, (K - K_0) \tag{2.2}$$

where the second term is a boundary term, or York-Gibbons-Hawking term (see A.1). The term K_0 is calculated by substituting the vacuum metric into the expression for the trace of the extrinsic curvature of the boundary K. The same

action in generic dimensions reads

$$I_{EH} = \frac{1}{\chi^2} \int_{\mathcal{M}} d^{n+1}x \, \sqrt{g} \, R + (-1)^d \, \frac{2}{\chi^2} \int_{\partial \mathcal{M}} d^n \Sigma \, K \, . \tag{2.3}$$

As usual, the dominant contribution to the path integral is given by the semi-classical saddle-point approximation $\mathcal{Z} \simeq e^{-I_{EH}(on-shell)}$ and the classical solution used to calculate the on-shell Euclidean action is for example the Wick rotated Schwarzschild's solution. After analytically continue the BH metric to Euclidean spacetime by rotating time as $t \to i\tau$ the manifold extend only from $r = \infty$ down to $r = r_+$. For this reason one has to integrate the action only in this range: The Euclidean BH manifold, contains only the region outside the outer horizon and is a smooth manifold with a single boundary at $r = \infty$. Moreover, in a thermal background, the Euclidean time τ is compact with period $\beta \equiv 1/T$ where T is the Hawking temperature. Using the Euclidean time transformation, one can find that at the horizon r_+, there is generically a conical singularity. One can calculate the length of a circle $\tau \to \beta + \tau$ and the thermodynamic is associated with a smooth Euclidean geometry where τ can be viewed as an angle in polar coordinates. Therefore, in this way, the Hawking temperature is obtained in terms of geometrical data. Like in other thermodynamic systems, one can define the standard thermodynamic potentials related to the action. A significant potential is the Gibbs free energy $F = M - TS \equiv I_E/\beta$.

2.2 Black Hole Thermodynamics

The Hawking's discovery was that, when the quantum effects produced by the existence of an event horizon are taken into account, BHs radiate as if they where black bodies. This black body radiation is called Hawking radiation and it was calculated in the framework of quantum field theory in curved spacetime. The electromagnetic radiation is produced as if emitted by a black body with a temperature inversely proportional to the mass of the black hole. Because of the Hawking radiation, the BH reduces its the mass and energy (givin rise to the so-called "black hole evaporation"). Black holes that lose more mass than they gain would emit more than they absorb and thereby lose mass and expected to shrink.

Using the Einstein-Hilbert action for the BH solution, it is possible to have a description of the system as a thermodynamic system with temperature and entropy,

respectively given by the following formulae:

$$T = \frac{\hbar \kappa_h}{2\pi c}, \quad S = \frac{A c^3}{4\hbar G_N} \tag{2.4}$$

where κ_h is the surface gravity, and A is the area of the event horizon. In particular, the Schwarzschild's BH has

$$T = \frac{\hbar c^3}{8\pi G_N M}, \quad S = \frac{4\pi G_N M^2}{\hbar c}. \tag{2.5}$$

Using the thermodynamic analogy, the first law of BH and the Smarr's formula [1] (that is an integral version of the first law obtained by applying Euler's theorem on homogeneous functions) for the Schwarzschild's BH read:

$$dM\, c^2 = T\, dS \qquad M c^2 = 2T\, S. \tag{2.6}$$

Considering all this, the thermodynamics of BHs has several characteristics:

- The temperature (2.5) of the Schwarzschild's BH decreases as the mass (the energy) increases, i.e., the BH has a negative specific heat

$$C^{-1} = \frac{\partial T}{\partial M} = -\frac{\hbar c^3}{8\pi G_N M^2} < 0 \tag{2.7}$$

  and, unlike ordinary thermodynamical systems, becomes colder when it absorbs matter instead of when it radiates. Thus, a BH cannot be in equilibrium with an infinite heat reservoir because it would absorb the energy and grow without bounds.

- The temperature (2.5) grows when the mass decreases (in the evaporation for example) and diverges near zero mass. At the same time the specific heat becomes bigger in absolute value and stays negative. So, in principle the final stage of the Hawking evaporation of a BH could be an explosion with consequent BH disappearance. However in the final state the horizon radius becomes of the order of the BH's Compton wavelength[1] and quantum-gravity effects should become important and should determine the BH's fate.

- If a BH can radiate, its entropy can diminish. This looks against the second law but the total entropy (BH plus radiation) never decreases.

[1] This happen when $M \sim M_{plank} = \sqrt{\hbar c/G}$ and implies that the horizon radius $r_+ \sim L_P = \sqrt{\hbar G/c^3}$

- The Hawking radiation seems to carry information about BH only related to M, J and Q. Why is that so? This is indeed an important difference between the black hole radiation and the usual thermal radiation emitted from a black body. While the former satisfies exactly the Planck's law of black body radiation, the latter is statistical in nature, and only its average satisfies the Planck's law. Thus thermal radiation contains information about the body that emitted it, while Hawking radiation seems to contain no such information, and depends only on the mass, angular momentum, and charge of the black hole (this is also named as the "no-hair theorem") and leads to the black hole information paradox.
  Maybe in a full quantum computation of the gravitational collapse of matter described by the theory of quantum gravity, the radiation contains more information and the whole process could be unitary. Or, on the other hand, maybe no information is carried by Hawking radiation and the BH evaporates indefinitely[2]. Or there is still another way out: the information is not carried out of the BH by Hawking radiation but the evaporation process stops at some point, leaving a BH *remnant* storing that information.
  Usually in models based on string theory BHs are standard quantum mechanical systems and information is always recovered (and never lost). The regularized solution based on the gaussian distribution, as will be show in Sec. 2.4, supports the idea of a *remnant* as a final state of the evaporation process.

2.3 Hawking Page Transition

In 1983, Hawking and Page discovered, by using path integral methods, that an AdS-BH has negative free energy (relatively to AdS spacetime) at high temperature and exhibits a *first-order phase transition* [2]. This phase transition is the so-called *Hawking-Page (HP) transition*: A phase transition between thermal AdS and BH in four spacetime dimensions. How can this happen? As said in subsec.1.1.3 an asymptotically AdS space acts as a confining box. As a result the thermal radiation remains confined close to the BH and cannot escape to infinity[3]. Therefore, one can always consider a canonical ensemble description for BHs at any given temperature T.

[2] In this case, the information about the initial state is completely lost and the theory of quantum gravity is non-unitary, in contrast to all the other physical theory.

[3] Although zero rest mass particles can escape to infinity but the incoming and outgoing fluxes at infinity are equal.

If the temperature of the thermal radiation is below a particular minimum ($T < T_{min}$), then the only possible equilibrium is the thermal radiation without BHs. On the other hand, if the temperature is higher than this minimum $T > T_{min}$ then there are two possible BHs that could be in equilibrium with the thermal radiation. According to the findings of Hawking and Page, there exists a critical mass value M_0 for BHs in AdS space. If the mass of the BH is below this critical value ($M < M_0$) then it appears with a negative heat capacity which means that the lower mass BH is unstable. Therefore, it may either decay ultimately to thermal radiation or to a larger mass BH ($M > M_0$) with a positive heat capacity which corresponds to a locally stable phase. In the second case the heat capacity changes from negative infinity to positive infinity at the minimum temperature T_{min}. Also, there is a change in the dominance from thermal AdS to BHs at some temperature T_{HP} which corresponds to a change in sign in the free energy of the system (see Fig. 2.2). Since the discovery of such a phenomenon in AdS-BHs, some investigations have been made regarding various thermodynamic aspects of AdS-BHs, for example in higher dimensions. In the following the thermodynamical aspects of AdS-RBHs are presented and compared to the HP behaviour (see Sec. 2.5.1).

2.3.1 Details about the Hawking-Page Transition

Let us consider the following solution:

$$ds^2 = -f(r)dt^2 + \frac{1}{f(r)}dr^2 + r^2 d\Omega^2 \tag{2.8}$$

in four dimensional spacetime, beside the AdS solution

$$f(r) = 1 + \frac{r^2}{b^2}\,, \tag{2.9}$$

another vacuum solution is

$$f(r) = 1 + \frac{r^2}{b^2} - \frac{2M}{r} \tag{2.10}$$

for each $M > 0$. This is the black hole solution known as the Schwarzschild anti-de Sitter (SAdS) solution. The SAdS solution has mass

$$M = \frac{r_+}{2}\left(1 + \frac{r_+^2}{b^2}\right) \tag{2.11}$$

and Hawking temperature

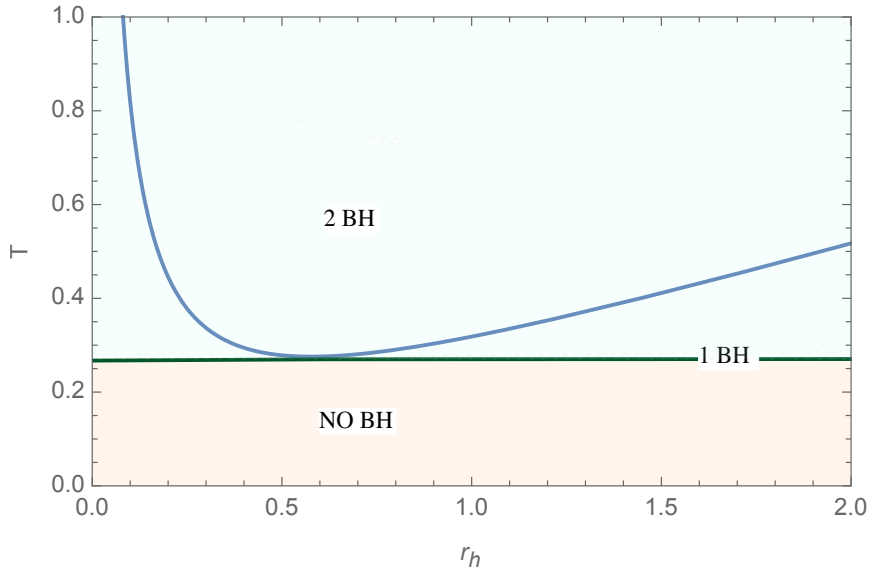

FIGURE 2.1: **AdS-BH Temperature vs r_+.** Temperature as function of horizon radius where b is fixed to one

$$T_H = \frac{1}{4\pi r_+}\left(1 + \frac{3r_+^2}{b^2}\right) \tag{2.12}$$

that has a minimum when

$$\frac{\partial T_H}{\partial r_+} = \frac{3}{4\pi b^2} - \frac{1}{4\pi r_{min}^2} = 0 \rightarrow r_{min} = \frac{b}{\sqrt{3}} \tag{2.13}$$

from which follow that

$$T_{min} = \frac{\sqrt{3}}{2\pi b}. \tag{2.14}$$

So it follow that (see for Fig. 2.1):

- For $T < T_{min}$, the only possible phase is the pure thermal AdS solution.
- For $T = T_{min}$, the possible phases are pure thermal AdS and one black hole Schwarzschild AdS solution.
- For $T > T_{min}$, the possible phases are pure thermal AdS and two black holes Schwarzschild AdS solutions.

To see where the phase transition occurs, we calculate the (Helmholtz) free energy difference between the phases with the same asymptotic physical temperature. In this way we see which phase is thermodynamically favorable. The free energy difference in the zero-loop approximation is given by the difference between the

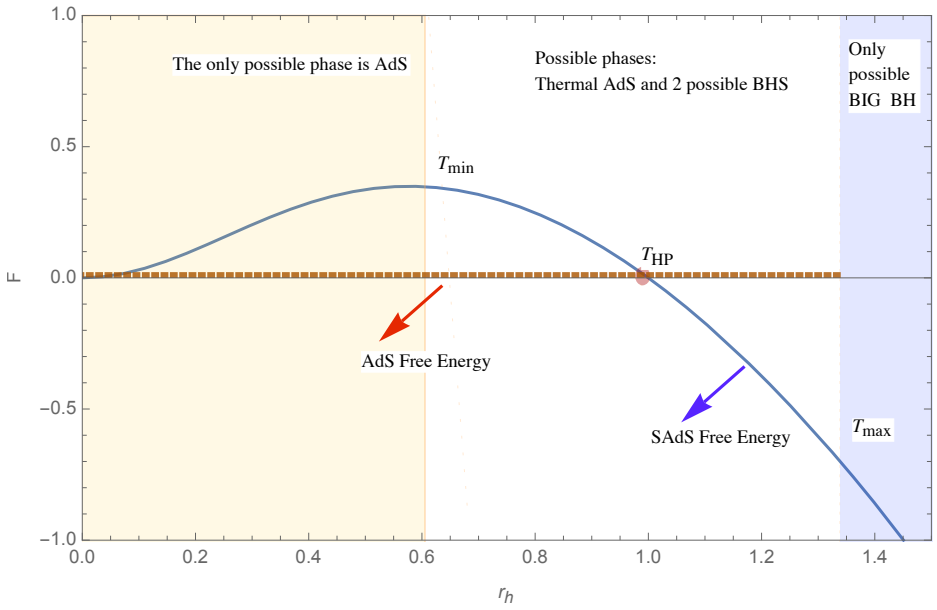

FIGURE 2.2: **Hawking-Page Free energy** as function of the horizon radius where b is fixed to one.

on-shell actions for SAdS and AdS

$$\Delta F = I_{SAdS} - I_{AdS} = M - T_H S = \frac{r_+}{2}\left(1 - \frac{r_+^2}{b^2}\right) \tag{2.15}$$

and, we have that $\Delta F < 0$ iff $r_+ > b$. So when $r_+ = b$ the temperature becomes

$$T_{HP} = \frac{1}{4\pi b}\left(1 + \frac{3b^2}{b^2}\right) = \frac{1}{\pi b} \tag{2.16}$$

at this temperature $T = T_{HP}$ the Hawking-Page phase transition occurs. Therefore, we can summarize:

- For $T > T_{HP}$, the SAdS solution is the solution with the lowest free energy, so the Schwarzschild black hole is preferred over thermal radiation.
- For $T = T_{HP}$, the (first-order) Hawking-Page phase transition takes place.
- For $T_{min} < T < T_{HP}$, thermal radiation is the energetically favorable solution, even though a stable black hole can exist. Thus for these temperatures the black hole is a metastable state.
- For $T < T_{min}$, thermal radiation is the only possible solution.

Including the gravitational effect of thermal radiation, one can show that at some very high temperature T_{max} the radiation would become unstable and collapse to a black hole. Hence the pure AdS solution is only stable at temperatures $T < T_{max}$.

In order to see this, one can suppose to have a perfect fluid given by the cosmological constant. The energy of the thermal radiation then can be estimated to be

$$< E > \simeq \frac{\pi}{30} g T^4 b^3 \tag{2.17}$$

where g is a constant and T is the thermal AdS temperature. When $< E >$ is larger then the BH mass, one has

$$\frac{\pi}{30} g T^4 b^3 \geq \frac{r_+}{2}\left(1 + \frac{r_+^2}{b^2}\right) \tag{2.18}$$

this inequality will be verified when the horizon radius is $r_+ \geq b$ and in case of equality we have

$$\frac{\pi}{30} g T_{max}^4 b^3 = \frac{b}{2}\left(1 + \frac{b^2}{b^2}\right) \tag{2.19}$$

and solving with respect to T_{max} one finds

$$T_{max} \approx \frac{1}{g^{1/4}\sqrt{b}} > T_{HP} = \frac{1}{\pi b}\,. \tag{2.20}$$

Now we can continue the phase diagram (see Fig. 2.3):

- For $T_{HP} < T < T_{max}$ the stable Schwarzschild black hole is the energetically favorable solution and pure thermal radiation is a metastable state.
- For $T > T_{max}$, pure thermal radiation always collapses to a black hole and the Schwarzschild black hole is the only possible solution.

2.4 Regular Black Hole Thermodynamics

In this section the regular BH metric (RBH) in generic spacetime dimensions is presented. The metric of a $(n+1)-$dimensional regularized Schwarzschild BH, in Minkowski space (where n is the number of spatial dimensions) is a generalization of the Schwarzschild-Tangherlini solution [3] that solves the $(n+1)$-dimensional Einstein's equations with $T_{\mu\nu}$ and reads

$$ds^2 = -V(r)\,dt^2 + \frac{dr^2}{V(r)} + r^2 d\Omega^2\,, \tag{2.21}$$

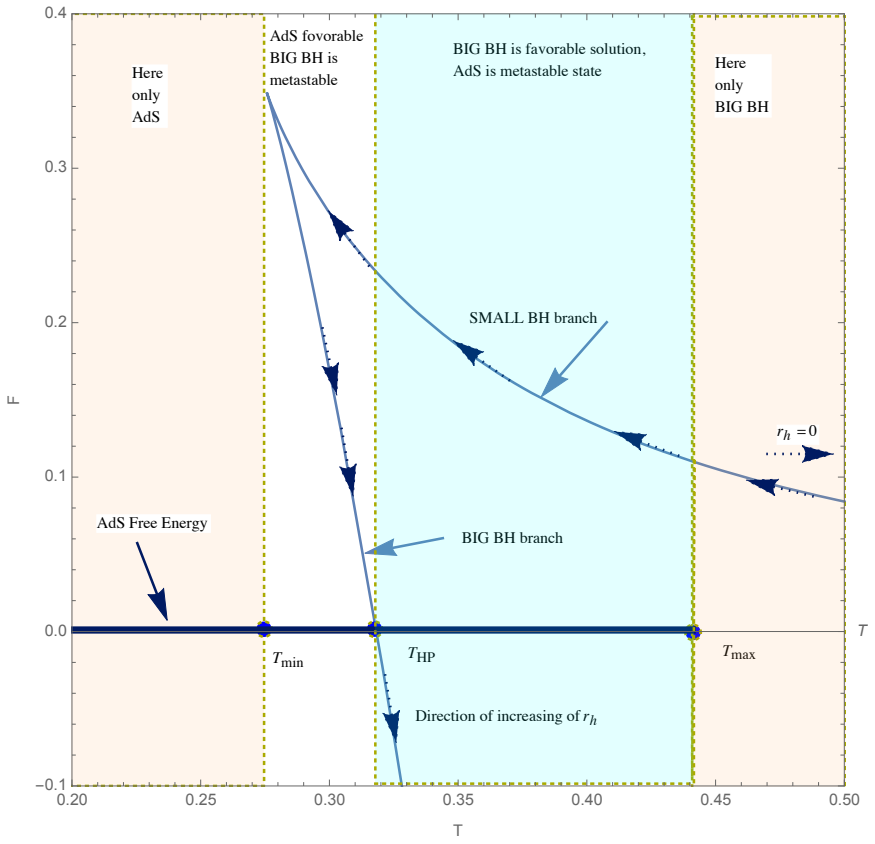

FIGURE 2.3: **Hawking-Page Free energy** as function of the temperature where b is fixed to one

where $d\Omega^2$ is the metric of a $(n-1)-$sphere and the function $V(r)$ is defined as

$$V(r) = 1 - \frac{\omega_n M \mu(r)}{r^{n-2}}, \qquad \mu(r) = \gamma\left(\frac{n}{2}, \frac{r^2}{4\theta^2}\right). \tag{2.22}$$

with mass coefficient defined by the following combination of constants

$$\omega_n = \frac{16\pi G_{\mathrm{N}}}{(n-1)\,\Gamma\left(\frac{n}{2}\right)\mathrm{Vol}\left(\mathrm{S}^{n-1}\right)}. \tag{2.23}$$

The Newton's constant G_{N} depends on the dimension of spacetime $(n+1)$ and $\mathrm{Vol}\left(\mathrm{S}^{n-1}\right)$ is the volume of a unit sphere in $n-1$ dimensions defined by

$$\mathrm{Vol}\left(\mathrm{S}^{n-1}\right) = \frac{2\pi^{n/2}}{\Gamma\left(\frac{n}{2}\right)}. \tag{2.24}$$

The BH's mass M (that correspond to the internal energy of the system) can be defined by the horizon equation $V(r_+) = 0$ and reads

$$M = \frac{(n-1)\, r_+^{n-2}\Gamma\left(\frac{n}{2}\right)\mathrm{Vol}\left(S^{n-1}\right)}{16\pi\, G_N\, \mu(r_+)} \tag{2.25}$$

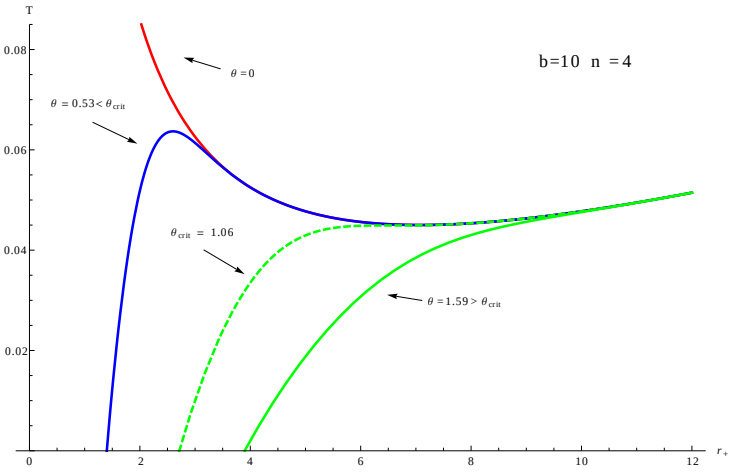

FIGURE 2.4: **Hawking Temperature in $n = 4$ for RBH in AdS background.** The temperatures should be compared with the red line that is the classical Hawking temperature.

using the definition (2.24), the mass simplify in

$$M = \frac{(n-1)\,\pi^{\frac{n}{2}} r_+^{n-2}}{8\pi\, G_N\, \mu\,(r_+)}\,. \tag{2.26}$$

The Hawking temperature can be easily calculated from the line element (2.21) using the following relation

$$T = \frac{1}{4\pi}\,\partial_r V\,(r)|_{r_+} \tag{2.27}$$

that for a RBH with (2.22) gives

$$T \;=\; \frac{(n-2)}{4\pi r_+}\left[1 - \frac{r_+\mu'(r_+)}{(n-2)\mu(r_+)}\right] \tag{2.28}$$

a temperature that reaches a value $T = 0$ for a horizon radius $r_+ \neq 0$. The temperature of the RBHs appears to be suppressed (or equal) relative to that of a vacuum BHs of equal horizon area (see Fig. 2.4). This is a common feature of static spherically symmetric BHs in interaction with various classical matter fields[4].

In the classical limit $r_+ \gg \theta$, i.e., when the solution should be the standard Schwarzschild BH, the temperature reads

$$T_{cl} = \frac{n-2}{4\pi r_+} \tag{2.29}$$

[4] Any BH in interaction with nonzero classical matter fields is usually referred to as "dirty" (such as electromagnetic fields, dilaton fields, axion fields, Abelian Higgs fields, non-Abelian gauge fields, etc.) [4].

and is exactly equal to the standard Hawking temperature. Using the formula of the energy-density (1.21) for a gaussian distribution

$$\rho_\theta\left(r_+\right)=\frac{M}{\left(4\,\pi\,\theta^2\right)^{n/2}}e^{-\frac{r_+^2}{4\theta^2}}$$

that define the RBH and substituting the RBH's mass (2.25), one gets

$$\rho_\theta\left(r_+\right) \;=\; \frac{(n-1)\theta^{-n}r_+^{n-2}}{2^{n+3}\pi G_N\,\mu(r_+)}e^{-\frac{r_+^2}{4\theta^2}}. \tag{2.30}$$

This equality allows to rewrite the temperature as function of the classical temperature (2.29) and the matter density distribution

$$T \;=\; \frac{1}{8\pi}\left[\frac{r_+}{\theta^2}+\frac{2\rho'_\theta(r_+)}{\rho_\theta(r_+)}\right] \tag{2.31}$$

$$\;=\; \frac{T_{cl}}{(n-2)}\left(\frac{r_+^2}{2\theta^2}+\frac{r_+\rho'_\theta(r_+)}{\rho_\theta(r_+)}\right). \tag{2.32}$$

Now, considering the specific function $\mu\left(r\right)=\gamma\left(\frac{n}{2},\frac{r^2}{4\theta^2}\right)$ one obtain the following result:

$$T \;=\; \frac{1}{4\pi r_+}\left[1-\frac{16\pi G_N\,r_+^2}{(n-2)\,(n-1)}\rho_\theta\left(r_+\right)\right] \tag{2.33}$$

$$\;=\; \frac{T_{cl}}{n-2}\left[1-\frac{16\pi G_N\,r_+^2}{(n-2)\,(n-1)}\rho_\theta\left(r_+\right)\right]. \tag{2.34}$$

The formula (2.34) reduces in the case $n=3$ (the standard four dimensional spacetime) to the nice relation

$$T=T_{cl}\left[1-8\pi G_N\,r_+^2\rho_\theta\left(r_+\right)\right] \tag{2.35}$$

typical of a general spherically symmetric distribution of matter with a black hole at the center [4].

If r_+ is the largest real positive root of $V\left(r\right)$, then in order for this RBH metric to describe a BH with a non-singular horizon at $r=r_+$, the temperature must satisfy the inequality $T\geq 0$, that gives

$$\frac{16\pi G_N\,r_+^2}{(n-2)\,(n-1)}\rho_\theta\left(r_+\right)\leq 1 \tag{2.36}$$

If the inequality is saturated, the horizon is degenerate and one gets an *extremal RBH*. The inequality (2.36) imposes a bound on the BH mass parameter of the

form[5] $M > M_e(\theta)$. When the Hawking temperature reaches the value $T = 0$, then one can use the expression to find the mass M_e of the extremal BH evaluated at a specific value of the horizon radius r_e. The extremal BH has interesting physical properties, for example, non-vanishing mass but zero temperature. The definition of the entropy for the extremal BH is still an open problem.

The study of BH thermodynamics implies the calculation of other important quantities such as the entropy and the free energy of the system. In order to calculate the free energy defined as

$$F = U - TS \tag{2.37}$$

one needs to integrate the entropy given by the first law of BH thermodynamic:

$$dS = \frac{dM}{T} = \frac{(n-1)\pi^{n/2} r_+^{n-2}}{2G_N \gamma\left(\frac{n}{2}, \frac{r_+^2}{4\theta^2}\right)} dr_+. \tag{2.38}$$

One way to calculate the free energy (2.37) is using (2.25), (2.28) and perform the integration numerically (assuming that the entropy is zero when the temperature is zero.

2.5 Regular Black Hole in Anti-deSitter Spacetime

In the case of AdS-RBH, the metric function (2.22) with $\mu(r) = \gamma\left(\frac{n}{2}, \frac{r^2}{4\theta^2}\right)$ becomes

$$V(r) = 1 + \frac{r^2}{b^2} - \frac{\omega_n M}{r^{n-2}} \gamma\left(\frac{n}{2}, \frac{r^2}{4\theta^2}\right) \tag{2.39}$$

where b is the AdS radius. The Hawking temperature can be again easily calculated from (2.27)

$$T = \frac{r_+}{4\pi b^2}\left(\frac{(n-2)\, b^2 + n r_+^2}{r_+^2} - \frac{2^{1-n} r_+^{n-2}\left(b^2 + r_+^2\right) e^{-\frac{r_+^2}{4\theta^2}} \theta^{-n}}{\gamma\left(\frac{n}{2}, \frac{r_+^2}{4\theta^2}\right)}\right) \tag{2.40}$$

$$= \frac{(n-2)\, b^2 + n r_+^2}{4\pi b^2 r_+} - \frac{r_+}{4\pi b^2}\left(\frac{2^{1-n} r_+^{n-2}\left(b^2 + r_+^2\right) e^{-\frac{r_+^2}{4\theta^2}} \theta^{-n}}{\gamma\left(\frac{n}{2}, \frac{r_+^2}{4\theta^2}\right)}\right) \tag{2.41}$$

[5] The same kind of bound can be built in the AdS case and lead to important consideration about the background and the definition of the thermodynamical system (see sub-sec. 2.5.1.2).

and the classical limit gives

$$T_{cl} = \frac{b^2(n-2) + nr_+^2}{4b^2\pi r_+}. \tag{2.42}$$

Also in this case the temperature reaches a value $T = 0$ for an horizon radius $r_+ \neq 0$ (see Fig. 2.4). The mass M can be defined by the horizon equation $V(r_+) = 0$ as

$$M = \frac{(n-1)r_+^{n-2}\left(b^2 + r_+^2\right)\Gamma\left(\frac{n}{2}\right)\mathrm{Vol}\left(S^{n-1}\right)}{16\pi\, b^2 G_N \gamma\left(\frac{n}{2}, \frac{r_+^2}{4\theta^2}\right)} \tag{2.43}$$

and depends from the AdS radius. Substituting the mass (2.43) into the density gives

$$\rho_\theta(r_+) = \frac{n-1}{4G_N}\left(\frac{2^{1-n}r_+^{n-2}\left(b^2 + r_+^2\right)e^{-\frac{r_+^2}{4\theta^2}}\theta^{-n}}{4\pi b^2\gamma\left(\frac{n}{2}, \frac{r_+^2}{4\theta^2}\right)}\right), \tag{2.44}$$

and also in the AdS background one can rewrite the temperature as a function of the classical AdS temperature in this way

$$T = T_{cl} - \rho_\theta(r_+)\frac{4G_N r_+}{n-1} \tag{2.45}$$

where the classical temperature is given in (2.42). Again, if r_+ is the largest real positive root of $V(r)$, then in order for this AdS-RBH metric to describe a black hole with an horizon at $r = r_+$, the temperature must satisfy $T_H \geq 0$ that means that

$$\frac{(n-1)\,r_+}{4G_N}T_{cl} \geq \rho_\theta. \tag{2.46}$$

If the inequality in Eq. (2.46) is saturated, the horizon is degenerate and we get an extremal BH. This inequality imposes a bound on the BH's mass parameter of the form $M > M_e(\theta, b)$ and all the solutions violating the bound (2.46) are BHs with a negative temperature.

2.5.1 Phase Structure in AdS Background

Now that all the thermodynamical quantities required to calculate the free energy $F = M - TS$ are defined, one only needs to fix the proper background. The regular AdS-BH solution shows a very interesting phase structures at intermediate temperatures as a result of studying two different thermodynamic ensembles:

1. *Ensemble 1.* A thermodynamic ensemble with fixed θ parameter in a thermal AdS bath.

2. *Ensemble 2.* A fixed θ ensemble, for which the background is provided by the extremal black hole with mass given by that θ parameter.

In both the cases, at sufficiently high temperature the physics is dominated by highly non-extremal BHs, and one recovers the " deconfined" behavior characteristic of the associated field theories. At intermediate temperatures, in the *Ensemble 2*, for example, the presence of the parameter θ allows a new branch of BH solutions to modify the qualitative phase structure in the low temperature regime, resulting in a very interesting phase structure (see Fig.2.6). The situation described by the *Ensable 2* is different from the case where the background is thermal AdS (*Ensamble 1*), and it represents the possibility that the regular black hole could decay into something else than thermal AdS, a kind of (perhaps "non-commutative") AdS spacetime. This subtlety does not arise in the standard Gibbons-Hawking calculus of the thermodynamics of BHs because the calculations are not sensitive to the ability of the BHs to decay into a remnant. The phase structure which one can obtain in each thermodynamic ensemble is summarized in Fig. 2.6. In the case of *Ensemble 2*, it is possible to recognize a van der Waals (VdW) system. The fact that this system appears in the AdS-BH thermodynamics is engaging, and it would not have been possible without the presence of the extra branches of solutions which appear when there is a negative cosmological constant. Besides, the shape of the free energy surface (as a function of θ and T) is that of the classic "swallowtail" catastrophe (see Fig. 3.2 for an example). This shape is familiar from the study of bifurcations in catastrophe theory (see for example [5]). Catastrophe theory is a classification of the possible different types of bifurcation shapes that can occur in a wide variety of complex systems. Indeed, catastrophe theory can help to understand what diverse models have in common. The fact that these shapes appear in this context suggests that there could be a universality class to be explored. Thus, perhaps, one could learn about a possible universal phase structures which can occur in the dual field theory.

2.5.1.1 Thermal AdS Background (*Ensemble 1*)

In this case, the free energy $\Delta F = F - F_0 = M - TS$ is given by Eq. (2.15) where $F_0 = F_{AdS}$ is the AdS background. In the AdS-RBH case, the entropy and, therefore, the free energy can be calculated numerically using $dS = dM/T$ for

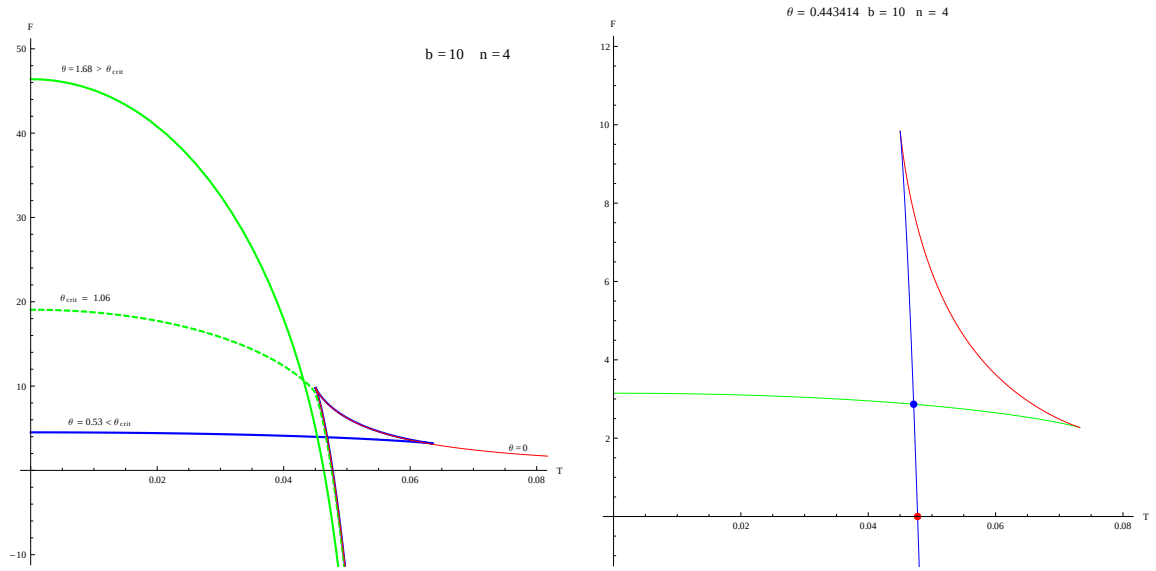

FIGURE 2.5: **Free energy vs Temperature and Swallowtail.** (Left) The blue curve shows the swallowtail for a particular value $\theta = 0.53 < \theta_{crit}$; the dashed green line shows the free energy for the $\theta_{crit} = 1.06$ which presents a cusp. The red curve corresponds to the classical case also showed in Fig. 2.3. (Right) Enlargement of the swallowtail for $\theta = 0.44 < \theta_{crit}$. The three braches of the solution are indicated in different colors. The unstable BH correspond to the red segment of the curve.

AdS-RBH. As seen in Sec. 2.3.1, the total energy will be finite. The free energy as function of the temperature is shown in Fig. 2.5 for some values of θ (included $\theta = 0$). For values of $\theta < \theta_{crit}$, the free energy exibits a swallowtail behaviour.

At $T = 0$ the free energy of the extremal RBH is $F_e = M_e$. Increasing the temperature the free energy becomes a multivalued function. This means that at fixed temperature there can be up to three possible RBH. When the three phases coexist, the one with highest free energy has negative heat capacity (red curve in Fig. 2.5), therefore it is unstable (see sec. 2.3.1). The favourite RBH solutions are those with lowest free energy. At low temperatures, the AdS system is the favorite system because $F > F_0$ (as in Hawking and Page's paper [2]).

The phase diagram for this configuration shows that there is only a *first-order phase transition* between AdS radiation and a large BH. A first-order phase transitions exhibit a discontinuity in the first derivative of the free energy with respect to temperature. In chemistry, the various solid/liquid/gas transitions are classified as first-order transitions. In this ensamble, case there is no second-order critical point. Second-order phase transitions are continuous in the first derivative but exhibit discontinuity in a second derivative of the free energy. For every value of θ there is always an Hawking-Page transition. See Fig. 2.6 on the left.

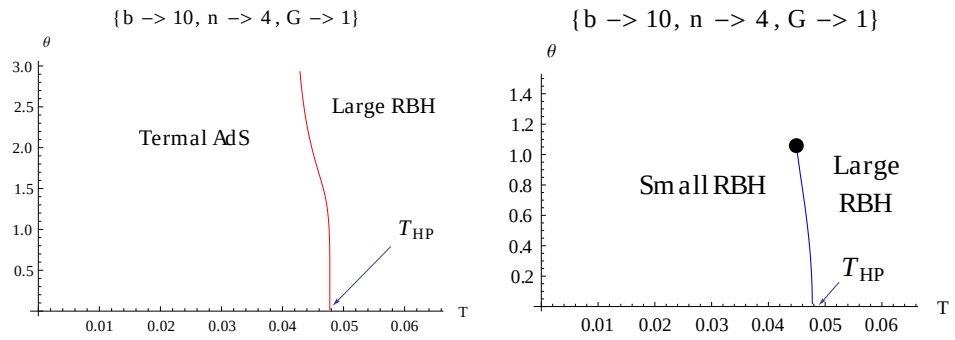

FIGURE 2.6: **Phase transition diagram for RBH.** Right: RBH in case of thermal AdS background: a first order phase transition is present for each value of θ. Left: RBH in extremal RBH bath: The first order phase transition ends in a second order critical point. At $\theta = 0$ the usual first-order Hawking-Page (HP) transition appears.

2.5.1.2 Extremal Regular Black Hole Background (*Ensemble 2*)

If one thinks that the presence of a minimal length always induce the presence of a "minimal" BH then one could also consider a background filled with small extremal black holes. In this case the definition of the free energy is

$$F = M - M_e - TS \tag{2.47}$$

where $F_0 = M_e$ is the mass of the extremal zero temperature configuration. This hypothesis completely change the phase diagram because in this case the swallow-tail is realized for negative values of the free energy. In this case there is not only a first order phase transition but also a second order critical point appears (see Fig. 2.6 on the right). The RBH has always negative free energy relative to AdS spacetime, also at low temperature, meaning that is always the favorite system. This phenomena happen also in the case of charged-Schwarzschild-AdS BHs [6]. The phase diagram illustrates in Fig. 2.6 right, shows a first-order transition line between small/large BHs that terminates in a second order critical point.

2.6 Higher Derivative Gravity

Following the line of reasoning presented in Chap. 1, now we move to investigate the thermodynamic properties of higher derivative gravity theories. In particular, in five dimensions, there is a non-vanishing topological term that one should consider: The so-called Gauss-Bonnet (GB) term. This is the 2-nd order term in the more general higher derivative theory of gravity, called Lovelock gravity. Since in AdS/CFT the gravity theory, considered to study a four-dimensional field theory,

has $d = 5$, here we present a study of the thermal structure of a GB Black Brane (BB) that is preliminary to the calculation of η/s of the dual field theory presented in Chap. 4. The BB solution for the RBH will be presente and discussed in Chap. 4.

2.6.1 Lovelock Gravity

Lovelock gravity [7] is a higher derivative theory that has received a lot of attention in recent years. Indeed, in any attempt to perturbatively quantize gravity as a field theory, one should expect that the Einstein-Hilbert action is only an effective gravitational action valid for small curvature or low energies and that it will be modified by higher-curvature terms. Lovelock gravity has also another interesting feature: Among higher derivative gravity theories, Lovelock gravities are the unique theories that give rise to field equations that are covariant and contain at most second order derivatives of the metric. In generic d spacetime dimensions, the Lagrangian of a Lovelock gravity theory is given by [7]

$$\mathcal{L} = \frac{1}{16\pi G_N} \sum_{k=0}^{k_{max}} \hat{\alpha}_{(k)} \mathcal{L}^{(k)} \,. \tag{2.48}$$

The $\hat{\alpha}_{(k)}$ are the Lovelock coupling constants and $\mathcal{L}^{(k)}$ are the $2k$-dimensional Euler densities, given by the contraction of k powers of the Riemann tensor

$$\mathcal{L}^{(k)} = \frac{1}{2^k} \delta^{a_1 b_1 \ldots a_k b_k}_{c_1 d_1 \ldots c_k d_k} R_{a_1 b_1}{}^{c_1 d_1} \ldots R_{a_k b_k}{}^{c_k d_k} \,, \tag{2.49}$$

where the "generalized Kronecker delta function" is totally antisymmetric in both sets of indices. The term $\mathcal{L}^{(0)}$ gives *the cosmological constant term*, $\mathcal{L}^{(1)}$ gives the Einstein–Hilbert action, and $\mathcal{L}^{(2)}$ corresponds to the quadratic Gauss–Bonnet term. The integer $k_{max} = \left[\frac{d-1}{2}\right]$ provides an upper bound on the sum, reflecting the fact that $\mathcal{L}^{(k)}$ contribute to the equations of motion for $d > 2k$, whereas they are topological in $d = 2k$, and vanish identically in lower dimensions. GR is recovered upon setting $\hat{\alpha}_{(k)} = 0$ for $k \geq 2$.[6] The vacuum equations of motion for

[6] Another interesting limit in odd dimensions arises for the following choice of Lovelock couplings

$$\alpha_p = \frac{\ell^{2p-2n+1}}{2n-2p-1} \binom{n-1}{p} \qquad p = 1, 2, \ldots, n-1 = \frac{d-1}{2} \tag{2.50}$$

for which the local Lorentz invariance of the Lovelock action is enhanced to a local (A)dS symmetry and the theory belongs to the class of Chern–Simons theories [8]. This case is not considered here.

Lovelock gravity, following from the Lagrangian density (2.48), are

$$\mathcal{G}^a_{\ b} = \sum_{k=0}^{k_{max}} \hat{\alpha}_{(k)} \mathcal{G}^{(k)\,a}_{\quad\ b} = 0\,, \tag{2.51}$$

where the Einstein-like tensors $\mathcal{G}^{(k)\,a}_{\quad\ b}$ are given by

$$\mathcal{G}^{(k)\,a}_{\quad\ b} = -\frac{1}{2^{(k+1)}} \delta^{a\,c_1 d_1 \ldots c_k d_k}_{b\,e_1 f_1 \ldots e_k f_k} R_{c_1 d_1}^{\quad\ e_1 f_1} \ldots R_{c_k d_k}^{\quad\ e_k f_k}\,, \tag{2.52}$$

and each of them independently satisfies a conservation law $\nabla_a \mathcal{G}^{(k)\,a}_{\quad\ b} = 0$.

2.6.1.1 Lovelock Charged Black Holes

The static charged AdS Lovelock BH has metric function

$$ds^2 = -f\left(r\right) dt^2 + f\left(r\right)^{-1} dr^2 + r^2 d\Omega^2_{(\kappa)d-2}\,, \qquad F = \frac{Q}{r^{d-2}} dt \wedge dr\,, \tag{2.53}$$

where $d\Omega^2_{(\kappa)d-2}$ denotes the line element of a $(d-2)$-dimensional compact space with constant curvature $(d-2)(d-3)\kappa$. One should note here that BHs in AdS spaces are rather different from BHs in flat or dS spaces. In fact, in asymptotically flat or dS spaces, the horizon topology of a $d = 4$ spacetime dimensions BH is constrained to be a round sphere S^2. On the other hand, in AdS spaces it is possible to have BHs with $\kappa = 0, +1, -1$ (respectively: flat, spherical, hyperbolic) horizon geometries [9, 10]. Due to the different horizon structure, the associated BH thermodynamic properties can be rather different.
Denoting by $\Sigma^{(\kappa)}_{d-2}$ the finite volume of this compact space, a $(d-2)$-dimensional unit sphere $\Sigma^{(\kappa)}_{d-2}$ takes the following standard form:

$$\Sigma^{(+1)}_{d-2} = \frac{2\pi^{(d-1)/2}}{\Gamma\left(\frac{d-1}{2}\right)}\,. \tag{2.54}$$

In terms of the rescaled Lovelock coupling constants

$$\alpha_0 = \frac{\hat{\alpha}_{(0)}}{(d-1)\,(d-2)}\,, \quad \alpha_1 = \hat{\alpha}_{(1)}\,, \quad \alpha_k = \hat{\alpha}_{(k)} \prod_{n=3}^{2k} (d-n) \quad \text{for} \quad k \geq 2\,, \tag{2.55}$$

the field equations (2.60) reduce to the requirement that $f(r)$ solves the following polynomial equation of degree k_{max} [11, 12, 13, 14, 15, 16]

$$\mathcal{P}(f)=\sum_{k=0}^{k_{max}}\alpha_k\left(\frac{\kappa-f}{r^2}\right)^k=\frac{16\pi G_N M}{(d-2)\Sigma_{d-2}^{(\kappa)}r^{d-1}}-\frac{8\pi G_N Q^2}{(d-2)(d-3)}\frac{1}{r^{2d-4}}\,. \tag{2.56}$$

Here M stands for the ADM mass of the black hole and Q is the electric charge integrated on the $(d-2)$-dimensional surface at spatial infinity

$$Q=\frac{1}{2\Sigma_{d-2}^{(\kappa)}}\int *F\,. \tag{2.57}$$

2.7 Black Brane Solutions of Lovelock Gravity

Let us consider the static, electrically charged, radially symmetric AdS Lovelock BB in d-dimensional spacetime, described by the following line element and electromagnetic (EM) field:

$$ds^2=-f(r)\,N^2dt^2+f(r)^{-1}\,dr^2+\frac{r^2}{L^2}d\Sigma_{d-2}^2\,,\qquad F=\frac{Q}{r^{d-2}}dt\wedge dr\,, \tag{2.58}$$

where $d\Sigma_{d-2}^2$ denotes the $(d-2)$-dimensional space with zero curvature and planar topology, whereas L is related to the cosmological constant $\hat{\alpha}_{(0)}$ by $L^{-2}=\hat{\alpha}_{(0)}/(d-1)(d-2)$. Notice that the metric in Eq.(2.58) differs from that in the usual Schwarzschild gauge by a (constant) rescaling $t\to Nt$ of the time coordinate t. It will be showed later in this thesis (see Sec. 4.6.1) that this rescaling is necessary in order to have a unit speed of light in the dual CFT. Using the rescaled Lovelock coupling constants

$$L^{-2}=\alpha_0=\frac{\hat{\alpha}_{(0)}}{(d-1)(d-2)}\,,\quad \alpha_1=\hat{\alpha}_{(1)}\,,\quad \alpha_k=\hat{\alpha}_{(k)}\prod_{n=3}^{2k}(d-n)\quad \text{for}\quad k\geq 2\,, \tag{2.59}$$

the field equations read

$$\sum_{k=0}^{k_{max}}\hat{\alpha}_{(k)}\mathcal{G}_{ab}^{(k)}=8\pi G_N\left(F_{ac}F_b{}^c-\frac{1}{4}g_{ab}F_{cd}F^{cd}\right) \tag{2.60}$$

where G_N is the d-dimensional Newton's constant. The higher-curvature terms contribute to the equations of motion only for $d>2k$. For $d=2k$ the higher-curvature corrections are topological, and they vanish identically in lower dimensions. Setting $\hat{\alpha}_{(k)}=0$ for $k\geq 2$, one can recover the standard form of general

relativity. In the notation (2.59), the field equations (2.60) reduce to the requirement that $f(r)$ solves the following polynomial equation of degree $k_{max} = \left[\frac{d-1}{2}\right]$ (see e.g., [11, 12, 13, 14, 15, 16, 17])

$$\mathcal{P}(f) = \sum_{k=0}^{k_{max}} \alpha_k \left(\frac{\kappa - f}{r^2}\right)^k = \frac{\omega_d M_{ADM}}{N r^{d-1}} - \frac{8\pi G_N Q^2}{(d-2)(d-3)} \frac{1}{r^{2d-4}}\,. \tag{2.61}$$

Here M_{ADM} is the ADM mass of the black brane and ω_d is

$$\omega_d = \frac{16\pi G_N}{(d-2)} \frac{L^{d-2}}{V^{d-2}} \tag{2.62}$$

where V^{d-2} is the volume of the $(d-2)$-dimensional space with curvature $\kappa = 0$. The electric charge Q of the brane is

$$Q = \frac{L^{d-2}}{2V_{d-2}} \int *F\,. \tag{2.63}$$

2.7.1 Universality of Black Brane Thermodynamics in Lovelock Gravity

Interestingly, even without knowing $f = f(r)$ in Eq.(2.61) explicitly, it is possible, using the Hamiltonian formalism [14, 18], to find the thermodynamic quantities characterizing the Lovelock black brane solution [14, 18, 19]. In the Hamiltonian picture the spacetime metric g_{ab} is split according to

$$g_{ab} = -n_a n_b + s_{ab} \tag{2.64}$$

where n_a is the unit timelike normal to a spatial slice Σ with induced metric s_{ab} and these satisfy the orthogonality relation $s_{ab}n_b = 0$. As in Einstein gravity the time-time and time-space components of the field equations act as constraints on initial data. After splitting space and time, the dynamical variables on the spatial surface Σ are the spatial metric s_{ab}, and its conjugate momentum π^{ab}. The derivation of the first law comes from a judicious evaluation of the Hamiltonian [19].

Let r_+ denotes the radius of the event horizon, determined as the largest root of $f(r) = 0$. Introducing the effective mass M and temperature T related to the usual ADM mass M_{ADM} and Hawking temperature T_H by the relations

$$M = \frac{M_{ADM}}{N}, \quad T = \frac{T_H}{N}, \tag{2.65}$$

the black brane mass M, the temperature T, the entropy S, and the gauge potential Φ are given by [14, 20]

$$M = \frac{1}{\omega_d L^2} r_+^{d-1} + \frac{V_{d-2}}{2(d-3)L^{d-2}} \frac{Q^2}{r_+^{d-3}}\,, \tag{2.66}$$

$$\begin{aligned} T &= \frac{1}{2\pi N} \frac{1}{\sqrt{g_{rr}}} \frac{d\sqrt{-g_{tt}}}{dr}\Big|_{r=r_+} \\ &= \frac{1}{4\pi r_+} \left[(d-1) \left(\frac{r_+}{L}\right)^2 - \frac{8\pi G_N Q^2}{(d-2) r_+^{2(d-3)}} \right]\,, \end{aligned} \tag{2.67}$$

$$S = \frac{V^{d-2}}{4G_N} \left(\frac{r_+}{L}\right)^{d-2}\,, \quad \Phi = \frac{V_{d-2}}{(d-3)L^{d-2}} \frac{Q}{r_+^{d-3}}\,. \tag{2.68}$$

The rescaling of the physical parameters (2.65) of the Lovelock BB having the dimensions of energy is essentially due to the presence of the constant N^2 in the metric. The two time coordinates t and Nt correspond to using two different units to measure the energy. However, when one deals with Einstein-Hilbert branes the rescaling of the time coordinate is not necessary and one can simply set $M = M_{ADM}$ and $T = T_H$. Notice that the area-law for the entropy S always hold for the generic Lovelock black brane.

A striking feature of these thermodynamic expressions is that *they do not depend on the Lovelock coupling constants* α_k *for* $k \geq 2$ but only on α_0 and α_1, i.e., they depend only on the cosmological constant and on the Newton constant. This means that the thermodynamic behaviour of the BB in Lovelock theory is universal, in the sense that *it does not depend on the higher order curvature terms* but only on the Einstein-Hilbert term, the cosmological constant and the matter fields content (in our case the EM field). This implies, in turn, that as thermodynamic system the charged BBs of Lovelock gravity are indistinguishable from the Reissner-Nordström BBs of Einstein-Hilbert gravity. Notice that this feature is not shared by the black hole solutions of the theory, i.e., solutions with spherical or hyperbolic horizons. In fact, in the Lovelock thermodynamic expressions (see Refs. [14, 20]) the dependence on the Lovelock coupling constants $\alpha_{k\geq 2}$ is introduced by the dependence on the curvature κ of the $(d-2)$-dimensional spatial sections. This dependence drops out when $\kappa = 0$.

The universal thermodynamic behaviour of charged Lovelock black branes is strictly true only when we choose $N = 1$ in the metric (2.58). The universality of the Lovelock BB thermodynamics is recovered simply by rescaling the units we use to measure the energy, i.e., by using in Eqs. (2.66) and (2.67) the effective parameters M and T instead of M_{ADM} and T_H.

2.8 $5d$ Reissner-Nordström Black Brane Solution

Let us preliminary review some known facts about the RN BB solutions of Einstein-Maxwell gravity. Setting $\alpha_k = 0$ for $k \geq 2$ and $d = 5$ in Eq (2.52), one has standard GR equations sourced by an electromagnetic field. For this choice of the parameters, Eq. (2.61) is a linear equation in f that gives the following solution:

$$f = \alpha_0 r^2 - \frac{\omega_5 M}{r^2} + \frac{4\pi}{3}\frac{G_N Q^2}{r^4}, \tag{2.69}$$

where ω_5 is given by Eq. (2.62) and G_N is the five dimensional Newton's constant. Performing the asymptotic limit $r \to \infty$, the function (2.69) reduces to $f = r^2/L^2$, i.e., AdS_5 with AdS length $L^2 = \alpha_0^{-1}$. Setting $r^2 = Y$ in Eq. (2.69), the RN BB horizons are determined by the cubic equation

$$Y^3 - \omega_5 M L^2 Y + \frac{4\pi}{3} G_N L^2 Q^2 = 0. \tag{2.70}$$

This equation has two positive roots for

$$M^3 \geq 12\pi^2 \frac{G_N^2 Q^4}{\omega_5^3 L^2}, \tag{2.71}$$

which gives the extremal (BPS [21, 22]) bound for the RN black brane in $5d$. In general, the solution will have an inner and outer horizon, when the bound is saturated the two horizons merge at r_0 and the RN BB becomes extremal. In the extremal case, Eq. (2.70) has a double root at $Y_0 = \sqrt{\omega_5 M L^2/3}$ and $f(r)$ can be factorized in the following way

$$f(r) = \frac{1}{L^2 r^4}\left(r^2 + r_0^2\right)(r - r_0)^2 (r + r_0)^2, \quad r_0 = \left(\frac{\omega_5 M L^2}{3}\right)^{1/4}. \tag{2.72}$$

The extremal near-horizon geometry can be determined expanding the metric near r_0 and keeping only the leading term in the metric

$$f(r) = \frac{12}{L^2}(r - r_0)^2, \tag{2.73}$$

a simple translation of the radial coordinate $r \to r + r_0$ gives the $AdS_2 \times R_3$ extremal near-horizon geometry with AdS_2 lenght l

$$ds^2 = -\left(\frac{r}{l}\right)^2 dt^2 + \left(\frac{l}{r}\right)^2 dr^2 + \left(\frac{r_0}{L}\right)^2 d\Sigma_3^2, \; l^2 = \frac{L^2}{12}. \tag{2.74}$$

The extremal solution given in Eq. (2.72) is a soliton interpolating between the asymptotic AdS_5 geometry in the UV and the $AdS_2 \times R_3$ geometry (2.74) in the IR.

2.9 Gauss-Bonnet Solution

For $k = 2$ and generic curvature κ, Eq. (2.61) reduces to a quadratic equation

$$\alpha_2 \frac{(\kappa - f)^2}{r^4} + \frac{(\kappa - f)}{r^2} + \alpha_0 - \frac{\omega_d M}{r^{d-1}} + \frac{8\pi G_N Q^2}{(d-2)(d-3)r^{2d-4}} = 0\,, \tag{2.75}$$

from which one obtains two possible solutions, $f_\pm$. In the following, we will refer to the solution f_- as the '*Einstein branch*' because it approaches the Einstein case when the Gauss–Bonnet coupling α_2 goes to zero and to f_+ as the '*Gauss–Bonnet branch*' [23]. The quadratic Eq. (2.75) gives the following necessary condition requirement for the existence of $f_\pm$ for large r:

$$1 - 4\alpha_0\alpha_2 \geq 0\,. \tag{2.76}$$

When this inequality is violated, the space becomes compact because of the strong nonlinear curvature [23]. Therefore, there is no asymptotic 'AdS region' and consequently no proper black hole with standard asymptotics.

2.9.1 $5d$ Gauss-Bonnet Black Brane

In this subsection, the special case of $5d$ GB BB ($\kappa = 0$) will be discussed. The parameter will be considered $\alpha_1 = 1$ in order to recover the usual Newtonian limit. It is easy to check that that for $d = 5$ and $\kappa = 0$, then Eq. (2.75) reduces to the following equation

$$\alpha_2 \frac{f^2}{r^4} - \frac{f}{r^2} + \alpha_0 - \frac{\omega_5 M}{r^4} + \frac{4\pi Q^2}{3r^6} = 0 \tag{2.77}$$

and the two branches are respectively

$$f_\pm = \frac{r^2}{2\alpha_2}\left[1 \pm \sqrt{1 - 4\alpha_0\alpha_2}\sqrt{1 + \frac{4M\alpha_2\omega_5}{(1 - 4\alpha_0\alpha_2)}\frac{1}{r^4} - \frac{16\pi G_N}{3}\frac{Q^2\alpha_2}{1 - 4\alpha_0\alpha_2}\frac{1}{r^6}}\right]. \tag{2.78}$$

In case of positive GB coupling $\alpha_2 > 0$ that satisfy the condition (2.76), the two branches describe two asymptotically AdS_5 spacetimes, however, from Eq. (2.78)

one can see that f_+ has no zeroes, hence the f_+ branch does not describe a BB but a solution with no event horizon. Thus, only the f_- branch describes a BB solution.

At leading order for $r \to \infty$ the metric coefficient $g_{tt} = N^2 f(r)$ in Eq.(2.58) becomes

$$g_{tt} \to N^2 \frac{r^2}{2\alpha_2} \left(1 \pm \sqrt{1 - 4\alpha_0\alpha_2}\right) . \tag{2.79}$$

In order to have the boundary of the asymptotic AdS_d conformal to $(d-1)$-Minkowski space with speed of light equal to 1, $ds^2 \approx \alpha_0 r^2(-dt^2 + d\Sigma_3^2)$, the constant N^2 has to be chosen as

$$N^2 = \frac{1}{2}\left(1 \mp \sqrt{1 - 4\alpha_0\alpha_2}\right), \tag{2.80}$$

where the $+$ sign is for the f_- branch, the BB solution, while the $-$ sign has to be used when we consider the f_+ branch. For $\alpha_2 < 0$, only the f_- branch is asymptotically AdS. Conversely, the f_+ branch describes a spacetime which is asymptotically de Sitter (dS) and can be therefore relevant as a cosmological solution.

2.9.2 Singularities

To determine the position of the singularities of the spacetime one can calculate the scalar curvature for both the $f_\pm$ branches:

$$R^{(\pm)} = \mp\frac{1}{2}\frac{\beta r^2(20r^{10} + 30\sigma r^6 - 31\rho r^4 + 6\sigma^2 r^2 - 9\rho\sigma) \pm 20r^3(r^6 + r^2\sigma - \rho)^{3/2} + 2\beta\rho^2}{\alpha_2 r^3(r^6 + \sigma r^2 - \rho)^{3/2}}, \tag{2.81}$$

where the $\pm$ sign refers respectively to the $f_\pm$ branches. To simplify expressions we used (here and after) the following notation

$$\beta = \sqrt{1 - 4\alpha_0\alpha_2}, \quad \sigma = \frac{4\alpha_2\omega_5 M}{\beta^2}, \quad \rho = \frac{16\pi G_N \alpha_2 Q^2}{3\beta^2}, \quad e = \frac{1}{\beta^2} - 1 = \frac{4\alpha_0\alpha_2}{\beta^2}, \; Y = r^2. \tag{2.82}$$

There are curvature singularities at $r = 0$ and at the zeroes of the argument of the square root in Eq. (2.81) (branch-point singularities). The position of the physical singularities of the spacetime is therefore determined by the pattern of zeroes of the function $g(Y)$, with

$$g(Y) = Y^3 + \sigma Y - \rho. \tag{2.83}$$

The singularity will be located at the biggest positive zero Y_1 of $g(Y)$ or at $r = 0$ when $g(Y)$ has no zeroes for positive Y. The singularity at $Y = Y_1$ is a branch point singularity. The pattern of zeroes of $g(Y)$ is determined by the signs of the coefficients ρ, σ and the discriminant $\Delta = \left(\frac{\rho}{2}\right)^2 + \left(\frac{\sigma}{3}\right)^3$.

- For $\sigma > 0$, the function $g(Y)$ is a monotonic increasing function of Y with a single zero which, depending on the sign of ρ, will be positive $Y = Y_1$ ($\rho > 0$) or negative ($\rho < 0$). The physical spacetime singularity will be therefore located at $r = \sqrt{Y_1}$ for $\rho, \sigma > 0$ and at $r = 0$ for $\rho < 0$, $\sigma > 0$.
- For $\sigma < 0$, the function $g(Y)$ is an oscillating function with a maximum at negative Y and a minimum at positive Y, it may therefore have one, two or three zeros. For $\sigma < 0$, $\rho > 0$, $g(Y)$ has at least a positive zero. For $\sigma < 0$, $\rho < 0$ we have a positive zero for $\Delta \leq 0$ and no positive zeros for $\Delta > 0$. For $\Delta = 0$ we have a double zero of $g(Y)$ so that Y_1 is not anymore a branch point singularity. In this latter case the singularity is at $r = 0$.

Summarising, the physical singularity is always located at $r = \sqrt{Y_1}$ unless $\sigma > 0, \rho < 0$ or $\sigma < 0, \rho < 0, \Delta \geq 0$ in which case the singularity is at $r = 0$.

2.9.3 f_- Branch

In this subsection, the horizons of the f_- branch, solution of Eq. (2.78), describing the GB black brane, is studied. In general the BB will have an inner ($r = r_-$) and outer ($r = r_+$) event horizon. The BB becomes extremal when $r_+ = r_-$. Using the notation (2.82), (2.83), one finds that the necessary condition for the existence of the BB is the positivity of the argument in the square root in Eq. (2.78), i.e., $g(Y) \geq 0$. The position of the event horizon(s) is determined by the *positive* roots of the cubic equation

$$h(Y) = eY^3 - \sigma Y + \rho = 0. \tag{2.84}$$

The case $\alpha_2 > 0$, which corresponds to $\sigma, \rho, e > 0$ (since also $\alpha_0 > 0$). The condition for the existence of real roots of the function $h(Y)$ can be easily found: The function $h(Y)$ has a maximum (minimum) for, respectively

$$Y = Y_{M,m} = \pm\sqrt{\frac{\sigma}{3e}} = \pm\sqrt{\frac{\omega_5 ML^2}{3}} \tag{2.85}$$

also, $h(Y = 0) = \rho > 0$, hence the cubic equation (2.84) always has a negative root. The existence of other roots is determined by the sign of $h(Y_m)$. We will have

two (one) positive roots hence a BB with two (one) event horizons for $h(Y_m) \leq 0$, i.e., for

$$\rho \leq \frac{2}{3}\sigma\sqrt{\frac{\sigma}{3e}}. \tag{2.86}$$

Using Eq. (2.82), the previous inequality can be written in terms of the charge Q and the effective mass M and gives *the same* Bogomol'nyi-Prasad-Sommerfield (BPS) bound (2.71) found in the RN case. However, the BPS bound is modified when we instead express it in terms of the ADM mass:

$$M_{ADM}^3 \geq 12N^3\pi^2\frac{G_N^2Q^4}{\omega_5^3L^2}. \tag{2.87}$$

When the bound is saturated, the inner and outer horizon merge at $r_- = r_+$, the BB becomes extremal, and the solution describes a soliton. The striking feature of the BPS bound (2.86) is that the *BPS bound of 5d Gauss-Bonnet BB does not depend on the Lovelock coupling constant, and it is exactly the same one gets for GR ($\alpha_2 = 0$), i.e., for the 5d Reissner-Nordström BB.* When M does not satisfy the inequality (2.86), the spacetime describes a naked singularity. For $\alpha_2 > 0$, the condition $M > 0$ implies $\sigma, \rho > 0$ and the function $g(Y)$ is a monotonic increasing function which cuts the Y-axis at the point Y_1, and, in view of the previous discussion, it also gives the position of the singularity. Since, the position of the event horizon Y_h is determined by the equation

$$\beta\sqrt{g(Y_h)} = Y\sqrt{Y_h}\,, \tag{2.88}$$

from which follow that $g(Y_h) > 0$ hence $Y_h > Y_1$, this checks that in the region where the bound (2.86) holds the condition $g(Y) > 0$ is always satisfied and that the physical singularity is always shielded by two (one in the extremal case) event horizons.

The behaviour of the metric function f_- for $\alpha_2, M > 0$ and selected values of the other parameters is shown in Fig. 2.7. The solid red, green and brown lines describe respectively a naked singularity, extremal and two-horizon BB geometry. The solid blue line represents a zero-charge, BB solution with single horizon. The case $\alpha_2 < 0, M > 0$ gives exactly the same BPS bound. Now, we have $\sigma, \rho, e < 0$. The function $h(Y)$ in Eq. (2.84) always has a negative root and a minimum (maximum) for

$$Y = Y_{m,M} = \pm\sqrt{\frac{\sigma}{3e}} = \pm\sqrt{\frac{\omega_5 ML^2}{3}}\,. \tag{2.89}$$

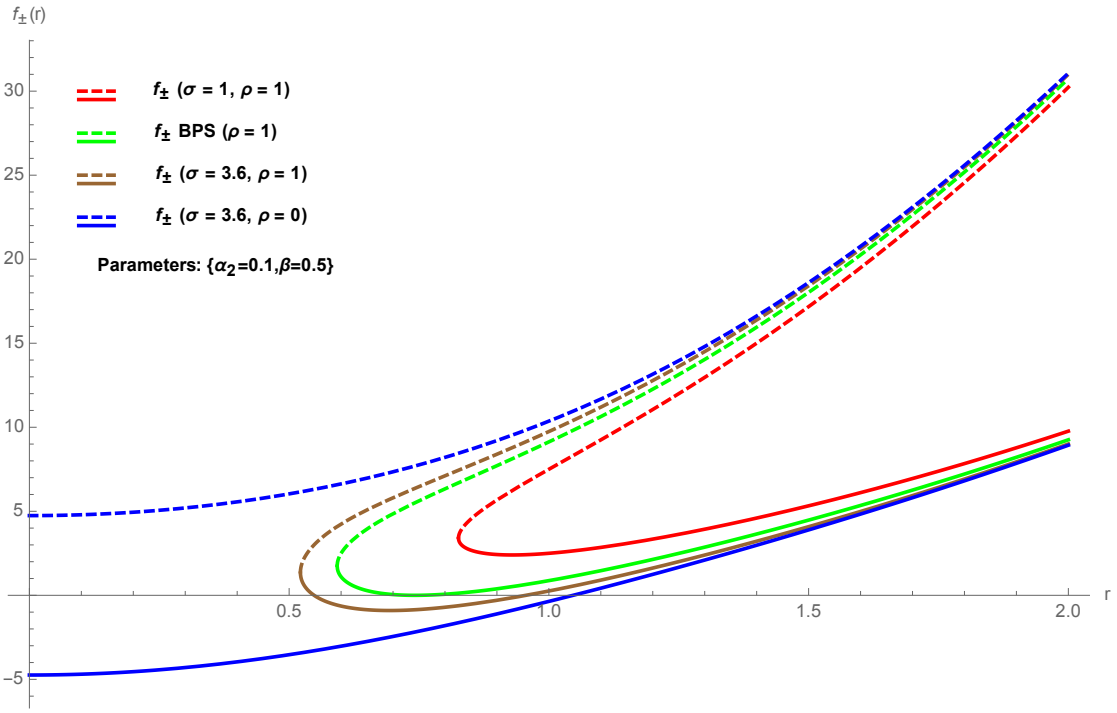

FIGURE 2.7: **Behaviour of the metric functions $f_\pm$ for $\alpha_2, M > 0$ and selected values of the other parameters.** The dashed (solid) lines describe the f_+ branch (f_- branch). The red, green, brown and blue solid lines describe respectively a naked singularity, an extremal, two-horizon and vanishing charge BB geometry. The corresponding dashed lines describe spacetimes with a naked singularity.

The conditions for the existence of two positive roots become $|\rho| \leq \frac{2}{3}|\sigma|\sqrt{\frac{\sigma}{3e}}$ leading to the same BPS bound (2.86). However, there is a crucial difference from the $\alpha_2 > 0$ case. When $\alpha_2 < 0$, the condition $M > 0$ implies $\sigma, \rho < 0$. Taking into account that $|e| < 1$ owing to (2.76), we see that the condition $\Delta < 0$ implies the BPS bound (2.86). This means that the two horizons are separated by a region in which the solution does not exist. The spacetime breaks into two disconnected parts. The physical part, having an asymptotic AdS region, describes a BB with singularity shielded by a *single* event horizon. The behaviour of the metric function f_- for $\alpha_2 < 0$ and selected values of the other parameters is shown in Fig. 2.8. The solid red, green and brown lines describe respectively a naked singularity, extremal and single-horizon BB geometry. The solid blue line represents a zero-charge, BB solution with horizon.

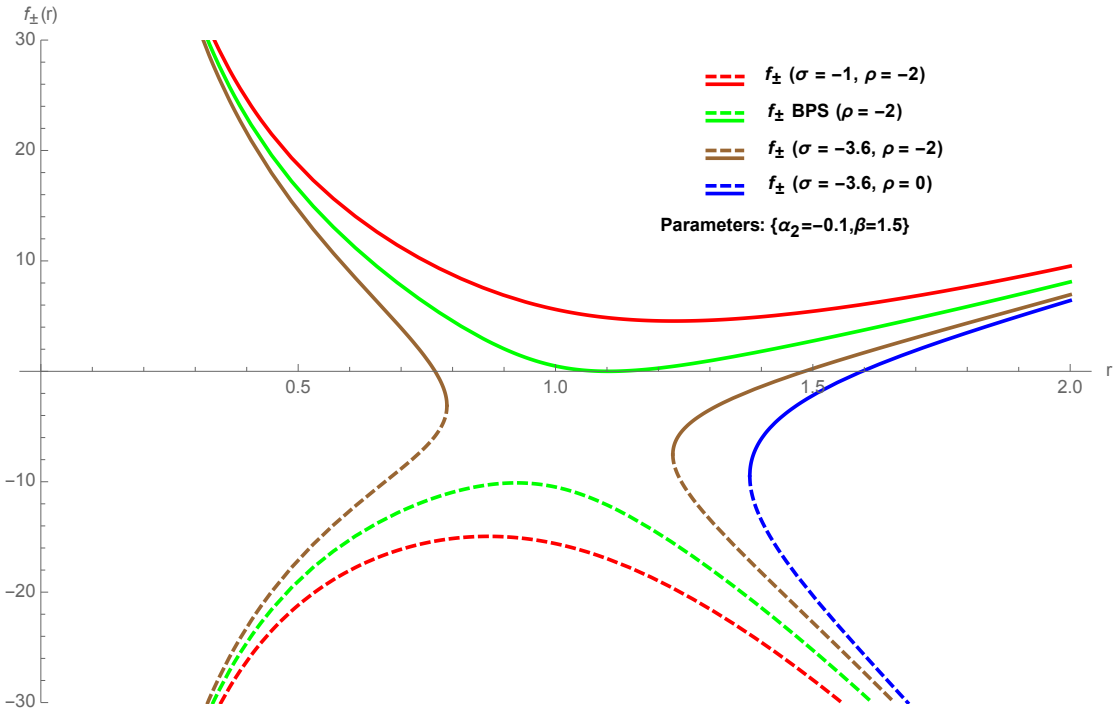

FIGURE 2.8: **Behaviour of the metric functions $f_\pm$ for $\alpha_2 < 0, M > 0$ and selected values of the parameters.** The dashed (solid) lines describe the f_+ branch (f_- branch). The red, green, brown, blue solid lines describe respectively a naked singularity, an extremal, single-horizon, vanishing charge BB geometry. The corresponding dashed lines describe cosmological solutions with a singularity which approach asymptotically to the dS spacetime.

2.9.3.1 Near Horizon Extremal Solution

When the bound (2.86) is saturated, the BB becomes extremal and the metric function (2.78) has a double zero at

$$Y_h = Y_m = \sqrt{\frac{\sigma}{3e}} = \sqrt{\frac{\omega_5 M L^2}{3}}, \tag{2.90}$$

thus, the solution f_- can be factorized as

$$f_-^{(ex)}(Y) = \frac{e\beta^2}{2\alpha_2} \frac{(Y+2Y_m)(Y-Y_m)^2}{Y^2+\beta\sqrt{Y^4+\sigma Y^2-\rho Y}}. \tag{2.91}$$

This solution represents the extremal GB soliton.

Let us now consider the near-horizon geometry. In this regime, the solution (2.91) can be expanded around $r = r_0 = \left(\frac{\sigma}{3e}\right)^{1/4}$. At the leading order the Einstein branch reads

$$f_-^{(ex)}(r) = 12\alpha_0(r-r_0)^2. \tag{2.92}$$

Translating the radial coordinate $r \to r + r_0$ and rescaling the time coordinate as $t \to t/N$ we get the extremal, near-horizon geometry:

$$ds^2 = -\left(\frac{r}{l}\right)^2 dt^2 + \left(\frac{l}{r}\right)^2 dr^2 + \left(\frac{r_0}{L}\right)^2 d\Sigma_3^2, \qquad l^2 = \frac{1}{12\alpha_0}\,. \tag{2.93}$$

i.e., $\mathrm{AdS}_2 \times R_3$ with the AdS_2 length l being determined uniquely by α_0. Thus, the extremal near-horizon geometry does not depend on α_2 and fully coincides with the extremal near-horizon geometry (2.74) one gets in the RN case.

2.9.4 Near Horizon Metric as Exact Solution of the Equations of Motion

In this section, we will show that the near-horizon solution given in Eq. (2.93) is an exact solution of the equations of motion (EOM). For the GB case, Eqs. (2.60) read

$$\begin{aligned} R_{ab} - \frac{1}{2}Rg_{ab} =& \frac{6}{L^2}g_{ab} + 8\pi G_N\left(F_{ac}F_b{}^c - \frac{1}{4}g_{ab}F_{cd}F^{cd}\right) \\ &+ \frac{\alpha_2}{2}g_{ab}\left(R_{cdef}R^{cdef} - 4R_{cd}R^{cd} + R^2\right) \\ &+ \alpha_2\left(-2RR_{ab} + 4R_{ac}R^c{}_b + 4R_{cd}R^c{}_a{}^d{}_b - 2R_{acde}R_b{}^{cde}\right)\,. \end{aligned} \tag{2.94}$$

We note that, since the Eq. (2.93) describes a spacetime with $\mathrm{AdS}_2 \times R_3$ geometry, the contribution to the curvature tensors coming from the planar geometry R_3 vanishes. Thus, the EOM includes only the contribution of the AdS_2 part of the metric which is a two dimensional maximally symmetric space.

For a generic n-dimensional maximally symmetric space with $R = \Lambda$ the two terms in Eqs. (2.94), that are quadratic in the curvature tensors, are given respectively by

$$\alpha_2\Lambda^2\frac{(n-2)(n-3)}{2n(n-1)}, \qquad -2\alpha_2\Lambda^2\frac{(n-2)(n-3)}{n^2(n-1)}. \tag{2.95}$$

These relations are consequence of the fact that the GB term in the action is topological for $d = 4$ and identically vanishes for $d = 2$ and $d = 3$. The previous equations imply that in the case of the $\mathrm{AdS}_2 \times R_3$ geometry, the contributions given by the GB terms to the EOM vanish; therefore, the near horizon metric (2.93) is an *exact* solution of both Einstein and GB EOM. In particular, the latter reduces to the usual Einstein-Maxwell equations in $5d$.
Thus, the $\mathrm{AdS}_2 \times R_3$ geometry is not only a near horizon approximation but it is

an exact solution of the field equations of GB-Maxwell gravity. The presence of two exact extremal solutions (the extremal soliton interpolating through a throat region the $AdS_2 \times R_3$ geometry with the asymptotic AdS geometry and the $AdS_2 \times R_3$ geometry itself) is a typical feature of extreme black branes describing BPS states (see e.g. Refs. [24, 25]). The two solutions correspond to two different extremal limits. As we will see in Sect. 2.10, the presence of two different extremal, exact, solutions give rise to a non-trivial extremal thermodynamic behaviour.

2.9.5 f_+ Branch

This branch does not describe a BB but a spacetime with a singularity for every value of the parameters $Q \neq 0, M \neq 0$. Depending on the value of the parameter α_2 we have either a spacetime with a naked singularity (for $\alpha_2 > 0$) or a cosmological, asymptotically de Sitter (dS) solution with a singularity (for $\alpha_2 < 0$.) This follows from the above discussion of the singularities of the scalar curvature (2.81). In the f_+ branch the spacetime always has a singularity, which can be located at $r = 0$ or $r = \sqrt{Y_1}$ depending on the values of the parameters. This is consistent with the results of Ref. [11], according to which the f_+ branch is unstable and contains ghosts.

For $M, \alpha_2 > 0$, the metric functions for the f_+ branch are the dashed lines shown in Figs. 2.7. An interesting, peculiar feature is that in this case, all the solutions of the f_- branch are continuously connected with the solution of the f_+ branch passing trough the singularity. This feature has a simple analytic explanation. In the cases under consideration the singularities are the zeros of the function $g(Y)$ and when $g(Y) = 0$ then $f_+ = f_-$. This fact can have interesting holographic implications: we have two CFTs with different central charges connected through the same singularity.

For $M > 0$ and $\alpha_2 < 0$, the f_+ branch describes a cosmological solution with a singularity. The corresponding metric functions are shown (dashed lines) in Fig. 2.8. Also in this case the solutions of the f_- branch with an horizon are continuously connected with the solution of the f_+ branch passing trough the singularity. We have now an asymptotically AdS solution continuously connected through a cosmological singularity to a late de Sitter geometry. On the other hand, the solutions of the f_- branch describing a naked singularity are disconnected from the cosmological solutions.

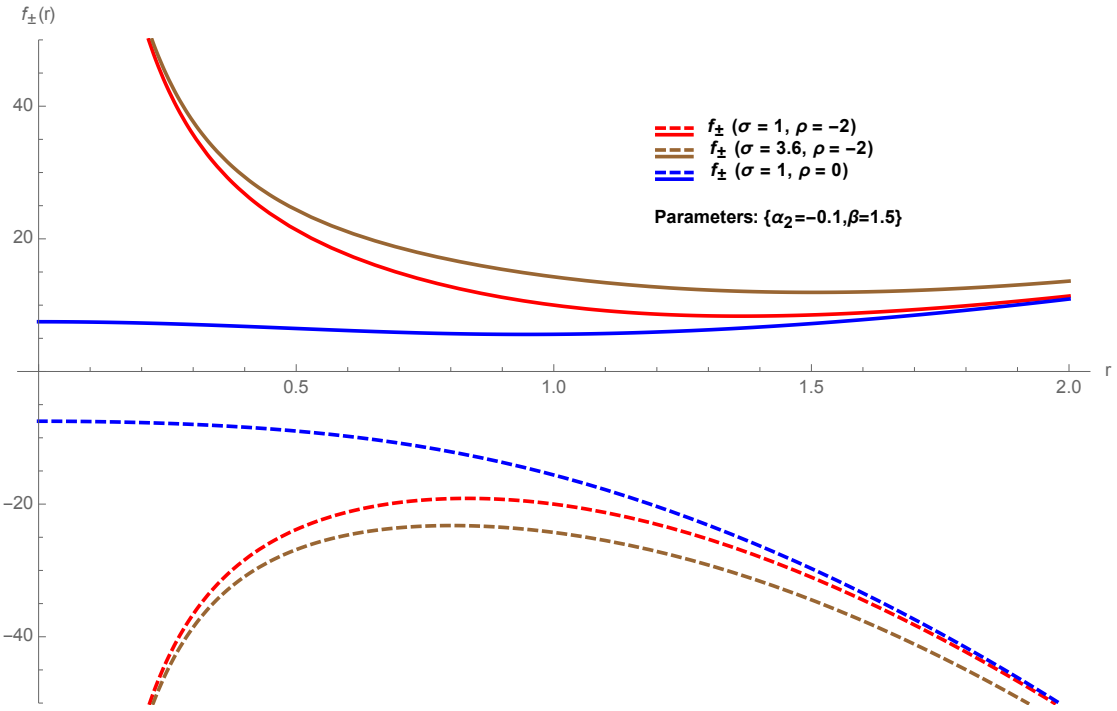

FIGURE 2.9: **Behaviour of the metric functions $f_\pm$ for $\alpha_2, M < 0$ and selected values of the other parameters.** The dashed (solid) lines describe the f_+ branch (f_- branch). The solid lines describe spacetimes with naked singularities, whereas the dashed lines describe cosmological, asymptotically dS solutions with a singularity.

For $\alpha_2, M < 0$, the f_+ branch describes a cosmological solution with a singularity with late de Sitter behaviour, whereas the f_- branch describes an asymptotically AdS spacetime with a naked singularity. However, here the two branches are disconnected. The metric functions for this case are shown in Fig. 2.9.

It should be stressed that in the $Q = 0$ case, the f_+ branch has ghosts in the spectrum [11]. We naturally expect this to extend to the charged case and is consistent with the intrinsic instability of these branch of solutions connected with the presence of naked singularities.

2.10 Charged Gauss-Bonnet Black Brane Thermodynamics

In this section, we will study the thermodynamics of the GB BB solutions,i.e., solutions in the f_- branch and make a comparison with the Reissner-Nordström black branes. The effective thermodynamic potentials $M = M_{ADM}/N, S, \Phi$ and the temperature $T = T_H/N$ can be written as functions of the horizon radius r_+ and the charge Q by specializing Eqs. (2.66),(2.67),(2.68) to $d = 5$. We obtain the

following equations

$$\begin{aligned} M &= \frac{r_+^4}{\omega_5 L^2}\left(1+\frac{4\pi}{3}\frac{G_N Q^2 L^2}{r_+^6}\right), \quad T=\frac{1}{\pi L^2}\left(r_+ - \frac{2\pi G_N Q^2 L^2}{3r_+^5}\right), \\ S &= \frac{V_3}{4G_N}\left(\frac{r_+}{L}\right)^3, \quad \Phi = \frac{V_3}{2L^3}\frac{Q}{r_+^2}, \end{aligned} \tag{2.96}$$

that satisfy the first principle $dM = TdS + \Phi dQ$. As pointed out in Sect. 2.7.1, because of the universality of the thermodynamic behaviour, the thermodynamic relations (2.96) hold for both for the charged GB and the RN BB. The only difference is that for the GB brane, with metric function (2.78), M and T are the effective parameters whereas in the RN case $M = M_{ADM}$ and $T = T_H$.

In order to have a clear and complete description of the GB BB thermodynamics, one should eliminate r_+ from the Eqs. (2.96) and write $M(T,Q), S(T,Q)$. This parametrization cannot be done in analytic form because we have to solve a 6^{th} grade equation in r_+. Thus, we will derive the explicit scaling behaviour of M and S as a function of the temperature in the large and small T limit. These relations will shed light on the holographic interpretation of the solutions.

2.10.1 Scaling Behaviour

The functions $M(T,Q)$ and $S(T,Q)$ can be obtained in implicit form by using the second equation in (2.96) as an implicit definition of the function $r_+(T,Q)$, and they read

$$M(T,Q) = \frac{r_+^3}{\omega_5 L^2}\left(3r_+ - 2\pi L^2 T\right), \qquad S(T,Q) = \frac{V_3}{4G_N}\left(\frac{r_+}{L}\right)^3. \tag{2.97}$$

Let us now consider separately the two limits of interest: $T \to \infty$ and $T \to 0$.

2.10.2 Large Temperature

The limit $T \to \infty$ corresponds to large radius BB, i.e., $r_+ \to \infty$. In this regime, the temperature scales linearly with r_+

$$T \simeq \frac{r_+}{\pi L^2} \tag{2.98}$$

and, at the leading order, we get for M and S

$$M = \frac{3V_3 L^3}{16\pi G_N}(\pi T)^4\,, \qquad S = \frac{V_3 L^3}{4G_N}(\pi T)^3\,. \tag{2.99}$$

This is exactly the scaling behaviour one expects for a UV fixed point described by a CFT_4.

Because of the universality of the thermodynamic behaviour, the relations (2.99) hold for both the RN and the GB BB. In the former case, Eqs. (2.99) hold when $M = M_{ADM}, T = T_H$, in the latter when M, T are given by the effective values in Eq. (2.65). Thus, for the GB BB, mass and entropy acquire a $1/N^3$ factor.

2.10.3 Small Temperature

The $T \to 0$ thermodynamic behaviour corresponds to extremal BBs in which the BPS bound (2.87) is saturated. This is achieved at non vanishing, constant value of the BB radius

$$r_+ = \left(\frac{2\pi G_N L^2 Q^2}{3}\right)^{1/6} \equiv r_0 \tag{2.100}$$

that corresponds, as expected for BPS states, to the extremal brane $T = 0$ state with non vanishing mass and entropy given by

$$M_{ext} = \frac{3r_0^4}{2\omega_5 L^2}, \qquad S_{ext} = \frac{V_3}{4G_N}\left(\frac{r_0}{L}\right)^3. \tag{2.101}$$

We can now expand in Taylor series the temperature near r_0 to obtain

$$T \simeq \frac{3}{\pi L^2}\left[2(r_+ - r_0) - \frac{5}{r_0}(r_+ - r_0)^2\right], \tag{2.102}$$

and the behaviour of M and S near $T = 0$ is of the form

$$M - M_{ext} = \frac{2r_0^2}{3\omega_5}(\pi L T)^2 + \mathcal{O}(T^4), \quad S - S_{ext} = \frac{\pi r_0^2 V_3}{8G_N L}T + \mathcal{O}(T^2)\,. \tag{2.103}$$

Again, universality of the thermodynamic behaviour imply that the relations in Eq. (2.103) hold both for the RN and for the GB BB. For the RN case, the relations take the same form with $M = M_{ADM}$ and $T = T_H$. For the GB case, when we express the relations (2.103) in terms of ADM mass and Hawking temperature we

get

$$\begin{aligned} M_{ADM} &= NM_{ext} + \frac{2r_0^2}{3N\omega_5}(\pi L T_H)^2 + \mathcal{O}(T^4) \\ S &= S_{ext} + \frac{\pi r_0^2 V_3}{8NG_N L} T_H + \mathcal{O}(T^2). \end{aligned} \tag{2.104}$$

2.10.4 Excitations Near Extremality and the Near-Horizon Limit

An important feature of the RN BB, which in view of the previous results extends to the charged GB BB, is that the semiclassical analysis of its thermodynamic behavior breaks down near extremality [24, 25]. In fact, the energy of an Hawking radiation mode is of order T_H and the semiclassical description breaks down when this energy is comparable with the energy above extremality $M - M_{ext}$ given by Eq. (2.103). This results in an energy gap for excitations above extremality [24], which in the case under consideration is $E_{gap} \sim (N\omega_5)/L^2 r_0^2$. The fact that the extremal limit is singular, can be also understood in geometrical terms. It has been observed that at extremality the geometry splits into two spacetimes: an extremal black hole and a disconnected AdS space [26].

The presence of this energy gap has important consequences for what concerns the spectrum of BB excitations near extremality. In particular, whereas in the extremal case the near-horizon geometry is given, as shown in Sect. 2.9.3.1, by $\mathrm{AdS}_2 \times R_3$, finite energy excitations of $\mathrm{AdS}_2 \times R_3$ are suppressed. Analogously to the RN case in $4d$ [24], one can consider near-horizon limits not restricted to zero temperature and excitation energy. These limits are obtained by letting the $5d$ Planck length L_P go to zero, holding fixed some of the other physical parameters of the BB (energy, charge and temperature).

References

[1] Larry Smarr. "Mass formula for Kerr black holes". In: *Phys.Rev.Lett.* 30 (1973), pp. 71–73.

[2] S.W. Hawking and Don N. Page. "Thermodynamics of Black Holes in anti-De Sitter Space". In: *Commun.Math.Phys.* 87 (1983), p. 577.

[3] F.R. Tangherlini. "Schwarzschild field in n dimensions and the dimensionality of space problem". In: *Nuovo Cim.* 27 (1963), pp. 636–651.

[4] Matt Visser. "Dirty black holes: Thermodynamics and horizon structure". In: *Phys.Rev.* D46 (1992), pp. 2445–2451. arXiv: hep-th/9203057 [hep-th].

[5] Robert Gilmore. *Catastrophe Theory for Scientists and Engineers*. 1St Edition. John Wiley & Sons Inc, June 1981.

[6] Andrew Chamblin et al. "Charged AdS black holes and catastrophic holography". In: *Phys.Rev.* D60 (1999), p. 064018. arXiv: hep-th/9902170 [hep-th].

[7] D. Lovelock. "The Einstein tensor and its generalizations". In: *J.Math.Phys.* 12 (1971), pp. 498–501.

[8] Jorge Zanelli. "Lecture notes on Chern-Simons (super-)gravities. Second edition (February 2008)". In: (2005). arXiv: hep-th/0502193 [hep-th].

[9] Rong-Gen Cai and Kwang-Sup Soh. "Topological black holes in the dimensionally continued gravity". In: *Phys. Rev.* D59 (1999), p. 044013. arXiv: gr-qc/9808067 [gr-qc].

[10] Ted Jacobson and Shankar Venkataramani. "Topology of event horizons and topological censorship". In: *Class. Quant. Grav.* 12 (1995), pp. 1055–1062. arXiv: gr-qc/9410023 [gr-qc].

[11] David G. Boulware and Stanley Deser. "String Generated Gravity Models". In: *Phys. Rev. Lett.* 55 (1985), p. 2656.

[12] James T. Wheeler. "Symmetric Solutions to the Gauss-Bonnet Extended Einstein Equations". In: *Nucl.Phys.* B268 (1986), p. 737.

[13] James T. Wheeler. "Symmetric Solutions to the Maximally Gauss-Bonnet Extended Einstein Equations". In: *Nucl.Phys.* B273 (1986), p. 732.

[14] Rong-Gen Cai. "A Note on thermodynamics of black holes in Lovelock gravity". In: *Phys.Lett.* B582 (2004), pp. 237–242. arXiv: hep-th/0311240 [hep-th].

[15] Xian O. Camanho and Jose D. Edelstein. "A Lovelock black hole bestiary". In: *Class.Quant.Grav.* 30 (2013), p. 035009. arXiv: 1103.3669 [hep-th].

[16] Tomohiro Takahashi and Jiro Soda. "Pathologies in Lovelock AdS Black Branes and AdS/CFT". In: *Class.Quant.Grav.* 29 (2012), p. 035008. arXiv: 1108.5041 [hep-th].

[17] Alejandra Castro et al. "On the Universality of Inner Black Hole Mechanics and Higher Curvature Gravity". In: *JHEP* 07 (2013), p. 164. arXiv: 1304.1696 [hep-th].

[18] David Kastor, Sourya Ray, and Jennie Traschen. "Mass and Free Energy of Lovelock Black Holes". In: *Class. Quant. Grav.* 28 (2011), p. 195022. arXiv: 1106.2764 [hep-th].

[19] Ted Jacobson and Robert C. Myers. "Black hole entropy and higher curvature interactions". In: *Phys.Rev.Lett.* 70 (1993), pp. 3684–3687. arXiv: hep-th/9305016 [hep-th].

[20] Xian-Hui Ge and Sang-Jin Sin. "Shear viscosity, instability and the upper bound of the Gauss-Bonnet coupling constant". In: *JHEP* 05 (2009), p. 051. arXiv: 0903.2527 [hep-th].

[21] E. B. Bogomolny. "Stability of Classical Solutions". In: *Sov. J. Nucl. Phys.* 24 (1976). [Yad. Fiz.24,861(1976)], p. 449.

[22] M. K. Prasad and Charles M. Sommerfield. "An Exact Classical Solution for the 't Hooft Monopole and the Julia-Zee Dyon". In: *Phys. Rev. Lett.* 35 (1975), pp. 760–762.

[23] Antonia M. Frassino et al. "Multiple Reentrant Phase Transitions and Triple Points in Lovelock Thermodynamics". In: *JHEP* 09 (2014), p. 080. arXiv: 1406.7015 [hep-th].

[24] Juan Martin Maldacena, Jeremy Michelson, and Andrew Strominger. "Anti-de Sitter fragmentation". In: *JHEP* 02 (1999), p. 011. arXiv: hep-th/9812073 [hep-th].

[25] M. Cadoni and C. N. Colacino. "Thermodynamical behavior of composite stringy black holes". In: *Nucl. Phys.* B590 (2000), pp. 252–260. arXiv: hep-th/0004037 [hep-th].

[26] Sean M. Carroll, Matthew C. Johnson, and Lisa Randall. "Extremal limits and black hole entropy". In: *JHEP* 11 (2009), p. 109. arXiv: 0901.0931 [hep-th].

Chapter 3

Black Hole Chemistry

As seen in the previous chapter, the study of BH thermodynamics provides crucial information to the underlying structure of quantum gravity. In this chapter, a recently new development in this area will be discussed: The proposal that the mass of an AdS BH should be interpreted as the enthalpy of spacetime H instead of the internal energy U (as in Chap. 2). The enthalpy H is defined as a thermodynamic potential, that consists of the internal energy of the system U plus the product of pressure P and volume V of the system: $H = U + PV$. This kind of total *gravitational enthalpy* takes into account the possibility of including in the first law of black hole thermodynamics the variation of physical "constants", such as the cosmological constant Λ [1, 2, 3].
The cosmological constant Λ can be considered as a thermodynamic variable analogous to pressure in the first law. This proposal has been shown to provide a rich panoply[1] of thermodynamic behaviors for both AdS and dS black holes. Furthermore, by introducing this pressure, it can be shown that there is a complete analogy between four-dimensional RN-AdS black holes and the Van der Waals liquid/gas system, with the critical exponents coinciding with those of the Van der Waals system as predicted by the mean field theory. These results, significantly modify previous considerations that emerged from the duality description [21, 22, 23, 24].

The *extended thermodynamic phase space* implied by this proposal is well motivated for a variety of reasons:

[1] These include the existence of *reentrant phase transitions* in rotating [4] and Born-Infeld [5] black holes and the existence of a tricritical point in rotating black holes analogous to the triple point in water [6] (see also [3, 7, 8, 9, 10, 11, 12, 13, 14, 15, 16, 17, 18, 19, 20]).

- In the extended phase space both the Smarr relations (which can be derived geometrically [2]) and the first law of thermodynamics hold, whereas in the conventional phase space only the latter relation is satisfied for nonzero Λ.
- The use of an extended thermodynamic phase space is consistent with considering more fundamental theories of physics that admit variation of physical constants.
- Finally, comparing the physics of black holes with real world thermodynamic systems becomes a much more reasonable possibility [25], insofar as tricriticality, reentrant phase transitions, and Van der Waals behaviour all have counterparts in laboratory physics[2].

This new perspective has been shown to provide some novel insights and new phenomena in BH thermodynamics, including the realization that the phase-transition between large AdS black holes and radiation can be understood as a liquid/solid phase transition. Also, the discovery that charged BHs behave as Van der Waals fluids and the findings of reentrant phase transitions, in which there are phase transitions from large BHs to small ones and then back to large again as the temperature monotonically increases or the presence of triple points for Kerr-AdS black holes [6], where a coalescence of small, medium, and large sized BHs merge into a single kind at a specific critical value of pressure and temperature, analogous to the triple point of water. A natural question is whether this new way to study black hole thermodynamics can be embedded in the AdS/CFT background (see Sec. 3.5). In Ref. [27], the author suggests that one can trace the dynamical pressure given by Λ to a dynamically changing N_c in the large N_c gauge theory story.

The purpose of this chapter is to provide a detailed thermodynamical analysis of some Einstein's gravity theories considering the cosmological constant as a dynamical pressure. In particular, the investigation of the thermodynamics of regular AdS black holes and (second and third order) Lovelock black holes in a canonical ensemble[3] will be presented. It will be showed that the thermodynamics of AdS black holes in both cases are, under certain circumstances, comparable to the "every day thermodynamics" of simple substances, such as reentrant phase transition of multicomponent liquids, multiple first order solid/liquid/gas phase transition and liquid/gas phase transitions of the Van der Waals type.

[2] An review of these issues in the context of rotating black holes was recently carried out in [26].

[3] This means that for generic black holes we study the thermodynamics for fixed charge Q in the case of charged black holes (and/or fixed black hole angular momenta J_i in the case of rotating black hole).

As explained in Sec. 2.3, an important example of transition in AdS-BH spacetime is the radiation/large black hole first order phase transition of Hawking and Page conjectured for Schwarzschild-AdS black holes immersed in a bath of radiation. Such a phenomenon has a dual interpretation for a boundary QFT via the AdS/CFT correspondence and is related to a confinement/deconfinement phase transition in the dual quark-gluon plasma. For charged or rotating black holes and regular black holes, one likewise observes a small/large black hole phase transition reminiscent of the liquid/gas transition of the Van der Waals (VdW) fluid. It is well known that in standard thermodynamics, the VdW equation approximates the behaviour of real fluids using a two parameter a, b closed form modification to the ideal gas law. The fluid parameters a and b are characteristics of a given fluid. The VdW equation takes into account the non-zero size of the fluid molecules (described by a constant parameter $b > 0$) and the attraction between them (described by a constant parameter $a > 0$) and is often used to describe qualitative features of the liquid-gas phase transition.
Moreover, new phenomena appear in higher dimensions: in Lovelock gravity, for example, it is possible to find a peculiar behaviour reminiscent of *reentrant phase transition* (RPT) observed for multicomponent fluid systems, gels, ferroelectrics, liquid crystals and binary gases. A system undergoes an RPT if a monotonic variation of any thermodynamic quantity results in two (or more) phase transitions such that the final state is macroscopically similar to the initial state.

3.1 Extended Phase Space Thermodynamics

By considering on AdS-BH, one can assume that the mass of black hole in AdS background should be understood as the enthalpy of the spacetime. It emerged from geometric derivations of the Smarr formula for AdS black holes that, the cosmological constant is a thermodynamic variable analogous to pressure in the first law of black hole thermodynamics, i.e.

$$P = -\frac{\Lambda}{8\pi} = \frac{(d-1)\,(d-2)}{16\pi b^2} \tag{3.1}$$

where $d = n + 1$ stands for the number of spacetime dimensions, Λ is the cosmological constant and b denotes the AdS radius. The conjugate quantity to the thermodynamic pressure is the thermodynamic volume V. The thermodynamic volume has dimensions of $(\text{length})^{d-1}$ and describes a spatial volume characterizing the black hole spacetime. Once the thermodynamic volume is known and

the cosmological constant identified with the volume, one can, for a given BH, write down the corresponding "fluid" equation of state relating pressure, temperature, volume and other external parameters characterizing the black hole, i.e. $P = P(V, T, J_i, Q)$ where there are N independent angular momenta J_i and Q is the charge. Then, the equation of state allows one to employ standard thermodynamic machinery and calculate the critical exponents associated with the critical point.

The equilibrium thermodynamics is usually governed by the Gibbs free energy, $G = G(T, P, J_i, Q)$ whose global minimum yields the state of a system for fixed (T, P, J_i, Q). Since in this case the pressure is considered as a thermodynamical variable, the BH mass M is interpreted as the enthalpy. Then one has the following thermodynamic relation

$$G = M - TS = G(P, T, J_i, Q) \tag{3.2}$$

where T and S stand for the horizon temperature and the BH entropy. Understanding the behaviour of G is essential in this context to find possible thermodynamics phase transitions. While in the case of RBH it is possible to write the Gibbs free energy explicitly, in the case of Lovelock gravity it is not. For this reason, in the charged Lovelock case (see Sec. 3.3), one needs to fix the pressure, the charge and the third order Lovelock parameter to particular values and plot G numerically to obtain information about the possible phase transitions.

Once the behaviour of the Gibbs free energy is known, one can construct the associated *phase diagrams*. These are drown in the $P - T$ plane and display the coexistence lines of various BH phases, interrelated by the first order phase transitions and the possible critical points where the coexistence lines terminate/merge together. The local thermodynamic stability of a canonical ensemble is characterized by positivity of the specific heat at constant pressure C_P (and so we take negativity of C_P as a sign of local thermodynamic instability). Once the behaviour of the Gibbs free energy is known, one can construct the associated *phase diagrams*. These are drown in the $P-T$ plane and display the coexistence lines of various BH phases, interrelated by the first order phase transitions and the possible critical points where the coexistence lines terminate/merge together. The local thermodynamic stability of a canonical ensemble is characterized by positivity of the specific heat at constant pressure C_P (and so we take negativity of C_P as a sign of local thermodynamic instability). Before going into detailed analysis for the two cases of interest, one can start seeing the thermodynamics of two simple examples when

we do not have the thermodynamic pressure corresponding to Λ.
In the asymptotically flat background one has:

1. *Schwarzschild black hole.* The Schwarzschild black hole has only negative specific heat which corresponds to local thermodynamic instability. In this case, the Gibbs free energy has no interesting features indicating the absence of phase transitions.

2. *Charged black hole.* When the charge Q is added to the Schwarzschild black hole, the Reissner-Nordstrom (RN) black hole is obtained. The specific heat capacity is positive for a small strongly charged black holes. This range corresponds to a thermodynamically stable branch of near extremal black holes which globally minimize the Gibbs free energy. Consequently and counter-intuitively (because the entropy is larger when $C_P < 0$), in a fixed charge canonical ensemble strongly charged small RN black holes are thermodynamically preferred to weakly charged (almost Schwarzschild-like) large black holes.

Now, the same two examples in case of asymptotically AdS background become:

1. *Schwarzschild-AdS black hole.* In the Schwarzschild-AdS spacetime , C_P is no longer always negative: it becomes positive for large BHs (when compared to the AdS radius). As we know from Hawking-Page (sec. 2.3), there is a minimum temperature T_{min} below which no BH can exist and there is only thermal AdS space.Above this temperature we have two branches of BHs. The upper one corresponding to small black holes with $C_P < 0$ that are thermodynamically unstable. While the large BHs at lowest branch (so lowest free energy) have $C_P > 0$ and hence are locally thermodynamically stable. However, just above T_{min} the Gibbs free energy of such BHs is positive and the thermal AdS space with approximately zero Gibbs free energy represents a globally preferred thermodynamic state. This continues until temperature $T_{HP} \approx 1/(\pi b)$ for which the Gibbs free energy becomes negative, with the corresponding BH radius given by $r_{HP} = b$. Black holes with $r_+ > r_{HP}$ have negative Gibbs free energy and represent the *globally* preferred state. This means that at a critical temperature $T = T_{HP}$ there is a first order Hawking-Page phase transition between thermal radiation and large black holes.
   Now, considering an extended phase space and rewriting the equation for the temperature

$$T = \frac{1}{4\pi\, r_+\, b^2}\left(b^2 + 3\, r_+^2\right) \tag{3.3}$$

in terms of the pressure (3.1), we get a corresponding *fluid equation of state*. At this point it is possible to plot the different isotherms in a $P-V$ diagram. For each isotherm there is a maximum at the volume $1/\pi T$ (i.e. when $r_+ = r_{min}$)

2. *Charged AdS black hole.* In a canonical (fixed charge) ensemble, RN-AdS BHs allow for a first order small/large BH phase transition reminiscent of the liquid/gas transition in a VdW fluid. This analogy becomes more complete in the extended phase space. In fact in this case, the $P-V$ diagram resembles the behaviour of the VdW equation. Below a certain critical pressure P_c, the Gibbs free energy displays a characteristic swallowtail behaviour, indicating a first order small/large BH phase transition indeed.

3.2 Phases of Regular Black Holes

As first simpler example, one can consider the RBH thermodynamic system. In the presence of an AdS cosmological term, also the regularized metric offers an extension of the Hawking-Page transition into a van der Waals-like phase diagram. Specifically, the regular Schwarzschild-Anti-deSitter geometry undergoes a first order small/large black hole transition similar to the liquid/gas transition of a real fluid. In the present analysis, the cosmological constant is considered as a dynamical quantity and its variation is included in the first law of BH thermodynamics. This introduces an extended thermodynamic phase space in which both the Smarr relations and the first law of thermodynamics should hold. In the beginning, the $n = 3$ case is consider then a $n-$dimensional generalization will be presented.

3.2.1 Thermodynamics and Equation of state

The temperature associated to the event horizon r_+ can be computed through the formula $T = \frac{1}{4\pi} V'(r)|_{r=r_+}$ and reads

$$T = \frac{1}{4\pi r_+}\left\{1 + \frac{r_+^2}{b^2}\left(3 - r_+\frac{\gamma'(r_+)}{\gamma(r_+)}\right) - r_+\frac{\gamma'(r_+)}{\gamma(r_+)}\right\} \tag{3.4}$$

where in this case one can use the following notation: $\gamma(r_+) \equiv \gamma\left(\frac{3}{2}, \frac{r_+^2}{4\theta^2}\right)$ and $\gamma'(r_+) = \frac{r_+^2}{4\theta^3} e^{-r_+^2/4\theta^2}$ is its derivative with respect to r_+. In contrast to the standard Schwarzschild-AdS case, extremal solution exists with vanishing Hawking

temperature given by Eq. (3.4). Using Eq. (3.1) to substitute b in (3.4), the *equation of state* $P(V,T)$ for the regular AdS-BH becomes

$$P = \frac{3\gamma(r_+)}{3\gamma(r_+) - r_+\gamma'(r_+)}\left\{\frac{T}{2r_+} - \frac{1}{8\pi r_+^2} + \frac{\gamma'(r_+)}{8\pi r_+\gamma(r_+)}\right\}. \tag{3.5}$$

Using the equation of state (3.5) it is possible to plot the isotherm functions in a $P-V$ diagram for a regular black hole (see Fig. 3.1) that resembles the van der Waals pressure-volume diagram.

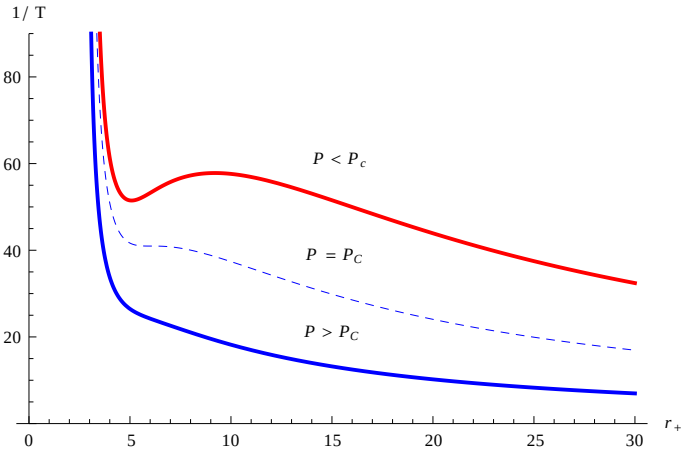

FIGURE 3.1: **Regular black hole inverse temperature as function of r_+ (with $\theta = 1$).** When$P < P_c$, there are three branches. The middle branch is unstable, while the branch with the smaller radii and the one with bigger radii are stable. This graph reproduces the pressure-volume diagram of the van der Waals theory, provided one identifies the black hole thermodynamic variables $\beta \equiv 1/T$, r_+ and P respectively with pressure pressure, volume and temperature of the van der Waals gas.

3.2.2 Gibbs Free Energy

To complete the analogy between the regular BH and a VdW gas, one proceeds by calculating the Gibbs free energy [9, 16]. This can be done by using the action of the Euclidean metric (see for example [28]). Such an action provides the Gibbs free energy via $G = I/\beta$ where β is the period of the imaginary time $\beta \equiv 1/T$. Then, the Gibbs free energy can be expressed as a function of pressure and temperature. The Hawking-Page transition takes place when the Gibbs energy changes its sign from positive to negative. In the regular black hole case, considering the cosmological constant as a pressure and using the Euclidean action given by $I = \int d^4x\sqrt{g}R$ one finds

$$G = \frac{r_+}{12\,G_N}\left[3 - 8P\pi r_+^2 + \frac{r_+\left(3 + 8P\pi r_+^2\right)\gamma'(r_+)}{\gamma(r_+)}\right]. \tag{3.6}$$

The Gibbs free energy (3.6) exhibits a characteristic swallowtail behavior (see Fig. (3.2)). This usually corresponds to a small black hole/large black hole first-order phase transition [16, 21] By performing the classical limit for $r_+ \gg \theta$ one gets the usual result for a classical uncharged Schwarzschild-AdS black hole that is

$$G(T,P) = \frac{1}{4G_N}\left(r_+ - \frac{8\pi}{3} P\, r_+^3\right) \tag{3.7}$$

as showed in Ref.[16]. Remarkably, in the regular Schwarzschild-AdS black hole case, as in the RN-AdS spacetime, there is a phase transition that occurs at positive Gibbs energy. This fact is visible from the presence of the swallowtail in Fig. (3.2). To investigate this aspect one needs to study the sign of the heat capacity. As underlined in [9], the specific heat related to the black hole is calculated at constant pressure

$$C_p = \left(\frac{\partial H}{\partial T}\right)_P = \left(\frac{\partial H}{\partial r_+}\right)_P \left(\frac{\partial r_+}{\partial T}\right)_P , \tag{3.8}$$

where the enthalpy H is identified with the black hole mass M. Now, the phase transitions can be studied from the change of the sign of the specific heat: the stability requires that the specific heat at fixed pressure is $C_p \geq 0$ and the specific heat at fixed volume is $C_v \geq 0$. In the case under investigation C_v is always equal to zero because the entropy is only volume dependent. This means that the heat capacity C_v does not diverge at the critical point and its critical exponent is $\alpha = 0$. By studying the sign of the function C_p, we can see that for $P > P_c$ the quantity C_p is always positive and the black hole is stable. In the limit $P \to P_c$ there is a critical value for r_+ for which C_p diverges. For $P < P_c$ there are two discontinuities of the specific heat and the situation is the same as in the RN-AdS black holes [29]. Thus, in the regular Schwarzschild-AdS case for $P < P_c$ it seems that a different phase transition is allowed because the heat capacity changes again from positive values to negative values. For large r_+ we have the Hawking-Page behavior in which the branch with negative specific heat has lower mass and thus falls in an unstable phase, while the branch with larger mass is locally stable and corresponds to a positive specific heat. Thus, the resulting phase diagram presents a critical point at a critical cosmological constant value in Plank units and a smooth crossover thereafter.

3.2.3 Critical Exponent

From the previous discussion, one can already establish the critical exponent $\alpha = 0$. Then, by defining the variable $t \equiv (T - T_c)/T_c$, one can compute the critical

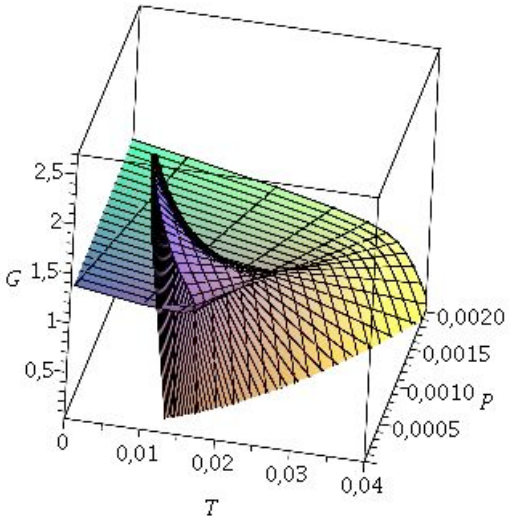

FIGURE 3.2: [
Gibbs free energy as function of the black hole pressure and temperature. The Gibbs free energy G changes its sign at a specific T and P (intersection of the function with the $T-P$-plane). As in the van der Waals case, the phases are controlled by the universal 'cusp', typical of the theory of discontinuous transitions. The Gibbs free energy shows the "swallowtail" shape, a region where $G(T,P)$ is a multivalued function. This region ends in a point (T_c, P_c). In the region with $P < P_c$ and $T < T_c$ we can see a transition between small black hole/large black hole. Note that r_+ is a function of temperature and pressure via the equation of state Eq. (3.5). For large value of P (or T) there is only one branch allowed.] **Gibbs free energy as function of the pressure and temperature.** The Gibbs free energy G changes its sign at a specific T and P (intersection of the function with the $T-P$-plane). As in the van der Waals case, the phases are controlled by the universal 'cusp', typical of the theory of discontinuous transitions [21]. The Gibbs free energy shows the "swallowtail" shape, a region where $G(T,P)$ is a multivalued function. This region ends in a point (T_c, P_c). In the region with $P < P_c$ and $T < T_c$ we can see a transition between small black hole/large black hole. Note that r_+ is a function of temperature and pressure via the equation of state Eq. (3.5). For large value of P (or T) there is only one branch allowed.

exponent of C_p by evaluating the ratio $\ln\left(C_p\left(t\right)\right)/\ln\left(t\right)$ in the limit $t \to 0$. This limit in this case is well-defined and the critical exponent is $\gamma = 1$. This result implies that the heat capacity diverges near the critical point like $C_p \propto |t|^{-1}$. Then using the scaling relations

$$\alpha + 2\beta' + \gamma = 2 = \beta'\left(1+\delta\right) \tag{3.9}$$

is possible to calculate the other two exponents, i.e., δ that determines the behaviour of the isothermal compressibility of a VdW system and β' that describes the behaviour of the difference between of the volume of the gas phase and the

liquid phase. For the regular black hole, the scaling relations give $\delta = 3$ and $\beta' = 1/2$, result that coincides with the case of charged black holes [16]. These critical exponents are consistent with the Ising mean field values

$$(\alpha, \beta', \gamma, \delta) = (0, 1/2, 1, 3) \tag{3.10}$$

allowing for an efficient mean field theory description. Since it is believed that the determination of critical exponents define universality classes , i.e., they do not depend on the details of the physical system (exept the number of dimensions), we can say that the phase transitions in the regular Schwarzschild-AdS black holes and in the RN-AdS black holes in four-dimensional spacetime have the same nature.

3.2.4 Extension to n-spacetime Dimensions

The results presented in the previous sections can be extended to a generic number of dimensions. The fundamental ingredient is the Euclidean action in generic number of dimensions. In the more specific case $n = 4$, the Gibbs free energy is given from the same equation $G = I/\beta$ and the equation of state can be easily calculated using the $n-$dimensional definition of the temperature. Performing the same calculation for the critical exponents one get the same result of mean-field theory: The critical exponents do not depend on the space dimension.

3.3 Phases of Lovelock Black Holes

Using the Hamiltonian formalism it is possible to derive the expression for gravitational entropy in Lovelock gravity and the corresponding first law of black hole thermodynamics [30]. More recently, both the first law and the associated Smarr formula in an extended phase space were obtained exploiting the Killing potential formalism [31].

In the *extended thermodynamic phase space*, all Lovelock coupling constants (including the cosmological constant $\hat{\alpha}_{(0)}$) are considered as thermodynamic variables and allowed to vary in the first law of black hole thermodynamics. The physical meaning of these variables along with their conjugates, apart from the cosmological constant which has an interpretation of pressure and its conjugate variable is an associated volume, remains to be explored.[4]

[4] A similar situation was seen to occur in Born–Infeld electrodynamics, in which the thermodynamics conjugate to the Born–Infeld coupling constant was interpreted as vacuum polarization [5].

3.3.1 Thermodynamic Considerations

Considering now Lovelock BH, charged under a Maxwell field, $F = dA$, with the action given by (cf. Eq.(2.48))

$$I = \frac{1}{16\pi G_N}\int d^dx\sqrt{-g}\Big(\sum_{k=0}^{k_{max}}\hat{\alpha}_{(k)}\mathcal{L}^{(k)} - 4\pi G_N F_{ab}F^{ab}\Big)\,, \tag{3.11}$$

the corresponding equations of motion read

$$\sum_{k=0}^{k_{max}}\hat{\alpha}_{(k)}\mathcal{G}^{(k)}_{ab} = 8\pi G_N\Big(F_{ac}F_b{}^c - \frac{1}{4}g_{ab}F_{cd}F^{cd}\Big)\,. \tag{3.12}$$

For a BH solution, characterized by mass M, charge Q, temperature T, and entropy S, the extended first law and the associated Smarr relation read [30, 31]

$$\delta M = T\delta S - \frac{1}{16\pi G_N}\sum_k \hat{\Psi}^{(k)}\delta\hat{\alpha}_{(k)} + \Phi\delta Q\,, \tag{3.13}$$

$$(d-3)\,M = (d-2)\,TS + \sum_k 2\,(k-1)\,\frac{\hat{\Psi}^{(k)}\hat{\alpha}_{(k)}}{16\pi G_N} + (d-3)\,\Phi Q\,. \tag{3.14}$$

In Lovelock gravity, the BH entropy is no longer given by one quarter of the horizon area, but rather reads

$$S = \frac{1}{4G_N}\sum_k \hat{\alpha}_k\mathcal{A}^{(k)}\,, \quad \mathcal{A}^{(k)} = k\int_{\mathcal{H}}\sqrt{\sigma}\mathcal{L}^{(k-1)}\,. \tag{3.15}$$

Here, σ denotes the determinant of σ_{ab}, the induced metric on the BH horizon $\mathcal{H}$, and the Lovelock terms $\mathcal{L}^{(k-1)}$ are evaluated on that surface. Potentials $\hat{\Psi}^{(k)}$ are the thermodynamic conjugates to $\hat{\alpha}_{(k)}$'s and are given by

$$\hat{\Psi}^{(k)} = 4\pi T\mathcal{A}^{(k)} + \mathcal{B}^{(k)} + \Theta^{(k)}\,, \tag{3.16}$$

where

$$\begin{aligned}\mathcal{B}^{(k)} &= -\frac{16\pi k G_N M(d-1)!}{b(d-2k-1)!}\left(-\frac{1}{\ell^2}\right)^{k-1}, \quad b = \sum_k \frac{\hat{\alpha}_k k(d-1)!}{(d-2k-1)!}\left(-\frac{1}{\ell^2}\right)^{k-1},\\ \Theta^{(k)} &= \int_\Sigma\sqrt{-g}\mathcal{L}^{(k)}[s] - \int_{\Sigma_{\rm AdS}}\sqrt{-g_{\rm AdS}}\mathcal{L}^{(k)}[s_{\rm AdS}]\,,\end{aligned} \tag{3.17}$$

and ℓ stands in this case for the AdS radius and b is given by a particular polynomial of the AdS radius. The potentials are a non-trivial function of the "bare"

cosmological constant $\Lambda = -\hat{\alpha}_0/2$ and the higher-order Lovelock couplings. Σ is a spatial hypersurface spanning from the BH horizon to spatial infinity, with timelike unit normal n^a and induced metric $s_{ab} = g_{ab} + n_a n_b$; quantities with "AdS subscript" are pure AdS space counterparts of the corresponding BH spacetime quantities, with no internal boundary and the same $\hat{\alpha}_0$.
In what follows, the (negative) cosmological constant $\Lambda = -\hat{\alpha}_0/2$ with the thermodynamic pressure and the conjugate quantity $\hat{\Psi}^{(0)}$ with the thermodynamic volume V, are defined according to an equation similar to (3.1),

$$P = -\frac{\Lambda}{8\pi G_N} = \frac{\hat{\alpha}_0}{16\pi G_N}\,, \quad V = -\hat{\Psi}^{(0)}\,. \tag{3.18}$$

3.3.2 Lovelock Thermodynamic Quantities

The black hole mass M, the temperature T, the entropy S, and the gauge potential Φ are given by [32]

$$M = \frac{\Sigma^{(\kappa)}_{d-2}\,(d-2)}{16\pi G_N}\sum_{k=0}^{k_{max}} \alpha_k \kappa^k r_+^{d-1-2k} + \frac{\Sigma^{(\kappa)}_{d-2}}{2(d-3)}\frac{Q^2}{r_+^{d-3}}\,, \tag{3.19}$$

$$T = \frac{|f'(r_+)|}{4\pi} = \frac{1}{4\pi r_+ D(r_+)}\left[\sum_k \kappa\alpha_k(d-2k-1)\Big(\frac{\kappa}{r_+^2}\Big)^{k-1} - \frac{8\pi G_N Q^2}{(d-2)r_+^{2(d-3)}}\right] \tag{3.20}$$

$$S = \frac{\Sigma^{(\kappa)}_{d-2}\,(d-2)}{4G_N}\sum_{k=0}^{k_{max}} \frac{k\kappa^{k-1}\alpha_k r_+^{d-2k}}{d-2k}\,, \quad \Phi = \frac{\Sigma^{(\kappa)}_{d-2} Q}{(d-3)r_+^{d-3}}\,, \tag{3.21}$$

where

$$D(r_+) = \sum_{k=1}^{k_{max}} k\alpha_k \left(\kappa r_+^{-2}\right)^{k-1}\,. \tag{3.22}$$

The leading term in the expression for S is one-quarter the horizon area; the other terms come from higher-curvature contributions. Note that S does not explicitly depend on the cosmological constant or the charge Q. Using the expression for M, one finds the following formulae for the potentials $\Psi^{(k)}$ conjugate to α_k, $\delta M = T\delta S + \Phi\delta Q + \sum_k \Psi^{(k)}\delta\alpha_k$:

$$\Psi^{(k)} = \frac{\Sigma^{(\kappa)}_{d-2}(d-2)}{16\pi G_N}\kappa^{k-1} r_+^{d-2k}\left[\frac{\kappa}{r} - \frac{4\pi k T}{d-2k}\right]\,, \quad k \geq 0\,. \tag{3.23}$$

and the thermodynamic volume

$$V = -\hat{\Psi}^{(0)} = \frac{16\pi G_N \Psi^{(0)}}{(d-1)(d-2)} = \frac{\Sigma^{(\kappa)}_{d-2} r_+^{d-1}}{d-1}\,, \tag{3.24}$$

while the other potentials read

$$\hat{\Psi}^{(1)} = \Psi^{(1)}\,, \quad \hat{\Psi}^{(k)} = -16\pi G_N \prod_{n=3}^{2k}(d-n)\Psi^{(k)}\,, \quad k \geq 2\,. \tag{3.25}$$

One can then verify that the Smarr relation (3.14) and the first law (3.13) are satisfied. Note that $\hat{\alpha}_{(1)}$ effectively captures a possible change in the gravitational constant G_N.In the following sections, the couplings α_k for $k \geq 1$ are treated as fixed external parameters and only the cosmological constant and hence α_0 is considered a thermodynamic variable.

Using (3.18) and (3.24), this allows to reinterpret equation (3.20) as the Lovelock "fluid equation of state"

$$\begin{aligned} P &= P(V, T, Q, \alpha_1, \ldots, \alpha_{k_{max}}) && (3.26)\\ &= \frac{d-2}{16\pi G_N} \sum_{k=1}^{k_{max}} \frac{\alpha_k}{r_+^2}\left(\frac{\kappa}{r_+^2}\right)^{k-1}\Big[4\pi k r_+ T - \kappa(d-2k-1)\Big] + \frac{Q^2}{2\alpha_1 r_+^{2(d-2)}} && (3.27) \end{aligned}$$

and study the possible phase transitions based on the behavior of the Gibbs free energy in the canonical ensemble, given by

$$G = M - TS = G(P, T, Q, \alpha_1, \ldots, \alpha_{k_{max}})\,. \tag{3.28}$$

where the favourite thermodynamic state corresponds to the global minimum of this quantity for fixed parameters P, T, Q and α's.

3.3.3 Constraint Conditions For Hyperbolic Black Holes

Before going to the general thermodynamic discussion, one should noting two phenomena present for hyperbolic black holes, $\kappa = -1$.

- First, for such BHs a "thermodynamic singularity" (also known as a "branch singularity" [33]), characterized by

$$\left.\frac{\partial P}{\partial T}\right|_{V=V_s} = 0\,, \tag{3.29}$$

will be present. Where $V = V_s$ is a value in the $P - V$ diagram, which is a $2d$ projection of the $3d$ $P = P(V, T)$ relation, where the isotherms will cross.

The above Eq. (3.29) lead to the condition

$$D(r_+)|_{\text{TD singularity}} = \sum_{k=1}^{k_{max}} k\,\alpha_k \left(\kappa^{d-1} \left[\frac{\Sigma_{d-2}^{(\kappa)}}{(d-1)V_s} \right]^2 \right)^{\frac{k-1}{d-1}} = 0\,, \tag{3.30}$$

upon using (3.24) in (3.22). For $\kappa = -1$, this equation will have at least one real solution for $k \geq 2$, and will have up to $(k-1)$ distinct solutions in k-th order Lovelock gravity. This generic situation stands in contrast to $k = 0$ Einstein-Maxwell gravity, where this relation is absent [5]. Upon inspection of equations (3.20) and (3.28), one can see that both the temperature and the Gibbs free energy diverge at $V = V_s$ (M and S are finite for all values of P and V), apart from a very special choice of the pressure $P = P_s$ for which both T and G are finite and T takes the special value $T = T_s$. By taking the derivative of the entropy (3.21) with respect to r_+ it straightforward to show that the entropy is maximized for V_s and P_s as well [33].
Apart from $P = P_s$, the thermodynamic singularity reflects the presence of a curvature singularity of the Riemann tensor, since the Kretschmann scalar at the horizon is

$$K(r_+) = R_{abcd}R^{abcd}|_{r=r_+} = \left[\left(\frac{d^2 f}{dr^2} \right)^2 + \frac{2(d-2)}{r^2} \left(\frac{df}{dr} \right)^2 + \frac{2(d-2)(d-3)}{r^4} \right]_{r=r_+} . \tag{3.31}$$

However by analytically continuing around (P_s, V_s, T_s) one can not only make sense of thermodynamics but also show that the Kretschmann scalar is finite. We shall discuss this for the concrete example in Sec. 3.4.4.5.

- Second, when $\kappa = -1$, the entropy S is given in (3.21), and it is not always positive. Demanding its positivity imposes the following condition:

$$\sum_{k=1}^{k_{max}} \frac{k\kappa^{k-1}\alpha_k r_+^{d-2k}}{d-2k} = \sum_{k=1}^{k_{max}} \frac{k\kappa^{k-1}\alpha_k}{d-2k} \left[\frac{(d-1)V}{\Sigma_{d-2}^{(\kappa)}} \right]^{\frac{d-2k}{d-1}} \geq 0\,. \tag{3.32}$$

In what follows BHs with negative entropy are considered unphysical and excluded from thermodynamic considerations.

3.3.4 Lovelock Parameters

In principle, one may consider α_k to have arbitrary positive or negative values[5]. However, for cubic (or higher order) Lovelock gravities, there are entire regions of the parameter space where there are no black holes at all, even if there is a well defined AdS vacuum. For 3rd-order Lovelock gravity, negative values of α_k yield solutions with naked singularities over a broad parameter range [37]. Moreover, in the low energy effective action of heterotic string theory α_2 is proportional to the inverse string tension and hence is positive. For all these reasons, in this section the Lovelock couplings $\alpha_2 > 0$ and $\alpha_3 > 0$ are considered positive. Moreover, from now the parameter α_1 is setted equal to one to recover general relativity in the small curvature limit and also $G_N = 1$.

3.3.4.1 2nd-order Lovelock Gravity

For $k = 2$ (i.e. Gauss-Bonnet solution) and generic curvature κ, Eq. (2.61) reduces to a quadratic equation

$$\alpha_2 \frac{(\kappa - f)^2}{r^4} + \frac{(\kappa - f)}{r^2} + \alpha_0 - \frac{\omega_d M}{r^{d-1}} + \frac{8\pi G_N Q^2}{(d-2)(d-3)r^{2d-4}} = 0\,, \tag{3.33}$$

from which one obtains two possible solutions, $f_\pm$. In the following, the solution f_- is referred as the '*Einstein branch*' because it approaches the Einstein case when the Gauss–Bonnet coupling α_2 goes to zero and f_+ as the '*Gauss–Bonnet branch*' [38]. The quadratic Eq. (3.33) gives the following necessary condition requirement for the existence of $f_\pm$ for large r:

$$1 - 4\alpha_0\alpha_2 \geq 0\,. \tag{3.34}$$

When this inequality is violated, the space becomes compact because of the strong nonlinear curvature [38]. Therefore, there is no asymptotic 'AdS region' and consequently no proper black hole with standard asymptotics.

[5] Up to now, most of the information needed to clarify the existence of black hole solutions for different values of the Lovelock couplings has relied on the behaviour of cubic polynomials, see, e.g., Eq. (2.61) in [34], or on the AdS/CFT calculations [35, 36].

3.4 $P - v$ Criticality in 3rd-order Lovelock Gravity

In this section thermodynamic phenomena of $U(1)$ charged black holes in 3rd-order Lovelock gravity are considered. After some general considerations we concentrate on $d = 7$ and $d = 8$, the lowest two dimensions for which 3rd-order Lovelock theory brings new qualitative features.

3.4.1 Maximal Pressure and Other Conditions

In Sec. 3.3.4.1, it has been seen that in the Gauss–Bonnet case, the requirement for the existence of an asymptotic "AdS region" imposes an important bound on how high the cosmological pressure can be in order the solution not to collapse into a compact region. Here the analogous discussion is presented for the 3rd-order Lovelock. In the Lovelock case the following cubic equation for the metric function f has to be satisfied to have an asymptotic AdS region :

$$\begin{aligned} &\alpha_3 \frac{(\kappa - f)^3}{r^6} + \alpha_2 \frac{(\kappa - f)^2}{r^4} + \frac{(\kappa - f)}{r^2} + A_0(r) = 0\,, \\ &A_0(r) = \alpha_0 - \frac{16\pi M}{(d-2)\Sigma^{(\kappa)}_{d-2} r^{d-1}} + \frac{8\pi Q^2}{(d-2)(d-3)r^{2d-4}}\,, \end{aligned} \tag{3.35}$$

whose solution is

$$f = \kappa + \frac{r^2}{\sqrt{\alpha_3}} X\,, \tag{3.36}$$

where X is a solution to the equation $X^3 - \frac{\alpha_2}{\sqrt{\alpha_3}} X^2 + X - \sqrt{\alpha_3} A_0(r) = 0$. The resulting three solutions can be labelled in the following way: *Einstein branch* ($f_{\rm E}$), the *Gauss-Bonnet branch* ($f_{\rm GB}$), and the *Lovelock branch* ($f_{\rm L}$). The solution $f_{\rm E}$ approaches the Einstein branch upon successively taking the limit $\alpha_3 \to 0$ and then $\alpha_2 \to 0$; $f_{\rm GB}$ approaches the Gauss-Bonnet branch (that does not exist in the limit $\alpha_2 \to 0$), and $f_{\rm L}$ represents a new branch which does not have a smooth limit when $\alpha_3 \to 0$. When the following condition is satisfied,

$$4\alpha_3 - \alpha_2^2 + 27\alpha_0^2\alpha_3^2 - 18\alpha_0\alpha_2\alpha_3 + 4\alpha_0\alpha_2^3 \leq 0\,. \tag{3.37}$$

all three branches admit an asymptotic "AdS region". Equality represents a quadratic equation for α_0, whose solution is

$$p_\pm = \frac{(d-1)(d-2)}{108\pi}\left[9\alpha - 2\alpha^3 \pm 2(\alpha^2 - 3)^{3/2}\right], \tag{3.38}$$

in terms of the following dimensionless parameters:

$$\alpha = \frac{\alpha_2}{\sqrt{\alpha_3}}, \quad p = 4\sqrt{\alpha_3}P = \frac{\alpha_0(d-1)(d-2)\sqrt{\alpha_3}}{4\pi}. \tag{3.39}$$

It is possible to define two parameter regions according to the asymptotics of solutions of the various branches.[6]

- Region I, occurs for values of α and p outside the envelope of the region bounded by the $p_\pm$ curves. In this region only the Lovelock branch has proper AdS asymptotics whereas the Gauss-Bonnet and Einstein branches either do not exist as real solutions or represent a compact space.
- Region II, is inside the region bounded by the $p_\pm$ curves. In this region all three branches admit proper AdS asymptotics. The situation is displayed in Fig. 3.3.

Regions I and II were defined according to the asymptotic structure. Further restriction ensue when horizons are taken into consideration. Consider for simplicity the uncharged case. When $\kappa = -1$ it can be shown that Region I always admits Lovelock BHs at least in a certain range of parameters, whereas region II admits all three kinds of BHs. The situation is more restrictive when $\kappa = +1$. Region II then admits only Einstein type BHs whereas region I splits into a Region Ia and Region Ib. In Region Ia, defined by ($\alpha < \sqrt{3}$) or ($\sqrt{3} < \alpha < 2$ and $p < p_-$), Lovelock black holes exist in a certain parameter range. In Region Ib, defined by ($\alpha > \sqrt{3}$ and $p > p_+$), no BHs can exist. This is illustrated in Fig. 3.4.

3.4.2 Equation of State

In terms of (3.39) and the following dimensionless quantities (v, t, m, q):

$$r_+ = v\,\alpha_3^{\frac{1}{4}}, \quad T = \frac{t\alpha_3^{-\frac{1}{4}}}{d-2}, \quad m = \frac{16\pi M}{(d-2)\Sigma_{d-2}^{(\kappa)}\alpha_3^{\frac{d-3}{4}}}, \quad Q = \frac{q}{\sqrt{2}}\alpha_3^{\frac{d-3}{4}}, \tag{3.40}$$

[6] Note that whereas the asymptotic structure is independent of the values of the charge and mass, the existence of horizons is affected by it.

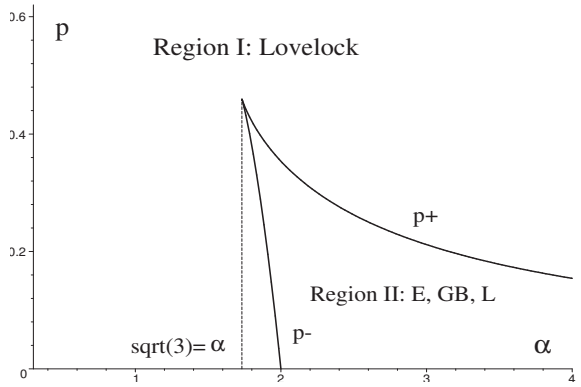

FIGURE 3.3: **Branches with 'AdS' asymptotics.** According to the asymptotics of solutions of the various branches the $\alpha - p$ space splits into 2 parameter regions. In region I only the Lovelock branch admits AdS asymptotics. In region II all three branches admit the correct asymptotics. In this case $d = 7$, for other dimensions the behavior is qualitatively similar ($p_\pm$ are appropriately scaled by d-dependent factor).

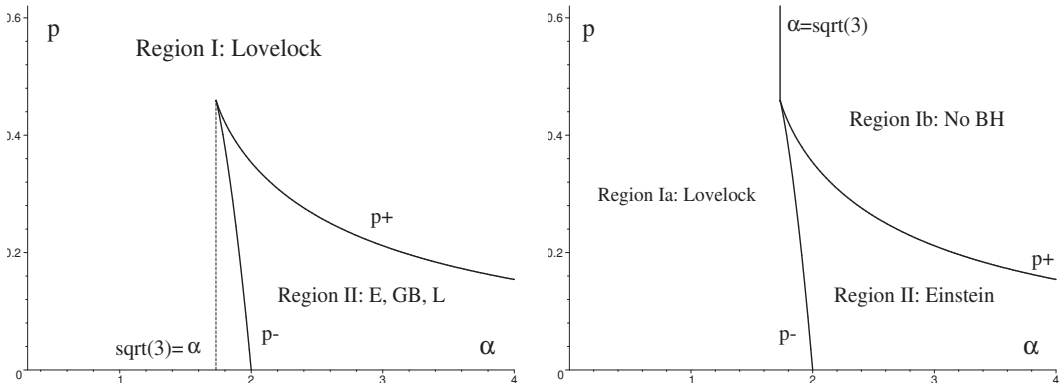

FIGURE 3.4: **Possible uncharged black holes.** *Left:* $\kappa = -1$ *case.* The Lovelock black holes may exist in region I for a certain range of parameters; all 3 kinds may exist in region II. *Right:* $\kappa = +1$ *case.* Region I now splits into 2 regions: the Lovelock region Ia and the no black hole region Ib. In region II only Einstein branch possesses horizons and can represent a black hole. We have displayed $d = 7$ case, for $d = 8$ the situation is qualitatively similar.

the equation of state (3.26) for 3rd-order Lovelock $U(1)$ charged black holes now reduces to ($\kappa = \pm 1$)

$$\begin{aligned} p \;=\; & \frac{t}{v} - \frac{(d-2)(d-3)\kappa}{4\pi v^2} + \frac{2\alpha\kappa t}{v^3} - \frac{(d-2)(d-5)\alpha}{4\pi v^4} + \frac{3t}{v^5} \\ & - \frac{(d-2)(d-7)\kappa}{4\pi v^6} + \frac{q^2}{v^{2(d-2)}}\,. \end{aligned} \tag{3.41}$$

Now, one can also investigate a dimensionless counterpart of the Gibbs free energy,

$$g = \frac{1}{\Sigma^{(\kappa)}_{d-2}} \alpha_3^{\frac{3-d}{4}} G = g(t, p, q, \alpha)\,, \tag{3.42}$$

which reads

$$\begin{aligned} g &= -\frac{1}{16\pi(3+2\alpha\kappa v^2+v^4)}\Big[\frac{4\pi p v^{d+3}}{(d-1)(d-2)}-\kappa v^{d+1}+\frac{24\pi\kappa p\alpha v^{d+1}}{(d-1)(d-4)} \\ &\quad -\frac{\alpha v^{d-1}(d-8)}{d-4}+\frac{60\pi p v^{d-1}}{(d-1)(d-6)}-\frac{2\kappa\alpha^2 v^{d-3}(d-2)}{d-4}+\frac{4\kappa v^{d-3}(d+3)}{d-6} \\ &\quad -\frac{3\alpha v^{d-5}(d-2)(d-8)}{(d-4)(d-6)}-\frac{3\kappa v^{d-7}(d-2)}{d-6}\Big] \\ &\quad +\frac{q^2}{4(3+2\alpha\kappa v^2+v^4)(d-3)v^{d-3}}\Big[\frac{v^4(2d-5)}{d-2}+\frac{2\alpha\kappa(2d-7)v^2}{d-4}+\frac{3(2d-9)}{d-6}\Big]. \end{aligned} \tag{3.43}$$

The thermodynamic state corresponds to the global minimum of this quantity for its fixed parameters t, p, q and α. A critical point occurs when $p = p(v)$ has an inflection point, i.e., when

$$\frac{\partial p}{\partial v} = 0\,, \quad \frac{\partial^2 p}{\partial v^2} = 0\,. \tag{3.44}$$

Together with the equation of state (3.41) this determines the critical values $\{p_c, v_c, t_c\}$ as functions of q and κ. To find a critical point we have to solve (higher-order polynomial) Eqs. (3.44) for t_c, v_c and insert the result into the equation of state (3.41) to find p_c, subject to the restriction that p_c, v_c, t_c are all positive in order the critical point be physical. Solving the first equation in (3.44) for t_c yields

$$t_c = \frac{(d-2)}{2\pi v_c(v_c^4+6\alpha\kappa v_c^2+15)}\Big[3\kappa(d-7)+2\alpha(d-5)v_c^2+(d-3)\kappa v_c^4-\frac{4\pi q^2}{v_c^{2(d-5)}}\Big]\,, \tag{3.45}$$

and the second equation in (3.44) then becomes

$$\begin{aligned} 0 &= (d-3)\,v_c^{2d-2}-12\,\alpha\,\kappa\,v_c^{2d-4}+6v_c^{2d-6}\big(2\alpha^2\,(d-5)+5-5d\big) \\ &\quad +12\,\kappa\,\alpha\,(2d-19)\,v_c^{2\,d-8}+45\,(d-7)\,v_c^{2\,d-10} \\ &\quad -4\pi\kappa q^2\big[(2\,d-5)\,v_c^4+6\kappa\alpha\,(2d-7)\,v_c^2+30d-135\big]\,. \end{aligned} \tag{3.46}$$

The thermodynamic singularity for the $\kappa = -1$ 3rd-order Lovelock black holes occurs when $v^4 - 2\alpha v^2 + 3 = 0$, i.e., for

$$v = v_{s\pm} = \sqrt{\alpha \pm \sqrt{\alpha^2-3}}\,. \tag{3.47}$$

A particularly interesting case occurs when the parameter $\alpha = \sqrt{3}$ (for which the two thermodynamic singularities 'coincide') and $q = 0$. In this case we find

$$v_s = 3^{1/4}\,, \quad t_s = \frac{d-2}{2\pi}3^{-1/4}\,, \quad p_s = \frac{(d-1)(d-2)}{36\pi}\sqrt{3}\,. \tag{3.48}$$

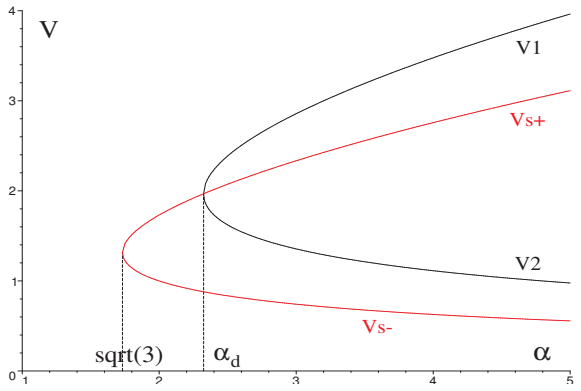

FIGURE 3.5: **Conditions for $\kappa = -1$ black holes.** The thermodynamic singularities occur on a thick red curve. The black hole entropy is positive to the left of the region outlined by thick black curve. We have chosen $d = 7$. As d increases, the red curve remains unchanged, whereas the black curve moves closer to it; the two curves coincide in the limit $d \to \infty$.

It is possible to check that the corresponding black hole has zero mass $M = 0$; such "massless" black holes can occur for hyperbolic geometries with appropriate identifications [39, 40, 41]. This very special case shall be discussed in Sec. 3.4.4.5. The positivity of entropy requires

$$(d-4)(d-6)v^4 - 2\alpha(d-2)(d-6)v^2 + 3(d-2)(d-4) > 0\,. \tag{3.49}$$

The corresponding admissible roots are

$$v_{1,2} = \sqrt{\frac{d-2}{d-4}\left(\alpha \pm \sqrt{\alpha^2 - \frac{3(d-4)^2}{(d-6)(d-2)}}\right)}\,, \tag{3.50}$$

and coincide when

$$\alpha = \alpha_d = \sqrt{\frac{3(d-4)^2}{(d-6)(d-2)}}\,. \tag{3.51}$$

For $\alpha < \alpha_d$ the entropy is always positive. The two conditions are displayed in Fig. 3.5. As one can see, for $\alpha < \sqrt{3}$ the BH entropy is always positive and there are no thermodynamic singularities. However, for $\alpha > \sqrt{3}$, we may have both positive and negative entropy BHs and thermodynamic singularities may be present. In the next two subsections the behavior of this equation in $d = 7$ and $d = 8$ dimensions, for various black hole topologies and various regions of the parameter space (q, α) is discussed.

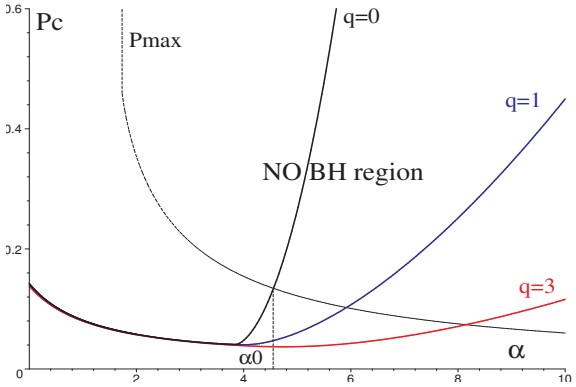

FIGURE 3.6: **Critical pressure: $d = 7$ and $\kappa = +1$.** In $d = 7$ and the spherical case we observe one critical point and the associated VdW behavior. The corresponding pressure p_c is displayed for $q = 0, 1, 3$. We observe that for $\alpha > \alpha_0 \approx 4.55$ there exists a minimum charge q_{min} such that for $q < q_{min}$ the critical pressure p_c exceeds the corresponding maximal pressure p_+ indicated as p_{max} in the plot.

3.4.3 Seven Dimensions

In seven dimensions the equation of state reduces to:

$$p = \frac{t}{v} - \frac{5\kappa}{\pi v^2} + \frac{2\alpha\kappa t}{v^3} - \frac{5\alpha}{2\pi v^4} + \frac{3t}{v^5} + \frac{q^2}{v^{10}}\,. \tag{3.52}$$

the critical temperature is

$$t_c = \frac{10}{\pi(v_c^4 + 6\alpha\kappa v_c^2 + 15)}\left[\alpha v_c + \kappa v_c^3 - \frac{\pi q^2}{v_c^5}\right], \tag{3.53}$$

and

$$v_c^{12} - 3\alpha\kappa v_c^{10} + 3(2\alpha^2 - 15)v_c^8 - 15\alpha\kappa v_c^6 - 3\pi\kappa q^2(3v_c^4 + 14\kappa\alpha v_c^2 + 25) = 0\,. \tag{3.54}$$

The AdS asymptotics of various branches is displayed in Figs. 3.3 and 3.4, positive entropy condition as well as thermodynamic singularities are displayed in Fig. 3.5, α_7 given by (3.51) now reads $\alpha_7 = 3\sqrt{3/5}$.

3.4.3.1 Spherical Case ($\kappa = +1$)

For BHs of spherical topology with charge or not, in the range $\alpha \in (0, 10)$, the equation of state admits exactly one critical point, characterized by the standard swallowtail mean field theory critical exponents (3.10), and the system demonstrates a VdW behavior. However, as α increases, the corresponding critical pressure, see Fig. 3.6, increases, and eventually exceeds the admissible pressure p_+,

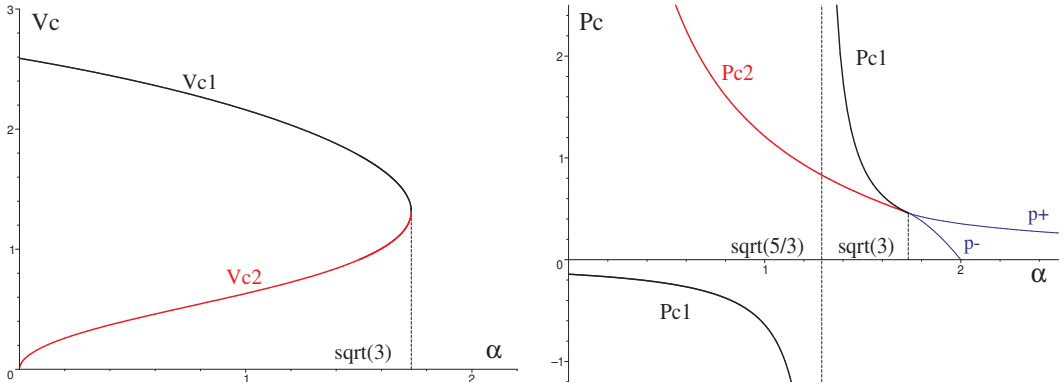

FIGURE 3.7: **Critical points in $d = 7$: $\kappa = -1, q = 0$ case.** Depending on the parameter α we may have up to two physical critical points. The special case is $\alpha = \sqrt{3}$ for which these two critical points 'coincide' forming a special critical point discussed in the next subsection.

that is occurs for a compact space solution. Alternatively, similar to the Gauss-Bonnet case, for each $\alpha > \alpha_0 \approx 4.55$ there exists a minimum charge q_{min} such that for $q < q_{min}$ the critical pressure p_c exceeds the corresponding maximal pressure set by p_+.

3.4.3.2 Hyperbolic Case ($\kappa = -1$): Multiple Reentrant Phase Transition

The hyperbolic case, $\kappa = -1$, is more interesting. When $q = 0$ and depending on the parameter α one may have up to two critical points (Fig. 3.7) and get various physical situations as summarized in Table 3.1. The corresponding $p - v$, $g - t$, and $p - t$ diagrams are displayed in Figs. 3.8–3.12. Namely, when $\alpha \in (0, \sqrt{5/3})$ one observes 1 physical critical point (with positive p_c, v_c and t_c) and the associated VdW-like first order small/large black hole phase transition terminating at a critical point characterized by the swallowtail critical exponents (3.10). Note however that, contrary to the $\kappa = +1$ case, the coexistence line terminates at a finite pressure p as $t \to 0$. At $\alpha = \sqrt{5/3}$ an additional physical critical point emerges with 'infinite' t_c that becomes finite and positive as α increases. In the range $\alpha \in (\sqrt{5/3}, \sqrt{3})$ two critical points and the associated VdW and "reverse VdW" behavior are present as shown in Figs. 3.9. At $\alpha = \sqrt{3}$, the two critical points merge together and a qualitatively new behaviour emerges. Increasing α even further, in the region $\alpha \in (\sqrt{3}, 3\sqrt{3/5})$ thermodynamic singularities appear.[7] However, these do not exist in the branches globally minimizing the Gibbs

[7] Associated with these singularities are the two reconnections of various branches—making the $g - t$ diagram quite complicated.

case	range of α	# critical points	behavior
I	$\alpha \in (0, \sqrt{5/3})$	1	VdW
II	$\alpha \in (\sqrt{5/3}, \sqrt{3})$	2	VdW & reverse VdW
III	$\alpha = \sqrt{3}$	1	special
IV	$\alpha \in (\sqrt{3}, 3\sqrt{3/5})$	0	infinite coexistence line
V	$\alpha > 3\sqrt{3/5}$	0	multiple RPT, infinite coexistence line

TABLE 3.1: Types of physical behavior in $d = 7, \kappa = -1, q = 0$ case.

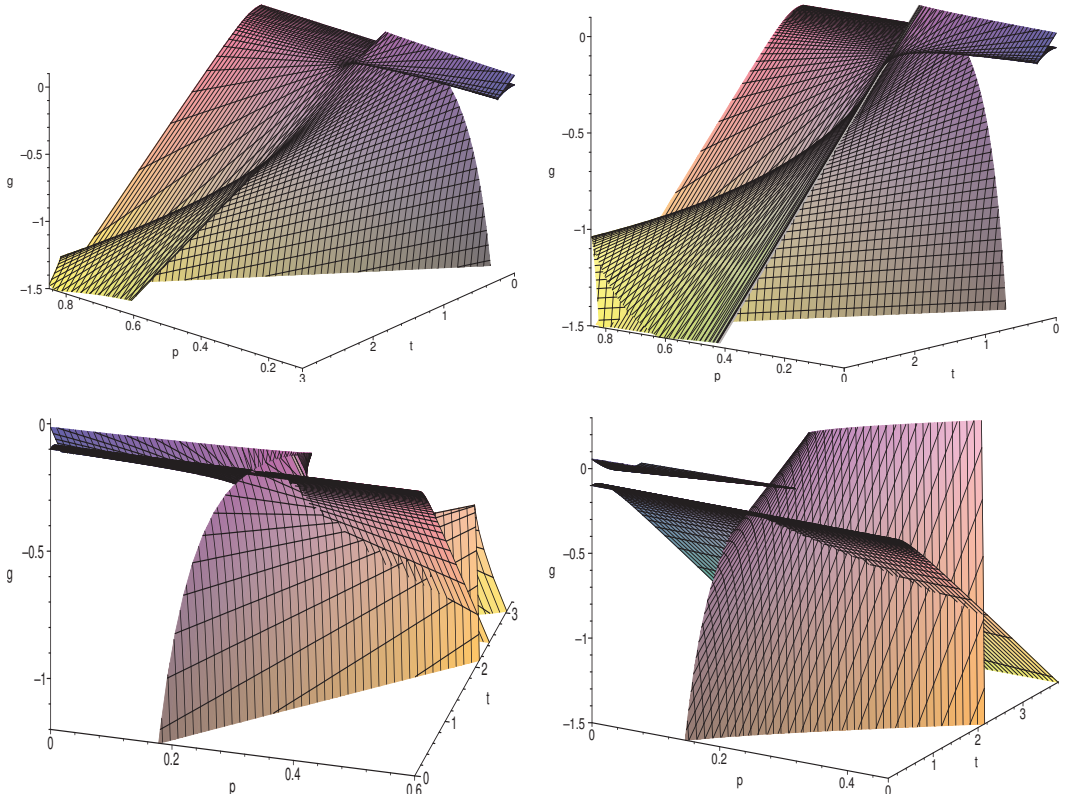

FIGURE 3.8: **Gibbs free energy: uncharged $d = 7, \kappa = -1$ case.** The Gibbs free energy is displayed successively for $\alpha = 1.65, \sqrt{3}, 1.85, 2.5$. In the $\alpha = 1.65$ case we observe a presence of two swallowtails that never occur at the same pressure. The $\alpha = \sqrt{3}$ is a special case for which the previous swallowtails emerge from the same isolated critical point, characterized by non-standard critical exponents. For $\alpha = 1.85 \in (\sqrt{3}, 3\sqrt{3/5})$ the behavior of g is quite complicated, however, the global minimum of g corresponds to one possible first-order phase transition. Finally, for $\alpha = 2.5 > 3\sqrt{3/5}$ the presence of negative entropy black holes effectively makes the admissible Gibbs 'discontinuous'. Besides the standard first-order phase transition, we can also observe, in a small range of pressures, the 'smooth' RPT and/or the zeroth-order phase transition, as displayed in Fig. 3.11 .

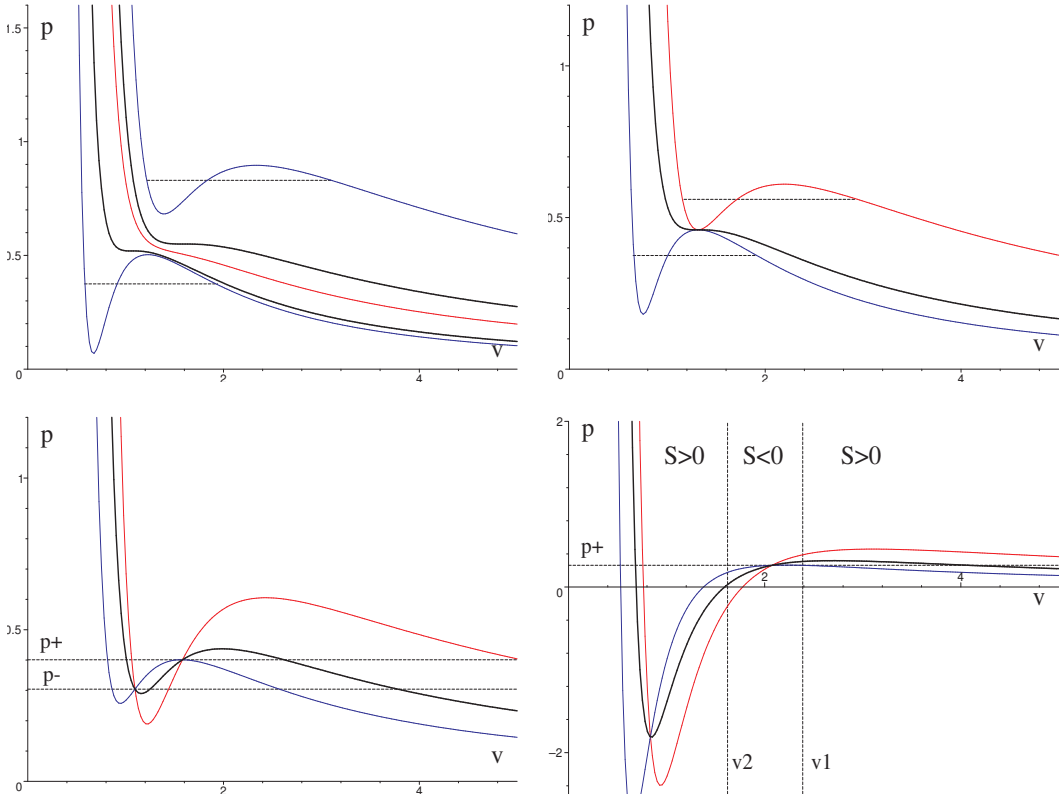

FIGURE 3.9: $p-v$ **diagram: uncharged** $d=7, \kappa=-1$ **case.** The $p-v$ diagram is displayed successively for $\alpha = 1.65, \sqrt{3}, 1.85, 2.5$. In the $\alpha = 1.65$ we observe two critical isotherms displayed by thick black curves, the isotherm with $(t_{c1}+t_{c2})/2$ is displayed by red curve and demonstrates the 'ideal gas behavior', whereas the isotherms with $t > t_{c2}$ and $t < t_{c1}$ display oscillations that are replaced according to Maxwell's equal area law. $\alpha = \sqrt{3}$ is a special case discussed in the next subsection. For $\alpha > \sqrt{3}$ we observe the presence of two thermodynamic singularities. The case $\alpha = 2.5 > 3\sqrt{3/5}$ moreover displays the region of negative entropy black holes, in between v_2 and v_1. We also display $p_\pm$ in these cases. Note that the temperatures 'reverse' in between the two thermodynamic singularities—hotter isotherms occur for lower pressures.

free energy.Therefore, solutions in this range of α have sensible thermodynamic behaviour, and a first-order phase transition as displayed in Fig. 3.10 d.

Similar behavior persists even for $\alpha > 3\sqrt{3/5}$. However in such a region some of the black holes may have negative entropy and hence are unphysical. Discarding such BHs, the Gibbs free energy is no longer continuous. Moreover, the hypersurface of large black holes displays interesting curved shape, see Fig. 3.11, leading to a *multiple reentrant phase transition* (RPT). To understand this phenomenon, one can look more closely at the 2d $g-t$ diagram displayed on RHS of Fig. 3.11. It is possible to observe that for $p \in (p_1 \approx 0.23209, p_2 \approx 0.23311)$ the branch of small BHs (displayed by a thick black curve that remains almost identical for various pressures) crosses twice the branches of large BHs -displayed by dashed colored curves- that moreover terminate at a finite temperature.

This indicates that there will be two first-order phase transitions, possibly accompanied, for $p \in (p_0 \approx 0.21809, p_2)$ and $t \in (0, t_z \approx 0.16864)$, by a *zeroth-order phase transition* like in [4]. Consider the constant pressure $p' = 1.002 \times p_1 \in (p_1, p_2)$ curves displayed in the diagram by thick black and dashed black lines. As the temperature decreases from say $t = 0.4$, the system follows the lower dashed black curve being a large black hole, until at $t_3 \approx 0.308$ the two branches cross and the system undergoes a first-order phase transition to a small BH. As t decreases even further the global minimum of g corresponds to the small BH on a thick black curve until at $t_2 \approx 0.20$ another first-order phase transition, this time to a large BH, occurs. Then the system follows the dashed black curve as a large BH until this terminates at $t_1 \approx 0.162$. If the temperature is decreased even further the system jumps to the thick black curve, undergoing the zeroth-order phase transition and becoming a small BH again. The RPT in chemistry was first observed in a nicotine/water mixture [42], and since seen in multicomponent fluid systems, gels, ferroelectrics, liquid crystals, and binary gases [43].

In summary, a reentrant large/small/large/small black hole phase transition is present. The corresponding $p - t$ phase diagram is displayed in Fig. 3.12.

3.4.3.3 Charged case.

When q is sufficiently small the behaviour is similar to the $q = 0$ case: namely, there are: one critical point in the range $0 < \alpha < \sqrt{5/3}$, two critical points for $\sqrt{5/3} < \alpha < \sqrt{3}$, and no critical points for $\alpha > \sqrt{3}$. More generally, the number of physical critical points in the (q, α)-parameter space is displayed on LHS of Fig. 3.13.
When $\alpha < \sqrt{5/3}$ there is the standard VdW behavior in the blue region with one critical point and no critical behavior in the grey region. For $\alpha \in (\sqrt{5/3}, \sqrt{3})$, as q increases one of the two critical temperatures decreases and soon becomes negative. Consequently, the VdW-like swallowtail disappears and for large q and one observes only the reverse VdW behavior; this is displayed in Fig. 3.14. The situation for $\alpha \geq \sqrt{3}$ is rather complicated because of the presence of thermodynamic singularities. The detailed study of this case can be considered for future study.

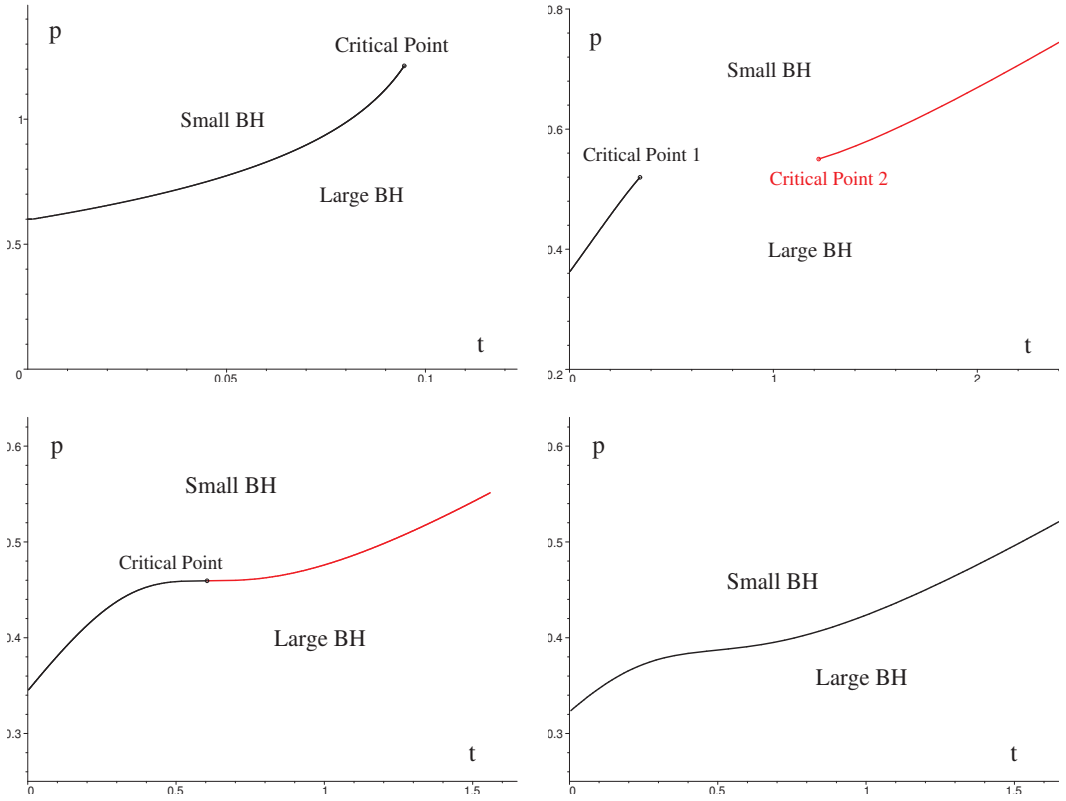

FIGURE 3.10: $p-t$ **phase diagram for** $\kappa=-1$**.** The distinct behaviour of the $p-t$ diagram is displayed for $\alpha=1, 1.65, \sqrt{3}, 1.85$. The $\alpha=\sqrt{3}$ case is a special case for which the two critical points 'coincide' forming an isolated critical point discussed in Sec. 4.5; for $\alpha\in(\sqrt{3}, 3\sqrt{3/5})$ we no longer observe a critical point, however, the first-order phase transition still persists. The case $\alpha>3\sqrt{3/5}$ demonstrates reentrant behavior and is discussed in the next figure.

3.4.4 Eight Dimensions

In eight dimensions there is the following equation of state:

$$p=\frac{t}{v}-\frac{15\kappa}{2\pi v^2}+\frac{2\alpha\kappa t}{v^3}-\frac{9\alpha}{2\pi v^4}+\frac{3t}{v^5}-\frac{3\kappa}{2\pi v^6}+\frac{q^2}{v^{12}}\,. \tag{3.55}$$

Eqs. (3.45) and (3.46) reduce to

$$t_c=\frac{3}{\pi v_c(v_c^4+6\alpha\kappa v_c^2+15)}\left[3\kappa+6\alpha v_c^2+5\kappa v_c^4-\frac{4\pi q^2}{v_c^6}\right], \tag{3.56}$$

and

$$5v_c^{14}-12\alpha\kappa v_c^{12}+6(6\alpha^2-35)v_c^{10}-36\alpha\kappa v_c^8+45v_c^6-4\pi\kappa q^2(11v_c^4+54\kappa\alpha v_c^2+105)=0\,. \tag{3.57}$$

The AdS asymptotics and various BH branches are qualitatively similar to those displayed in Figs. 3.3 and 3.4, positive entropy condition as well as thermodynamic

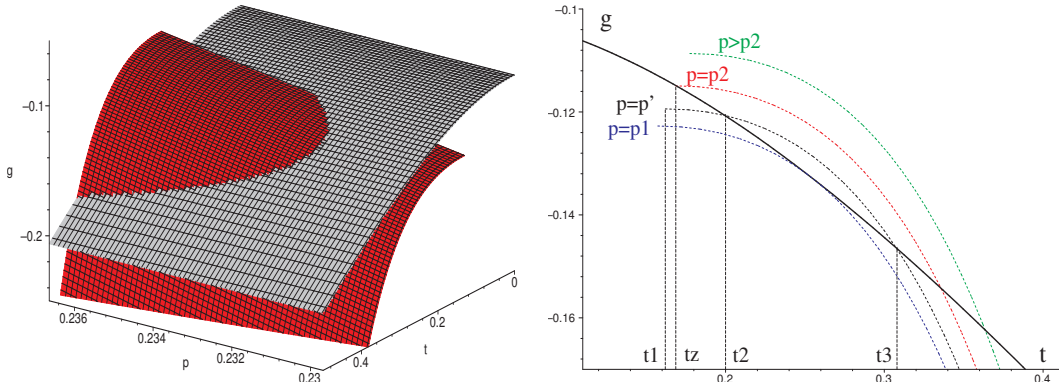

FIGURE 3.11: **Multiple RPT: Gibbs free energy.** The Gibbs free energy is displayed for $d = 7, q = 0, \kappa = -1, \alpha = 2.5 > 3\sqrt{3/5}$ case. *Left* figure is a close up of Fig. 3.8. *Right* figure represents $p = const.$ slices of the left one. We observe two branches: the branch of small black holes (displayed by a thick black curve—almost identical for various pressures) and the branch of large black holes displayed by dashed coloured curves. We do not display the surfaces of g for negative entropy black holes. Consequently, the Gibbs free energy seems discontinuous—the large black hole branch terminates at finite t. For $p \in (p_0 \approx 0.218088, p_2 \approx 0.2331108665$ we observe the zeroth-order phase transition. More interestingly, for any $p \in (p_1, p_2)$, the global minimum of g alternates from branch to branch: small and large black hole branches double cross indicating the presence of multiple RPT behavior. Namely, consider a constant pressure $p' = 1.002 \times p_1 \in (p_1, p_2)$ displayed by thick black and dashed black curves. As the temperature decreases from say $t = 0.4$, the system follows the lower dashed black curve being a large black hole, until at $t_3 \approx 0.308$ the two branches cross and the system undergoes a first-order phase transition to a small black hole. As t decreases even further the global minimum of g corresponds to the small black hole on a thick black curve until at $t_2 \approx 0.20$ another first-order phase transition, this time to a large black hole occurs. Then the system follows the dashed black curve as a large black hole until this terminates at $t_1 \approx 0.162$. If the temperature is decreased even further the system jumps to the thick black curve, undergoing the zeroth-order phase transition and becoming a small black hole again. In summary, we observe reentrant large/small/large/small black hole phase transition.

singularities behave as in Fig. 3.5, with $\alpha_8 = 2$. The number of possible critical points with positive (p_c, v_c, t_c) as we probe the (q, α)-parameter space is displayed in Figs. 3.13 and 3.15.

3.4.4.1 Spherical Case

The thermodynamic behavior is qualitatively different for uncharged and charged black holes. There are two important cases: i) reentrant phase transitions, present for uncharged black holes and ii) multiple first order phase transitions accompanied by a triple point, in the weakly charged case.

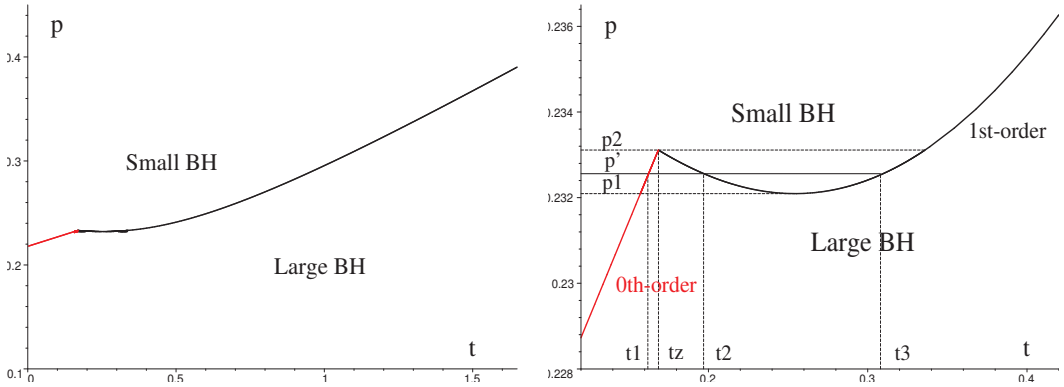

FIGURE 3.12: **Multiple RPT: $p-t$ phase diagram.** The $p-t$ phase diagram is displayed for $d=7, q=0, \kappa=-1, \alpha=2.5>3\sqrt{3/5}$. The thick black curve displays the first-order phase transition between small and large black holes, the red curve stands for the corresponding zeroth-order phase transition. *Right* figure represents a close up of the left figure. For a fixed pressure $p' \in (p_1, p_2)$ as temperature increases we may observe multiple phase transitions showing the reentrant behavior. Namely, we observe a phase transition from small black holes to large black holes, back to small black holes again, and finally to large black holes. The first transition is of the zeroth-order while the other two are of the first-order; the temperatures t_1, t_2 and t_3 coincide with those in Fig. 3.11 . The zeroth-order phase transition terminates at (t_z, p_2).

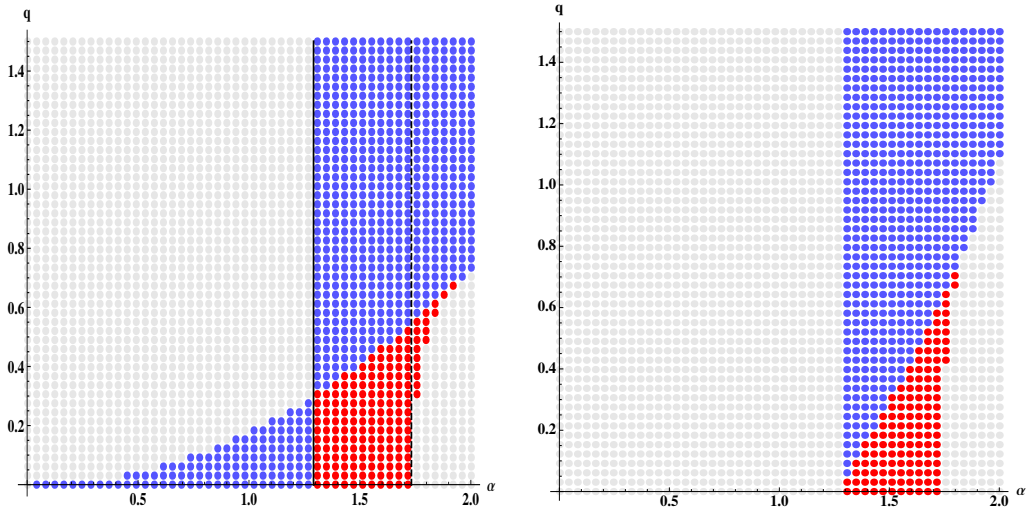

FIGURE 3.13: **Critical points in (q,α)-parameter space: $\kappa=-1$ case.** The number of critical points with positive (p_c, v_c, t_c) is displayed in the (q,α)-parameter space for $\kappa=-1$. Grey dots correspond to no critical points, blue to one critical point, and red to two; black solid and dashed lines highlight $\alpha=\sqrt{5/3}$ and $\alpha=\sqrt{3}$, respectively. Contrary to $d=7$ (*left*) case, in $d=8$ (*right*) there are no critical points for $\alpha<\sqrt{5/3}$.

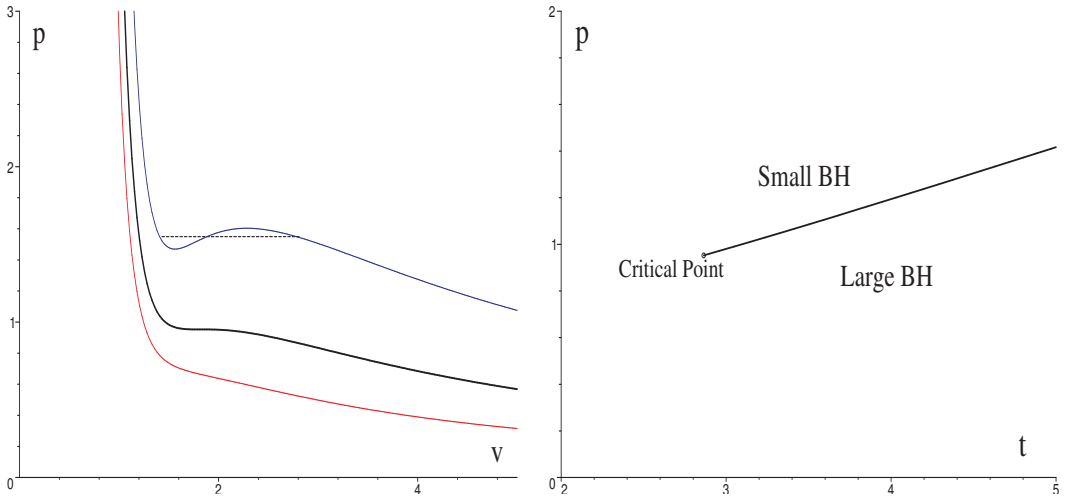

FIGURE 3.14: **Reverse VdW behavior.** The characteristic reverse VdW behavior is displayed for $d = 7, \kappa = -1, q = 1, \alpha = 1.5$ case. *Left:* the $p - v$ diagram. *Right:* the $p - t$ phase diagram.

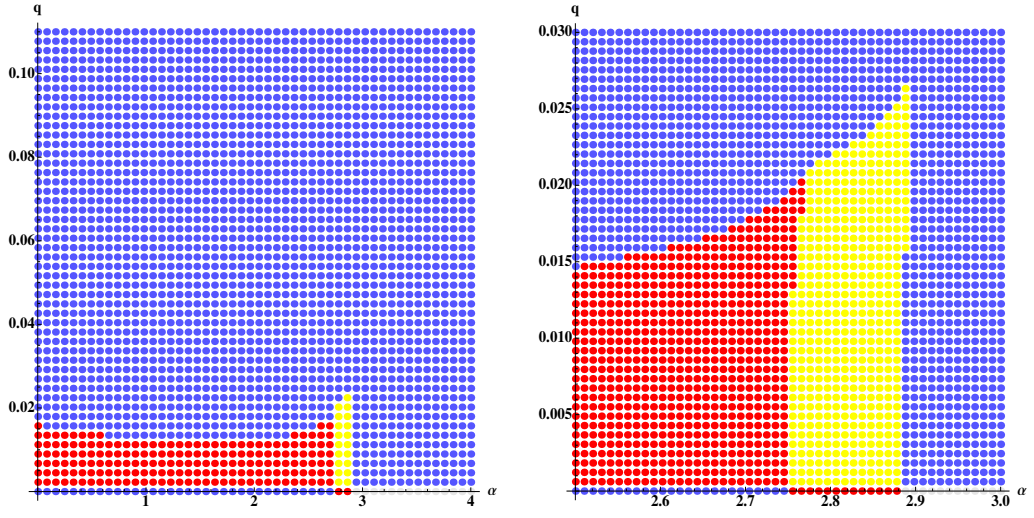

FIGURE 3.15: **Critical points in (q, α)-parameter space: $d = 8, \kappa = +1$ case.** The number of critical points with positive (p_c, v_c, t_c) is displayed in the (q, α)-parameter space; grey dots correspond to no critical points, blue to one critical point, red to two, and yellow to three. The corresponding diagram for $d = 7$ is trivial (contains only the blue region with one critical point) and hence is not displayed. Although all critical points have positive (p_c, v_c, t_c), some p_c may exceed the maximum pressure p_+ and hence occurs for a compact space. Note also the qualitatively different behavior for $q = 0$.

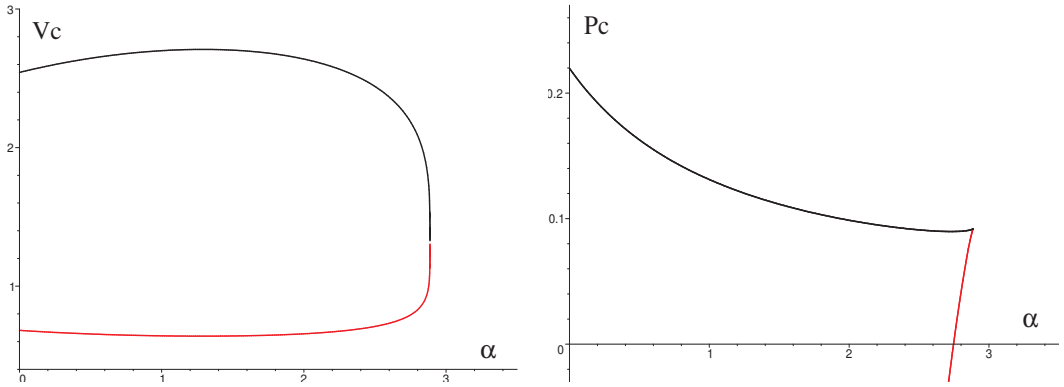

FIGURE 3.16: **Critical points:** $d = 8, q = 0, \kappa = 1$**.** Critical volume v_c and pressure p_c are displayed as functions of α. We observe that for $\alpha \in (\alpha_1 \approx 2.747, \alpha_2 \approx 2.886)$ we have two critical points with positive (p_c, v_c, t_c). However, only one of them occurs in a branch globally minimizing the Gibbs free energy.

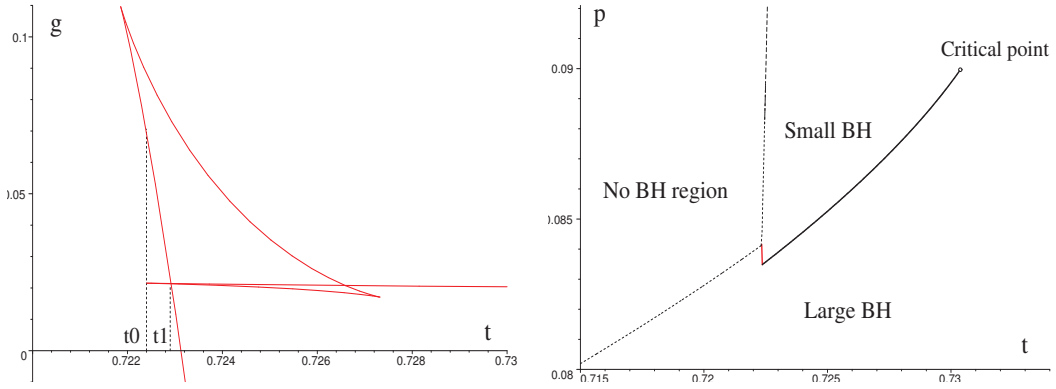

FIGURE 3.17: **Reentrant phase transition:** $d = 8, q = 0, \kappa = 1$**.** *Left:* $g - t$ diagram. The characteristic behavior of the Gibbs free energy when the RPT is present is displayed for $p = 0.08384$. The temperature t_1 indicates the standard large/small BH first-order phase transition; t_0 the peculiar small/large BH zeroth-order phase transition. *Right:* $p - t$ diagram. The zeroth-order phase transition is displayed by thick red curve. The dashed curve outlines the 'no black hole region'. We have set $\alpha = 2.8$.

3.4.4.2 Reentrant Phase Transition

When $q = 0$ there could be up to two critical points, the corresponding v_c and p_c are displayed in Fig. 3.16. Namely, for $\alpha < \alpha_1 \approx 2.747$ we observe one critical point, for $\alpha_1 < \alpha < \alpha_2 \approx 2.886$ two critical points, and above α_2 there are no critical points.

In even dimension and in the absence of charge, small BHs may have arbitrarily high temperature [44]. Consequently, for $\alpha < \alpha_2$ and certain range of pressures, one observe a reentrant phase transition, similar to the one observed in [4]. The characteristic behaviour of the Gibbs free energy is displayed on the LHS of

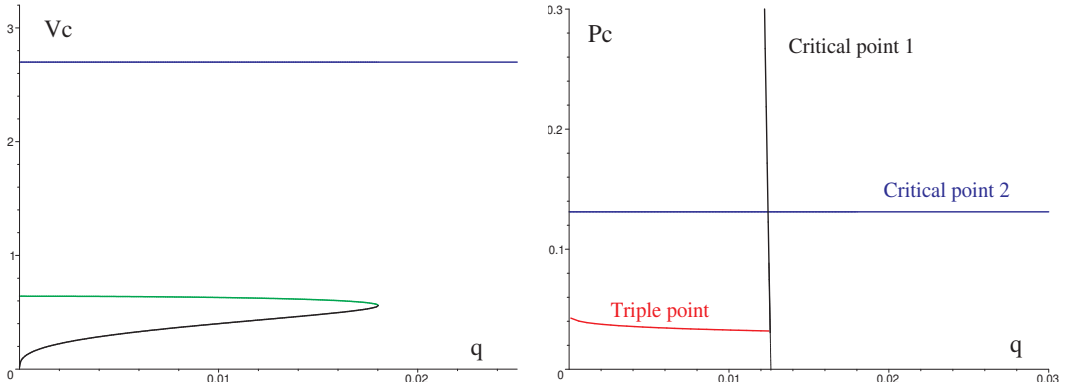

FIGURE 3.18: **Critical points:** $d = 8, \kappa = 1, \alpha = 1$. *Left:* critical volume v_c is displayed for $q \in (0, 0.03)$. *Right:* critical pressures. For certain range of q's we observe the existence of a triple point.

Fig. 3.17 for $\alpha = 2.8$. Looking at this figure, one observes that for high temperature, large BHs (lower vertical curve) globally minimize the Gibbs free energy. As temperature decreases, at t_1 there is a first order phase transition to small BHs displayed by horizontal curve. Following this curve further, at $t = t_0$, this curve terminates and the system cannot be a small BH anymore. Rather it undergoes a zeroth order phase transition and "jumps" to the upper vertical curve denoting the large BHs again. Hence as temperature monotonously changes from high to low the system undergoes phase transitions from large to small and back to large BH, a phenomenon known as a reentrant phase transition. The corresponding $p - t$ phase diagram is displayed on r.h.s of Fig. 3.17.

3.4.4.3 Triple Point

When a small charge q is added to the BH, there could be up to three critical points, shown in Fig. 3.18 for $\alpha = 1$. Consequently the small/intermediate and intermediate/large BH phase transitions as well as a triple point may be present. The Gibbs free energy exhibits two swallowtails that terminate at critical points on one side and merge together to form a triple point on the other side, see Fig. 3.19. triple point for example occurs at

$$q = 0.012\,, \quad p_{3c} = 0.03209\,, \quad t_{3c} = 0.54729\,, \tag{3.58}$$

where BHs of three different sizes, $v_1 = 0.3948, v_2 = 0.4855, v_3 = 9.7190$ "coexist". The corresponding phase diagram is displayed on RHS of Fig. 3.19.

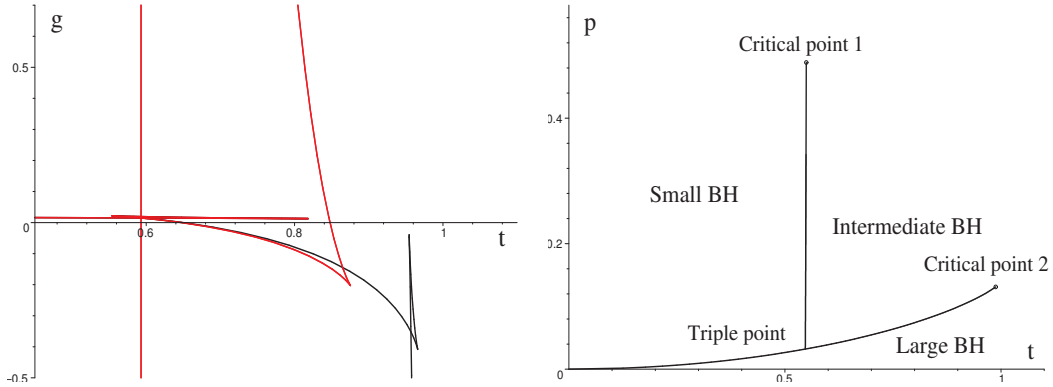

FIGURE 3.19: **Triple point:** $d = 8, \kappa = 1, \alpha = 1$. *Left: $g - t$ diagram.* The characteristic double swallowtail indicating the presence of two first-order phase transitions is displayed by thick black curve. When two such swallowtails 'coincide' one can observe a triple point. *Right: $p - t$ diagram.* The phase diagram possesses two first-order phase transitions that eventually terminate at critical points on one side and merge together to form a triple point on the other side. To signify these features we have set different charges in the two figures. Whereas left figure is displayed for $q = 0.00161$ (for which the two swallowtails are apparent), for right figure we have set $q = 0.012$ for which the two critical pressures are comparable.

3.4.4.4 Hyperbolic Case

The thermodynamic behavior of $d = 8$ hyperbolic Lovelock BHs is very similar to the $d = 7$ case. The structure of possible critical points in the (q, α)-parameter space is illustrated on the RHS of Fig. 3.13 - apart from the absence of small blue region associated with the VdW behavior for $\alpha < \sqrt{3}$ the figures seem very much alike.

3.4.4.5 $\alpha = \sqrt{3}$: Isolated Critical Point

A special case occurs when the parameter α takes the particular value $\alpha = \sqrt{3}$; the system can be solved analytically and the solution expressed in the simple form [34, 45]

$$f = \kappa + \frac{r^2}{\sqrt{3\alpha_3}}\left[1 - \left(1 - 3\sqrt{3\alpha_3}\left(\alpha_0 - \frac{16\pi M}{(d-2)\Sigma^{(\kappa)}_{d-2} r^{d-1}} + \frac{8\pi Q^2}{(d-2)(d-3)r^{2d-4}}\right)\right)^{\frac{1}{3}}\right]. \tag{3.59}$$

In what follows only the $Q = 0$ case is considered. The equation of state and the Gibbs free energy are given by (3.41) and (3.43), taking the $\alpha = \sqrt{3}$ limit. While certain properties of this case in the context of $p - v$ criticality have been studied previously [46, 47, 48], we here point out an interesting novel feature. For $\kappa = +1$,

we find one physical critical point, with positive (p_c, v_c, t_c), characterized by

$$\begin{aligned} v_c &= 3^{\frac{1}{4}} \times \sqrt{\frac{d+3+2\tilde{d}}{d-3}}\,, \quad t_c = \frac{3^{\frac{3}{4}}(d-2)(d-3)^2(d-2+\tilde{d})}{6\pi\big(\tilde{d}+3d-6\big)\sqrt{(d+3+2\tilde{d})(d-3)}}\,, \\ p_c &= \frac{\sqrt{3}(d-2)(d-3)^2\big[3(d+1)(69-5d)(d-2)-\tilde{d}(d^2-160d+255)\big]}{36\pi(\tilde{d}+3d-6)(d+3+2\tilde{d})^3}\,, \end{aligned} \tag{3.60}$$

where $\tilde{d} = \sqrt{(d-2)(12-d)}$. Obviously, there is no solution for $d > 12$ and so the range of d admitting critical points is $7 \leq d \leq 12$. In $d = 10, 11$ an additional critical point emerges which, however, occurs in a branch that does not globally minimize the Gibbs free energy.

3.4.4.6 Critical Exponents

Recapitulating, for $\kappa = +1$ critical behavior occurs in $d = 7, 8, 9, 10, 11$ dimensions: in $d = 7$ the critical point is associated with the VdW behavior, whereas in $d = 8, 9, 10, 11$ we observe a reentrant phase transition similar to the one studied in the previous subsection for $d = 8$. To study the nature of the critical point (3.60) we study its critical exponents. One procedure is to Taylor expand the equation of state around this critical point. By introducing the new variables

$$\omega = \frac{v}{v_c} - 1\,, \quad \tau = \frac{t}{t_c} - 1\,, \tag{3.61}$$

and the equation of state expands as

$$\frac{p}{p_c} = 1 + A\tau + B\tau\omega + C\omega^3 + \dots\,, \tag{3.62}$$

with A, B, C non-trivial d-dependent constants—implying the standard critical exponents (3.10). The situation is considerably different for $\kappa = -1$. Here in any dimension $d \geq 7$ we find a single critical point [46, 47] at

$$v_c = 3^{1/4}\,, \quad t_c = \frac{d-2}{2\pi}3^{-1/4}\,, \quad p_c = \frac{(d-1)(d-2)}{36\pi}\sqrt{3} = p_+ = p_-\,. \tag{3.63}$$

Note that this critical point occurs exactly at the thermodynamic singular point (3.48), and implies that the BH is massless ($M = 0$). This leads to a very peculiar behaviour as described below. Namely, in the $p - v$ diagram this critical point corresponds to a place where various isotherms merge together as displayed in

Fig. 3.9b.[8] The Gibbs free energy displays two swallowtails, both emanating from the same origin given by (3.63), shown in Fig. 3.8b. In the $p-t$ diagram, Fig. 3.10c, we consequently observe an *isolated critical point*. Such a critical point is special as can be seen from the following expansion of the equation of state, using variables (3.61):

$$\frac{p}{p_c} = 1 + \frac{24}{d-1}\tau\omega^2 - 8\frac{(d-4)}{(d-1)}\omega^3 + \cdots \tag{3.64}$$

Together with the fact that the specific heat at constant volume, $C_v \propto T\frac{\partial S}{\partial T}\Big|_v \propto |t|^{-\tilde{\alpha}}$, identically vanishes for our Lovelock BHs as $S = S(V, \alpha_2, \alpha_3, \dots)$, one can conclude that the critical exponents associated with the isolated critical point are

$$\tilde{\alpha} = 0\,, \quad \tilde{\beta} = 1\,, \quad \tilde{\gamma} = 2\,, \quad \tilde{\delta} = 3\,. \tag{3.65}$$

Such exponents are different from the swallowtail exponents (3.10). This means that not all scaling relations remain valid for this critical point. In fact we find that the following scaling relation:

$$\tilde{\gamma} = \tilde{\beta}(\tilde{\delta} - 1) \tag{3.66}$$

remains valid, whereas the equality between $2 - \tilde{\alpha} = 2\tilde{\beta} + \tilde{\gamma}$ is violated; in other words three instead of two of the critical exponents $\tilde{\alpha}, \tilde{\beta}, \tilde{\gamma}$ and $\tilde{\delta}$ are independent.

The presence of the thermodynamic singularity that occurs exactly at $v = v_c$ seems puzzling. Is there any pathology hiding in the black hole spacetime? In particular are the black holes at the critical point and its nearby vicinity non-singular at the horizon? To answer this question, one can try to study the tidal forces that an observer falling through the black hole horizon would experience. Such forces are determined by the orthonormal components of the Riemann tensor and, in this case, depend on $f'(r_+)$ and $f''(r_+)$.[9] One can show that both these quantities when expressed as functions of p and v are smooth and finite at $p = p_c$, however they diverge at $v = v_c$ for pressures slightly off p_c. Therefore, the thermodynamics around the special isolated critical point (3.63) seems well defined and there is nothing pathological about the corresponding BH spacetimes. One can also show that the branches of BHs that globally minimize the Gibbs free energy (and possess non-negative temperature) have always non-negative specific heat C_P and hence

[8] Contrary to the previous cases concerning thermodynamic singularities, the isotherms do not cross here but rather merge and depart again. This is a direct consequence of the fact that in fact two thermodynamic singularities coincide at $v = v_s$.

[9] Alternatively, one may want to study various curvature invariants, for example the Kretschmann scalar, given by (3.31). In either case the conclusions remain qualitatively the same.

are locally thermodynamically stable, while at the critical point we find $C_P = 0$. Further discussion of this interesting isolated point can be found in [49].

3.5 AdS/CFT Interpretation and Conclusions

New ideas about dynamical pressure and holography in this context has been recently proposed [27]. The question is: How does one interpret the pressure and the volume in the extended thermodynamics in terms of the dual field theory? The first idea could be that they are the pressure and the volume of the fluid but this hypothesis does not seem to be valid (as can be seen by studying the stress-energy tensor of a Schwarzschild BH in AdS). The stress tensor's properties are consistent with that of with that of a conformally invariant fluid with density $\rho \propto p$. Both are set by the energy (so the mass M of the black hole, plus the Casimir energy, if we are in global AdS). Thus, the fluid pressure is not the p of the AdS thermodynamics that is set by the cosmological constant. They simply do not match. In the standard holographic dictionary, the BH thermodynamic quantities (M, T, S) map[10] to (U, T, S) of the dual non–gravitational theory. However, considering the extended phase space, one has a BH thermodynamics where P and V are dynamical, and M is interpreted as the enthalpy $H = U + pV$ of the gravity theory. Thus, it is reasonable to think that there should be a map from the BH quantities (H, T, S, P, V) and the dual field theory [27, 50, 51]. The question remains on the field theory side, what is the meaning of P, given that it is not a thermodynamic variable?

In this chapter, a study of different gravitational systems in the framework of black hole chemistry has been presented.

It has been showed that various thermodynamic phenomena, such as Van der Waals behaviour, reentrant phase transitions (RPT), and tricritical points occur in the context of RBH and 3rd-order Lovelock gravity. For example, it is possible to confirm the existence of a tricritical point in $d = 8, 9, 10$ dimensions in the case of charged Lovelock black holes and the existence of RPT in $d = 8, 9, 10, 11$ dimensions for the electrically neutral ones. Moreover, a 'multiple RPT' behaviour is present, in which the Gibbs free-energy is continuous at the phase transition point. This feature has not previously been noted.
In the case of hyperbolic $\kappa = -1$ Lovelock black holes one generically finds thermodynamic singularities, in which all isotherms cross at a particular value of v in

[10] after putting in the value of Newton's constant G

the $p-v$ diagram. The corresponding Gibbs free energy suffers from 'infinite jump' and undergoes 'reconnection'. In particular, one may observe a form of swallowtail in which one end of the swallowtail 'goes to infinity'. Since the global minimum of the Gibbs free energy is always well-defined, it is still possible to make sense of thermodynamics. Regions where black holes have negative entropy have been excluded from thermodynamic considerations. However there has been a recent proposal in which negative entropy is interpreted in terms of heat flow out of a volume [50, 51, 52]. It would be interesting to see if a similar interpretation holds for Lovelock black holes.

It has been showed that the thermodynamic behaviour when $\alpha = \sqrt{3}$ and $\kappa = -1$ for 3rd-order uncharged Lovelock black holes is very peculiar [46, 47]. In this interesting special case has been found [38] that the equation of state has non-standard expansion about a special critical point. Rather than $p/p_c = 1 + A\tau + B\tau\omega + C\omega^3 + \dots$ (characteristic for mean field theory critical exponents and swallowtail catastrophe behaviour), one obtains

$$\frac{p}{p_c} = 1 + \frac{24}{d-1}\tau\omega^2 - \frac{8(d-4)}{d-1}\omega^3 + \dots , \tag{3.67}$$

suggesting a violation of certain scaling relations and non-standard critical exponents. Beyond $p = p_{max}$ the asymptotic structure of the spacetime changes, being compact for $p > p_{max}$. Perhaps there is a phase transition to such solutions? One might also consider a possibility of identifying an effective cosmological constant, rather than the bare cosmological constant, with pressure [53] and describing the thermodynamics from that perspective, analogous to the approach taken for boson stars [54].

References

[1] Jolien D. E. Creighton and Robert B. Mann. "Quasilocal thermodynamics of dilaton gravity coupled to gauge fields". In: *Phys. Rev. D* 52 (8 Oct. 1995), pp. 4569–4587.

[2] D. Kastor, S. Ray, and J. Traschen. "Enthalpy and the Mechanics of AdS Black Holes". In: *Class.Quant.Grav.* 26 (2009), p. 195011. arXiv: 0904.2765 [hep-th].

[3] M. Cvetic et al. "Black Hole Enthalpy and an Entropy Inequality for the Thermodynamic Volume". In: *Phys.Rev.* D84 (2011), p. 024037. arXiv: 1012.2888 [hep-th].

[4] Natacha Altamirano, David Kubiznak, and Robert B. Mann. "Reentrant Phase Transitions in Rotating AdS Black Holes". In: *Phys.Rev.* D88 (2013), p. 101502. arXiv: 1306.5756 [hep-th].

[5] S. Gunasekaran, R. B. Mann, and D. Kubiznak. "Extended phase space thermodynamics for charged and rotating black holes and Born-Infeld vacuum polarization". In: *JHEP* 1211 (2012), p. 110. arXiv: 1208.6251 [hep-th].

[6] Natacha Altamirano et al. "Kerr-AdS analogue of tricritical point and solid/liquid/gas phase transition". In: (2013). arXiv: 1308.2672 [hep-th].

[7] Brian P. Dolan et al. "Thermodynamic Volumes and Isoperimetric Inequalities for de Sitter Black Holes". In: *Phys.Rev.* D87 (2013), p. 104017. arXiv: 1301.5926 [hep-th].

[8] M. M. Caldarelli, G. Cognola, and D. Klemm. "Thermodynamics of Kerr-Newman-AdS black holes and conformal field theories". In: *Class.Quant.Grav.* 17 (2000), pp. 399–420. arXiv: hep-th/9908022 [hep-th].

[9] Brian P. Dolan. "The cosmological constant and the black hole equation of state". In: *Class.Quant.Grav.* 28 (2011), p. 125020. arXiv: 1008.5023 [gr-qc].

[10] B. P. Dolan. "Pressure and volume in the first law of black hole thermodynamics". In: *Class.Quant.Grav.* 28 (2011), p. 235017. arXiv: 1106.6260 [gr-qc].

[11] B. P. Dolan. "Compressibility of rotating black holes". In: *Phys.Rev.* D84 (2011), p. 127503. arXiv: 1109.0198 [gr-qc].

[12] B. P Dolan. "Where is the PdV term in the fist law of black hole thermodynamics?" In: *Open Questions in Cosmology*. Ed. by G. J. Olomo. InTech, 2012. arXiv: 1209.1272 [gr-qc].

[13] A. Larranaga and A. Cardenas. "Geometric Thermodynamics of Schwarzschild-AdS black hole with a Cosmological Constant as State Variable". In: *J.Korean Phys.Soc.* 60 (2012), pp. 987–992. arXiv: 1108.2205 [gr-qc].

[14] A. Larranaga and S. Mojica. "Geometric Thermodynamics of Kerr-AdS black hole with a Cosmological Constant as State Variable". In: *Abraham Zelmanov J.* 5 (2012), pp. 68–77. arXiv: 1204.3696 [gr-qc].

[15] G.W. Gibbons. "What is the Shape of a Black Hole?" In: *AIP Conf.Proc.* 1460 (2012), pp. 90–100. arXiv: 1201.2340 [gr-qc].

[16] David Kubiznak and Robert B. Mann. "P-V criticality of charged AdS black holes". In: *JHEP* 1207 (2012), p. 033. arXiv: 1205.0559 [hep-th].

[17] A. Belhaj et al. "On Thermodynamics of AdS Black Holes in Arbitrary Dimensions". In: *Chin.Phys.Lett.* 29 (2012), p. 100401. arXiv: 1210.4617 [hep-th].

[18] H. Lu et al. "AdS and Lifshitz Black Holes in Conformal and Einstein-Weyl Gravities". In: (2012). arXiv: 1204.1062.

[19] A. Smailagic and E. Spallucci. "Thermodynamical phases of a regular SAdS black hole". In: (2012). arXiv: 1212.5044 [hep-th].

[20] S.H. Hendi and M.H. Vahidinia. "P-V criticality of higher dimensional black holes with nonlinear source". In: (2012). arXiv: 1212.6128 [hep-th].

[21] Andrew Chamblin et al. "Charged AdS black holes and catastrophic holography". In: *Phys.Rev.* D60 (1999), p. 064018. arXiv: hep-th/9902170 [hep-th].

[22] A. Chamblin et al. "Holography, thermodynamics and fluctuations of charged AdS black holes". In: *Phys.Rev.* D60 (1999), p. 104026. arXiv: hep-th/9904197 [hep-th].

[23] M. Cvetic and S.S. Gubser. "Phases of R charged black holes, spinning branes and strongly coupled gauge theories". In: *JHEP* 9904 (1999), p. 024. arXiv: hep-th/9902195 [hep-th].

[24] M. Cvetic and S. S. Gubser. "Thermodynamic stability and phases of general spinning branes". In: *JHEP* 9907 (1999), p. 010. arXiv: hep-th/9903132 [hep-th].

[25] David Kubiznak and Robert B. Mann. "Black Hole Chemistry". In: (2014). arXiv: 1404.2126 [gr-qc].

[26] N. Altamirano et al. "Thermodynamics of rotating black holes and black rings: phase transitions and thermodynamic volume". In: (2014). arXiv: 1401.2586 [hep-th].

[27] Clifford V. Johnson. "Holographic Heat Engines". In: *Class.Quant.Grav.* 31 (2014), p. 205002. arXiv: 1404.5982 [hep-th].

[28] Edward Witten. "Anti-de Sitter space, thermal phase transition, and confinement in gauge theories". In: *Adv.Theor.Math.Phys.* 2 (1998), pp. 505–532. arXiv: hep-th/9803131 [hep-th].

[29] Chao Niu, Yu Tian, and Xiao-Ning Wu. "Critical Phenomena and Thermodynamic Geometry of RN-AdS Black Holes". In: *Phys.Rev.* D85 (2012), p. 024017. arXiv: 1104.3066 [hep-th].

[30] Ted Jacobson and Robert C. Myers. "Black hole entropy and higher curvature interactions". In: *Phys.Rev.Lett.* 70 (1993), pp. 3684–3687. arXiv: hep-th/9305016 [hep-th].

[31] David Kastor, Sourya Ray, and Jennie Traschen. "Smarr Formula and an Extended First Law for Lovelock Gravity". In: *Class.Quant.Grav.* 27 (2010), p. 235014. arXiv: 1005.5053 [hep-th].

[32] Rong-Gen Cai. "A Note on thermodynamics of black holes in Lovelock gravity". In: *Phys.Lett.* B582 (2004), pp. 237–242. arXiv: hep-th/0311240 [hep-th].

[33] Hideki Maeda, Steven Willison, and Sourya Ray. "Lovelock black holes with maximally symmetric horizons". In: *Class. Quant. Grav.* 28 (2011), p. 165005. arXiv: 1103.4184 [gr-qc].

[34] M.H. Dehghani and R. Pourhasan. "Thermodynamic instability of black holes of third order Lovelock gravity". In: *Phys.Rev.* D79 (2009), p. 064015. arXiv: 0903.4260 [gr-qc].

[35] Xian O. Camanho and Jose D. Edelstein. "Causality in AdS/CFT and Lovelock theory". In: *JHEP* 1006 (2010), p. 099. arXiv: 0912.1944 [hep-th].

[36] Xian O. Camanho, Jose D. Edelstein, and Miguel F. Paulos. "Lovelock theories, holography and the fate of the viscosity bound". In: *JHEP* 1105 (2011), p. 127. arXiv: 1010.1682 [hep-th].

[37] Robert C. Myers and Jonathan Z. Simon. "Black Hole Thermodynamics in Lovelock Gravity". In: *Phys.Rev.* D38 (1988), pp. 2434–2444.

[38] Antonia M. Frassino et al. "Multiple Reentrant Phase Transitions and Triple Points in Lovelock Thermodynamics". In: *JHEP* 09 (2014), p. 080. arXiv: 1406.7015 [hep-th].

[39] W.L. Smith and Robert B. Mann. "Formation of topological black holes from gravitational collapse". In: *Phys.Rev.* D56 (1997), pp. 4942–4947. arXiv: gr-qc/9703007 [gr-qc].

[40] Robert B. Mann. "Pair production of topological anti-de Sitter black holes". In: *Class.Quant.Grav.* 14 (1997), pp. L109–L114. arXiv: gr-qc/9607071 [gr-qc].

[41] Robert B. Mann. "Black holes of negative mass". In: *Class.Quant.Grav.* 14 (1997), pp. 2927–2930. arXiv: gr-qc/9705007 [gr-qc].

[42] C. Hudson. In: *Z. Phys. Chem.* 47 (1904), p. 113.

[43] T. Narayanan and A. Kumar. "Reentrant phase transitions in multicomponent liquid mixtures". In: *Physics Reports* 249 (1994), pp. 135–218.

[44] David Kastor, Sourya Ray, and Jennie Traschen. "Mass and Free Energy of Lovelock Black Holes". In: *Class. Quant. Grav.* 28 (2011), p. 195022. arXiv: 1106.2764 [hep-th].

[45] M.H. Dehghani and M. Shamirzaie. "Thermodynamics of asymptotic flat charged black holes in third order Lovelock gravity". In: *Phys.Rev.* D72 (2005), p. 124015. arXiv: hep-th/0506227 [hep-th].

[46] Jie-Xiong Mo and Wen-Biao Liu. "$P - V$ criticality of topological black holes in Lovelock-Born-Infeld gravity". In: *Eur.Phys.J.* C74.4 (2014), p. 2836. arXiv: 1401.0785 [gr-qc].

[47] Hao Xu, Wei Xu, and Liu Zhao. "Extended phase space thermodynamics for third order Lovelock black holes in diverse dimensions". In: *Eur.Phys.J.* C74.9 (2014), p. 3074. arXiv: 1405.4143 [gr-qc].

[48] A. Belhaj et al. "Ehrenfest Scheme of Higher Dimensional Topological AdS Black Holes in Lovelock-Born-Infeld Gravity". In: (2014). arXiv: 1405.3306 [hep-th].

[49] Brian P. Dolan et al. "Isolated critical point from Lovelock gravity". In: *Class.Quant.Grav.* 31.24 (2014), p. 242001. arXiv: 1407.4783 [hep-th].

[50] Clifford V. Johnson. "Thermodynamic Volumes for AdS-Taub-NUT and AdS-Taub-Bolt". In: *Class.Quant.Grav.* 31.23 (2014), p. 235003. arXiv: 1405.5941 [hep-th].

[51] Clifford V. Johnson. "The Extended Thermodynamic Phase Structure of Taub-NUT and Taub-Bolt". In: (2014). arXiv: 1406.4533 [hep-th].

[52] Scott MacDonald. "Thermodynamic Volume of Kerr-bolt-AdS Spacetime". In: (2014). arXiv: 1406.1257 [hep-th].

[53] Rong-Gen Cai et al. "P-V criticality in the extended phase space of Gauss-Bonnet black holes in AdS space". In: *JHEP* 1309 (2013), p. 005. arXiv: 1306.6233 [gr-qc].

[54] Laura J. Henderson, Robert B. Mann, and Sean Stotyn. "Gauss-Bonnet Boson Stars with a Single Killing Vector". In: *Phys.Rev.* D91.2 (2015), p. 024009. arXiv: 1403.1865 [gr-qc].

Chapter 4

Holographic Application

During the past years, the AdS/CFT correspondence has yielded several insights into the dynamics of strongly coupled gauge theories. A strongly coupled QFT at finite temperature T can be obtained using, as gravitational dual, a black brane (that is a black hole whose horizon is $\mathbf{R}^3$) in asymptotically Anti-de-Sitter space. Indeed, BHs and black branes are thermal objects associated with a Hawking temperature that, in the gauge/gravity dictionary, correspond to the temperature T of the dual field theory. The entropy and the energy density of the boundary theory are also equal to the corresponding black brane quantities (see Fig. 4.1).
The components of the retarded two-point correlator functions of the $T_{\mu\nu}$ of a CFT in four-dimensional Minkowski space at finite temperature can be expressed in terms of the bulk metric fluctuations $h_{\mu\nu}$ around the black brane solution. These metric fluctuations depend on the various symmetries of the gravitational system.

In this chapter, the Gauss-Bonnet and the regular black brane metrics, will be used to calculate the shear viscosity of a strongly coupled gauge theory on the AdS boundary, in the hydrodynamic limit. The hydrodynamic limit corresponds to $\omega, k << T$, where ω is the frequency, k is the wavelength number and T is the temperature of the dual thermal QFT. In this limit, the theory describes a sort of "CFT plasma" for which transport coefficients can be calculated using the rules of the AdS/CFT correspondence.
In particular, during this chapter, it will be used the duality between the hydrodynamic modes in field theory and the quasi-normal modes of the AdS black brane metric. This identification was initially used to calculate the ratio of the shear viscosity η to the entropy density s for a class of gauge theories with a classical Einstein gravity dual.

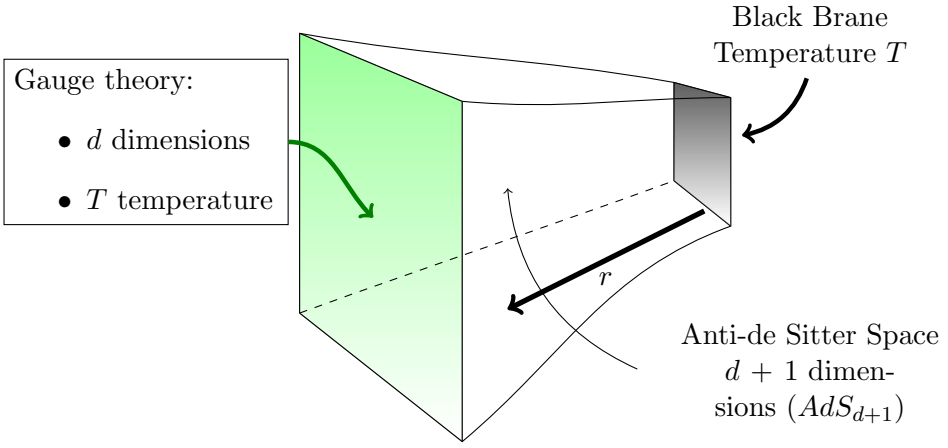

FIGURE 4.1: **Cartoon representation of the AdS/CFT correspondence.**

In the hydrodynamic description, the shear viscosity η parametrizes how efficiently the momentum of a layer of fluid (assuming the momentum to be in the plane defined by that layer) diffuses in the direction orthogonal to the momentum[1]. Interestingly, it has been found that there is some *universality* on the value of the ratio η/s calculated for all gauge theories described by classical gravity. Using AdS/CFT it has been calculated that the ratio of the shear viscosity η to the entropy density s is specifically

$$\frac{\eta}{s} = \frac{1}{4\pi}. \tag{4.1}$$

The ratio $\eta/s = 1/4\pi$ is conjectured to be a universal lower bound, called KSS bound [1], that by now all known materials in nature satisfy [2]. One piece of evidence for the KSS conjecture came from string theory, because the leading finite corrections in the 't Hooft coupling λ always give a positive contribute raising η/s above the bound. However, in Refs. [8, 9, 10] a study on AdS Gauss-Bonnet gravity (i.e., R^2 higher derivative gravity corrections[3]) showed that the lower bound is violated and a new lower bound $4/25\pi$ based on causality condition on the dual field theory, is proposed. From the point of view of AdS/CFT, an interesting feature of the KSS bound is that it seems to be *saturated* by Einstein gravity. This gives that at the linearized order, small corrections to Einstein gravity often violate the bound. One can expect that corrections to Einstein gravity occurring in any quantum theory of gravity can violate the bound [9].

[1] Or in other words, η governs the relaxation of small deviations away from thermodynamic equilibrium.

[2] At the present, all known substances, among which for example water and liquid helium, satisfy the bound. However, certain cold atomic gas systems in the unitarity limit (see e.g. [2]) and the quark-gluon plasma created at Relativistic Heavy Ion Collider (RHIC) [3, 4, 5, 6, 7] seem to be the closest to the bound.

[3] The higher derivative gravity corrections, as it was also stated in Chapter 3, can be considered as generated from string theory corrections.

The bound on the lowest value of the ratio has been considered from the point of view of heavy-ion collision physics. The idea that holography provides a useful, experimentally testable model for heavy ion collisions was further supported when the results from the Relativistic Heavy Ion Collider (RHIC) indicated that the quark-gluon plasma could be understood as a near-perfect fluid with shear viscosity numerically close to the AdS/CFT result. Moreover, the ratio η/s for pure gluon QCD slightly above the deconfinement temperature has also been calculated on the lattice [11, 12] and it seems to be larger than (4.1). This difference between the two approaches further motivates investigations of the universality of the KSS bound in holographic models to clarify its physical origin by correlating bulk pathologies and the violation of the bound. In this chapter, the shear viscosity will be calculated for:

- A plasma dual to Gauss-Bonnet (GB) black branes, and
- A gauge theory dual to an AdS RBH background.

In the case of extremal and non-extremal GB black branes in five spacetime dimensions, the shear viscosity to entropy ratio η/s is calculated using the method recently proposed in Refs. [13, 14, 15]. Different methods will be used to calculate η in the case of regular black brane metric [16, 17, 18].

4.1 The Gauge/gravity Correspondence

The topic of the AdS/CFT duality has been briefly presented in Chapter 1 (see Sect. 1.4.3). In general, the duality states that there is a map from string theory in ten dimensions to a QFT in a lower number of dimensions. Indeed, in the string theory framework, it is quite natural to construct $SU(N_c)$ gauge field theories on hypersurfaces embedded in a higher dimensional space containing gravity. Although the AdS/CFT correspondence should be valid at all regimes, the duality between the two theories can be used to give insights into the non-perturbative regime (i.e., strong coupling dynamics) of one theory, from the computable weak coupling perturbative regime of the other. This is obtained in the so-called 't Hooft limit ($N_c \to \infty$) and $\lambda_{tH} \to \infty$. The original example of AdS/CFT correspondence is between $\mathcal{N} = 4$ supersymmetric Yang-Mills (SYM) theory and a specific string theory (type IIB) on $AdS_5 \times S^5$ space. The $\mathcal{N} = 4$ SYM theory is a gauge theory with a gauge field, four Weyl fermions, and six real scalars, all in the

adjoint representation of the color group. The Lagrangian of this theory can be written down explicitly, but is not very important for the purposes of this thesis. It has a vanishing beta function and is a conformal field theory (CFT) (thus the CFT in AdS/CFT).

A picture of the duality in superstring theory is obtained using a stack of N parallel $D3$-branes[4] [19]. The CFT side of the duality is realized using the open string point of view, i.e., the stings that begin and end on the $D3$-branes. There are N^2 types of open strings stretched between the $D3$-branes. As the distance between the branes decreases, the masses of the stretched strings go to zero, and the strings do behave as the components of a $U(N)$ gauge field living on the world volume of the branes [20]. On the other hand, closed strings contain gravitons in the spectrum of their excitations. In the low energy limit, this can be modeled by a supergravity theory, in which the metric on spacetime is affected by massive objects, like D-branes. The interaction between the stack of $D3$-branes and closed strings curves the space, generating an extremal black three-brane, a higher-dimensional analog of an extremal charged BH. It can be seen that the space near the event horizon is warped into anti-de Sitter space. Thus, the AdS part of the duality is realized as the near-horizon limit of a stack of $D3$-branes.

4.1.1 Anti-de Sitter Geometry

On the string theory side, we have type IIB string theory, which contains a finite number of massless fields, including the graviton, the dilaton ϕ, some other fields (forms), their fermionic superpartners and an infinite number of massive string excitations. It has two parameters: the string length l_s and the string coupling g_s. In the long-wavelength limit, when all fields vary over length scales much larger than l_s, the massive modes decouple and one is left with type IIB supergravity in a ten dimensional spacetime, which can be described by an action. The type IIB string theory lives in a ten-dimensional space-time with metric that is a direct product of a five-dimensional sphere ($d\Omega_5$) and another five-dimensional space-time spanned by t, x, and r

$$ds^2 = \frac{r^2}{b^2}\left(-dt^2 + d\vec{x}^2\right) + \frac{b^2}{r^2}dr^2 + b^2 d\Omega_5^2. \tag{4.2}$$

[4] D-branes (or Dirichlet branes) are higher dimensional non-perturbative solitonic objects contained in supersymmetric string theory.

The AdS_5 geometry is described by the metric [21]

$$ds^2 = \frac{r^2}{b^2}\left(-dt^2 + d\vec{x}^2\right) + \frac{b^2}{r^2}dr^2 \tag{4.3}$$

where slices of constant radial coordinate r are four-dimensional Minkowski space, with the boundary at $r \to \infty$, and b is the AdS radius of curvature. Even if the duality regards a ten dimensional string theory, one does not generally consider the S^5 part of the metric, assuming that the theory is compactified on S^5. When the dual of the string theory is $\mathcal{N} = 4$ super-Yang-Mills, the AdS radius of curvature is related to the rank of the gauge group N_c by

$$b^3/\left(8\pi G_5\right) = \left(N_c/2\pi\right)^2 \ , \tag{4.4}$$

where G_5 is the five-dimensional gravitational coupling. The metric (4.2) has the isometry group[5] $SO\,(4;\,2)$, which is also the conformal group in four spacetime dimensions. Because of this property, the dual quantum field theory has no scale and is a conformal field theory (CFT). The isometry realizing overall scale transformations in AdS, corresponds to a translation in the fifth (radial) direction along with an overall rescaling of the coordinates shared with the field theory. Consequently the fifth, holographic direction r can be identified with a *change of scale*, with the region near the boundary corresponding to the high energy (UV) limit and the region far from the boundary encoding the low energy (IR) physics (see Fig. 4.1); this is realized by the redshift factor r^2/b^2 weighting the Minkowski metric in Eq. (4.2). Other gauge symmetries of the gravity side are mapped to globally conserved currents in the field theory. The fields in AdS are sources of operators on the field theory side. Therefore, analyzing the dynamics of the sources in the curved spacetime one can learn about the dual operators.

4.1.2 Black Brane in Anti-de Sitter Spacetime

There is the possibility to generalize the original AdS/CFT duality introducing features that break the conformal symmetry, producing in this way a duality with a non-conformal field theory. In a non-conformal theory there is a fundamental scale. One notable way to break conformality and introduce a scale is to consider

[5]The isometry group of a metric space is the set of all distance-preserving maps from the metric space onto itself, with the function composition as group operation. The conformal group is the group of transformations from a space to itself that preserve all angles within the space.

in the bulk a black brane (BB) in AdS space

$$ds^2 = \frac{r^2}{b^2}\left(-h\left(r\right)dt^2 + d\vec{x}^2\right) + \frac{b^2}{r^2 h\left(r\right)}dr^2, \quad h\left(r\right) \equiv 1 - u^2,\ u = \frac{r_+^2}{r^2}\ . \tag{4.5}$$

These are theories at finite temperature. The BB is interpreted as being dual to a thermal state of the dual field theory. The surface gravity and surface area of the BB horizon coincide with the temperature and entropy density of the QFT [22]. Therefore, even though the vacua of the QCD and $\mathcal{N} = 4$ SYM theory have very different properties, when one compares $\mathcal{N} = 4$ SYM at temperature different from zero with QCD at a temperature above the critical temperature T_c of the crossover from the hadron gas to QGP, many of the qualitative differences disappear or become unimportant.

4.2 Hydrodynamics

Hydrodynamics can be thought of as an effective theory describing the dynamics of the system at large length scales with respect to the mean free path of its microscopic components. Thus, in hydrodynamics the fluctuations about thermal equilibrium are small and the system is locally in equilibrium.
Using (i) the conservation law of energy and momentum ($\partial_\mu T^{\mu\nu} = 0$), (ii) the hypothesis of *local thermal equilibrium*[6] and (iii) the expansion in powers of spatial derivatives of the hydrodynamic variables; then the zeroth order expression of the energy-momentum tensor $T^{\mu\nu}$ can be written in this form:

$$T^{\mu\nu} = \left(\epsilon + P\right)u^\mu u^\nu + P g^{\mu\nu} \tag{4.6}$$

where u_μ is the relativistic velocity with $u_\mu u^\nu = -1$. The expression (4.6) is the typical formula for ideal fluid where $\epsilon = \langle T^{tt}\rangle$ is the energy density and $P = \langle T^{ii}\rangle$ is the pressure[7]. The notion of *ideal* is related to the fact that the fluid does not dissipate energy (e.g., there is no friction). However, the ideal fluid does not generate entropy (that is a conserved quantity in the ideal case). In order to have entropy production, one needs to go to the next order in the derivative expansion. This expansion is obtained by allowing the temperature T and the velocity u^μ to be slowly varying functions of the boundary coordinates. The coefficients in this

[6] If perturbations have long wavelengths, the state of the system, at a given time, is determined by the temperature $T\left(\boldsymbol{x}\right)$ and the local fluid velocity $u^\mu\left(\boldsymbol{x}\right)$ as a function of coordinates. Note that because $u^\mu u_\mu = -1$, only three components of u^μ are independent.

[7] Note that the quantities ϵ and P are not independent, they are related via the equation of state of thermodynamics.

expansion are the so-called *transport coefficients* [23].
The derivative expansion modifies the previous energy-momentum tensor (4.6) in

$$T^{\mu\nu} = (\epsilon + P)\, u^{\mu\nu} + P g^{\mu\nu} - \sigma^{\mu\nu} \tag{4.7}$$

where $\sigma^{\mu\nu}$ is proportional to derivatives of the temperature $T(x)$ and the local fluid velocity $u^{\mu}(x)$ and it corresponds to the dissipative part of $T^{\mu\nu}$. In a generic frame, the dissipative part of the energy momentum tensor can be defined as [24]

$$\sigma^{\mu\nu} = P^{\mu\alpha} P^{\nu\beta} \left[\eta \left(\partial_\alpha u_\beta + \partial_\beta u_\alpha - \frac{2}{3} g_{\alpha\beta} \partial_\lambda u^\lambda \right) + \zeta g_{\alpha\beta} \partial_\lambda u^\lambda \right] \tag{4.8}$$

where $P^{\mu\nu} = g^{\mu\nu} + u^\mu u^\nu$ is the projection operator onto the directions perpendicular to u^μ while η and ζ are respectively the *shear* and *bulk* viscosity. The shear viscosity η is the coefficient of the symmetric traceless contribution while the bulk viscosity ζ is the coefficient of the trace part[8]. The generalization of the equation (4.8) to curved space-time is

$$\sigma^{\mu\nu} = P^{\mu\alpha} P^{\nu\beta} \left[\eta \left(\nabla_\alpha u_\beta + \nabla_\beta u_\alpha \right) + \left(\zeta - \frac{2}{3} \eta \right) g_{\alpha\beta} \nabla \cdot u \right] \tag{4.9}$$

where ∇ is the covariant derivative. Thus, using (4.7) and (4.8) one can write the energy-momentum tensor as a function of the shear and bulk viscosity. In the next section, it will be described how it would be possible to use these equations to extract information about the low-momentum behavior of Green's functions of the boundary QFT. In particular, it will be shown how the transport coefficient η is related to the retarded Green's functions. The connection between the macroscopic hydrodynamic transport coefficient and the microscopic Green' s functions is given by the Kubo formula.

4.2.1 The Kubo Formula

To understand the connection between hydrodynamic and the Green's functions, we need to introduce *the linear response theory* and Green's functions that respect the causal structure. The idea behind linear response theory is to consider small space-perturbations and time-perturbations around the equilibrium state of the physical system. As first step, let us recall how two-point correlation functions are usually calculated. If one couples sources $J_a(x)$ to a set of (bosonic) operators

[8] In CFT theories that are defined by a traceless energy-momentum tensor, the bulk viscosity is equal to zero.

$\hat{\mathcal{O}}_a(x)$, so that the new action is given by the sum of the free action S_0 and the coupled part

$$S = S_0 + \int dt\, d\mathbf{x}\, J^a(x)\, \hat{\mathcal{O}}_a(x) \tag{4.10}$$

then the source $J_a(x)$ will introduce a perturbation of the system. In particular, the average values of $\hat{\mathcal{O}}_a$ will differ from zero, which is usually assumed to be the equilibrium value. The field theory path integral representation of the one-point function with a source is

$$\left\langle \hat{\mathcal{O}}_a(x) \right\rangle = \int [D\psi]\, \hat{\mathcal{O}}_a(x)\; e^{S_0 + \int_y J^a(y)\hat{\mathcal{O}}_a(y)} \tag{4.11}$$

where ψ denotes the field of the QFT. Now, one can expand the exponent in (4.11) in a power series of the source and, if the sources J^a's are small, maintain the terms up to the linear order

$$\left\langle \hat{\mathcal{O}}_a(x) \right\rangle = \left\langle \hat{\mathcal{O}}_a(x) \right\rangle_{J=0} + \int dt\, d\mathbf{y}\, \left\langle \hat{\mathcal{O}}_a(x)\, \hat{\mathcal{O}}_b(y) \right\rangle J^b(y) + \dots \tag{4.12}$$

Considering normal-ordered observables, the two-point function is the retarded Green's function G^R_{ab}

$$iG^R_{ab}(x-y) = \theta\left(x^0 - y^0\right) \left\langle \left[\hat{\mathcal{O}}_a(x)\,,\, \hat{\mathcal{O}}_b(y) \right] \right\rangle . \tag{4.13}$$

Thus, if the sources J^a's are small, the quantity $\delta\left\langle \hat{\mathcal{O}}_a(x) \right\rangle$, defined by $\left\langle \hat{\mathcal{O}}_a(x) \right\rangle - \left\langle \hat{\mathcal{O}}_a(x) \right\rangle_{J=0}$ in (4.12), measures the fluctuations of the observable away from the expectation value, i.e., the linear response of the system to the external perturbation as

$$\delta\left\langle \hat{\mathcal{O}}_a(x) \right\rangle = -\int dt\, d\mathbf{y}\, G^R_{ab}(x-y)\, J^b(y)\,. \tag{4.14}$$

The fact that the linear response is determined by the retarded Green's function is given by causality: The source can influence the system only after it has been turned on.

Now, to determine the correlation functions of $T^{\mu\nu}$, one needs to couple a weak source to $T^{\mu\nu}$ and determine the average value of $T^{\mu\nu}$ after this source is turned on. To find these correlators at low momenta, one can use the hydrodynamic theory. So far, in the Sec.4.2 about hydrodynamics, there was no source coupled to $T^{\mu\nu}$. However, this lack can be easily corrected, as the source of the energy-momentum tensor is the metric $g^{\mu\nu}$. One must then use the hydrodynamic equations generalized to curved spacetime and from them determine the response of the thermal

medium to a weak perturbation of the metric. By comparison with the result from the linear response theory, one can see that the contributions to the traceless spatial components correspond to the zero spatial momentum, low-frequency limit of the retarded Green's function of T^{xy}

$$G^R_{xy,\,xy}\left(\omega,\,\mathbf{0}\right)=\int dt\,d\boldsymbol{x}\,e^{i\omega t}\theta\left(t\right)\left\langle\left[T_{xy}\left(t,\,\boldsymbol{x}\right),\,T_{xy}\left(0,\,\mathbf{0}\right)\right]\right\rangle=-i\eta\omega+O\left(\omega^2\right). \tag{4.15}$$

In this way one can derive the Kubo's formula relating the shear viscosity and the Green's function

$$\eta=-\lim_{\omega\to 0}\frac{1}{\omega}\,\mathrm{Im}\,G^R_{xy,\,xy}\left(\omega,\,\mathbf{0}\right). \tag{4.16}$$

The Kubo's formula encodes the dynamical properties of a thermal gauge theory in its Green's functions. In particular the kinetic coefficients are connected, via the Kubo's formula, to a certain limit of the real-time thermal Green's functions. In the framework of AdS/CFT, it is possible to compute the retarded Green's function by making a small perturbation of the bulk metric.

4.3 Holographic Correlation Functions

This section will show how to deal with the calculation of correlation functions of the type $\left\langle\mathcal{O}\left(x_1\right)\cdots\mathcal{O}\left(x_n\right)\right\rangle$ from gravity. We will recall how to transfer the Euclidean approach to calculate the holographic two-point functions to the Lorentzian case and how to impose boundary condition compatible with causality [23].

Usually, in QFT the correlation functions can be calculated from the generating functional

$$Z_{\mathrm{QFT}}\left[\,J\,\right]=\left\langle e^{\int\mathcal{L}_J}\right\rangle \tag{4.17}$$

where $\mathcal{L}_J$ is obtained by perturbing the Lagrangian by a source term in this way:

$$\mathcal{L}\to\mathcal{L}+J\left(x\right)\mathcal{O}\left(x\right)\equiv\mathcal{L}+\mathcal{L}_J \tag{4.18}$$

and $\mathcal{O}\left(x\right)$ is a gauge invariant operator of the d-dimensional field theory. The connected correlators then are given by the functional derivatives of the partition function:

$$\left\langle\prod_i\mathcal{O}\left(x_i\right)\right\rangle=\left(\prod_i\frac{\delta}{\delta J\left(x_i\right)}\right)\log Z_{\mathrm{QFT}}\left[\,J\,\right]\Big|_{J=0}. \tag{4.19}$$

Now, in Euclidean spacetime, the gauge/gravity duality is encoded[9] in the following way:

$$Z_{\text{QFT}}\left[\phi_0\right] = \left\langle e^{\int_{\partial\mathcal{M}} \phi_0 \hat{\mathcal{O}}} \right\rangle = Z_{\text{gravity}}\left[\phi \to \phi_0\right] \tag{4.20}$$

where $\hat{\mathcal{O}}$ is some boundary CFT operator and ϕ is the bulk field in the $d+1$-dimensional theory that couples to it. The field ϕ_0 is the boundary value of ϕ

$$\phi_0\left(x\right) = \phi\left(r \to \infty, x\right) = \phi\left(x\right)|_{\partial AdS}\,. \tag{4.21}$$

The generating functional $Z_{\text{gravity}}\left[\phi \to \phi_0\right]$ is the partition function (or the path integral) in the gravity theory evaluated over all the functions which have the value ϕ_0 at the boundary of AdS[10]

$$Z_{\text{gravity}}\left[\phi \to \phi_0\right] = e^{-S_{cl}[\phi_0]}. \tag{4.22}$$

In Euclidean space, Eq. (4.20) implies that finding $\left\langle \hat{\mathcal{O}}\left(x\right)\hat{\mathcal{O}}\left(0\right)\right\rangle$ means to compute the second functional derivative of the gravitational action S_{cl} on the boundary value ϕ_0

$$\left\langle \hat{\mathcal{O}}\left(x_1\right)\hat{\mathcal{O}}\left(x_1\right)\right\rangle = \left.\frac{\delta^2 S_{cl}\left[\phi\right]}{\delta\varphi\left(x_1\right)\delta\varphi\left(x_2\right)}\right|_{\varphi=0} \tag{4.23}$$

where $\varphi = \left(b/r\right)^{\Delta-d}\phi$ and Δ is the mass scaling dimension. In order to calculate the $\left\langle \hat{\mathcal{O}}\hat{\mathcal{O}}\right\rangle$ correlator, one can follow the following three steps[11] [17]:

1. Write the classical gravitational action for the scalar perturbation ϕ and then extract the function $A\left(u\right)$ staying in front of $\left(\partial_u\phi\right)^2$ in the kinetic term

$$S_{cl} = \frac{1}{2}\int du\, d^4x\, A\left(u\right)\left(\partial_u\phi\right)^2 + \ldots \tag{4.24}$$

   where u is an alternative radial coordinate defined as r_0^2/r^2 with r_0 an arbitrary length. In terms of this new coordinate, the boundary is at $u = 0$.

2. After performing the Fourier transformation of the boundary coordinates and imposing the boundary condition $\phi\left(u=0,p\right) = \phi_0\left(p\right)$, find the solution of

[9] Based on the Maldacene discovery, Witten and independently Gubser, Klebanov and Polyakov deduced the general rule (4.20) relating the bulk and the boundary in 1998, thus, this formula is usually called GPKW.

[10] The action is the on-shell classical gravity action. The on-shell gravity action typically diverges and it needs to be renormalized following the procedure of *holographic renormalization*. Thus, in general, the classical action should be substituted by a renormalized version.

[11] One should take in mind that these three steps work because the classical action for classical solutions, reduces to the boundary term $\sim A\phi\phi'$.

the linearized field equation for ϕ in the following form

$$\phi\left(u,\, q\right) = f_q\left(u\right)\phi_0\left(q\right) \quad \text{with} \quad p = \left(\omega, \vec{q}\right). \tag{4.25}$$

3. The Euclidean Green's function is then defined as

$$G_E\left(q\right) = -\, A\left(u\right)\, f_{-q}\left(u\right)\partial_u f_q\left(u\right)\big|_{u\to 0} \tag{4.26}$$

and in doing the limit $u \to 0$ one may need to throw away the contact terms.

Now, one can proceed with the formulation of the prescription for the Minkowskian correlators:

1. Find the Euclidean Green's function following the previous procedure.
2. In Minkowki space one has to specify the boundary condition at the horizon $u = 1$ in addition to that at the boundary. A reasonable decision (based on the black hole physics) turns out to be to impose the incoming-wave boundary condition, i.e. waves are only absorbed by the black hole but not emitted from there.
3. The retarded[12] thermal Green's function then can be defined as

$$G^R\left(q\right) = A\left(u\right) f_{-q}\left(u\right)\partial_u f_q\left(u\right)\big|_{u\to 0}. \tag{4.27}$$

The sign of (4.27) corresponds to the standard convention of the retarded (minus sign in the front) and advanced (plus sign) Green's functions, in particular:

$$G^R\left(\omega,\, \vec{q}\right) = -i\int d^4x\, e^{-iq\cdot x}\theta\left(t\right)\left\langle\left[\hat{\mathcal{O}}\left(x\right),\, \hat{\mathcal{O}}\left(0\right)\right]\right\rangle. \tag{4.28}$$

In ref. [25] has been verified that this procedure gives indeed the correct retarded Green's function in several cases where an independent verification is possible. This prescription will be used in this section for the regular black brane solution.

[12] Choosing the outgoing-wave function, boundary condition would give the advanced Green's function instead.

4.3.1 Classical Black Three-brane Example

As an illustrative example before proceed with the next calculations based on the regular black three-brane described in Sec. 4.4.1, one can consider a black three-brane metric $g^{\mu\nu}$ given in (4.5) and write the equation of motion of a scalar field ϕ in this background[13]

$$\Box\phi = \frac{1}{\sqrt{-g}}\partial_\mu\left(\sqrt{-g}g^{\mu\nu}\partial_\nu\phi\right) = 0. \tag{4.29}$$

The solution to this equation with the boundary condition $\phi = \phi_0$ when $u = 0$ is $\phi(p,u) = f_p(u)\,\phi_0(p)$ where the function $f_p(u)$ satisfy the following equation

$$\frac{\partial^2 f_p(u)}{\partial u^2} - \left(\frac{1+u^2}{uf}\right)\frac{\partial f_p(u)}{\partial u} + \frac{w^2}{uf^2}f_p(u) - \frac{q^2}{uf}f_p(u) = 0. \tag{4.30}$$

For a standard black three-brane described by the line element (see also Eq. (4.5))

$$ds^2 = \frac{r_+^2}{ub^2}\left(-f(u)\,dt^2 + \sum_{i=1}^{3} dx_i^2\right) + \frac{b^2}{4u^2 f(u)}du^2 + b^2 d\Omega_5^2 \tag{4.31}$$

the differential equation (4.30) near the boundary $u = 0$ has two solutions $f_1 \sim 1$, $f_2 \sim u^2$ and also near the horizon $u = 1$ has two solutions

$$f_p(u) \sim (1-u)^{i\omega/2} \tag{4.32}$$

$$f_p^*(u) \sim (1-u)^{-i\omega/2}. \tag{4.33}$$

These two solutions oscillate rapidly as $u \to 1$, but the amplitude of the oscillation is constant. In virtue of this, one can accept as solution any linear combination of f_1 and f_2 near the boundary, which means that there is no unique solution to the differential equation (4.30). The two solutions f_p and f_p^*, have very different behaviour at the horizon: one correspond to a wave that moves toward the horizon (incoming wave) and the other to a wave that moves away from the horizon (outgoing wave) [23].

Motivated by the fact that nothing should escape from the horizon, one can impose the incoming-wave boundary condition at $r = r_+$. At this point the action for the bulk field plays an important role: if one writes down this action, after integrating

[13] The equation of motion can be obtained from the variation of the action of the scalar field ϕ in the AdS_{d+1} space.

by parts one get contribution from both the boundary and the horizon

$$S = \int \frac{d^4p}{(2\pi)^4}\phi_0(-p)\,\mathcal{F}(p,z)\,\phi_0(p)\Big|_{z=0}^{z=z_h}. \tag{4.34}$$

where $z = b^2/r$. If one tried to differentiate the action with respect to the boundary value ϕ_0, one would find

$$G(p) = \mathcal{F}(p,z)|_0^{z_h} + \mathcal{F}(-p,z)|_0^{z_h} \tag{4.35}$$

and this quantity is real (because the imaginary part of $\mathcal{F}(z,p)$ does not depend on z). However, this is not the expected result, as the retarded Green's functions are in general complex. A partial solution to this problem was suggested in [25] where is postulated that the retarded Green's function is related to the function $\mathcal{F}$ by the same formula that is usually used at zero temperature:

$$G_R(p) = -2\lim_{z\to 0}\mathcal{F}(p,\,z)\,. \tag{4.36}$$

In particular in this way, all the contributions from the horizon are threw away. Using the "postulate" (4.36) one can extract physical results. For instance, using the Kubo's formula (4.16) one can get the shear viscosity by studying a mode with $\vec{q} = 0$ in the low-frequency limit $\omega \to 0$. As showed in [8], the above prescription for computing the retarded Green's functions in AdS/CFT works well only if the bulk scalar field has second-order derivatives as in Gauss-Bonnet. If the bulk action contains more than two derivative, complication could arise even if one treats the higher derivative part as a perturbation. For example one needs to add Gibbons-Hawking terms to ensure a well-posed variational problem.

4.4 Regular Black Brane

The $(n+1)-$dimensional line element of a non-singular (i.e., regular) Schwarzschild BH in AdS spacetime has been introduced in Chap.1 and Chap.2 (e.g., see Eq. 2.21). The metric function for a $(n+1)$-dimensional RBH in AdS background reads:

$$ds^2 = -V_n dt^2 + \frac{1}{V_n}dr^2 + r^2 d\Omega^2 \tag{4.37}$$

where $d\Omega^2$ is the metric of the unit $(n-1)$-sphere and the function V_n is of the form

$$V_n = 1 + \frac{r^2}{b^2} - \frac{\omega_n M}{r^{n-2}}\,\gamma\left(\frac{n}{2},\,\frac{r^2}{4\theta^2}\right) \tag{4.38}$$

and b is the AdS radius which is related to the cosmological constant Λ by the equation

$$\Lambda = -\frac{n\,(n-1)}{2b^2}\ . \tag{4.39}$$

The topology of the solution (4.37) is $\boldsymbol{R}^2 \times \boldsymbol{S}^{n-1}$ but in order to describe the regular black brane, one needs to go to a solution with boundary $\boldsymbol{R}^{n-1} \times \boldsymbol{S}^1$. This solution can be obtained performing the *large mass limit* [26], because when $M >> \infty$, the $\boldsymbol{S}^{n-1}$ becomes flat and looks exactly like $\boldsymbol{R}^{n-1}$. So, in the large M limit the horizon equation $V_n\,(r) = 0$ reads

$$r_+^n = \omega_n M\,\gamma\left(\frac{n}{2},\,\frac{r_+^2}{4\theta^2}\right)\,b^2 \to \frac{r_+^n}{\gamma\left(\frac{n}{2},\,\frac{r_+^2}{4\theta^2}\right)} = \omega_n M\,b^2. \tag{4.40}$$

A scaling that reduces the metric (4.37) to a solution with boundary $\boldsymbol{R}^{n-1} \times \boldsymbol{S}^1$ is given by setting

$$r = \left(\frac{r_+}{b}\right)\rho \equiv K\rho, \qquad t = \left(\frac{r_+}{b}\right)^{-1}\tau \equiv K^{-1}\tau \tag{4.41}$$

then

$$V_n = K^2\left[\frac{\rho^2}{b^2} - \frac{\omega_n M}{K^n \rho^{n-2}}\,\gamma\left(\frac{n}{2},\,\frac{K^2\rho^2}{4\theta^2}\right)\right] \tag{4.42}$$

and the line elements reads

$$ds^2 \;=\; -\frac{V_n}{K^2}d\tau^2 + \frac{K^2}{V_n}d\rho^2 + K^2\rho^2 d\Omega^2. \tag{4.43}$$

If one introduce in the line element the explicit value for K and then consider its power to n, then

$$K^n = \left(\frac{r_+}{b}\right)^n = \frac{\omega_n M}{b^{n-2}}\,\gamma\left(\frac{n}{2},\,\frac{r_+^2}{4\theta^2}\right) \tag{4.44}$$

and one gets the complete non-singular $(n+1)$-dimensional metric

$$\begin{aligned} ds^2 \;=\; & -\frac{\rho^2}{b^2}\left[1 - \frac{b^n}{\rho^n}\cdot\frac{\gamma\left(\frac{n}{2},\,\frac{K^2\rho^2}{4\theta^2}\right)}{\gamma\left(\frac{n}{2},\,\frac{K^2b^2}{4\theta^2}\right)}\right]d\tau^2 + \frac{b^2}{\rho^2}\frac{d\rho^2}{\left[1 - \frac{b^n}{\rho^n}\cdot\frac{\gamma\left(\frac{n}{2},\,\frac{K^2\rho^2}{4\theta^2}\right)}{\gamma\left(\frac{n}{2},\,\frac{K^2b^2}{4\theta^2}\right)}\right]} + \\ & + \frac{\rho^2}{b^2}\left[\omega_n M\,\gamma\left(\frac{n}{2},\,\frac{r_+^2}{4\theta^2}\right)b^2\right]^{\frac{2}{n}} d\Omega^2. \end{aligned} \tag{4.45}$$

The metric (4.45) has interesting properties, e.g., one should notice that:

1. This metric has horizon at $\rho_+ = b$;

2. The last term describes an $\boldsymbol{S}^{n-1}$ sphere with radius

$$\frac{\rho}{b}\left[\omega_n M\,\gamma\left(\frac{n}{2},\,\frac{r_+^2}{4\theta^2}\right)b^2\right]^{\frac{1}{n}} \tag{4.46}$$

that in the limit $M \to \infty$ diverges as $M^{1/n}$ (because the gamma function is bounded). Hence, for $M \to \infty$, locally $\boldsymbol{S}^{n-1} \to \boldsymbol{R}^{n-1}$. If one introduces near a point $P \in \boldsymbol{S}^{n-1}$ coordinates y_i such that, $d\Omega^2 = \sum_i dy_i^2$, and then set

$$y_i = \left[\omega_n M\,\gamma\left(\frac{n}{2},\,\frac{r_+^2}{4\theta^2}\right)b^2\right]^{\frac{2}{n}} x_i \tag{4.47}$$

then the metric becomes

$$ds^2 \;=\; \frac{\rho^2}{b^2}\left(-f d\tau^2 + \sum_{i=1}^{n-1} dx_i^2\right) + \frac{b^2}{\rho^2 f}d\rho^2 \tag{4.48}$$

where

$$f = 1 - \frac{b^n}{\rho^n}\cdot\frac{\gamma\left(\frac{n}{2},\,\frac{K^2\rho^2}{4\theta^2}\right)}{\gamma\left(\frac{n}{2},\,\frac{K^2 b^2}{4\theta^2}\right)}. \tag{4.49}$$

3. The asymptotic formula for the gamma function $\gamma\left(\frac{n}{2},\,z\right)$ in case $z \gg 1$ gives

$$\gamma\left(\frac{n}{2},\,z\right) \sim \Gamma\left(\frac{n}{2}\right) - z^{\frac{n}{2}-1}e^{-z}\left[1 + \frac{\frac{n}{2}-1}{z} + \frac{\left(\frac{n}{2}-1\right)\left(\frac{n}{2}-2\right)}{z^2} + \ldots\right]. \tag{4.50}$$

So the expansion for $M \gg 1$ gives[14]

$$f \simeq 1 - \frac{b^n}{\rho^n}\cdot\left[1 - \frac{\left(\frac{K^2\rho^2}{4\theta^2}\right)^{\frac{n}{2}-1} e^{-\frac{K^2\rho^2}{4\theta^2}}}{\Gamma\left(\frac{n}{2}\right)}\right]. \tag{4.51}$$

The black brane metric (4.48) can also be described using an alternative radial coordinate u, defined as $u = (b/\rho)^v$. In terms of the radial coordinate u, the boundary is at $u = 0$, the horizon at $u = 1$ and the

$$du = \frac{b^v\,(-v)}{\rho^{v+1}}d\rho = \frac{b^v\,(-v)}{\rho^v\rho}d\rho \tag{4.52}$$

writing explicitly ρ one gets

$$d\rho = \frac{du}{b^v\,(-v)}\,\frac{b^v}{u}\cdot\frac{b}{u^{1/v}} = du\cdot\frac{b}{(-v)\,u\cdot u^{1/v}} \tag{4.53}$$

[14] (the same expansion would occur for $\theta \to 0$)

while

$$f \to \tilde{f} = 1 - u^{n/v} \cdot \frac{\gamma\left(\frac{n}{2}, \frac{K^2\left(b/u^{1/v}\right)^2}{4\theta^2}\right)}{\gamma\left(\frac{n}{2}, \frac{K^2 b^2}{4\theta^2}\right)} \tag{4.54}$$

and the metric (4.48) in the new coordinate reads

$$ds^2 = \frac{b^2}{u^{2/v}} \cdot \frac{1}{b^2}\left(-\tilde{f}\, d\tau^2 + \sum_{i=1}^{n-1} dx_i^2\right) + \frac{b^2 u^{2/v}}{b^2 f} \cdot \frac{b^2}{(-v)^2 \left(u \cdot u^{1/v}\right)^2} du^2 \tag{4.55}$$

and finally one can write the black brane metric as

$$ds^2 = \frac{1}{u^{2/v}}\left(-\tilde{f}\,(u)\; d\tau^2 + \sum_{i=1}^{n-1} dx_i^2\right) + \frac{b^2}{v^2 u^2 \tilde{f}\,(u)} du^2. \tag{4.56}$$

Now, one last variables transformation is needed to bring the metric in the usual black brane form: the time variable goes like $\tau \to t/K$ (that is the inverse of (4.41)) and the flat coordinates x^i can be rescaled as $dx^i \to d\tilde{x}^i/K$, giving the well-know

$$ds^2 = \frac{r_+^2}{b^2 u^{2/v}}\left(-\tilde{f}\,(u)\; d\tau^2 + \sum_{i=1}^{n-1} dx_i^2\right) + \frac{b^2}{v^2 u^2 \tilde{f}\,(u)} du^2 \tag{4.57}$$

that is the regular black brane metric in generic n space dimensions.

4.4.1 Black Brane Metric

In this section the black brane metric (4.56) in the case $n = 4$ and $v = 2$ is considered. Using the $K^2 = r_+^2/b^2$

$$ds^2 = \frac{r_+^2}{b^2\, u}\left(-\tilde{f}\,(u)\; d\tau^2 + \sum_{i=1}^{n-1} dx_i^2\right) + \frac{b^2}{4u^2 \tilde{f}\,(u)} du^2, \qquad \tilde{f} = 1 - u^2 \cdot \frac{\gamma\left(2, \frac{r_+^2}{4\theta^2 u}\right)}{\gamma\left(2, \frac{r_+^2}{4\theta^2}\right)} \tag{4.58}$$

where the horizon is at $u = 1$ and the AdS boundary is at $u = 0$. Now, one can perform the calculation directly in the case of five spacetime dimensions. Starting from Eq. (4.38)

$$ds^2 = -V_4\,(r)\, dt^2 + V_4^{-1}\,(r)\, dr^2 + r^2 d\Omega_3^2 \tag{4.59}$$

where the function $V_4\,(r)$ (that corresponds to $n = 4$ and spacetime $d = 5$) reads explicitly

$$V_4\,(r) = 1 - \frac{M\, G_5}{r^2}\gamma\left(2, \frac{r^2}{4\theta^2}\right) + \frac{r^2}{b^2}. \tag{4.60}$$

In the large M limit, the horizon equation $V_4(r) = 0$ gives

$$\frac{M\,G_5}{r_+^2}\gamma\left(2,\,\frac{r_+^2}{4\theta^2}\right) = \frac{r_+^2}{b^2} \tag{4.61}$$

from which one can obtain

$$M\,G_5 = \frac{r_+^4}{b^2\gamma\left(2,\,\frac{r_+^2}{4\theta^2}\right)} \tag{4.62}$$

and using the M in (4.60) then

$$V_4(r) = -\left(\frac{r_+^4}{b^2r^2}\right)\frac{\gamma\left(2,\,\frac{r^2}{4\theta^2}\right)}{\gamma\left(2,\,\frac{r_+^2}{4\theta^2}\right)} + \frac{r^2}{b^2} \tag{4.63}$$

$$= \frac{r^2}{b^2}\left[1 - \left(\frac{r_+^4}{r^4}\right)\frac{\gamma\left(2,\,\frac{r^2}{4\theta^2}\right)}{\gamma\left(2,\,\frac{r_+^2}{4\theta^2}\right)}\right] \tag{4.64}$$

One can go to the standard form of the black brane metric, performing the coordinate transformation

$$u = \frac{r_+^2}{r^2} \tag{4.65}$$

that gives,

$$V_5(u) = \frac{r_+^2}{b^2u}\left[1 - u^2\frac{\gamma\left(2,\,\frac{r_+^2}{4u\,\theta^2}\right)}{\gamma\left(2,\,\frac{r_+^2}{4\theta^2}\right)}\right] \tag{4.66}$$

and defines

$$f(u) = 1 - u^2\frac{\gamma\left(2,\,\frac{r_+^2}{4u\,\theta^2}\right)}{\gamma\left(2,\,\frac{r_+^2}{4\theta^2}\right)} \tag{4.67}$$

giving finally the metric (4.57) in $d = 5$ spacetime dimensions

$$ds^2 = \frac{r_+^2}{b^2u}\left[-f(u)\,dt^2 + d\vec{x}^2\right] + \frac{b^2}{4u^2f(u)}du^2. \tag{4.68}$$

4.4.2 Black Brane Temperature

Let us now look at the Hawking temperature for a general class of black brane metrics of the form

$$ds^2 = g(r)\left[-f(r)\;dt^2 + d\vec{x}^2\right] + \frac{1}{h(r)}dr^2 \tag{4.69}$$

where $f(r)$ and $h(r)$ have a first order zero at the horizon, whereas $g(r)$ is non-vanishing there. Now one demands that the Euclidean continuation of the metric (4.69),

$$ds^2 = g(r)\left[f(r)\, dt_E^2 + d\vec{x}^2\right] + \frac{1}{h(r)} dr^2 \tag{4.70}$$

obtained by the change of variables $t \to -it_E$, be regular at the horizon. Expanding the euclidean metric (4.70) near the horizon $r = r_+$ one gets

$$ds^2 \approx \rho^2 d\varphi^2 + d\rho^2 + g(r_+)\, d\vec{x}^2 \tag{4.71}$$

with the new variable ρ, φ defined as

$$\rho = 2\sqrt{\frac{r - r_+}{h'(r_+)}} \qquad \varphi = \frac{t_E}{2}\sqrt{g(r_+)\, f'(r_+)\, h'(r_+)}. \tag{4.72}$$

The first two terms in (4.71) describe a plane in polar coordinates, so in order to avoid a conical singularity at $\rho = 0$, one need require φ having period 2π. From (4.72) one finally gets that the period $\beta = 1/T$ of the Euclidean time must be

$$\beta = \frac{1}{T} = \frac{4\pi}{\sqrt{g(r_+)\, f'(r_+)\, h'(r_+)}}. \tag{4.73}$$

Equation (4.73) can be applied to the metric (4.58) giving the temperature

$$T = \frac{r_+}{\pi b^2}\left(1 - \frac{r_+^4 e^{-\frac{r_+^2}{4\theta^2}}}{32\,\theta^4 \gamma\left(2, \frac{r_+^2}{4\theta^2}\right)}\right). \tag{4.74}$$

The temperature (4.74) for the regular black three-brane is lower than the temperature of the black three-brane (see Fig. 4.2).

4.4.3 Scalar Perturbations

Now that we have the black brane metric, it is possible to compute the stress tensor correlators for a boundary CFT described by a particular action S. The fluctuations of the boundary stress-energy tensor are described, in the gravity language, by small metric fluctuations $h_{\mu\nu}$ around the black brane solution. Taking into account the various symmetries and gauge degrees of freedom, only certain components can mix.

For example, if one considers perturbations to the black brane background with frequency ω and momentum p_3 along the x_3 axis, the system manifest an $O(2)$

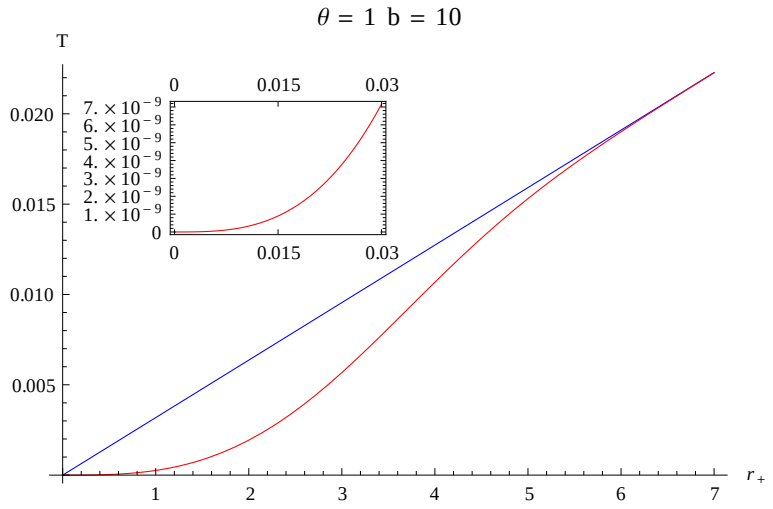

FIGURE 4.2: **Black Brane temperture vs horizon radius.** Temperature of a black three brane (blue line) and a regular black three brane (red). The temperature for both the metrics reaches the zero value only at $r_+ = 0$.

symmetry in the plane (x_1, x_2). In this case the perturbation h_{12} does not mix with any other components, whereas components h_{01} and h_{31} mix only with each other. Therefore, the metric fluctuations can be combined into three independent scalar fields ϕ_a with $a = 1, 2, 3$ (because only these three metric components are different from zero). These three independent scalar fields given by the fluctuation of the metric are dual to the Green's function on the boundary. In particular for the calculation of the shear viscosity the so-called *scalar perturbation* $\phi = h^1_2$ is used. Adding the perturbation h^1_2 to the black brane metric (4.58), the quadratic part of the gravitational action (without the contribution of the matter part L_m) in terms of the scalar field reads

$$S_{quad} = \frac{1}{16\,\pi G_N} \int d^4x\, dr\, \sqrt{-g} \left(-\frac{1}{2} g^{\mu\nu} \partial_\mu \phi \partial_\nu \phi \right). \tag{4.75}$$

4.4.4 Equation of Motion for the Scalar Channel

To compute the shear viscosity, one needs to study small metric fluctuation $\phi = h^x_y$ around the black brane background and compute the two-point correlation function of T^{xy}. Varying the action for the scalar perturbation (4.75), one gets the field equation for ϕ

$$\partial_\mu \left(\sqrt{-g}\, g^{\mu\nu}\, \partial_\nu \phi \right) = 0. \tag{4.76}$$

The equation of motion for the black three-brane metric

$$ds^2 = \frac{r_+^2}{u\, b^2} \left(-f dt^2 + d\boldsymbol{x}^2 \right) + \frac{b^2}{4u^2} \frac{du^2}{f} \tag{4.77}$$

where f is defined as in Eq. (4.67), is obtained from (4.76) and gives

$$\left(\frac{w^2}{u\,f^2}-\frac{q^2}{uf}\right)\phi\left(u,\,q\right)+\left(\frac{f'}{f}-\frac{1}{u}\right)\phi'\left(u,\,q\right)+\phi''\left(u,\,q\right)=0 \tag{4.78}$$

where the primes denote the derivative with respect to the variable u. The variables q, w are defined as

$$q=p_3\left(\frac{b^2}{2r_+}\right)\qquad w=\omega\left(\frac{b^2}{2r_+}\right). \tag{4.79}$$

In (4.78), the scalar field ϕ is written in the Fourier decomposition and it is defined to be independent of x_1 and x_2

$$\phi\left(t,\,u,\,x_3\right)=\int\frac{d\omega\,dp_3}{\left(2\pi\right)^2}\phi\left(u,\,p_3\right)e^{-i\omega t+ip_3x_3},$$
$$p=\left(\omega,\,0,\,0,\,p_3\right),\qquad \phi\left(u,\,p_3\right)=\phi^*\left(u,\,-p_3\right). \tag{4.80}$$

Usually, i.e., in the classical limit $r_+\gg\theta$, Eq. (4.78) is the Heun differential equation (second-order differential equation with four regular singular points). Global solutions to the Heun equation are unknown. However, for computing the shear viscosity one needs to consider only the regime of low frequency and momentum, $\omega,p_3\ll T$. In this regime, the solution representing the incoming wave at the horizon is given by

$$\phi_{p_3}\left(u\right)=\left(1-u\right)^{-iw/2}F_{p_3}\left(u\right), \tag{4.81}$$

where $F_{p_3}\left(u\right)$ is regular at $u=1$ and can be written as a series

$$F_{p_3}\left(u\right)=1-\left(\frac{iw}{2}+q^2\right)\ln\frac{1+u}{2}+O\left(w^2,wq^2,q^4\right). \tag{4.82}$$

Let us now study the equation of motion for the regular black three-brane. Substituting the metric function f of the regular black brane (4.58)

$$f=1-u^2\cdot\frac{\gamma\left(2,\,\frac{r_+^2}{4\theta^2u}\right)}{\gamma\left(2,\,\frac{r_+^2}{4\theta^2}\right)} \tag{4.83}$$

in the coefficients of the differential equation (4.78), in this way

$$\mathfrak{q}\left(u\right)\phi\left(u,\,q\right)+\mathfrak{p}\left(u\right)\phi'\left(u,\,q\right)+\phi''\left(u,\,q\right)=0 \tag{4.84}$$

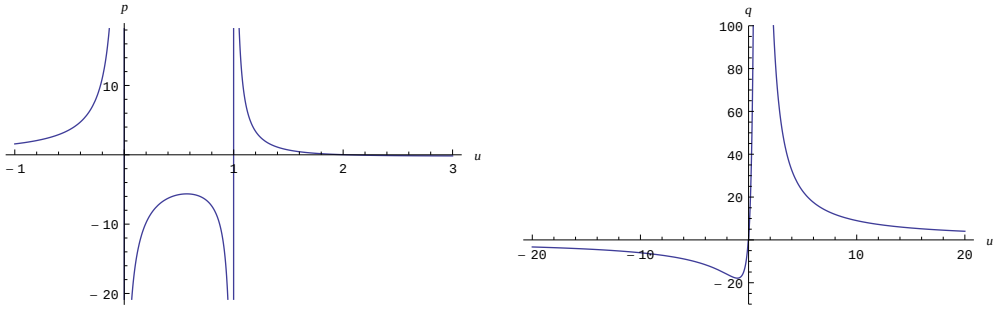

FIGURE 4.3: **Scalar perturbation equation of motion.** Details of the coefficients around the poles. *(Left)* Plot of the function $\mathfrak{p}(u)$ for values $\theta = 12$, $r_+ = 10.1$. *(Right)* Plot of the function $\mathfrak{q}(u)$ for values $\theta = 12$, $r_+ = 10.1, w = 1, q = 1$.

one obtains that the two functions are given by

$$\mathfrak{p}(u) = \frac{r_+^4 e^{-\frac{r_+^2}{4\theta^2 u}} - 16\theta^4 \left[\gamma\left(2, \frac{r_+^2}{4\theta^2}\right) + u^2\gamma\left(2, \frac{r_+^2}{4u\theta^2}\right)\right]}{16\theta^4 u \left[\gamma\left(2, \frac{r_+^2}{4\theta^2}\right) - u^2\gamma\left(2, \frac{r_+^2}{4u\theta^2}\right)\right]} \tag{4.85}$$

and

$$\mathfrak{q}(u) = \frac{1}{u}\left(\frac{q^2u^2\gamma\left(2, \frac{r_+^2}{4u\theta^2}\right)}{\gamma\left(2, \frac{r_+^2}{4\theta^2}\right)} - q^2 + w^2\right)\left(\frac{u^2\gamma\left(2, \frac{r_+^2}{4u\theta^2}\right)}{\gamma\left(2, \frac{r_+^2}{4\theta^2}\right)} - 1\right)^{-2}. \tag{4.86}$$

From a numerical study (see Fig. 4.3) one finds that $\mathfrak{p}(u)$ has two divergences, one in $u = 0$ and the other in $u = 1$ while $\mathfrak{q}(u)$ has only one divergence in $u = 0$. One can also see that

$$\lim_{u\to 1^-} \mathfrak{p}(u)(u-1) = 1 \tag{4.87}$$

$$\lim_{u\to 0^+} \mathfrak{p}(u)\, u = -1 \tag{4.88}$$

$$\lim_{u\to 0^+} \mathfrak{q}(u)\, u = w^2 - q^2 \tag{4.89}$$

$$\lim_{u\to 0^+} \mathfrak{q}(u)\, u^2 = 0. \tag{4.90}$$

that means that the two functions have first order poles. Therefore, in the regular black three-brane solution, there are only three regular singular points at $u = 0, 1, +\infty$.

4.5 Calculation of η/s for the Regular Black Brane

In general, if the field theory at temperature $T \neq 0$ is translational and rotational invariant, the gravitational metric (4.48) can be written as

$$ds_5^2 = -g_{tt}dt^2 + g_{rr}d^2r + g_{xx}\delta_{ij}dx^i dx^j = g_{NM}dx^M dx^N \tag{4.91}$$

with metric components that depend only on r. As seen before, a non-zero temperature field theory has a dual theory characterized by the presence of an event horizon. Thus, one can assume that in the non-extremal case, g_{tt} has a zero of order one while g_{rr} has a first order pole at the horizon $r = r_+$.
In order to compute the transport coefficient η associated to some operator $\hat{\mathcal{O}}$ in this theory, one can use the Kubo formula (4.16).

$$\eta = -\lim_{\omega\to 0}\lim_{\vec{k}\to 0}\frac{1}{\omega}\,\mathrm{Im}G_R\left(\omega,\vec{k}\right) \tag{4.92}$$

where $k_\mu = \left(\omega,\vec{k}\right)$. Assuming that the quadratic effective action for the bulk mode ϕ dual to $\hat{\mathcal{O}}$ has the form of the massless scalar field

$$S = -\frac{1}{2}\int d^{n+1}x\,\sqrt{-g}\,\frac{1}{q\,(r)}g^{MN}\partial_M\phi\partial_N\phi, \tag{4.93}$$

where $q\,(r)$ is a function of r and can be considered a spacetime dependent coupling constant. Using the Kubo formula (4.16) with the general expression for the retarded correlators, one finds that [18]

$$\eta = -\lim_{k_\mu\to 0}\lim_{r\to 0}\frac{\Pi\,(r,\,k_\mu)}{i\omega\phi} \tag{4.94}$$

where Π is the canonical momentum of the field ϕ:

$$\Pi = \frac{\delta S}{\delta\partial_r\phi} = -\frac{\sqrt{-g}}{q\,(r)}g^{rr}\,\partial_r\phi. \tag{4.95}$$

The equation (4.94) follows from the fact that the real part of $G_R\,(k)$, when $k \to 0$,vanishes faster then linearly in ω. Moreover, in (4.94), both Π and ϕ are solutions of the classical equation of motion. The evaluation of η using (4.92), requires the determination of both $\omega\phi$ and Π in the small four momentum $k_\mu \to 0$.
In the Hamiltonian formalism the equations of motions are given by (4.95) together with

$$\partial_r\Pi = -\frac{\sqrt{-g}}{q\,(z)}g^{\mu\nu}k_\mu k_\nu\phi. \tag{4.96}$$

In the limit $k_\mu \to 0$, the e.o.m. (4.95) and the Eq. (4.96) are trivial

$$\partial_r \Pi = 0 + O\left(k_\mu \omega \phi\right), \ \partial_r\left(\omega\phi\right) = 0 + O\left(\omega \Pi\right), \tag{4.97}$$

and both quantities become independent of r, which allows their evaluation at any r. Since the only restriction on the general metric (4.91) is that it possesses an horizon, one can simply evaluate the e.o.m. at the horizon r_+ where the infalling boundary condition should be imposed.

In the near-horizon approximation $r \to r_+$, the metric functions can be written as in (B.7)

$$g_{tt} = -c_0\left(r_+ - r\right), \quad g_{rr} = \frac{c_r}{r_+ - r} \tag{4.98}$$

and from the equation of motions one find the following differential equation

$$\sqrt{\frac{c_0}{c_r}}\left(r_+ - r\right)\partial_r\left(\sqrt{\frac{c_0}{c_r}}\left(r_+ - r\right)\partial_r\phi\right) + \omega^2\phi = 0. \tag{4.99}$$

As seen before, the two general solutions for this equations are

$$\phi \propto e^{-i\omega t}\left(r_+ - r\right)^{\pm i\omega\sqrt{c_r/c_0}}. \tag{4.100}$$

The infalling boundary condition imposes to take the negative sign in the exponent. Therefore, from Eq. (4.100), one find that at the horizon

$$\partial_r\phi = \sqrt{\frac{g_{rr}}{-g_{tt}}}\left(i\omega\phi\right), \tag{4.101}$$

and using (4.95) and (4.100) one obtains that (4.94)

$$\eta = \frac{1}{q\left(r_+\right)}\sqrt{\frac{-g}{-g_{rr}g_{tt}}}\bigg|_{r_+}. \tag{4.102}$$

One can now apply this result to the regular black brane where

$$\begin{aligned} q\left(r_+\right) &= 16\pi G_N \\ g &= g_{tt}g_{rr}\left(g_{xx}\right)^3 \end{aligned}$$

and the shear viscosity (4.102)

$$\eta = \frac{1}{16\pi G_N}\left(\frac{b}{r_+}\right)^3 \tag{4.103}$$

depends from the parameter θ only via the horizon radius r_+. The same result

can be obtained using other methods (see Appendix B). The result (4.103) is the standard result that one can obtain for a general black brane. To obtain the entropy density $s = S/\text{ Vol }(x_1x_2x_3)$, necessary for the calculation of the ratio η/s, one should integrate the first law of black brane thermodynamics

$$dS = \frac{dM}{T} \tag{4.104}$$

$$= \frac{3r_+^2 \text{Vol}(x_1x_2x_3)}{4\,b^3\,G_N\,\gamma\left(2, \frac{r_+^2}{4\theta^2}\right)} dr_+. \tag{4.105}$$

Since the temperature goes to zero faster then the derivative of the mass, the function (4.105) diverges as $r_+ \to 0$. In the IR limit, $r_+ >> \theta$, the brane behaves like a classical black brane and its entropy is $S = \frac{\text{Vol}(x_1x_2x_3)}{4G_N}\left(\frac{r_+}{L}\right)^3$.

4.6 Calculation of η/s for the Gauss-Bonnet Black Brane

The *universality* of the shear viscosity η to entropy density s ratio for Einstein-Hilbert gravity represents a very important result of the gauge/gravity correspondence. First found for the hydrodynamic regime of the QFT dual to black branes and black holes of the Einstein-Hilbert theory [1, 16, 27]. The KSS bound $\eta/s \geq 1/4\pi$ has been extended to a variety of cases including the Einstein-Hilbert gravity with all possible matter terms in the action, hence, among others the QFT dual to Reissner-Nordström $5d$ gravity [1, 27] and the important case of the quark-gluon plasma (see e.g. [28]). As already discussed in the introduction, it has been also conjectured that the KSS bound holds for any fluid in nature. For a detailed discussion on the shear viscosity to entropy ratio see Refs. [1, 8, 16, 27, 28, 29, 30, 31].

In the previous sections, it has been showed that also the non-extremal *regular* black brane satisfies the bound. However, the KSS bound seems to lose its universality when one introduces, in the Einstein-Hilbert action, higher powers of the curvature tensors. This is, for instance, the case of Lovelock (and Gauss-Bonnet) gravity that it will be discussed in the following sections. In particular, the KSS bound acquires a dependence on the coupling constant for the higher curvature terms [8].

Following the notation of [8], we rewrite the Gauss-Bonnet (GB) black brane (BB) solution (2.78) as follows

$$f_{-}=\frac{r^{2}}{2\lambda L^{2}}\left[1-\sqrt{1-4\lambda\left(1-\frac{\omega_{5}ML^{2}}{r^{4}}+\frac{4\pi}{3}\frac{G_{N}Q^{2}L^{2}}{r^{6}}\right)}\right], \tag{4.106}$$

where L now is the AdS radius and $\alpha_0\alpha_2 = \alpha_2/L^2 = \lambda$. In $5d$ Gauss-Bonnet gravity, the shear viscosity to entropy ratio is [8]

$$\frac{\eta}{s}=\frac{1}{4\pi}\left(1-4\lambda\right). \tag{4.107}$$

The KSS bound still holds if $\lambda \leq 0$, and it is violated for $0 < \lambda \leq 1/4$ (the upper bound follows from Eq. (2.76)). The dependence of the bound from the coupling constant λ makes the bound not anymore universal as in the Einstein-Hilbert theory. In terms of the dual gauge theory, the curvature corrections to the Einstein-Hilbert action correspond to finite N_c (rank of the gauge group) and λ_{tH} ('t Hooft coupling) effects. It has been argued that the universality of the KSS bound strictly holds in the limit $N_c \to \infty$ whereas, in general, finite N_c effects will give lower bounds for η/s [10].
A crucial issue is that the relation (4.107) seems to allow for arbitrary violations of the KSS bound. However, consistency of the QFT dual to bulk GB gravity as a relativistic field theory constrains the allowed values of λ. For instance, in [9, 32, 33] it was found that causality and positivity of the energy for the dual QFT describing the Gauss-Bonnet plasma require $-7/36 < \lambda < 9/100$ implying $4\pi\eta/s > 16/25$, a bound lower then the KSS bound. On the other hand, the hydrodynamic description of the dual GB plasma is valid in the IR regime,i.e., for $\omega, k << T$, whereas causality is determined by the propagation of modes in the $\omega, k > T$, UV regime. Thus, *the existence of lower bounds for η/s implies a higher non-trivial relationship between the transport properties in the IR and causality requirements in the UV regime of the QFT dual to GB gravity.*

Recent investigations have shown that if translation symmetry is broken in the IR then one may have strong violation of the KSS bound even in the context of Einstein gravity, in the form of $\eta/s \sim T^{2\nu}$, $\nu \leq 1$ [13, 34, 35]. Although, for these backgrounds, the breaking of translational invariance prevents an hydrodynamical interpretation of the viscosity, this behaviour of η/s is clearly related to the emergence of extremely interesting physics in the far IR. A way to shed light on these questions is to investigate the behaviour of η/s in the case of a gravitational bulk background for which there is a temperature flow of η/s. The charged GB

BB represents a nice example of this behaviour, particularly in view of the universality of the IR $AdS_2 \times R_3$ fixed point. This will be the subject of the next three subsections.

4.6.1 η/s for the Charged Gauss-Bonnet Black Brane

A standard way to calculate the shear viscosity for a QFT is by using the Kubo formula for the transverse momentum conductivity

$$\eta = \lim_{\omega \to 0} \frac{1}{\omega} Im G^R_{xy}, \tag{4.108}$$

where G^R_{xy} is the retarded Green function for the T_{xy} component of the stress-energy tensor. The application of the usual AdS/CFT procedure for the computation of correlators gives for the $U(1)$-charged Gauss-Bonnet black brane in five dimensions [30, 31]

$$\eta = \frac{s}{4\pi}\left[1 - 4\lambda\left(1 - \frac{a}{2}\right)\right] \tag{4.109}$$

where $a = \frac{4\pi}{3}\frac{G_N Q^2 L^2}{r_+^6}$ and s is the entropy density S/V following from (2.96).

4.6.1.1 Extremal Black Brane

A drawback of the usual computation of the shear viscosity is that it does not work in the extremal $T_H = 0$ case because the metric function has a double zero at the horizon. For this reason, η in the case of extremal BB cannot be simply computed by taking the $T_H = 0$ limit in Eq. (4.109). Building on [36], a method of dealing with this problem has been developed in [37]. Recently, a very simple and elegant formula for computing correlators of the form (4.108) in QFTs dual to a gravitational bulk theory has been proposed in [15] (see also [13, 14]). This method also works in the extremal case; thus, in the following, we will use it to compute η for the charged GB BB. The extremal case will be discussed in Sect. 4.6.3.

Considering perturbations $g_{ab} = g^{(0)}_{ab} + h_{ab}$ of the background (4.106), at the linear level the field equations (2.94) give for the $h^y_x(t,r) = \phi(r)e^{-i\omega t}$ component of the perturbation

$$\partial_r\left[\sqrt{\gamma(r)} f_-(r) F(r) \partial_r \phi\right] + \omega^2 \frac{\sqrt{\gamma(r)} F(r)}{N^2 f_-(r)}\phi = 0, \tag{4.110}$$

where $\gamma(r) = (r/L)^3$ is the determinant of the spatial metric, $f_-(r)$ is given by Eq. (4.106) and $F = N\left(1 - \frac{\lambda L^2}{r}\partial_r f_-(r)\right)$. Notice that in the background (4.106), the component h^y_x decouples from the other perturbation modes.

Let us first consider the *non-extremal charged GB black brane*. Following Ref. [15] we now denote with $\phi_0(r)$ the time independent solution of (4.110) which is regular on the horizon $r = r_+$ and such that $\phi_0 \to 1$ as $r \to \infty$. The other linearly independent solution $\phi_1(r)$ of Eq. (4.110) behaves as $1/r^4$ for $r = \infty$ and can be computed using the Wronskian method,

$$\phi_1 = \phi_0 \int_r^\infty \frac{dr}{\phi_0^2 \sqrt{\gamma} F f_-}. \tag{4.111}$$

Expanding near the horizon $r = r_+$ we get at leading order

$$\phi(r) = -\frac{1}{\phi_0(r_+)} \frac{\ln(r - r_+))}{4\pi T_H \sqrt{\gamma(r_+)}\left[1 - 4\lambda(1 - \frac{a}{2})\right]}, \tag{4.112}$$

where T_H is the Hawking temperature of the BB and a is defined as in Eq. (4.109). Solving now Eq. (4.110) near the horizon with infalling boundary conditions and for small ω, one gets at leading order in ω

$$\phi(r) = \phi_0(r_+)\left[1 - \frac{i\omega}{4\pi T_H}\ln(r - r_+)\right]. \tag{4.113}$$

Comparing Eq. (4.112) with Eq. (4.113) and expanding near the $r \to \infty$ boundary of AdS, one gets

$$\phi(r) = 1 + i\omega\phi_0^2(r_+)\sqrt{\gamma(r_+)}\left[1 - 4\lambda\left(1 - \frac{a}{2}\right)\right]\frac{1}{r^4}. \tag{4.114}$$

The usual AdS/CFT rules for computing boundary correlators tell us that the retarded Green function is $1/(16\pi G_N)$ the ratio between normalizable and non-normalizable modes, so that we have

$$\eta = \frac{s}{4\pi}\phi_0(r_+)^2\left[1 - 4\lambda\left(1 - \frac{a}{2}\right)\right]. \tag{4.115}$$

Because $\phi_0(r)$ goes to 1 as $r \to \infty$ and must be regular on the horizon, we have $\phi_0(r_+) = 1$ and Eq. (4.115) reproduces correctly the previous result (4.109).

Now, the second Eq. (2.96) can be used to define, implicitly, the horizon radius as a function of the BB Hawking temperature and the electric charge, thus allowing

us to write also the shear viscosity (4.109) as a function of T_H and Q

$$\eta(T_H, Q) = \frac{1}{16\pi G_N}\left(\frac{r_+(T_H, Q)}{L}\right)^3\left[1 - 4\lambda\frac{\pi L^2 T_H}{N r_+(T_H, Q)}\right]. \tag{4.116}$$

In the same way, the entropy density in Eq. (2.96) can be written as a mere function of T_H and Q, so that we can write the shear viscosity to entropy ratio in the form

$$\frac{\eta}{s} = \frac{1}{4\pi}\left[1 - 4\lambda\frac{\pi L^2}{N r_+(T_H, Q)}T_H\right]. \tag{4.117}$$

It is also of interest to write explicitly the dependence of η/s from the normalization constant N:

$$\frac{\eta}{s} = \frac{1}{4\pi}\left[1 - 4N\pi L^2(1 - N^2)\frac{T_H}{r_+}\right] \tag{4.118}$$

When the electric charge is set to zero, the ratio T_H/r_+ in Eq. (4.117) is $N/(\pi L^2)$ and η/s reaches the value in Eq. (4.107), as one expects. On the other hand, the dependence of η/s on T_H and N in the generic case is rather puzzling.

In view of the universality of the thermodynamic behaviour of GB BB described in Chap. 2, one would naively expect that also the shear viscosity to entropy ratio should be universal, i.e., that Eq. (4.118) becomes the same as in the RN case just by using the effective temperature $T = T_H/N$ instead of T_H. This is not the case. Only for $N = 1$, which corresponds to $\alpha_2 = 0$, i.e., exactly the RN case, η/s assumes the universal value $1/4\pi$, while for N generic we have a quite complicated dependence on N and T_H. This strongly indicates that the transport features of the dual QFT in the hydrodynamic regime contain more information about the underlying microscopic theory than that contained in the thermodynamic description.

An investigation on the behaviour of η/s at large and small T_H can shed light on this issue. In fact, as we have seen in Chap. 2, in these limits the BB allows for a simple thermodynamic description. We, therefore, expect this to be true also for the shear viscosity to entropy ratio. This will be the subject of the next sections.

4.6.2 η/s in the Large and Small T_H Regime

The behavior of the shear viscosity (4.116) for large and small temperatures can be investigated in a way similar to that used for the GB BB thermodynamics.

4.6.2.1 Large T_H

For large T_H, the Hawking temperature is given by Eq. (2.98), thus leading to the following expression for the shear viscosity in Eq. (4.116),

$$\eta = \frac{1}{16\pi G_N}\left(\frac{\pi L T_H}{N}\right)^3 (1-4\lambda)\,. \tag{4.119}$$

The shear viscosity at large T_H scales as T_H^3. In this limit, the entropy density also depends on the temperature as T_H^3 (see Eq. (2.99)), the shear viscosity to entropy density ratio approaches Eq. (4.107) and reduces to the universal value $1/4\pi$ when $\lambda \to 0$. This is rather expected, because at large T_H the contribution of the electric charge can be neglected.

4.6.2.2 Small T_H

To investigate the small T_H behaviour we invert Eq. (2.102) and we write the horizon radius as

$$r_+ - r_0 \simeq \frac{\pi L^2}{6N} T_H\,, \tag{4.120}$$

where r_0 is defined by Eq. (2.100). At small temperature the sub-leading term in the shear viscosity scales linearly in T_H

$$\eta \simeq \frac{1}{16\pi G_N}\left(\frac{r_0}{L}\right)^3 \left[1 + \left(\frac{1}{2} - 4\lambda\right)\frac{\pi L^2 T_H}{N r_0}\right]\,. \tag{4.121}$$

The behavior of the entropy density in the small T_H regime is given by the second equation in (2.103). Hence, in this limit, also the subleading term of the shear viscosity to entropy density ratio scales linearly

$$\frac{\eta}{s} \simeq \frac{1}{4\pi}\left[1 - 4\lambda\frac{\pi L^2 T_H}{N r_0}\right]\,. \tag{4.122}$$

The result $\eta/s = 1/4\pi$ for $T_H = 0$ has been already found and discussed in the literature in the case of the RN solution [36, 37]. It has been argued that at small temperatures, the dual QFT behaves as a "strange RN metal". The optical conductivity exhibits the generic perfect-metal behaviour, but although we have a non-vanishing ground-state entropy, for the strange metal hydrodynamics continues to apply and energy and momentum can diffuse.

In the limit $T_H = 0$, the ratio becomes $\eta/s = 1/4\pi$ attaining the universal value one expects from the KSS bound. This result is what one naturally expects in view

of the fact that at $T_H = 0$ the near-horizon solution of the GB brane gives exactly the same $AdS_2 \times R_3$ geometry of the RN solution. However, extra care is needed when one takes the $T_H \to 0$ limit in Eq. (4.117). Taking $T_H \to 0$ directly in Eq. (4.117) is not save for several reasons. First, as discussed in Sect. (2.10.4) the semiclassical description for the BB breaks down at small temperature when the energy gap above extremality prevents excitations with finite energy. Second, as noted by Cai [31], although the $T_H \to 0$ limit is well defined, the usual computation of the shear viscosity to entropy ratio fails in the extremal case because the metric function as a double zero at the horizon. Third, also the computations of Sect. 4.6.1 do not hold for $T_H = 0$ because the expressions (4.112) and (4.113) are ill defined for $T_H = 0$. However, the general method based on [15] and used in Sect. 4.6.1 for calculating η, works also for extremal BB.

4.6.3 η/s in the Extremal Case

Let us now extend the calculations of η described in Sect. 4.6.1 to the case of the extremal brane. In the extremal case the function f_- given by Eq. (4.106) and its first derivative vanish when evaluated on the horizon. We have therefore at leading order near the horizon

$$f_-(r_+) = f'_-(r_+) = 0, \quad F(r_+) = N, \quad f_-(r) \simeq k(r - r_+)^2, \tag{4.123}$$

where k is some non zero constant. Using the previous expression in (4.111) one gets

$$\phi_1(r) = \frac{1}{kN\phi_0(r_+)\sqrt{\gamma(r_+)}} \frac{1}{(r - r_+)}. \tag{4.124}$$

On the other hand the near-horizon, small ω expansion gives now

$$\phi(r) = \phi_0(r_+) \left[1 + \frac{i\omega}{kN(r - r_+)}\right]. \tag{4.125}$$

Comparing Eqs. (4.124) and (4.125), near the $r \to \infty$ boundary of AdS_5 we find the expansion

$$\phi(r) = 1 + i\omega\phi_0^2(r_+)\sqrt{\gamma(r_+)} \left(\frac{1}{r^4}\right), \tag{4.126}$$

from which follows the shear viscosity

$$\eta = \frac{s}{4\pi}\phi_0(r_+)^2. \tag{4.127}$$

Using the same argument used in Sect. (4.6.1) to infer that $\phi_0(r_+) = 1$, we get for the shear viscosity to entropy ratio of the extremal GB black brane the universal value

$$\frac{\eta}{s} = \frac{1}{4\pi}\,. \tag{4.128}$$

It is interesting to notice that the universality of η/s for the extremal GB BB is a direct consequence of the universality of the $\mathrm{AdS}_2 \times R_3$, extremal, near-horizon geometry. In fact the extremal, near-horizon metric background (2.93) does not depend on λ. The other source for a λ- or Q-dependence of η is the function F in Eq. (4.110). However, this contribution, hence the dependence of η from λ and Q, is removed by the condition $f'(r_+) = 0$, which implies that near the horizon the two-dimensional sections of the metric behave as AdS_2.

To conclude, let us now discuss the global behaviour of η/s as a function of the temperature in order to gain some insight about the η/s bounds. Taking into account that $r_+(T_H)$ is a monotonically increasing function, one easily finds that also the function $P(T_H) = \pi L^2 T_H/(N r_+) = 1 - 2\pi G_N Q^2 L^2/(3 r_+^6)$ in Eq. (4.117) is a monotonically increasing function of T_H, with $P(0) = 0$ and $P(\infty) = 1$. The global behaviour of η/s in Eq. (4.117) therefore is ruled by the sign of λ. For $\lambda < 0$, η/s is a monotonically *increasing* function of T_H, which raises from its minimum value $1/4\pi$ at $T_H = 0$ to its maximum value $(1 + 4|\lambda|)/4\pi$ for $T_H = \infty$, in full agreement with the KSS bound. On the other hand, for $0 < \lambda < 1/4$, η/s is a monotonically *decreasing* function of T_H, which drops from its maximum value $1/4\pi$ at $T_H = 0$ to its minimum value $(1 - 4\lambda)/4\pi$ for $T_H = \infty$, violating the KSS bound.

4.7 The Gauss-Bonnet Black Hole Case

The second part of this chapter has been focused on the charged black brane solutions of GB gravity. However we would conclude with some comments on the black hole solutions of the theory, i.e., solutions with $\kappa = 1$ in Eq. (2.56). In the case of spherical black holes the discussion considerably changes. In fact, in $5d$, from Eq. (2.56) we find that the metric function can be written as

$$f(r) = 1 + \frac{r^2}{2\alpha_2}\left[1 \mp \sqrt{1 - 4\alpha_2\left(\alpha_0 - \frac{\omega_5 M}{r^4} + \frac{4\pi}{3}\frac{G_5 Q^2}{r^6}\right)}\right], \tag{4.129}$$

where $\omega_5 = \frac{16\pi G_5}{3\Sigma_3}$ and Σ_3 is the volume of the 3-sphere. We have two branches of solutions, but similarly to the BB case, the only one admitting horizon solutions is f_- with α_0, α_2 constrained by (2.76). The black hole mass, can be expressed in terms of the horizon radius r_+ [38]

$$M = \frac{r_+^4}{\omega_5}\left[\alpha_0 + \frac{\alpha_2}{r_+^4} + \frac{1}{r_+^2} + \frac{4\pi G_5 Q^2}{3r_+^6}\right]. \tag{4.130}$$

Due to the presence of the curvature ($\kappa = 1$), now the mass depends explicitly both on the AdS radius, $L^2 = \alpha_0^{-1}$ and on the GB coupling constant, α_2.

The other important aspect which makes black holes different from black branes is that also temperature and entropy depend explicitly from α_2 through the coupling with the curvature since all the higher curvature corrections (like the Gauss Bonnet one) enter in the expression for the temperature trough a coupling with κ. As found by Cai [38], for a charged $5d$ GB black hole one gets

$$T = \frac{1}{4\pi r_+(r_+^2 + 2\alpha_2)}\left[4\alpha_0 r_+^4 + 2r_+^2 - \frac{4\pi G_5 Q^2}{3r_+^4}\right], \qquad S = \frac{\Sigma_3 r_+^3}{4G_5}\left(1 + \frac{6\alpha_2}{r_+^2}\right). \tag{4.131}$$

We see that since M, T, S depend explicitly on the GB coupling constant α_2, differently from the black branes case, it is not anymore true that the thermodynamic behaviour of the Reissner-Nordström and Gauss-Bonnet black hole is the same. From the previous equation one can also realize that for the entropy, the area law no longer holds and that it receives a correction from α_2.

Let us now consider the extremal of the GB black hole. In the BB case we have found the remarkable property that the extremal, near-horizon solution of the charged GB black brane is exactly the same as the RN black brane. One can easily show that this is not the case for the extreme, near-horizon GB black hole. In the RN case the extremal, near-horizon, solution, which actually is an exact solution of the field equation is the $\mathrm{AdS}_2 \times S_3$ geometry (S_3 is the three sphere), i.e., the direct product of two maximally symmetric spaces, respectively with negative curvature $R^{(2)} = -2/l^2$ and positive curvature $R^{(3)} = \Lambda$, where l and Λ can be written in terms of the $5d$ cosmological constant and the $U(1)$ charge Q.

Using Eqs. (2.95) one can show that the individual contributions of the AdS_2 and S_3 spaces, to the two terms in Eq. (2.94) that are quadratic in the curvature tensors vanish. Nevertheless there are still some cross-product contributions arising from the mixing of AdS_2 and S_3 terms. Splitting the $5d$ indices (a, b) into $\mu, \nu = 0, 1$

(running on AdS_2) and $i, j = 1, 2, 3$ (running on S_3) we find a contribution to the μ, ν components of the field equations given by $2\alpha_2\Lambda/l^2 g_{\mu\nu}$ and a contribution $4\alpha_2\Lambda/3l^2 g_{ij}$ to the ij components of the field equations.

We see that the $AdS_2 \times S_3$ solution of the RN field equations cannot be also solution of the GB field equations. Obviously, this not prevents the existence of a *different* $AdS_2 \times S_3$ solution, i.e., a solution with different curvatures for AdS_2 and S_3. However, from the structure of the field equations and from Eqs. (2.95) one can infer that these solutions, if existing, imply a dependence of l and/or Λ not only from the 5d cosmological contant and from the black hole charge Q but also from the GB coupling constant α_2.

References

[1] Pavel Kovtun, Dam T. Son, and Andrei O. Starinets. "Holography and hydrodynamics: Diffusion on stretched horizons". In: *JHEP* 10 (2003), p. 064. arXiv: hep-th/0309213 [hep-th].

[2] Sunao Sakai and Atsushi Nakamura. "Lattice calculation of the QGP viscosities: Present results and next project". In: *PoS* LAT2007 (2007). [AIP Conf. Proc.893,5(2007)], p. 221. arXiv: 0710.3625 [hep-lat].

[3] Derek Teaney. "The Effects of viscosity on spectra, elliptic flow, and HBT radii". In: *Phys. Rev.* C68 (2003), p. 034913. arXiv: nucl-th/0301099 [nucl-th].

[4] Paul Romatschke and Ulrike Romatschke. "Viscosity Information from Relativistic Nuclear Collisions: How Perfect is the Fluid Observed at RHIC?" In: *Phys. Rev. Lett.* 99 (2007), p. 172301. arXiv: 0706.1522 [nucl-th].

[5] Huichao Song and Ulrich W. Heinz. "Suppression of elliptic flow in a minimally viscous quark-gluon plasma". In: *Phys. Lett.* B658 (2008), pp. 279–283. arXiv: 0709.0742 [nucl-th].

[6] A. Adare et al. "Energy Loss and Flow of Heavy Quarks in Au+Au Collisions at s(NN)**(1/2) = 200-GeV". In: *Phys. Rev. Lett.* 98 (2007), p. 172301. arXiv: nucl-ex/0611018 [nucl-ex].

[7] K. Dusling and D. Teaney. "Simulating elliptic flow with viscous hydrodynamics". In: *Phys. Rev.* C77 (2008), p. 034905. arXiv: 0710.5932 [nucl-th].

[8] Mauro Brigante et al. "Viscosity Bound Violation in Higher Derivative Gravity". In: *Phys. Rev.* D77 (2008), p. 126006. arXiv: 0712.0805 [hep-th].

[9] Mauro Brigante et al. "The Viscosity Bound and Causality Violation". In: *Phys. Rev. Lett.* 100 (2008), p. 191601. arXiv: 0802.3318 [hep-th].

[10] Yevgeny Kats and Pavel Petrov. "Effect of curvature squared corrections in AdS on the viscosity of the dual gauge theory". In: *JHEP* 01 (2009), p. 044. arXiv: 0712.0743 [hep-th].

[11] Harvey B. Meyer. "Transport Properties of the Quark-Gluon Plasma: A Lattice QCD Perspective". In: *Eur.Phys.J.* A47 (2011), p. 86. arXiv: 1104.3708 [hep-lat].

[12] Harvey B. Meyer. "Transport properties of the quark-gluon plasma from lattice QCD". In: *Nucl.Phys.* A830 (2009), pp. 641C–648C. arXiv: 0907.4095 [hep-lat].

[13] Sean A. Hartnoll, David M. Ramirez, and Jorge E. Santos. "Entropy production, viscosity bounds and bumpy black holes". In: (2016). arXiv: 1601.02757 [hep-th].

[14] Richard A. Davison, Blaise Goutéraux, and Sean A. Hartnoll. "Incoherent transport in clean quantum critical metals". In: *JHEP* 10 (2015), p. 112. arXiv: 1507.07137 [hep-th].

[15] Andrew Lucas. "Conductivity of a strange metal: from holography to memory functions". In: *JHEP* 03 (2015), p. 071. arXiv: 1501.05656 [hep-th].

[16] G. Policastro, Dan T. Son, and Andrei O. Starinets. "The Shear viscosity of strongly coupled N=4 supersymmetric Yang-Mills plasma". In: *Phys. Rev. Lett.* 87 (2001), p. 081601. arXiv: hep-th/0104066 [hep-th].

[17] Giuseppe Policastro, Dam T. Son, and Andrei O. Starinets. "From AdS / CFT correspondence to hydrodynamics". In: *JHEP* 0209 (2002), p. 043. arXiv: hep-th/0205052 [hep-th].

[18] Miguel F. Paulos. "Transport coefficients, membrane couplings and universality at extremality". In: *JHEP* 1002 (2010), p. 067. arXiv: 0910.4602 [hep-th].

[19] Juan Martin Maldacena. "The Large N limit of superconformal field theories and supergravity". In: *Int.J.Theor.Phys.* 38 (1999), pp. 1113–1133. arXiv: hep-th/9711200 [hep-th].

[20] Edward Witten. "Bound states of strings and p-branes". In: *Nucl.Phys.* B460 (1996), pp. 335–350. arXiv: hep-th/9510135 [hep-th].

[21] Oliver DeWolfe et al. "Heavy ions and string theory". In: *Prog.Part.Nucl.Phys.* 75 (2014), pp. 86–132. arXiv: 1304.7794 [hep-th].

[22] Edward Witten. "Anti-de Sitter space and holography". In: *Adv.Theor.Math.Phys.* 2 (1998), pp. 253–291. arXiv: hep-th/9802150 [hep-th].

[23] Martin Ammon and Johanna Erdmenger. *Gauge/Gravity Duality: Foundations and Applications*. 1st ed. Cambridge University Press, May 2015.

[24] Dam T. Son and Andrei O. Starinets. "Viscosity, Black Holes, and Quantum Field Theory". In: *Ann. Rev. Nucl. Part. Sci.* 57 (2007), pp. 95–118. arXiv: 0704.0240 [hep-th].

[25] Dam T. Son and Andrei O. Starinets. "Minkowski space correlators in AdS / CFT correspondence: Recipe and applications". In: *JHEP* 0209 (2002), p. 042. arXiv: hep-th/0205051 [hep-th].

[26] Edward Witten. "Anti-de Sitter space, thermal phase transition, and confinement in gauge theories". In: *Adv.Theor.Math.Phys.* 2 (1998), pp. 505–532. arXiv: hep-th/9803131 [hep-th].

[27] P. Kovtun, Dan T. Son, and Andrei O. Starinets. "Viscosity in strongly interacting quantum field theories from black hole physics". In: *Phys. Rev. Lett.* 94 (2005), p. 111601. arXiv: hep-th/0405231 [hep-th].

[28] Sera Cremonini. "The Shear Viscosity to Entropy Ratio: A Status Report". In: *Mod. Phys. Lett.* B25 (2011), pp. 1867–1888. arXiv: 1108.0677 [hep-th].

[29] Xian-Hui Ge and Sang-Jin Sin. "Shear viscosity, instability and the upper bound of the Gauss-Bonnet coupling constant". In: *JHEP* 05 (2009), p. 051. arXiv: 0903.2527 [hep-th].

[30] Xian-Hui Ge et al. "Viscosity Bound, Causality Violation and Instability with Stringy Correction and Charge". In: *JHEP* 10 (2008), p. 009. arXiv: 0808.2354 [hep-th].

[31] Rong-Gen Cai, Zhang-Yu Nie, and Ya-Wen Sun. "Shear Viscosity from Effective Couplings of Gravitons". In: *Phys. Rev.* D78 (2008), p. 126007. arXiv: 0811.1665 [hep-th].

[32] Alex Buchel and Robert C. Myers. "Causality of Holographic Hydrodynamics". In: *JHEP* 08 (2009), p. 016. arXiv: 0906.2922 [hep-th].

[33] Diego M. Hofman. "Higher Derivative Gravity, Causality and Positivity of Energy in a UV complete QFT". In: *Nucl. Phys.* B823 (2009), pp. 174–194. arXiv: 0907.1625 [hep-th].

[34] Sachin Jain et al. "A Strongly Coupled Anisotropic Fluid From Dilaton Driven Holography". In: *JHEP* 01 (2015), p. 005. arXiv: 1406.4874 [hep-th].

[35] Sachin Jain, Rickmoy Samanta, and Sandip P. Trivedi. "The Shear Viscosity in Anisotropic Phases". In: *JHEP* 10 (2015), p. 028. arXiv: 1506.01899 [hep-th].

[36] Thomas Faulkner et al. "Emergent quantum criticality, Fermi surfaces, and AdS(2)". In: *Phys. Rev.* D83 (2011), p. 125002. arXiv: 0907.2694 [hep-th].

[37] Mohammad Edalati, Juan I. Jottar, and Robert G. Leigh. "Transport Coefficients at Zero Temperature from Extremal Black Holes". In: *JHEP* 01 (2010), p. 018. arXiv: 0910.0645 [hep-th].

[38] Rong-Gen Cai. "A Note on thermodynamics of black holes in Lovelock gravity". In: *Phys.Lett.* B582 (2004), pp. 237–242. arXiv: hep-th/0311240 [hep-th].

Chapter 5

Conclusions

Gauge/gravity duality is a significant progress in theoretical physics that, based on string theory, provides new links between quantum field theory and gravity. It realises the *holographic principle* because the boundary quantum field theory, with a gauge symmetry, encodes all the information about the gravity theory in the bulk. In particular, in a special case of the coupling constant regimes, the duality maps strongly coupled quantum field theories (e.g., low energy QCD) to more tractable (weakly curved) classical gravity theories.
The most striking and, at the moment, best-understood example of gauge/gravity duality is the AdS/CFT correspondence that is characterised by a high degree of symmetry. However, recent generalisations of AdS/CFT to gauge/gravity dualities have given useful contributions to the description of some aspects of strongly coupled systems. In particular, it has been introduced a combination of gauge/-gravity duality methods with linear response theory in order to describe transport processes.

During the past years, interesting phenomena related to QCD at low energies have been investigated using gauge/gravity duality. The most studied examples are the applications to the physics of the quark-gluon plasma. The quark-gluon plasma is a new strongly coupled state of matter at a temperature above the QCD deconfined temperature. This new phase of matter has been observed experimentally at the RHIC accelerator (in Brookhaven) and is currently under experimental study at the LHC in CERN (Geneva). In the context of strong coupling phenomena, the gauge/gravity duality has been used to estimate an important quantity: the ratio of shear viscosity to entropy density η/s. The result of η/s agrees well with the experimental measurements and gives rise to a phenomenon of *universality* in the gauge/gravity duality. This universality property of the ratio means that

gravity theories with different structures are all bounded by the KSS bound $\eta/s \leq 1/4\pi$ and that the precise form of the microscopic d.o.f of the field theory on the boundary is irrelevant for the dynamics. In particular, the duality can be generalized to non-conformal and finite temperature examples, which are obtained, for instance, by considering a black hole in AdS spacetime.

In this thesis, we have discussed in detail geometrical, thermodynamic and holographic properties of the charged $5d$ GB black branes, the charged Lovelock black holes and the *regular* black holes and black branes. From this research emerges that UV modifications of GR although important for a complete theory of gravity, do not seem to be relevant for the phenomenology of the dual field theory in the hydrodynamic regime.
After an introduction to the most important concepts used in this thesis (Chap.1), then Chap.2 and Chap.3 were dedicated to the study of the thermodynamic of charged Lovelock and regular BH solutions in different ensembles.
In Chap.3, it has been considered the possibility of identifying the cosmological constant, that parametrize the AdS space, as a thermodynamic variable (i.e., a thermodynamic pressure). The role of the variable pressure enrich the possible phases of the spacetime with complicated phenomena that were previously found only in the framework of some chemical systems. However, its interpretation in the gauge/gravity dictionary is not yet fully understood, and it deserves future studies.
Chap. 4 is completely dedicated to the calculation of η/s. It has been discussed the gauge/gravity correspondence at finite temperature in Lorentzian signature and how to obtain a causal structure which allows us to introduce retarded Green's functions. The concept of quasi-normal modes is crucial as well as their relation to the pole structure of the Green's functions. The first part of the chapter includes calculation of η/s for a regular black brane while the second part deals with the Gauss-Bonnet gravity. Although the discussion in the second part of Chap. 4 has been mainly confined to the GB case, because of the thermodynamic independence from higher order Lovelock parameters $\alpha_i,\ i \geq 3$, we expect that most of our results can be generalised to Lovelock gravity theories in any spacetime dimensions.

The interest in studying strongly correlated $4d$ quantum field theories motivates the study of higher dimensional gravity theories. In a five-dimensional spacetime, GR is not the most general theory with second order equations of motion. Higher curvature terms in the Lagrangian and a new coupling constant α_2 need to be considered. This is the Gauss-Bonnet theory of gravity that is generalized in higher

dimensions ($d > 5$) by Lovelock gravity. It should be noticed that the gravity theory in the bulk does not necessary need of a direct physical interpretation as a "physical" spacetime. Therefore, the parameters of the model are not constrained by gravitational experiments but, rather by the physical phenomena of the dual field theory on the boundary. Moreover, the rich phase structure of higher dimensional (Lovelock) gravity theory can be even more interesting once a dynamical model for the compactification or dimensional reduction of the extra-dimensions will be understood.

5.1 Results

5.1.1 Thermodynamics

In Chap.2 and Chap.3, it has been shown that the thermodynamics of the regular black holes and of black holes in Gauss-Bonnet and 3rd-order Lovelock gravity contains interesting and qualitatively new thermodynamic behaviour.
Moreover, it has also been shown that the particular combination of GB higher curvature terms added to the Einstein gravity action have three main effects for the brane ($\kappa = 0$) solutions:

(1) They introduce a new branch of brane solutions, which are however not black branes but describe naked singularities. The global structure of the RN geometry of Einstein gravity is preserved only for $\alpha_2 > 0$. For $\alpha_2 < 0$ the spacetime splits into two disconnected regions (an inner and outer region), with the external region having a single event horizon also in the non-extremal case. An interesting feature is that the solutions of the two branches may be, in some cases, continuously connected one with the other through the singularity. When this is the case, they describe transitions of the kind: $AdS_5 \rightarrow$ singularity $\rightarrow AdS_5$, AdS_5-black brane $\rightarrow$ singularity $\rightarrow AdS_5$ or AdS_5-black brane $\rightarrow$ singularity $\rightarrow dS_5$. Although it is known that one of the two branches of the solution (f_+) is unstable, one expects that the first two of these transitions have a holographic interpretation as the flow between two CFTs of different central charge through a singularity.

(2) The thermodynamic behaviour of charged GB black brane is universal, i.e., when expressed in terms of effective mass and temperature is indistinguishable from that of the RN black brane.

(3) Higher curvature terms modify the asymptotics (the AdS length) of the $5d$ AdS-RN gravity leaving unchanged the $\mathrm{AdS}_2 \times R_3$, extremal near-horizon geometry of the RN black brane. At thermodynamic level, when expressed in terms of M_{ADM} and T_H a dependence on the normalization factor N of the metric is introduced but not for the extremal, near-horizon geometry $\mathrm{AdS}_2 \times R_3$. In terms of the dual CFTs, this property can be described as a deformation of the CFT which changes the UV behaviour but leaves unchanged the IR.

In Chap. 3, we have seen that various thermodynamic phenomena, such as Van der Waals behaviour, reentrant phase transitions (RPT), and tricritical points appear when the cosmological constant is treated as a dynamical variable. All these phenomena naturally and generically occur in the context of 3rd-order Lovelock gravity. We confirmed the existence of a tricritical point in $d = 8, 9, 10$ dimensions in the case of Lovelock charged black holes and the existence of RPT in $d = 8, 9, 10, 11$ dimensions for the neutral ones. Moreover, we have seen "multiple RPT" behaviour, in which the Gibbs free-energy is continuous at the phase transition point. This appears to be an entirely new feature for gravitational systems, and it has not previously been noted. In the case of hyperbolic ($\kappa = -1$) charged Lovelock black holes, we generically find thermodynamic singularities, in which all isotherms cross at a particular value of v in the $p-v$ diagram. The corresponding Gibbs free energy suffers from 'infinite jump' and undergoes 'reconnection'. In particular, we may observe a form of swallowtail in which one end of the swallowtail 'goes to infinity'. Since the global minimum of the Gibbs free energy is always well-defined, we can still study the thermodynamics of the system.
In Chap. 3, we also further elucidated the thermodynamic behaviour when $\alpha_3 = \sqrt{3}$ and $\kappa = -1$ for 3rd-order uncharged Lovelock black holes (see Sec.3.4.4.5). In this interesting special case we find that the equation of state has non-standard expansion about a special critical point. Rather than $p/p_c = 1 + A\tau + B\tau\omega + C\omega^3 + \ldots$ (characteristic for mean field theory critical exponents and swallowtail catastrophe behaviour) we obtain

$$\frac{p}{p_c} = 1 + \frac{24}{d-1}\tau\omega^2 - 8\frac{(d-4)}{d-1}\omega^3 + \ldots \tag{5.1}$$

suggesting a violation of certain scaling relations and non-standard critical exponents.
An interesting question is whether one could observe a *quatri-critial point*, in which four first-order phase transitions coalesce. Such a point would correspond to three swallowtails merging together, or alternatively, to three Van der Waals

oscillations of a single isotherm such that the equal areas occur for the same pressure. A necessary (not sufficient) condition for the existence of a quatrocritical point is the existence of 3 maxima and 3 minima for a single isotherm; in other words $\partial p/\partial v = 0$ would have to have 6 solutions. This can never happen for $U(1)$ charged Gauss–Bonnet black holes. However, it might in principle occur for 3rd-order Lovelock black holes, though our results and preliminary study in higher dimensions shows this unlikely.

5.1.2 η/s

In QCD, the comparison between data and calculations done using relativistic viscous hydrodynamic yields the current estimate that η/s seems to lie within the range $\eta/s = (1-2)\,/\,(4\pi)$ (see also [1]). In Chap.4 the shear viscosity to entropy density ratio has been computed, using the gauge/gravity duality, for the GB charged black brane (both in the non-extremal and in the extremal case) and for the regular black brane (only in the non-extremal case).
In the GB case, it has been found that consistently with the geometrical and thermodynamic picture, the universality of η/s is lost in the UV, but it is restored in the IR. The ratio η/s has a non-universal temperature-dependent behaviour for non-extremal black branes but attains the universal $1/4\pi$ value at extremality. This result implies that η/s is completely determined by the IR behaviour and is completely insensitive to the UV regime of the dual QFT. On the one hand, this is largely expected because transport features in the hydrodynamic regime should be determined by IR physics. However, it is not entirely clear if this result has a general meaning or it is a just a consequence of the peculiarities of the charged GB black brane (higher curvature corrections vanish on the $\mathrm{AdS}_2 \times R_3$ background). Also, the result for the regular black brane suggests that the universal $1/4\pi$ value does not depend from the UV corrections to the gravity theory.
We have found that η/s for the charged GB black brane is a smooth monotonic function of the temperature. By going to small temperatures, it always flows to the universal value $1/4\pi$ but this value is a *minimum* for $\lambda < 0$ and a *maximum* for $\lambda > 0$, where $\lambda = \alpha_0\alpha_2 = \alpha_2/b^2$. Thus, the QFT dual to GB-Maxwell gravity with $\lambda < 0$ gives a nice example of temperature-flow of η/s always bounded from below by $1/4\pi$. On the other hand, the KSS-bound-violating flow we obtain in the theory for $0 < \lambda < 1/4$ remains open to further investigations.

5.2 Outlook

The research presented in this thesis can be used as a step towards the following three directions:

1. **The investigation of time-dependent processes, non-equilibrium Physics and thermalization using gauge/gravity duality.**
   An extensive study of the physical properties of the gauge theories would require also investigating time-dependent processes. This is important, for instance, to study transport effects and correlations in hot, dense and charged QCD-matter out of the equilibrium. Further steps in this direction involve the study of time-dependent metrics (e.g., for collapsing matter), and the understanding of the relevant thermal and non-thermal quantities for these out-of-equilibrium models (e.g., the *radiation flux* [2]). A first inspection of the time-dependent models for charged and regular black holes has been conducted in the past months. These preliminary studies already show interesting behaviors of the charged and regular black hole radiation flux.

2. **Understanding the role of the extended phase space in the gauge/gravity duality framework.**
   The rich phase structure emerged in the study of Lovelock extended phase space (i.e., considering the cosmological constant Λ as dynamical quantity) could imply new features of a boundary gauge theory once a duality dictionary is provided. Such a dictionary is nowadays an hot topic in the research community of holography (see [3] and [4]).

3. **Extra-dimensions, higher derivatives and non-local theories.**
   The tools developed to investigate the complicated dynamics of the Lovelock gravity and regular black holes, in this thesis, can be naturally applied to the study of $f(R)$ theories, generalized uncertainty principle (GUP) and promising extra-dimensional theories (e.g., Randall-Sundrum model [5]) in extended phase spaces. Moreover, in the past years, theories involving extensions of Einstein gravity have been developed to explain cosmological data at the price of introducing non-locality in the theory of gravity [6]. Such a framework shares many technical features with the regular solutions of Einstein gravity, and it needs further studies such as the determination of Lagrangians from which one can derive the non-local equation of motion.

References

[1] Iu. A. Karpenko et al. "Estimation of the shear viscosity at finite net-baryon density from $A+A$ collision data at $\sqrt{s_{\rm NN}} = 7.7-200$ GeV". In: *Phys. Rev.* C91.6 (2015), p. 064901. arXiv: 1502.01978 [nucl-th].

[2] Eugenio Bianchi, Tommaso De Lorenzo, and Matteo Smerlak. "Entanglement entropy production in gravitational collapse: covariant regularization and solvable models". In: *JHEP* 06 (2015), p. 180. arXiv: 1409.0144 [hep-th].

[3] Clifford V. Johnson. "An Exact Efficiency Formula for Holographic Heat Engines". In: (2016). arXiv: 1602.02838 [hep-th].

[4] Andreas Karch and Brandon Robinson. "Holographic Black Hole Chemistry". In: *JHEP* 12 (2015), p. 073. arXiv: 1510.02472 [hep-th].

[5] Lisa Randall and Raman Sundrum. "A Large mass hierarchy from a small extra dimension". In: *Phys. Rev. Lett.* 83 (1999), pp. 3370–3373. arXiv: hep-ph/9905221 [hep-ph].

[6] Michele Maggiore and Michele Mancarella. "Nonlocal gravity and dark energy". In: *Phys. Rev.* D90.2 (2014), p. 023005. arXiv: 1402.0448 [hep-th].

Appendix A

Gravitational Action

A.1 Boundary Term for Spherically Symmetric Metrics

In Chap.2, we introduced the York-Gibbons-Hawking boundary term. The boundary term is defined for a generic manifold M of dimension $N = n + 1$ as

$$I_{GH} := \underbrace{\frac{1}{8\pi G_N}}_{1/\kappa} \int_{\partial M} d^n x \sqrt{h}\, K\,, \tag{A.1}$$

where [1, 2] K is the extrinsic curvature and h_{ab} the the intrinsic-metric [1] (or the *projector* [2]). They read respectively

$$K = h^a{}_b \nabla_a n^b, \quad h_{ab} = g_{ab} - \sigma n_a n_b \quad \sigma := n_a n^a \tag{A.2}$$

where n^a is an (inward) normal vector to the n-dimensional boundary ∂M. A useful review of the topic is in [3]. We are interested in a n-spherical hypersurface defined as $r = \text{const}$ (i.e., $r = R$). In particular, we will be interested in $R \to \infty$ so let us consider a generic diagonal spherical symmetric metric like

$$ds^2 = \mp V(r)\, dt^2 + \frac{1}{V(r)} dr^2 + r^2 d\Omega^2_{n-1} \tag{A.3}$$

where the inward-pointing normal vector orthogonal to ∂M can be written as $n^a = -\mathfrak{c}\,(0, 1, 0, \ldots, 0)$. The normal vector can be normalized if

$$n^a n_a = 1 = n^a n^b g_{ab} = \mathfrak{c}^2 g_{11} = \frac{\mathfrak{c}^2}{V(r)}$$

and written as

$$n^a = -\sqrt{V(r)}\delta^a_1 \Rightarrow \quad n_a = g_{ab}n^b = g_{a1}n^1 = -\frac{1}{\sqrt{V(r)}}\delta_{a1}. \tag{A.4}$$

Now we need to calculate the extrinsic curvature K given in (A.2). Since $h^a{}_b = \delta^a{}_b - n^a n_b$, recalling that the covariant derivative is defined as $\nabla_a n^b = \partial_a n^b + \Gamma^b_{ac} n^c$ and that n^a is not zero only in the radial component $n^r \equiv n^1$, we can finally write K as

$$\begin{aligned} K &= h^a{}_b \nabla_a n^b = (\delta^a{}_b - n^a n_b)\left(\partial_a n^b + \Gamma^b_{ac}\, n^c\right) \\ &= \partial_a n^a + \Gamma^a_{ac}\, n^c - (n^r n_r \partial_r n^r + n^r n_r \Gamma^r_{rr}\, n^r) \\ &= \partial_r n^r + \Gamma^a_{ar}\, n^r - (\partial_r n^r + \Gamma^r_{rr}\, n^r) \end{aligned}$$

where in the last line we have used $n^r n_r = \sqrt{V(r)/V(r)}$. Now, let us look at the Christoffel symbols defined by

$$\Gamma^a_{bc} = \frac{1}{2} g^{a\rho}\left(g_{\rho c,b} + g_{b\rho,c} - g_{bc,\rho}\right). \tag{A.5}$$

Specifically, we need to calculate the Γ^a_{ar} and Γ^r_{rr} components. Using the definition (A.5), we can write:

$$\begin{aligned} \Gamma^a_{ar} &= \frac{1}{2} g^{a\rho}\left(g_{\rho r,a} + g_{a\rho,r} - g_{acr,\rho}\right) = \\ &= \frac{1}{2}\left(g^{rr} g_{rr,r} + \sum_a g^{aa} g_{aa,r} - g^{rr} g_{rr,r}\right) \\ &= \frac{1}{2}\left(g^{00} g_{00,r} + g^{rr} g_{rr,r} + \sum_{i=2}^{n} g^{ii} g_{ii,r}\right) \end{aligned}$$

notice that $g_{ii} = r^2 \mathsf{g}(\theta, \ldots)$ so

$$g_{ii,r} = 2r\, \mathsf{g} = 2r\, \frac{g_{ii}}{r^2} = \frac{2}{r} g_{ii}$$

and that $g^{ii} g_{ii} = 1$ so we get $\sum_{i=2}^{n} g^{ii} g_{ii,r} = \frac{2}{r}(n-1)$ and finally we can write

$$\Gamma^a_{ar} = \frac{1}{2}\left(g^{00} g_{00,r} + g^{rr} g_{rr,r} + \frac{2}{r}(n-1)\right) \qquad \Gamma^r_{rr} = \frac{1}{2} g^{rr}\left(g_{rr,r}\right).$$

Coming back to K we have

$$K = (\Gamma^a_{ar} - \Gamma^r_{rr})\, n^r = -\sqrt{V(r)}\frac{1}{2}\left(g^{00}g_{00,r} + \frac{2}{r}(n-1)\right) \tag{A.6}$$

$$= -\sqrt{V(r)}\left(\frac{\partial_r V(r)}{2\,V(r)} + \frac{n-1}{r}\right). \tag{A.7}$$

The interesting point is that K (A.7) is independent from the metric signature (it is the same for Euclidean and Lorentzian metrics). To write the final action we can plug (A.7) into (A.1), the determinant of the intrinsic metric is the determinant of the metric

$$ds^2_{\partial M} = \mp V(R)\, dt^2 + R^2 d\Omega^2_{n-1} \tag{A.8}$$

namely $h = \frac{g}{g_{rr}}$. In n-dimensions, the spherical element in (A.4) and (A.8) can be written as [4]

$$d\Omega^2_{n-1} = d\theta_2^2 + \sin^2\theta_2\, d\theta_3^2 + ... + \prod_{i=2}^{n-1}\sin^2\theta_l d\theta_n^2. \tag{A.9}$$

Just to be precise, we know that for this diagonal metrics the determinant is $g = \prod_{a=0}^{n} g_{aa}$ and the element of volume $\prod_{a=2}^{n}\sqrt{g_{aa}}dx_a$ once integrated gives the $\mathrm{Vol}\,(S^{n-1})$ so the action reads

$$I_{GH} := -\frac{1}{\kappa}\int_{\partial M} d^n x\ \sqrt{\frac{g}{g_{rr}}}\sqrt{V(r)}\left(\frac{\partial_r V(r)}{2\,V(r)} + \frac{n-1}{r}\right)\Big|_{r=R}. \tag{A.10}$$

Integrating Eq. (A.10) over the components θ_i and t, we get:

$$I_{GH} = -\int_0^\beta dt \frac{1}{\kappa}\mathrm{Vol}\left(S^{n-1}\right)\sqrt{V(r)}\times \tag{A.11}$$

$$\times\sqrt{\pm V(r)\, r^{2(n-1)}}\left(\frac{\partial_r V(r)}{2\,V(r)} + \frac{n-1}{r}\right)\Big|_{r=R} \tag{A.12}$$

$$= \frac{\beta_{Sh}}{\kappa}\mathrm{Vol}\left(S^{n-1}\right)\left[-\ r^{(n-1)}\left(\frac{1}{2}\partial_r V(r) + \frac{(n-1)}{r}V(r)\right)\Big|_{r=R}\right]. \tag{A.13}$$

In table A.1 are reported the results for different cases.

To evaluate the free energy, we have to regularize the boundary term subtracting the background contribute K_0

$$I_B = \int_{\partial M} d^n x\sqrt{h}\,(K - K_0). \tag{A.14}$$

This is a necessary procedure since (A.13) often diverge (for example, Minkowski background or AdS background). Precise requirement of all the literature is the "synchronizing" of the geometries at a given point R that eventually goes to infinity. In other words, we want that the compactification of the time occurs at a given time and it has to be the same in both the spaces (or that the BH has to be in thermal equilibrium with the background at a a given $R \to \infty$). In the case of Schwarzschild black hole with asymptotically Minkowski spacetime the equality $\int_0^{\beta_M} ds = \int_0^{\beta_{Sh}} ds$ have to be soddisfied and since $dr = 0$ and all the others are also 0 then the equality becomes $\int_0^{\beta_M} \sqrt{g_{tt}^M} dt = \int_0^{\beta_{Sh}} \sqrt{g_{tt}^{Sh}} dt$ and gives $\beta_M \sqrt{1} = \beta_{Sh} \sqrt{1 - \frac{2G_N M}{r}}\Big|_{r=R}$ where g_{tt}^M and g_{tt}^{Sh} are the time components, respectively of the Minkowski and Schwarzschild metric.

In the case $d = 4$, we get the boundary term for a black hole in Minkowski spacetime subtracting

$$\begin{aligned} I_B &= \frac{1}{\kappa} \mathrm{Vol}\left(S^2\right) [- \ (-3G_N M + 2R)] \, \beta_{Sh} + \frac{2}{\kappa} \mathrm{Vol}\left(S^2\right) \left(\beta_{Sh} \sqrt{1 - \frac{2G_N M}{R}} \right) R \\ &= \frac{1}{\kappa} \mathrm{Vol}\left(S^2\right) \beta_{Sh} \left\{ 3GM - 2R \left(1 - \sqrt{1 - \frac{2G_N M}{R}} \right) \right\}. \end{aligned} \tag{A.15}$$

In the case of interest, as final step we have to provide the limit $R \to \infty$. Using the expansion $\sqrt{1 - \epsilon A} \cong 1 - \epsilon \frac{1}{2} A$

$$\lim_{R \to \infty} I_B = \lim_{R \to \infty} \frac{1}{\kappa} \mathrm{Vol}\left(S^2\right) \beta_{Sh} \left\{ 3G_N M - 2R \left(\frac{G_N M}{R} \right) \right\} \tag{A.16}$$

$$= \lim_{R \to \infty} \frac{1}{\kappa} \mathrm{Vol}\left(S^2\right) \beta_{Sh} G_N M = \frac{\beta_{Sh} G_N \ M \, \mathrm{Vol}\left(S^2\right)}{\kappa} \tag{A.17}$$

substituting $\kappa = 8\pi G_N$ and the $\mathrm{Vol}\left(S^2\right)$, we finally get

$$I_B = \frac{4\pi M \, \beta_{Sh}}{8\pi} = \frac{1}{2} \beta_{Sh} M = \frac{\beta^2}{16\pi G_N} \tag{A.18}$$

where we use the relation

$$\beta_{Sh} := 4\pi \left(\frac{\partial V(r)}{\partial r} \right)^{-1} \Big|_{r=r_+} = 4\pi \left(\frac{2MG_N}{r_+^2} \right)^{-1} = 4\pi r_+ \tag{A.19}$$

and the horizon radius is defined by the horizon equation $V(r_+) = 0$ as $r_+ = 2MG_N$.

Metric	$V(r)$	I_{GH}
Schw 4D	$\left(1-\frac{2GM}{r}\right)$	$\frac{1}{\kappa}\mathrm{Vol}\left(S^2\right)\left[-\ r^2\left(\frac{GM}{r^2}+\left(\frac{2}{r}-\frac{4GM}{r^2}\right)\right)\Big\vert_{r=R}\right]\beta$ $=\frac{1}{\kappa}Vol\left(S^2\right)\left[-\ (-3GM+2r)\vert_{r=R}\right]\beta_{Sh}$
Mink $(n+1)$D	1	$\frac{1}{\kappa}\mathrm{Vol}\left(S^{n-1}\right)\left[-\ r^{(n-1)}\left(\frac{(n-1)}{r}\right)\Big\vert_{r=R}\right]\beta_M$
Mink 4D	1	$-\frac{2}{\kappa}Vol\left(S^2\right)R\beta_M$

TABLE A.1: Gibbons-Hawking term for different metrics.

Then, as in [5], one computes the energy

$$E=\frac{\partial I}{\partial\beta_{sh}}=M \tag{A.20}$$

and the entropy

$$S=\beta_{Sh}E-I=\frac{1}{4G_N}r_+^2\mathrm{Vol}\left(S^2\right). \tag{A.21}$$

A.1.1 Generalization to n Dimensions.

The entropy of a black hole in Minkowski spacetime is fully determined by the action boundary term. One can generalize the previous procedure to a generic number of spacetime dimensions $d=n+1$. The boundary term for the black hole geometry reads:

$$I_{GB}^{BH} = \frac{1}{\kappa}\left[\frac{8\pi\,G_N M\,n}{(n-1)}\right]\beta_{Sh}-\frac{1}{\kappa}\left[(n-1)R^{n-2}\mathrm{Vol}\left(S^{n-1}\right)\right]\beta_{Sh} \tag{A.22}$$

while for the Minkowski background, one has

$$I_{GB}^{M}=-\frac{1}{\kappa}\left[\sqrt{1-\frac{16\pi\,G_N M R^{2-n}}{(n-1)\mathrm{Vol}\left(S^{n-1}\right)}}\right](n-1)R^{n-2}\mathrm{Vol}\left(S^{n-1}\right)\beta_{Sh}. \tag{A.23}$$

The subtraction is

$$\begin{aligned} I_{GB}^{BH}-I_{GB}^{M} &= \frac{1}{\kappa}\left[\frac{8\pi\,G_N M\,n}{(n-1)}\right]\beta_{Sh}+ \\ &+\frac{1}{\kappa}\left[-1+\sqrt{1-\frac{16\pi\,G_N M R^{2-n}}{(n-1)\mathrm{Vol}\left(S^{n-1}\right)}}\right](n-1)R^{n-2}\mathrm{Vol}\left(S^{n-1}\right)\beta_{Sh} \end{aligned} \tag{A.24}$$

that in the limit for $R \to \infty$ (using the series expansion) becomes:

$$\lim_{R\to\infty}\left[I_{GB}^{BH} - I_{GB}^{M}\right] = \frac{1}{\kappa}\left[\frac{8\pi\, G_N M\, n}{(n-1)}\right]\beta_{Sh} - \frac{1}{\kappa}\left(8\pi\, G_N M\right)\beta_{Sh} \tag{A.25}$$

$$= \frac{1}{n-1} M\, \beta_{Sh}. \tag{A.26}$$

A.2 Boundary Term for Regular Schwarzschild Black Hole.

We investigate the boundary term in the case of a regular black hole. Using the general definition for the boundary term Eq. A.13

$$I_{GB}^{Sh} = \frac{1}{\kappa}\mathrm{Vol}\left(S^{n-1}\right)\left[-\; r^{(n-1)}\left(\frac{1}{2}\partial_r V\left(r\right) + \frac{(n-1)}{r}V(r)\right)\Big|_{r=R}\right]\beta_{Sh} \tag{A.27}$$

$$= \frac{1}{2\kappa}\mathrm{Vol}\left(S^{n-1}\right)\beta_{Sh}\left[-2\left(n-1\right)r^{n-2}\right] + \tag{A.28}$$

$$+\frac{1}{2\kappa}\mathrm{Vol}\left(S^{n-1}\right)\beta_{Sh}\left[2^{1-n}e^{-\frac{r^2}{4\theta^2}} M\left(\frac{r}{\theta}\right)^n \omega_n + Mn\omega_n\,\gamma\left(\frac{n}{2}, \frac{r^2}{4\theta^2}\right)\Big|_{r=R}\right]$$

so using the mass coefficient it becomes

$$I_{GB}^{Sh} = \frac{1}{\kappa}\left[\frac{8\pi G_N\, M\left(2^{1-n}e^{-\frac{R^2}{4\theta^2}}\left(\frac{R}{\theta}\right)^n + n\,\gamma\left(\frac{n}{2}, \frac{R^2}{4\theta^2}\right)\right)}{(n-1)\,\Gamma\left(\frac{n}{2}\right)(n-1)R^{n-2}\mathrm{Vol}\left(S^{n-1}\right)} - 1\right](n-1)R^{n-2}\mathrm{Vol}\left(S^{n-1}\right)\beta_{Sh} \tag{A.29}$$

while the Minkowski boundary term reads:

$$I_{GB}^{M} = -\frac{1}{\kappa}\mathrm{Vol}\left(S^{n-1}\right)R^{n-1}\left(\frac{n-1}{R}\right)\beta_M \tag{A.30}$$

$$= \frac{1}{\kappa}\mathrm{Vol}\left(S^{n-1}\right)R^{n-2}\left(n-1\right)\left[-\sqrt{1 - \frac{\omega_n M}{R^{n-2}}\gamma\left(\frac{n}{2}, \frac{R^2}{4\theta^2}\right)}\right]\beta_{Sh} \tag{A.31}$$

The final result for the boundary term is given taking the limit $R \to \infty$ of the subtraction (we note that this limit includes the classical limit i.e. corresponds

also to consider $\theta \to 0$)

$$
\begin{aligned}
I_{GB}^{Sh} - I_{GB}^{M} \;=\; & \frac{1}{\kappa}\Bigg[\underbrace{\frac{8\pi G_N M\ (2^{1-n})\, e^{-\frac{R^2}{4\theta^2}} \left(\frac{R}{\theta}\right)^n}{(n-1)^2\ \Gamma\left(\frac{n}{2}\right) R^{n-2}\mathrm{Vol}\left(S^{n-1}\right)}}_{\to 0} -1 + \\
& + \underbrace{\frac{8\pi G_N M\, n\, \gamma\left(\frac{n}{2}, \frac{R^2}{4\theta^2}\right)}{(n-1)^2\ \Gamma\left(\frac{n}{2}\right) R^{n-2}\mathrm{Vol}\left(S^{n-1}\right)}}_{\to const} + \\
& + \sqrt{1 - \frac{16 G_N M \pi R^{2-n} \gamma\left(\frac{n}{2}, \frac{R^2}{4\theta^2}\right)}{(n-1)\,\Gamma\left(\frac{n}{2}\right)\mathrm{Vol}\left(S^{n-1}\right)}}\Bigg] (n-1)\ R^{n-2}\mathrm{Vol}\left(S^{n-1}\right)\beta_{Sh}.
\end{aligned}
$$

in the limit for $R \to \infty$ the first term goes to zero, the second term goes to a constant and for the last two terms we can use the expansion $\sqrt{1-\epsilon A} \cong 1 - \epsilon\frac{1}{2}A$then the limit $L = \lim_{R\to\infty}\left[I_{GB}^{Sh} - I_{GB}^{M}\right]$ is equal to

$$
\begin{aligned}
L \;=\; & \frac{1}{\kappa}\beta_{Sh}\left(\frac{8\pi G_N M\, n}{n-1}\right) + \\
& + \frac{1}{\kappa}\beta_{Sh}\Bigg\{ - \lim_{R\to\infty}\left[1 - \sqrt{1 - \frac{16 G_N M \pi R^{2-n} \gamma\left(\frac{n}{2}, \frac{R^2}{4\theta^2}\right)}{(n-1)\,\Gamma\left(\frac{n}{2}\right)\mathrm{Vol}\left(S^{n-1}\right)}}\right](n-1) R^{n-2}\mathrm{Vol}\left(S^{n-1}\right)\Bigg\} \\
& (n-1) R^{n-2}\mathrm{Vol}\left(S^{n-1}\right)\Big\}
\end{aligned}
$$

that can be approximate to

$$
\begin{aligned}
\lim_{R\to\infty}\left[I_{GB}^{Sh} - I_{GB}^{M}\right] \;\approx\; & \frac{1}{\kappa}\left(\frac{8\pi G_N M\, n}{n-1}\right)\beta_{Sh} + \\
& - \frac{1}{\kappa}\left[\frac{8 G_N M \pi \Gamma\left(\frac{n}{2}\right)}{(n-1)\,\Gamma\left(\frac{n}{2}\right)\mathrm{Vol}\left(S^{n-1}\right)}\right](n-1)\mathrm{Vol}\left(S^{n-1}\right)\beta_{Sh} \\
= \;& \frac{1}{n-1}\, M\beta_{Sh} = \frac{M}{n-1}\cdot\frac{1}{T} = I_B. \qquad \text{(A.32)}
\end{aligned}
$$

As we expected, the boundary term for a regular black hole is the same of the classical calculation (because the limit $R \to \infty$ corresponds in some sense to the semiclassical limit $r \gg \theta$). In the case of a regal black hole we see that the temperature defined as $T = 1/\beta$ reaches zero for a non zero value of the horizon radius that means that the action has a divergences for that value of the radius.

A.2.1 ADM Mass and Komar Mass

The gravitational mass of an asymptotically flat spacetime is defined to be the limit of the gravitational Hamiltonian (with the fields h_{ab} and K_{ab} satisfy the vacuum field equations) when the boundary surface S_t is a two-sphere at spatially infinity evaluated with the following lapse and shift [3]: $N = 1$, $N^{\alpha} = 0$ such that

$$M_{ADM} = -\frac{1}{8\pi G_N} \lim_{S_t \to \infty} \oint_{S_t} (k - k_0) \sqrt{\sigma}\, d^2\theta. \tag{A.33}$$

The procedure so is precisely the same as for Eq. (A.14); however, in this case there is no integration over the time. The ADM mass calculation in the case of regular black hole follow the same steps as the previous calculations and it is possible to find that also in the case of a regular black hole the ADM mass coincides with $M(r_+)$.

The Komar integral can be defined as the integral at spatial infinity

$$E_K = \frac{1}{4\pi G} \int_{\partial\Sigma} d^2x \sqrt{\gamma^{(2)}} n_\mu \sigma_\nu \nabla^\mu K^\nu \tag{A.34}$$

where n^μ is the unit normal (normalized as $n_\mu n^\nu = -1$) vector associated with the spacelike hypersurface Σ. σ^μ(normalized as $\sigma_\mu \sigma^\mu = 1$) is the normal vector associated with the boundary $\partial\Sigma$ of the surface Σ. K^μ is the timelike Killing vector.

For a stationary spherically-symmetric metric

$$ds^2 = -f(r)\ dt^2 + f(r)^{-1}\ dr^2 + r^2\, d\theta^2 + r^2 \sin(\theta)^2\ d\phi^2 \tag{A.35}$$

the normal vectors have the only non-null components

$$n_0 = -f(r)^{1/2} \quad \sigma_1 = f(r)^{-1/2}. \tag{A.36}$$

We therefore have

$$n_\mu \sigma_\nu \nabla^\mu K^\nu = -\nabla^0 K^1. \tag{A.37}$$

The Killing vector for the static metric (A.35) is $K^\mu = (1, 0, 0, 0)$ and we can calculate

$$\begin{aligned} \nabla^0 K^1 &= g^{00} \nabla_0 K^1 = g^{00} \left(\partial K^1 + \Gamma^1_{01} K^\lambda\right) \\ &= g^{00} \Gamma^1_{00} K^0 = \frac{1}{2} \frac{\partial f(r)}{\partial r}. \end{aligned} \tag{A.38}$$

The metric of the two-sphere at infinity is

$$\gamma_{ij}^{(2)} dx^i\, dx^j = r^2 \left(d\theta^2 + \sin^2\theta\, d\phi\right) \tag{A.39}$$

so that

$$\sqrt{\gamma^{(2)}} = r^2 \sin\theta. \tag{A.40}$$

Finally

$$E_K = \frac{1}{4\pi G} \int_0^{\pi} d\theta \int_0^{2\pi} d\phi\, r^2 \sin\theta \frac{1}{2} \frac{\partial f\,(r)}{\partial\, r}. \tag{A.41}$$

The case where the metric involves the semi-classical correction of the quantum gravity has coefficients

$$f_\ell\,(r) = 1 - \frac{2\,M\,(\ell)}{r} \qquad M\,(\ell) = \frac{2\,M}{\sqrt{\pi}} \gamma\left(\frac{3}{2}; \frac{r^2}{4\ell^2}\right) \tag{A.42}$$

and derivative

$$\partial_r\, f_\ell\,(r) = \frac{M}{\sqrt{\pi}} \left(\frac{4\gamma\left(\frac{3}{2}\frac{r^2}{4\ell^2}\right)}{r^2} - \frac{e^{-\frac{r^2}{4\ell^2}} \sqrt{\frac{r^2}{\ell^2}}}{\ell^2} \right). \tag{A.43}$$

Therefore, the Komar energy reads

$$E_K = \frac{M}{2\sqrt{\pi}} \left(-e^{-\frac{r^2}{4\ell^2}} \left(\frac{r^2}{\ell^2}\right)^{3/2} + 4\ \gamma\left(\frac{3}{2}; \frac{r^2}{4\ell^2}\right) \right) \tag{A.44}$$

that in the limit $r \to \infty$, this becomes $E_K = M$.

Appendix B

Shear Viscosity Calculations

In this section, other methods to calculate the shear viscosity directly from the Lagrangian density are presented.

B.1 Pole Method

This method has been presented in [6] for computing the zero frequency limit of transport coefficients in strongly coupled field theories described holographically by higher derivative gravity theories. In this method, called *pole method*, the hydrodynamic parameters such as shear viscosity and conductivity can be obtained by computing residues of poles of the off-shell Lagrangian density. These coefficients can be thought of as effective couplings at the horizon. Using this method one can obtain an analytic, Wald-like formulae for the shear viscosity and conductivity in a large class of general higher derivative Lagrangians. If one applies this method to systems at zero temperature but finite chemical potential. The results imply that such theories satisfy $\eta/s = 1/4\pi$ universally in the Einstein-Maxwell sector [6].

In Refs. [7, 8] it is clear that generically transport coefficients associated to massless modes are given by effective couplings at the horizon. There is a quick, efficient procedure for extracting these couplings from the Lagrangian density. By evaluating the Lagrangian on an off-shell perturbation, it will generically develop a pole at the horizon. *The residue of the pole is precisely the desired transport coefficient up to a known factor.* Boundary terms cannot contribute as in general they yield higher order singularities. The single pole behaviour can be traced back to horizon

regularity of the generalized canonical momentum in the hydrodynamical approximation. This procedure for computing transport coefficients, which we name the pole method, works for any higher derivative theory and reproduces all the previously known results in the literature in a simple fashion. With this method the shear viscosity to entropy density ratio may be computed solely within the near horizon geometry, and therefore in Einstein gravity it can be used to deduce the universality of $\eta/s = 1/4\pi$ at extremality.

In this section, the ratio of the shear viscosity to entropy density for five dimensional regular black brane gravity is calculated using the pole method [6]. The metric for the planar regular AdS black hole given in eq. (4.77), reported again here for convenience

$$ds^2 = \frac{r_+^2}{u\,R^2}\left(-f dt^2 + d\boldsymbol{x}^2\right) + \frac{R^2}{4u^2}\frac{du^2}{f} \qquad f = 1 - u^2 \cdot \frac{\gamma\left(2,\, \frac{r_+^2}{4\theta^2 u}\right)}{\gamma\left(2,\, \frac{r_+^2}{4\theta^2}\right)} \tag{B.1}$$

An important feature of these coordinates is that $f(z)$ has a simple zero at the horizon. Following the pole method [6], one considers the perturbed metric of the brane by shifting

$$dx \to dx + \epsilon e^{-i\omega t} dy \tag{B.2}$$

where ϵ is treated as an infinitesimal parameter. Then one evaluates the Lagrangian density, with the matter part $L_m = 0$, on the shifted background up to quadratic order in ϵ. The presence of the off-shell perturbation (B.2) produces a pole at $z = 0$ in the (otherwise) on-shell action. The shear viscosity is then given directly by the 'time' formula [6]

$$\eta = -8\pi T \lim_{\omega,\epsilon\to 0} \frac{\mathrm{Res}_{z=0}\mathcal{L}}{\omega^2\epsilon^2} \tag{B.3}$$

where $\mathrm{Res}_{z=0}\mathcal{L}$ denotes the residue of the pole in the Lagrangian density. In the explicit case of a regular black brane in five spacetime dimensions,

$$\mathrm{Res}_{z=0}\mathcal{L} = \frac{7\theta^2\omega^2\epsilon^2\left[4\theta^2\left(e^{\frac{r_+^2}{4\theta^2}} - 1\right) - r_+^2\right]e^{-2it\omega}}{R\left[r_+^4 + 8\theta^2 r_+^2 - 32\theta^4\left(e^{\frac{r_+^2}{4\theta^2}} - 1\right)\right]} \tag{B.4}$$

Recall the Hawking temperature for the above regular black brane metric (B.1) is given in Eq. (4.74).

The final result of this calculation for regularized gravity is

$$\eta = \frac{1}{16\pi G_N}\left(\frac{r_+}{R^2}\right)^3 . \tag{B.5}$$

This result coincides with the result found in the previous section, eq. (4.103).

B.2 Numerical Method

A possible numerical solution is presented.

B.2.1 Near the Horizon Boundary Condition

As seen in Chap. 4, both the horizon and the boundary are regular singular points, i.e. first order poles of the equation of motion (4.78). For this reason, it is possible to apply the Froebenius method to solve the differential equation. The Frobenius method provides a solution of the equation (4.78) in terms of a series expansion around the horizon of the form

$$\phi(u) = (1-u)^A \sum_{n=0}^{\infty} a_n (u-1)^n . \tag{B.6}$$

Like in the standard black brane also for this regular black brane there are no other singularities between the boundary and the horizon and one expects that the series should be convergent. The first step is to study the solution (B.6) near the horizon. In this regime the metric function (4.83) reads

$$f_{NO}(u) = \kappa(u-1) + \frac{1}{2}\kappa_2 (u-1)^2 + O(u-1)^3 \tag{B.7}$$

where $\kappa = -4\pi T$ and $\kappa_2 = (\kappa+2)\frac{r_0^2}{4\theta^2} + \kappa$ and it is possible to truncate the series (B.6)

$$\phi_{NO}(u) = (1-u)^A (a_0 + a_1(1-u)) . \tag{B.8}$$

Plugging (B.6) and (B.7) into the equation of motion (4.78) and keeping only the dominant terms, the differential equation becomes

$$\left(A^2 + \frac{w^2}{\kappa^2}\right) a_0 (u-1)^{-2} + O(u-1)^{-1} = 0 \tag{B.9}$$

which is divergent at the horizon. The divergence can be avoided setting the parameter A (the exponent in (B.6))

$$A = \pm i\frac{w}{\kappa}. \tag{B.10}$$

The infalling boundary conditions[1] requires that the exponent is the one with minus sign $A = -i\frac{w}{\kappa} = i\frac{w}{4\pi T}$. Plugging the approximate solution near the horizon (B.8) into (4.78) gives a divergent result. The divergence of order $(u-1)^{-1}$ can be avoided appropriately fixing the free parameter a_1. In particular, the parameter a_1 in (B.8) can be fixed requiring that the coefficient of the expansion of order $(u-1)^{-1}$ is zero. This involves the second order of the metric function (B.7), and performing the calculation, the parameter a_1 reads

$$a_1 = \frac{a_0}{2\kappa^2}\left(-\frac{2\kappa\left(w^2+q^2\kappa+iw\kappa\right)}{(2iw+\kappa)} + iw\kappa_2\right) \tag{B.11}$$

$$= \frac{r_0^2 w(2w-i\kappa)(2+\kappa) + 4\theta^2\kappa\left(4w^2+2q^2\kappa+iw\kappa\right)}{8\theta^2\kappa^2(2iw+\kappa)}a_0. \tag{B.12}$$

Notice that parameter a_0 is an overall constant (it multiply both the terms of (B.9)) of the truncated solution and can be set $a_0 = 1$, in this way it satisfies the condition at the boundary. The solution (B.8) can be used as boundary condition for the numerical calculation of the solution on the whole range.

B.2.2 Near the Boundary

Near $u = 0$ the equation has two solutions, $f_1 \sim 1$ and $f_2 \sim u^2$. It is possible to see this by expanding the coefficients of the differential equation near the boundary and finding the indicial exponents $\Delta_+ = 2$ and $\Delta_- = 0$. Plot of the numeric solution $\phi(u)$ at the boundary are given in Fig. B.1 as functions of w.

B.3 Retarded Green's function

At this point, it is possible to extract the Green's function as

$$G_u(w,q) = \frac{f(u)}{u}\frac{\phi'(u)}{\phi(u)}. \tag{B.13}$$

[1] Imposing boundary condition on the horizon is an important step in the calculation of the Minkowskian Green's function (see Sec. B.3)

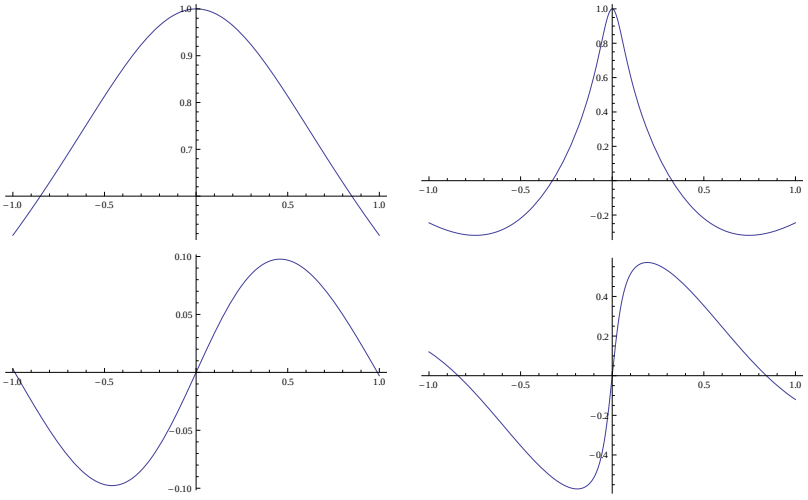

FIGURE B.1: **Numerical results.** Upper row: On the left, the real part of the solution at the boundary, $\Re[\phi(u=0,w,q=0)$ in the "classical" regime, namely $\theta=0.1$, $r_0=10$. On the right, in the "quantum" regime, $\theta=r_0=1$. Down row: On the left, the imaginary part of the solution at the boundary, $\Im[\phi(u=0,w,q=0)$ in the "classical" regime, namely $\theta=0.1$, $r_0=10$. On the right, in the "quantum" regime, $\theta=r_0=1$.

This is based on the postulate that the retarded Green's function is related to the quadratic part of the action as described in (4.26). Using the numerical solution for the perturbation ϕ, one can plot the imaginary part of the retarded Green's function.

In order to visualize the poles of the $\mathrm{Im}G_u\,(w,q)$, and therefore observe the effect of non-zero temperature, one needs to subtracts background. If one does not subtract this contribute then the two-point function is dominated by a large zero temperature that diverges as w^4. One could expect that in this case there are two solutions corresponding to $T=0$: one is the standard solution corresponding to a spacetime without a black hole while the other one should be a spacetime with a remnant.
In the case of the black brane the temperature

$$T=\frac{r_+}{\pi b^2}\left(1-\frac{r_+^4 e^{-\frac{r_+^2}{4\theta^2}}}{32\,\theta^4\gamma\left(2,\,\frac{r_+^2}{4\theta^2}\right)}\right) \tag{B.14}$$

where the[2]

$$\gamma\left(2,\,\frac{r_+^2}{4\theta^2}\right)=1-e^{-\frac{r_+^2}{4\theta^2}}\left(1+\frac{r_+^2}{4\theta^2}\right) \tag{B.15}$$

is always different from zero except for $r_+=0$ (see Fig. 4.2).

[2]Using the relation $\gamma\,(n+1,\,z)=n!\,\left(1-e^{-z}\sum_{k=0}^{n}z^k/k!\right)$.

Therefore, the only difference can be done with the background without a black hole. In that case the equation of motion is just Bessel's equation. The oscillatory solutions to the Bessel equation are the Hankel functions. Therefore the solution in this case can be written in terms of the spherical Hankel function of the second type. The same procedure then can be applied to calculate the two-point correlation function that gives

$$\mathrm{Im}G_{T=0} = \pi \left(w^2 - q^2\right)^2 . \tag{B.16}$$

The difference between the full two-point function and the zero temperature two-point function is the thermal excitation can be plotted. Unfortunately, numerical errors in this kind of calculation starts to be extremely severe and one cannot proceed further in this way to the calculation of η/s.

References A and B

[1] R.M. Wald. *General Relativity*. University of Chicago Press, 2010.

[2] S.M. Carroll. *Spacetime and Geometry: An Introduction to General Relativity*. Addison-Wesley Longman, Incorporated, 2004.

[3] E. Poisson. *A Relativist's Toolkit: The Mathematics of Black-Hole Mechanics*. Cambridge University Press, 2004.

[4] F.R. Tangherlini. "Schwarzschild field in n dimensions and the dimensionality of space problem". English. In: 27.3 (1963), pp. 636–651.

[5] S.W. Hawking and Don N. Page. "Thermodynamics of Black Holes in anti-De Sitter Space". In: *Commun.Math.Phys.* 87 (1983), p. 577.

[6] Miguel F. Paulos. "Transport coefficients, membrane couplings and universality at extremality". In: *JHEP* 1002 (2010), p. 067. arXiv: 0910.4602 [hep-th].

[7] Robert C. Myers, Miguel F. Paulos, and Aninda Sinha. "Holographic Hydrodynamics with a Chemical Potential". In: *JHEP* 06 (2009), p. 006. arXiv: 0903.2834 [hep-th].

[8] Nabamita Banerjee and Suvankar Dutta. "Higher Derivative Corrections to Shear Viscosity from Graviton's Effective Coupling". In: *JHEP* 03 (2009), p. 116. arXiv: 0901.3848 [hep-th].

Acknowledgements

I would like to thank all the people that contributed to the work described in this thesis. First and foremost, I would like to thank my academic advisors Dr. Piero Nicolini and Prof. Marcus Bleicher. During my years at FIAS and Goethe University, they contributed to a rewarding graduate school experience by giving me intellectual freedom in my work, engaging me in new ideas, and demanding a high quality of work. In particular, I would like to thank Piero, who has carefully reviewed this thesis, for his encouragement, understanding, patience and for guiding me through my graduate education.

I am grateful for the funding sources that allowed me to pursue my graduate studies: FIAS, HIC for FAIR and HGS-HIRE. I want to thank also the members of the HGS-HIRe management board that were so helpful and kind with me.

My deep gratitude goes to my external supervisor Dr. Orlando Panella for his support during throughout the work. His work in Physics has been of inspiration since my bachelor studies in Perugia, and I have really appreciated continuing working with him during my graduate studies. My sincere gratitude also goes to Prof. Giorgio Immirzi, who always supported me and taught me the beauty of Physics.

I am very grateful to Prof. Robert Mann, who introduced me to the Lovelock theory of gravity and supported me during my first period abroad in the wonderful Canada. I would like to thank David Kubzniak for his collaboration and supervision during my six-month visit at the Perimeter Institute. I am thankful to all the people that I have met at Perimeter Institute. It was an honor to work at PI. My appreciation extends to Jonas Mureika and Matthias Kaminski for their discussions, the interest they showed in my projects and the organization, together with Piero, of the incredible KSM meetings in Frankfurt.

Many thanks to all the friends I have met at FIAS and HGS-HIRe events, Alessandro, Lucas and his lovely family, Daniel, Sven, Michael, Gabriele and the whole class HQ-M, for making the working hours even more pleasant. In particular, I thank Michael, who helped me translating the abstract of this thesis into German. A sincere thanks also goes to the former FIAS postdoc Hannu for showing me the beauty of Frankfurt.

Finally, I want to thank the incredible support I received from my amazing sister, Francesca, and my awesome brother, Matteo. Without them and the support of my whole family, this work would not have been possible. I will never thank enough my dearest friend Marialucia that constantly fill me with her deep friendship and support. Above ground, I owe a gigantic debt of gratitude to D for his invaluable love.